MINISTRY
OF EDUCATION, RESEARCH,
DEVELOPMENT AND YOUTH
OF THE SLOVAK REPUBLIC

univnet

STU
SLOVAK UNIVERSITY OF
TECHNOLOGY IN BRATISLAVA

PROGRESSIVE AUTOMOTIVE WASTE UTILISATION TECHNOLOGIES AS DRIVING FORCES OF SUSTAINABLE DEVELOPMENT

Editors
Iveta Čabalová
Jozef Krilek

PROGRESSIVE AUTOMOTIVE WASTE UTILISATION TECHNOLOGIES AS DRIVING FORCES OF SUSTAINABLE DEVELOPMENT

Editors
Iveta Čabalová
Jozef Krilek

Zvolen, 2024

UNIVNET – University and Industrial Research and Education Platform of the Recycling Society

Members of the UNIVNET Association:
Slovak University of Technology in Bratislava
University of Economics in Bratislava
Technical University of Košice
University of Žilina
Technical University in Zvolen
Automotive Industry Association of the Slovak Republic

Editors:
Iveta Čabalová 1*
Jozef Krilek 1*
1 Technical University in Zvolen, T.G Masaryka 24, Zvolen*

Reviewers:
prof. Ing. Stanislav Legutko, PhD.
Poznan University of Technology
Institut of Mechanical Technology (PL)
prof. Ing. Dagmar Juchelková, Ph.D.
University J.E. Purkině Ústí nad Labem
Faculty of Mechanical Engineering (CZ)
prof. Ing. Pavel Kovac, PhD.
University of Novi Sad
Faculty of Technical Science (SRB)

Cover design:
Ing. Tibor Dzuro, PhD.,
Technical University of Košice,
Faculty of Mechanical Engineering,

Published by: **RAM-Verlag, Germany**

ISBN: **978-3-96595-042-9**

UNIVNET, Zvolen, November 2024

LIST OF AUTHORS

1. **Trends in the transformation of economies due to the penetration of electric mobility in passenger car sales and production**
Ochotnický Pavol, Sivák Rudolf, Lábaj Martin, Majzlíková Erika, Zábojník Stanislav, Belanová, Katarína, Hocman František

2. **Recycling of laminated glass – research on suitable plate material for the line scraper module**
Ľubomír Šooš, Marcela Pokusová, Iveta Čačková, Viliam Čačko

3. **Traction battery dischargers**
Ľubomír Šooš

4. **Development of technology for the recovery of waste foam into new products**
Ľubomír Šooš, Miloš Matúš, Ondrej Chlebo, Jozef Bábics

5. **Material recycling perspectives of discarded lithium-ion automotive batteries**
Tomáš Havlik, Dušan Oráč, Jakub Klimko

6. **Analysis and design of innovative material and design solutions for noise barriers based on recycled materials**
Miroslav Badida, Lýdia Sobotová, Marek Moravec, Tibor Dzuro, Miriama Piňosová

7. **Mechanical-physical and ecotoxicological properties of new wood-plastic composites**
Jozef Krilek, Iveta Čabalová, Helena Hybská, Marek Potkány, Vladimír Mancel, Anna Darabošová

8. **Energy recovery/disposal of waste sludge from the automotive industry**
Marek Patsch, Peter Pilát, Jozef Jandačka

Contents

Foreword 1

1 Trends in the Transformation of Economies Due to the Penetration of Electric Mobility in Passenger Car Sales and Production **3**
1.1 Introduction 3
1.2 Development of electric mobility in Europe and Slovakia 4
  1.2.1 Main defining factors and barriers to the development of electric Mobility in Europe 4
  1.2.2 Main trends and short-term development of electric mobility in Europe 5
  1.2.3 Empirical verification of the economic determinants of EV sales in Europe 7
  1.2.4 Regional aspects of e-mobility penetration in the Slovak Republic and scenarios 11
1.3 The energy context of fleet transformation 14
1.4 Modelling of changes in the technological mix in the automotive industry of the Slovak Republic on selected socio-economic and ecological indicators 21
References 31

2 Recycling of Laminated Glass – Research on Suitable Plate Material for the Line Scraper Module **35**
2.1 Introduction 35
2.2 Design of the scraper module of the laminated glass processing line 35
  2.2.1 Plate design for the scraper module 38
2.3 Objectives and assumptions of the experimental research 41
2.4 Analysis for the relevant investigation of wear of the plates in the scraper module 43
2.5 Experiment to determine the appropriate surface treatment for the scraper plat 45
2.6 Experiment implementation and measured data for the fired plates 48
2.7 Conclusion 57
References 57

3 Traction Battery Dischargers **58**
3.1 Introduction and definition of the analysis 58
3.2 Motivational introduction and description of the need for a traction battery dischargers 58
3.3 Using apps 59
  3.3.1 Car service 59
  3.3.2 The basics of discharging 60
  3.3.3 Types of discharge systems 62

3.4 Current status of discharger manufacturers in the world 63
3.5 Current situation in Slovakia 69
3.6 Discharge system requirements 70
3.7 Risk analysis for the design and construction of discharge facilities 72
3.8 Safety requirements 73
  3.8.1 Operation of the discharging device 73
  3.8.2 Qualification and proficiency to operate unloading equipment falling under the definition of work on electrical equipment 73
3.9 Design of the basic technical specification of the discharger (discharging into a resistive load) 75
  3.9.1 Technical specifications 75
  3.9.2 Typical discharge device design 76
  3.9.3 Reference technical standards 76
  3.9.4 Service and discharge process [3] 77
  3.9.5 Basic schemes of discharge equipment 78
  3.9.6 Selection of key components 81
References 82

4 Development of Technology for the Recovery of Waste Foam into New Products 83
4.1 Introduction 83
4.2 Characteristics of PUR foam 84
4.3 Environmental impacts of recovery of PUR foams from old vehicles in Slovakia 85
4.4 Analysis of technological options for the recovery of polyurethane foams 86
4.5 Mechanical recycling 87
  4.5.1 Disintegration of waste materials 87
4.6 Known mechanical recycling methods 90
4.7 Proposal of the appropriate technology for the stated project objectives 91
  4.7.1 Detailed description of the technology 92
4.8 Utilization of products from secondary raw materials 93
4.9 Experimental development and optimization of the proposed technology 96
4.10 Parameters affecting the quality of the moulding 97
4.11 Further research developments 99
4.1.2 Conclusion 99
References 100

5 Material Recycling Perspectives of Discarded Lithium-Ion Automotive Batteries **101**
5.1 Introduction 101
5.2 Current state of the issue 103
5.3 Experimental part 108
5.4 Conclusion 127
References 128

6 Analysis and Design of Innovative Material and Design Solutions for Noise Barriers Based on Recycled Materials 133
6.1 Introduction 133
6.2 Analysis of current material and design solutions for noise barriers 134
  6.2.1 Criteria for the design and implementation of noise reduction measures 134
  6.2.2 Categories of noise reduction measures 135
  6.2.3 Design, construction, material used and location of noise reduction barriers 137
6.3 Requirements for the material, construction and acoustic properties of noise reduction barrier 147
  6.3.1 Selected data on NRBs in the Slovak road network 150
  6.3.2 Selected NRB parameters 151
6.4 Design solution of the original damper applicable to the noise reduction barrier system 154
6.5 Investigation of acoustic conditions on a selected motorway section 158
6.6 Conclusion 162
References 162

7 Mechanical-Physical and Ecotoxicological Properties of New Wood-Plastic Composites 165
7.1 Introduction 165
7.2 Automotive industry 165
7.3 Plastics in the automotive industry 166
7.4 Use of waste plastics from the automotive industry 167
7.5 Particleboard containing plastic filler 170
  7.5.1 Material used for the production of single and three-layer particleboards with plastic/rubber content 170
7.6 Analysis of thermophysical properties of single-layer particleboards containing plastic 173
7.7 Analysis of the physical properties of particleboards containing plastic and rubber 176
7.8 Analysis of mechanical properties of wood composites containing plastic and rubber 177
7.9 Ecotoxicological testing of single-layer PBs containing plastic 178
7.10 Economic demand from the point of view of calculations of the innovated product – three-layer PB with plastic content 181
7.11 Conclusion 185
References 186

8 Energy Recovery/Disposal of Waste Sludge from the Automotive Industry 191
8.1 Introduction 191
8.2 Waste sludge treatment 191
  8.2.1 Threaded sludge press 193
  8.2.2 Band sludge press 194
  8.2.3 Chamber sludge press 196

8.2.4 Membrane sludge press 197
8.2.5 Frame sludge press – sheet filter 197
8.2.6 Sludge press accessories 197
8.3 Methods of recovery of industrial sludge 198
8.3.1 Landfill 198
8.3.2 Incineration and co-incineration 198
8.3.3 Pyrolysis and gasification 201
8.4 Measurement of moisture and calorific value of waste sludge 203
8.4.1 Sample preparation prior to laboratory testing 203
8.4.2 Fuel moisture measurement 204
8.4.3 Measurement of waste sludge calorific value 205
8.4.4 Elemental analysis of waste sludge sample 209
8.5 Conclusion 214
References 221

Foreword

Dear readers,

The current era brings new challenges for the environment and economy, which are in many cases interlinked and interacting. The dynamic changes in the automotive industry, including the advent of e-mobility and increasing demands for sustainability, are driving the need for innovative approaches to waste utilization and recovery. This publication focuses on advanced waste recovery technologies that are becoming a key pillar of the circular economy.

The aim of the publication is to provide a comprehensive view of waste management in the context of the automotive industry, which is one of the main driving forces of the global economy. Rapid technological progress, increasing demand for electric vehicles and ever-changing legislative requirements strongly demand changes in the approaches to waste treatment and recycling. The output hereof should also be an optimized design of the material (or energy) technology recovery of various types of automotive waste (glass, batteries, foam, rubber, plastic). The publication provides a detailed overview of current strategies, technologies and trends shaping the future of waste recovery.

At the same time, this book is the result of an extensive collaboration between universities, research institutions and industrial partners. This collaboration has been key to gathering the latest knowledge and examples of good practice that can serve as an inspiration for further development in this area. Thanks to this, the publication offers not only theoretical foundations, but also practical solutions that are applicable in real conditions.

An important part of this publication is the reference to socio-economic implications of the transition to electric mobility, which are the subject of extensive analysis in individual chapters. Electric mobility, which is closely linked to the concept of the circular economy, brings new challenges but also opportunities for sustainable development. The book also addresses employment issues in this sector, the potential of recycling, and the economic challenges that the European Union and Slovak Republic are facing.

UNIVNET currently represents an important research infrastructure in the field of circular economy across sectors with a national scope, and with initiatives and activities in research projects and collaborations on a European scale. It has ambitions to become a National Circular Economy Platform and to initiate the creation of a new European Research Infrastructure in the framework of ESFRI (European Strategy Forum on Research Infrastructures). The aim of this initiative will be to minimize the negative environmental impact and save primary energy sources and raw materials at an EU level. The UNIVNET association will strive to ensure in the future, in addition to research and development activities, also professional and educational activities based on the achieved results of the implemented activities, for example in the form of workshops with the authors and researchers of UNIVNET topics. One such activity is the presentation of results at the international scientific conference Environmental Protection Technology – TOP.

Dear readers, professionals in the field, dear students,
UNIVNET has published several publications over the period of its existence. You are now getting your hands on the sixth publication as a thematic continuation of the monographs
published since 2020. We believe that this publication will also be positively received by the professional as well as non-professional public and will provide you with the necessary information and answers to your questions.
Finally, we would like to thank all those who contributed to this publication, whether as authors, reviewers or supporters. We believe it will provide valuable information to readers and contribute to the development of new approaches in the field of sustainability and waste recovery. It is our sincere wish for this publication not only to be a source of knowledge, but also an impetus to further innovation and improved practices in the environmental management of automotive waste recovery.

In Zvolen, 13 November 2024

Assoc. prof. Iveta Čabalová
prof. Jozef Krilek

1 Trends in the Transformation of Economies Due to the Penetration of Electric mobility in Passenger Car Sales and Production

1.1 Introduction

The automotive industry in Europe and the Slovak Republic is undergoing huge technological changes, which significantly affect the structure of production and supply sectors, as well as the structure of offer or demand for new car models. A major impetus for change has been the adoption of the strategy document "A European Strategy for Low-Emission Mobility" by the European Commission in 2016 [1]. The strategy is a response to the long-term risks of the depletion of traditional fossil fuels in the world, and the risks of rising prices associated with the extraction, transport and use of traditional fuels in the growing transport sector. And nowadays also with the consequences of war conflicts, interference in the market of these energy sources and the diversification of transit flows.

The strategy also relies on new incentives and policies to increase the demand for advanced energy in transport and a target has been set for 2030 to replace around 15 – 17 % of the original demand for petroleum products in transport. In relation to the automotive market, the pillars of the above strategy have focused in particular on:

- increasing the efficiency of the transport system, using digital technologies and switching to lower-emission transport modes,
- the introduction of low-emission alternative energy in transport, e.g. advanced biofuels, renewable electricity and renewable synthetic fuels, but also the removal of barriers to the electrification of transport
- a shift to low- and zero-emission vehicles
- continuing incentives at city and municipal level for low-emission alternative energies and vehicles.

As reported by [2], road transport is a major source of air pollution and upper emission limits for the most harmful nitrogen oxides (NO_x), ground-level ozone (O_3) and solid particles have been significantly exceeded in the EU. The EU estimates that 100 million people have been affected by harmful noise levels above 55 dB during the day and 60 million people above 50 dB at night. Road traffic has been assessed as the dominant source of noise and its impact on the health of the population [3].

The wider Green Deal aims to make Europe the first climate neutral continent by 2050. This target [4] became legally binding with the adoption of the Climate Act by the European Parliament and the Council in 2021. The EU's 2030 emissions reduction target has been updated to a more ambitious level of 55 %.

The transport sector is considered one of the largest consumers of oil out of total oil consumption, contributes significantly to total final energy consumption and according to [5], road transport directly contributes 20 % of Europe's CO_2 emissions. The advent and development of electric mobility, across the entire life cycle of low to zero emission cars from production, through use to end-of-life recycling, is therefore an important element on the path to carbon neutrality in Europe, despite some open questions.

The authors aim to contribute to the discussion on the penetration of electric mobility in EU countries and the Slovak Republic with their preliminary findings, findings from other studies, and contributions to the following research questions:

(a) What is the penetration/sales of passenger electric vehicles in EU countries and how are sales affected?
(b) What is the trend in the penetration/sales of passenger electric cars in the Slovak Republic and its regions and what influences the demand for this type of vehicle?
(c) What is the energy context for the development of electric mobility?
(d) What changes can be expected from the transition to the production of electric vehicles in the economy of the Slovak Republic as the largest producer of passenger cars per capita and in the sectors of the Slovak Republic economy?

1.2 Development of electric mobility in Europe and Slovakia

With regard to the offer and demand for electric vehicles (EV), the development of electric mobility in Europe is the result of a whole complex of technological, economic, environmental and psychological influences.

1.2.1 Main defining factors and barriers to the development of electric mobility in Europe

As detailed in [6] and [7], the transition to EVs is one of potential sources to significantly decrease or even eliminate emissions in the energy supply chain, both in the production and use of EVs. This depends on the energy source used. For example, public charging stations that supply electricity from renewable energy sources (water, solar, wind and, to some extent, nuclear power) contribute to the fact that some types of electric vehicles can indeed be described as zero-emission vehicles. According to [8], [9] this is also true for the use of energy sources, which are not considered clean with respect to emissions, for the operation of different groups of electric vehicles, the overall environmental impact of vehicles powered by electricity generated from coal is better than that of a vehicle fitted with an internal combustion engine.

In addition, electric vehicles are also seen as having the storage capacity not only for variable renewable energy generation, optimizing the use of tariffs and electricity consumption times and its temporary storage, but also for precious metals storage and their subsequent recovery.

In conjunction with other breakthrough technologies such as electrification, automation, robotics, and artificial intelligence, renewable energy technologies are a prerequisite for the sustainability of the entire circular economy of the automotive industry.

A considerable and rather psychological influence is the efforts of the population (especially the younger representatives) to resist the potential negative aspects of transport and the effects of economic growth on the state of the environment. As reported by [10], [11], [12], [13] this is an important determining factor which affects the public interest in using electric vehicles.

The study [14] also provided empirical evidence that the dominant factor in the development of electric mobility and EVs sales is the purchase price of EVs in conjunction with the level of income of a country's population. According to [15], [16], EV prices are on average much higher than their petrol equivalents, around €35,000, and in many non-European countries these prices are 2- to 2.5-times higher than comparable conventionally powered vehicles. As such, electric vehicles are out of economic reach for many drivers, especially in emerging countries. However, studies by [14] and [17] have provided evidence that demand incentives are therefore increasingly successful in stimulating demand for EVs and their models.

In addition to the economic barriers mentioned above, the study [18] identified age, gender and education as factors playing a role in the EVs purchasing decision. According to [19], [20] a portion of the population believes that by purchasing a vehicle, regardless of price, and using it, they will contribute to reducing the consumption of natural resources, feel socially responsible and contribute to the advancement of technology.

Supportive policies for charging infrastructure development are another important factor in determining EVs adoption rates. The lack of charging facilities causes discomfort when using electric vehicles [21], [22], as well as the maximum range offered by electric vehicles on a single charge and also longer charging times. Concerns about EVs discharge and fear of failures also play a significant role. Security of supply of critical minerals is also a barrier to the development of electric mobility in the EU. According to the International Energy Agency (IEA), "clean energy technologies are becoming the fastest growing demand segment" for critical minerals. In particular, the expansion of the battery industry may put pressure on the supply chain of selected metals and materials.

1.2.2 Main trends and short-term development of electric mobility in Europe

Despite the above barriers and the slowdown in dynamics in recent years in some EU countries, the penetration of electromobility, as measured by sales, has appeared to be a success story in recent years. This is also documented in the following Table 1.1 and in Fig. 1.1.

Table 1.1

Development of sales of electric vehicles in million units and their share of sales in %.

Year	Battery electric cars	Plug-in electric cars	Total cars	Share of electric cars
2016	54065	65011	12027051	1
2017	83491	88334	12574590	1.4
2018	132377	106502	12753440	1.9
2019	242966	137632	12991283	2.9
2020	536186	525311	9924123	10.7
2021	878092	862569	9694858	18.0
2022	1126682	873042	9252358	21.6

Source: https://www.eea.europa.eu/en/analysis/indicators/new-registrations-of-electric-vehicles

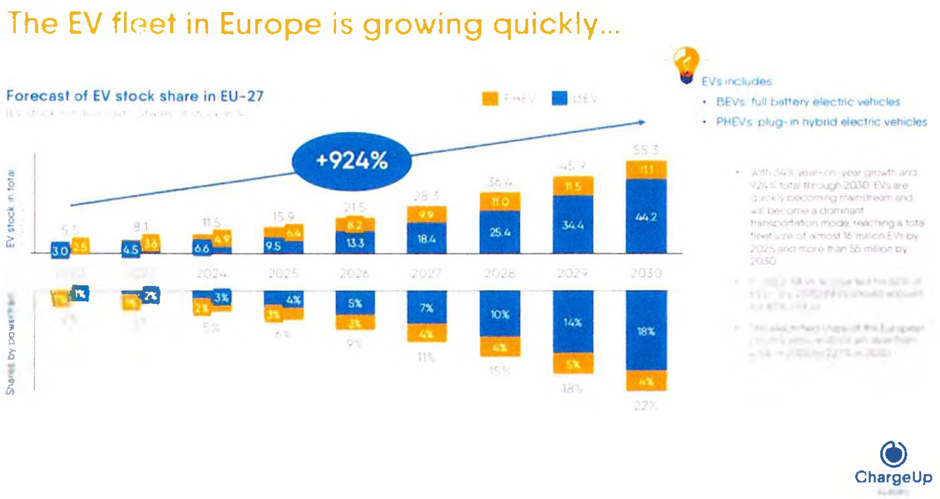

- With 34% year-on-year growth and 924% total through 2030, EVs are quickly becoming mainstream and will become a dominant transportation mode, reaching a total fleet size of almost 16 million EVs by 2025 and more than 55 million by 2030

Source: https://www.chargeupeurope.eu/state-of-the-industry

Fig. 1.1 Forecast of electric vehicle sales in 2023 in million units by 2030

In short term and based on ACEA data, there was a sharp drop (-18.3%) in new car registrations in the EU in August 2024, with significantly negative changes affecting the four main regional markets. Significant losses were recorded in Germany (-27.8%), France (-24.3%), and Italy (-13.4%), Spain (-6.5%). In addition to the change in the downward trend of new vehicle registrations, there was a further decrease in the share of battery-powered vehicle sales in August. The 14.4% share of the EU car market in August was down from 21% the previous year and was the fourth consecutive month of decline for 2024. Registrations of plug-in hybrid cars were also marked by a significant drop. This not only sharply contrasts with the relatively consistent month-on-month increases in the past year, but it is a distinct signal in changing trends in the penetration of electromobility in EU countries for the following years as well.

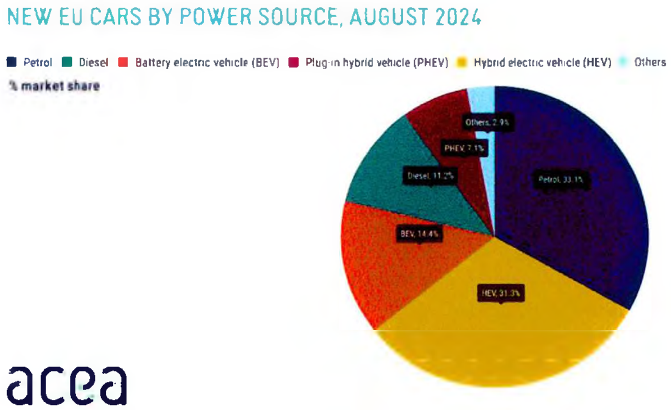

Source: https://www.acea.auto/pc-registrations/new-car-registrations-18-3-in-august-2024-bev-market-share-down-by-almost-one-third/

Fig. 1.2 Structure of newly registered cars

Battery electric vehicle (BEV) registrations in the EU fell by 43.9% in August to 92,627 units (compared to 165,204 in the same period in 2023) and overall market share fell to 14.4% of 21% in the previous year. This was mainly influenced by a dramatic decrease in Germany (-68.8%) and in France (-33.1%). For the year 2024, 902,011 new battery electric cars were registered, which represents 12.6% market. Registrations of plug-in hybrid cars also fell last month (-22.3%) in the EU, and all major European markets also fell. In August, plug-in hybrids (PHEV) accounted for 7.1% of the total car market, down from 7.4% last year with 45,590 units sold. Hybrid electric vehicles were the only vehicle type to see growth in August. Their registration increased in August by 6.6% to 201,552 units. In August 2024, petrol car sales fell only slightly slower than the overall vehicle market, by 17.1%. Market share of petrol cars represented 33.1% of the market in August 2024, compared to 32.6% in August last year. The market with diesel cars recorded in August 2024 a larger decline than the overall market - by 26.4%.

The data indicates that the entire automotive industry and the adaptation of consumers in EU countries to electromobility are undergoing unexpected changes in trends, the causes of which will need to be investigated in more depth.

1.2.3 Empirical verification of the economic determinants of EV sales in Europe

Based on a review of studies on the sale of electric vehicles in the EU, the study [14] defined and transferred empirical evidence of the impact of three main (non-price and non-behavioral) determinants of e-mobility penetration in EU countries, namely:

- economic maturity,
- density of the charging network, and
- support incentives from governments.

The study authors go on to extend these findings with a regression spatial analysis that can serve the shift towards the development of scenarios to forecast the dependence of the electrically chargeable vehicles (ECVs)[1] sales in countries on the three factors mentioned above. It could also help the development of more complex models based on spatial data.

The dependent variable is the market share of ECVs in the new registered cars (MSE) for each EU country – Table 1.2 The cumulative penetration of e-mobility in 2022 confirms that Sweden has the highest market share of ECVs (56.1 %), which in 2022 exceeded more than half of the sales of ECVs in its market, while compared to 2020, the share of ECVs increased by 24 %. Sweden is followed by Denmark, Finland, the Netherlands, Germany, Belgium, Luxembourg, Austria and France. In line with the long-term trend, the converging Central and Eastern Europe (CEE) and Visegrád Group (V4) countries are at the bottom of the ranking.

Table 1.2

Market share of ECVs in 2022 (%), according to the European Automobile Manufacturers Association (ACEA).

Country	MSE	Country	MSE	Country	MSE
Austria	22.1	Germany	31.4	Poland	5.0
Belgium	26.5	Greece	7.9	Portugal	21.7
Croatia	5.0	Hungary	8.6	Romania	9.0
Cyprus	5.4	Ireland	22.2	Slovakia	3.7
Czech Republic	3.9	Italy	8.7	Slovenia	6.2
Denmark	38.6	Latvia	8.1	Spain	9.6
Estonia	5.4	Lithuania	7.9	Sweden	56.1
Finland	37.6	Luxembourg	24.3		

Source: [30]

***The economic maturity factor of countries** is expressed in terms of the real expenditure of countries in purchasing power parity per capita (REppp) according to Eurostat data. Compared to the traditionally used GDP per capita model variable, this indicator also takes into account differences in price and, for some EU countries, exchange rate differences (non-euro area members) across countries (Table 1.3).*

---

[1] BEV plus PHEV.

Table 1.3

Real per capita expenditure (in PPS) in 2022 (according to Eurostat database).

Country	REpps	Country	REpps	Country	REpps
Austria	27,400	Germany	27,500	Poland	19,800
Belgium	26,700	Greece	18,100	Portugal	19,600
Croatia	17,400	Hungary	16,700	Romania	20,400
Cyprus	22,600	Ireland	20,100	Slovakia	16,800
Czech Republic	19,200	Italy	23,000	Slovenia	20,800
Denmark	25,700	Latvia	18,400	Spain	19,700
Estonia	18,300	Lithuania	21,900	Sweden	25,000
Finland	25,300	Luxembourg	32,000		
France	25,200	Netherlands	26,900		

The network density factor *is expressed in terms of the number of charging stations per 100 km (ChD) (Table 1.4). Compared to the indicator for the number of charging stations, it also reflects differences in population density between countries, which may influence the consumer's decision to buy an electric vehicle for shorter distance trips.*

Table 1.4

Charging network in EU countries in 2022 (number per 100 km).

Country	CHD	Country	CHD	Country	CHD
Austria	6.1	Germany	19.4	Poland	0.4
Belgium	5.1	Greece	0.2	Portugal	14.9
Croatia	2.3	Hungary	0.6	Romania	0.5
Cyprus	0.5	Ireland	1	Slovakia	2
Czech Republic	0.9	Italy	5.1	Slovenia	1.6
Denmark	4.4	Latvia	0.5	Spain	1.1
Estonia	0.7	Lithuania	0.2	Sweden	5
Finland	3.3	Luxembourg	34.5		
France	4.1	Netherlands	47.5		

Source: [30]

The government ***support incentive factor*** is used in accordance with the methodology of [14] as the government support intensity index*(SIG)* for e-mobility, the construction of which is based on the ACEA survey and data for 2022. The SIG index relies on an expert assessment of the level of e-mobility support in a country for 3 sub-indicators *(SI)* of taxation (tax benefits TB type) and one of purchase incentives type:

- SI_1 *acquisition (type TB),*
- SI_2 *ownership (type TB),*
- SI_3 *company vehicles (type TB),*
- SI_4 *purchase incentiveness (type PI).*

The multi-criteria method of variant evaluation (for country j) generates an $_{IIGj}$ index, which is the weighted sum of the country's rating by level of individual support (criteria) j and by individual expert i:

$$IIG_{s,j} = \sum_{s=1}^{4} SI_{s,i,j}, v_i \qquad (1)$$

The methodology is detailed in [14], where the values $v_1 = 0.141$, $v_2 = 0.154$, $v_3 = 0.205$, $v_4 = 0.5$ were used for v_i, and the level of support for the sub-indicators $SI_{s,i,j}$ were determined by a holistic expert method, where each of the co-authors s evaluates each sub-indicator $_i$ for country $_j$ with a value of $SI_{i,j,s}$ in the interval 1 to 100.

The arithmetic average of the value of $IIG_{s,j}$ indexes was used to determine the value of the e-mobility support indicator in country $_j$ (Table 1.5) as follows:

$$SIG_j = \left(\sum_{s=1}^{4} IIG_{s,j}\right)/4 \qquad (2)$$

Table 1.5

EU e-mobility support index SIG 2022 [14]

Country	**SIG**	**Country**	**SIG**	**Country**	**SIG**
Austria	83.61	Germany	64.76	Poland	25.00
Belgium	58.80	Greece	28.30	Portugal	48.43
Croatia	23.81	Hungary	67.74	Romania	21.26
Cyprus	22.80	Ireland	59.13	Slovakia	13.39
Czech Republic	18.39	Italy	43.32	Slovenia	6.68
Denmark	17.81	Latvia	13.26	Spain	27.73
Estonia	0.00	Lithuania	32.85	Sweden	55.89
Finland	62.67	Luxembourg	45.82		
France	77.05	Netherlands	61.85		

Empirical estimates of the dependence of the market share of ECVs on the economic maturity of countries, on the density of the charging station network and on the supporting fiscal instruments (Annex 1a., 1b., 1.c) confirm that the market share of ECVs in EU countries increases by 0.0012 for a €1 increase in the standard of living. For an increment in charging network density by 1 %, it increases by 0.386 and a 1unit increase in the sales promotion index results in a 0.192 increase in the market share of ECVs. The above findings confirm the fact that without a faster catch-up in living standards or convergence to the most advanced European countries, without massive fiscal support for the purchase of ECVs, and without the development of charging infrastructure from public, private or combined sources, a "two-speed path" of ECVs penetration between old and new EU Member States is highly likely. This will be a source of divergent approaches to meeting Europe's global targets for e-mobility penetration and acceptance of the EU global regulatory policies.

1.2.4 Regional aspects of e-mobility penetration in the Slovak Republic and scenarios

According to the Slovak Electric Vehicle Association (SEVA), the Slovak Republic takes the last ranking place of European Union countries in terms of the country's adoption of battery electric vehicles in 2022. This is a consequence of a whole complex of negative impacts of the pandemic and energy crisis, when the purchasing power of the population relatively to EU average decreased. According to the SIG indicator, the Slovak Republic also lags far behind in incentives for ECVs sales from public sources. In contrast, HEVs sales and their share in the car fleet in the Slovak Republic enjoyed until 2022 10 times higher interest compared to ECVs.

The following figures for the regions of the Slovak Republic also confirm that regional income disparities or population density also cause huge differences in the penetration of ECVs within the regions of individual countries. In all regions of the Slovak Republic, hybrid types of HEVs vehicles are more popular.

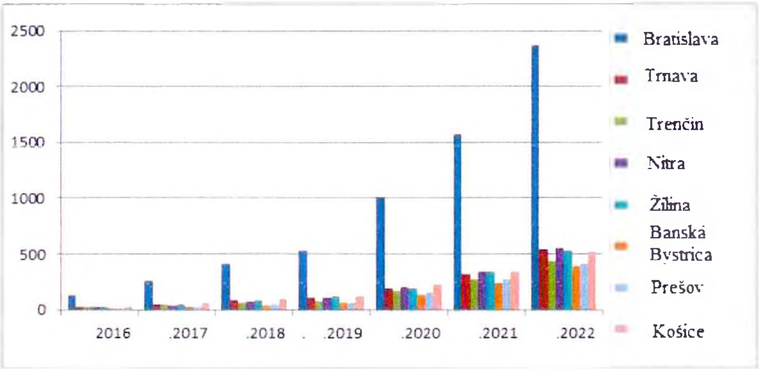

Fig. 1.4 Total registered ECVs for the regions of the Slovak Republic (end of year), source: own elaboration based on the Ministry of Interior of the Slovak Republic database.

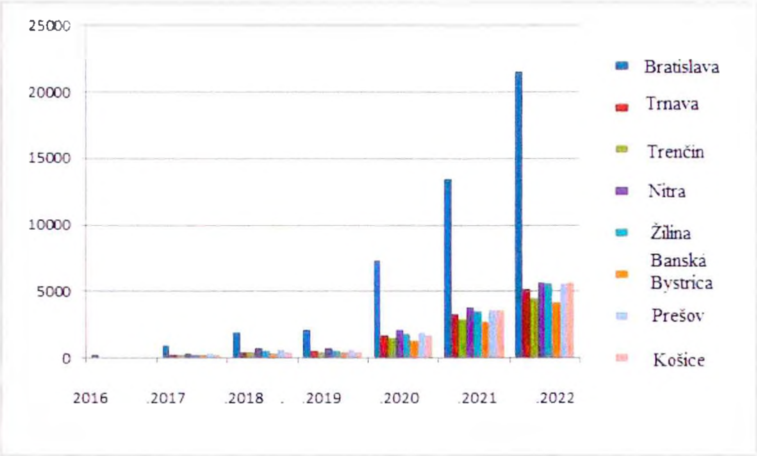

Fig. 1.5 Total registered HEVs for the regions of the Slovak Republic (end of year), source: own elaboration based on the Ministry of Interior of the Slovak Republic database.

The following three existing scenarios for the penetration of electromobility by 2030, which reflected developments in the Slovak Republic until 2022, are more of a signaling value. Without changes in measures to support the sale of electric vehicles and without a more positive inclination towards the purchase of ECVs by consumers, companies and institutions, the scenarios signal the risk of Slovakia lagging behind economically developed countries in the country's adaptation to electromobility.

The first scenario is based on the trend in the development of registered ECVs and HEVs vehicles (Fig. 1.6).

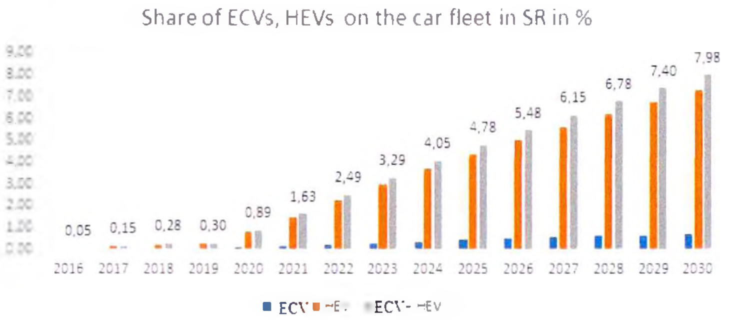

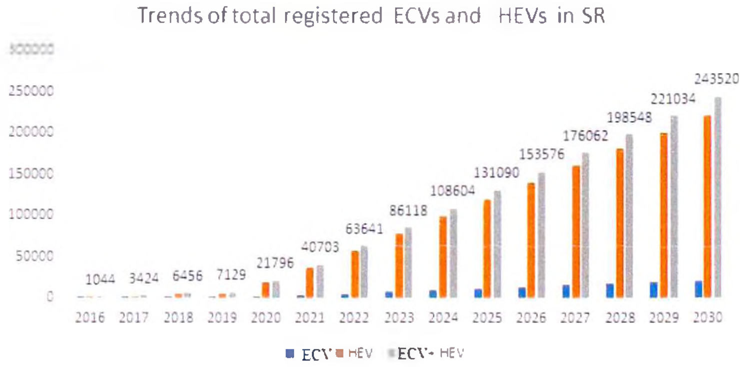

Fig. 1.6 Trend scenarios of ECVs and HEVs penetration into the car fleet in the Slovak Republic [23]

Next SEVA's two scenarios [24] foresee as a key determinant for higher electromobility penetration in SR a convergence of prices between ECVs and traditional ICEs vehicles by the turn of 2027 and 2028.

The first basic scenario foresees virtually no major support measures and assumes 117.060 ECVs for 2030, which is about 4.5 % of the fleet. The scenario, in line with the trend, assumes a continued growth in the share of individually imported and used electric vehicles of older generations from abroad. This is due to insufficient support from the state, which, similarly to other countries, could potentially bring impulses for changing customer preferences.

The second scenario assumes an acceleration of ECVs sales, taking into account support measures such as direct subsidies for the purchase of vehicles or tax benefits for companies, in addition to the change in price parity at the turn of 2027 and 2028. Enforcement of support measures, such as a subsidy for the purchase of zero-emission vehicles, a reduction in the income tax of an employee using a company electric vehicle for private purposes, or an accounting measure for charging of company ECVs at home by employees will, however, be conditional on the consolidation of public finances or the ability to flexibly draw on resources from the Resilience and Recovery Plan or other European and domestic sources.

The SEVA acceleration scenario assumes that in 2030 the number of battery electric vehicles in the Slovak Republic will reach 213,553 vehicles, which would mean reaching a share of 8% of the Slovak vehicle fleet. The scenario of accelerating ECVs penetration is almost identical to the trend scenario for ECVs plus HEVs combined, which signals even more the need for a deeper analysis of car sells factors in Slovakia and for setting appropriately targeted policies. This is despite the fact that more recent data indicate an increase in ECVs new registration in SR.

1.3 The energy context of fleet transformation

Alongside overall productivity and innovative capacity, energy costs are becoming a major challenge to the competitiveness of European car manufacturers and ultimately to their carbon footprint, which is the lowest in the world. The strategies of cross-border automotive concerns and the dynamics of international direct flows of investments reflect the growing importance of energy costs. An example of the fundamental impact of energy costs on international competitiveness is the energy crisis, which caused unprecedented costs (inflation), especially in EU countries, mainly CEE. Since this period, Asian car companies have come to the fore even more strongly at the expense of European car manufacturers (especially Chinese car companies not only exporting but also investing in the EU). Further risks in the CEE region are posed by the cessation of imports of relatively cheap energy carriers from the Russian Federation after the end of the sanction's exemption for Russian energy carriers. The exponentially increasing importance of energy costs is mainly determined by the high energy intensity of battery production and metal processing for BEV and PHEV production.

Convergence of energy intensity towards the advanced developed market economies of the OECD is a natural process in almost every CEE country. The energy intensity of the Slovak Republic was marked by high energy consumption with relatively low added value, especially during the 1990s. After the initiation of economic reforms towards transformation of the investment environment, the first waves of foreign direct investments (FDI) brought also advanced "Western" technologies and a sharp decline in the energy intensity of the Slovak economy. The second wave of investments came mainly after 2004 and with the arrival of key car companies and the convergence of the Slovak economy to a model based on a more dominant commercial services sector [25]. This trend, similar to the economic convergence of several developed market economies, is likely to result in a continuously decreasing energy intensity of Slovak GDP in the case of a successful and sustainable development model in Slovakia. The accelerator for these changes is to be the EU's strict environmental regulation, which is likely to remain at the heart of the reforms despite growing dissent in the European Parliament.

On the other hand, however, it should be clearly emphasised that from the economical point of view, Slovakia is one of the most industrialised countries in the EU, with a significant share of industrial production in GDP. In this context, therefore, at least until 2035, energy costs will play a similarly important function, which is also pointed out by German industrial producers from 2022. Only an affordable, stable supply of energy carriers can ensure not only investment attractiveness but also sustainable cost competitiveness for automotive manufacturers and downstream industries. The latest research results clearly show that also due to rising energy costs, large multinational investors have slowed down or redirected their capital flows within some EU regions to other countries [26].

Quantifying the impact of electricity prices in the automotive industry

Based on the methodology of [27], [28] and [29], data on UEC – unit energy costs for the Slovak Republic at the level of the overall industry (Fig. 1.8) and at the level of the automotive industry have been processed. At the level of the industry in general, as well as directly at the level of the automotive industry, the results look unfavourable for investment attractiveness and maintaining cost competitiveness in the case of the Slovak Republic.

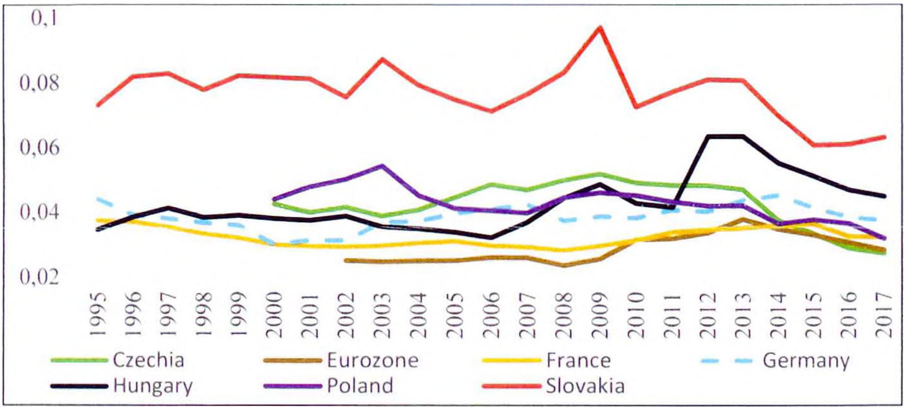

Fig. 1.8 UEC (unit energy cost in electricity) values at industry level, source: own elaboration based on Eurostat data

In the post-2007 period, the impact of decarbonization in the Slovak Republic is demonstrable through more intensive support for subsidized electricity generation from RES/CHP. This rapidly growing trend of decarbonization in the EU energy policy has had a decisive impact on the Slovak industry UECEE. Without the above subsidy scheme under decarbonization activities of the European Commission, the Slovak industry UECEE level would be 51.6 % higher than that of the EU27 (UECEE 0.047 vs. 0.031). However, when this support is financed through electricity prices borne by industrial consumers, the level of UECEE of the Slovak Republic compared to the EU27 is higher by up to 103 % (at the level of total industrial production). Therefore, it can be concluded that the active decarbonization policy of the EU in the form of support for RES/CHP in the Slovak Republic has caused a decline in energy intensity, especially since 2010, when the spot prices of energy carriers started to rise again.

Specifically, the unit energy cost parameters for electricity in the automotive sector reached 0.038 at EU level for the last known period before the energy crisis in 2017, i.e. the share of electricity costs in total costs was 3.8 % of the value added generated at industry level. Within the EU, the value of these UECs for the automotive industry was only 0.017, i.e. 1.7 % of the value added generated in the automotive industry. It should be stressed that these figures, according to the latest known data on Eurostat [30], were recorded even without the more intensive trend towards the advent of e-mobility and more energy-intensive battery production for BEVs and PHEVs. Taking this new trend into account, the parameters can be expected to be at an even slightly higher level.

However, the most important finding of the UEC analysis remains the fact that UEC values in the electricity sector are for industrial production (value added) of the Slovak Republic at a level of up to 0.063, i.e. 6.3 % share of electricity costs in the total value added of Slovak industrial producers [31]. Due to new technological equipment and modern production processes of mainly foreign shareholders, the UEC in electricity for the Manufacture of motor vehicles, trailers and semi-trailers sector was at 0.029, i.e. 2.9 % share of the cost of electricity bills in the total value added of these manufacturers. This share is at a surprisingly high level compared to the European average (1.7 %) which may negatively affect the cost competitiveness of established automotive producers (domestic or foreign) in the Slovak Republic, or the investment attractiveness of the sector. On the other hand, it should be noted that these differences are not as pronounced and do not have such a negative dynamic in the case of the Slovak Republic as is the case, for example, in the area of ULC or labor productivity as pointed out by some authors [32] and [33].

The above analysis leads to the conclusion that the automotive industry in the Slovak Republic is either highly energy intensive (which, given the period of the inflow of foreign producers cannot be assumed), or Slovak car producers have relatively high prices for the electricity they purchase for their production process. An undeniable influence on these prices is the "green tariff", which is a tariff for operating the system, the value of which and its share in electricity prices has been steadily increasing up to 2020.

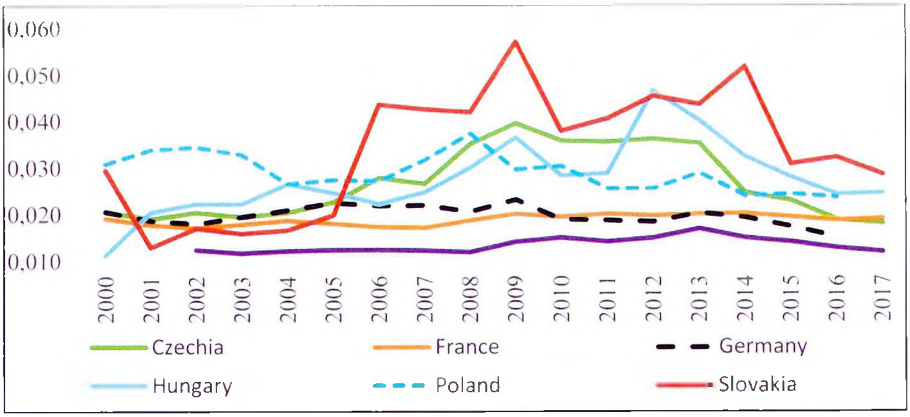

Fig. 1.9 UEC (unit energy cost in electricity) values at automotive industry level, source: own elaboration based on Eurostat data

Increase in electricity demand driven by the rise of BEV and PHEV

Based on the methodology of [29], two additional scenarios for the development of the number of ECVs (for this purpose only BEVs and PHEVs) and their numbers up to 2030 have been estimated. It should be stressed that a critical factor in the development of e-mobility is the level of regulation and legislative measures at the Member State level (individual incentives), which are likely to have a decisive impact on the pace of progress of BEVs and PHEVs. The above scenarios produce concrete results: the reference scenario, reflecting the current ambitious decarbonization plans of the European Commission, foresees a share of approximately 41.7 % of green cars (BEVs and PHEVs) in total fleet sales in 2030. A more optimistic scenario, the environmental one, assumes that in 2030 up to 74.3 % of cars in Slovakia will be sold with a fully electric or hybrid drive. This assumption would mean that more than 58,000 BEVs will be sold in 2030, and this share will increase thereafter. In the event of a further escalation of European emission standards and pressure on European car makers, the issue regarding the questionable impact on the competitiveness of European car makers arises. In terms of innovation capacity, they are already lagging behind the Chinese manufacturers in the lower-end affordable car segment.

Table 1.6.

Additional electricity consumption induced by the growth in the number of electric vehicles, source: own elaboration based on Eurostat data

Reference scenario	2022 (real)	2023	2025	2027	2029	2030	2032	2034	2035	AC
Electricity consumption (BEV)	21,789	5,251	13,977	18,659	26,027	60,508	88,229	124,987	145,906	727,796
Electricity consumption (PHEV)	10,885	3,722	6,316	11,990	23.585	29,845	35,503	45,339	46,979	345.764
Ecological scenario	**2022 (real)**	**2023**	**2025**	**2027**	**2029**	**2030**	**2032**	**2034**	**2035**	
Electricity consumption (BEV)	21,789	7,340	18,041	42.490	95.500	145.162	160.321	173,997	180,460	1,273,331
Electricity consumption (PHEV)	10,885	5.150	6,667	10.507	22,376	35,228	38,157	46,577	47,503	328.105

AC – Annual Consumption

The above UEC analyses show another crucial factor for the Slovak economy – the high sensitivity of the Slovak Republic to price shocks of energy raw materials. This conclusion results primarily from the fact that few EU countries have such a significant energy dependence on imports of energy carriers from third countries. This problem naturally gained momentum after Russia's invasion of Ukraine and the subsequent energy crisis, which fundamentally affected Slovak industry, including the automotive industry.

One explanation for the unproven statistically significant effect of electricity prices or UECEE on the export performance of Slovak car manufacturers is the fact that the vast majority of the triggers of the Porter effect, are innovations by large companies. The innovation potential (technologies, processes, but also energy equipment) of the Slovak economy and within it especially of small and medium-sized enterprises (SMEs), is considerably limited [34], [35], which is also shown by Eurostat statistics according to the size of enterprises in individual industrial sectors. This makes it more difficult for small and medium-sized companies, especially those with a high share of energy-intensive production, to absorb high electricity costs.

A very specific problem of Slovak exporters (especially in the automotive industry) is the huge dependence on FDI inflows and the high concentration of exports in the hands of the largest exporters. More than 50 % of Slovak exports are made by only 60 companies, 97 % of which are owned by foreign shareholders [36]. The study [37] even comes to the same conclusion in the case of French companies. A significant problem until 2019 was the limited targeting of green electricity tariff relief exclusively to large industrial producers (legal conditions). On the other hand, pro-export support for Slovak SMEs has the potential to partially address high electricity prices. This stems primarily from the higher productivity of exporting firms [37]. In the case of Slovak firms, the pro-export orientation of SMEs is also essential because they also import to a greater extent, which allows them to achieve the Porter effect by importing goods of an investment nature. The final argument is the conclusion of [37] pointing to the higher rate of product, process and R&D innovation of exporting companies.

A separate topic of cost competitiveness of companies from the automotive industry in the Slovak Republic is the issue of electricity and its availability. According to the available Eurostat data, in the first half of 2023, electricity prices for a major passenger car manufacturer (Kia or Stellantis type in Slovakia) with an annual consumption of around 250 GWh were at the seventh highest level in the EEA. The price was 268.7 €/MWh. Higher electricity prices for car producers were only in island European countries or some Eastern European countries with lower industrial or car production (Romania 328.9 €/MWh, Liechtenstein 325.5 €/MWh, Hungary 303.0 €/MWh, Croatia 292.5 €/MWh, Ireland 282.9 €/MWh, Cyprus 276.2 €/MWh). On the other hand, the main automotive competitors from Europe had electricity costs at a significantly lower level (e.g. Germany 219.2 €/MWh, Czech Republic 197.4 €/MWh, Serbia 138.4 €/MWh) (Eurostat, 2022). The way to higher cost competitiveness of Slovak producers is to reduce electricity prices in the B2B segment through a targeted energy policy and a regulatory policy that minimizes transmission and distribution costs and environmental charges paid by industrial producers.

The second important consequence of high UECs in the electricity sector is the investment attractiveness for energy-intensive investors in the Slovak Republic.

Conclusions can be drawn from specific cases of SARIO investment projects that the potential arrival of new industrial investors to the Slovak Republic in the automotive industry (VW, CATL and others) is very problematic, if not unlikely, in the field of energy-intensive battery production. Compared to other countries in the region (especially the Czech Republic), the foreign investor is responding to both the innovation potential and significantly lower electricity prices in neighboring countries. This factor either demotivates a potential foreign investor to establish themselves in the Slovak industry or requires investment incentives as a condition of entry, usually compensating for high electricity prices (this was the reason for VW's unrealized investment in Slovakia). The Porter effect is not possible in such a case, and when assessing the investment environment in energy-intensive automotive manufacturing, positive dynamics cannot be expected without a systematically more intensive waiver of TPS payments. The second issue, also very important for potential foreign investors in the field of e-mobility, is the "cleanness" of electricity contracted in Slovakia. In this case, this factor can be assessed as a significant positive, since a large part of electricity in the Slovak Republic is generated from nuclear sources (power plants) with a very low level of CO_2 emissions or is generated from renewable sources (currently around 20 %). This factor has a positive impact on the CSR and ESG policies of multinational producers in the field of e-mobility. It is clear from the above decomposition chart of UEC EE dynamics in the Slovak Republic that the system operation tariff (TPS) represents the dominant element in the dynamics of these energy costs in the Slovak Republic. On a positive note, despite record inflation in the Slovak Republic, the TPS parameter has been on a downward trend for the last two years (2022 and 2023), but this has only been partially offset by sharply rising energy prices and their unit costs.

Assuming that energy costs are of some importance to automobile producers (lower than, for example, ULC or the cost of intermediate goods), it is a legitimate question how European energy policy and Slovak energy policy can eliminate environmental components in electricity prices for industrial producers. In addition to the above-mentioned recommendations for general reductions in industrial electricity prices (lower rates for distribution, transmission, and costs for auxiliary services), a possible solution is the financing of decarbonization and more extensive use of renewables from the state budget, or a larger part of the financing is transferred to the household segment. Otherwise, there is a risk not only for the lower cost competitiveness of car manufacturers within Europe, but also vis-à-vis US and especially Asian competitors. It should be pointed out that Asian competitors, in particular, are flooding the European market with electric vehicles that use lower-priced electricity.

The results of the electricity consumption research show a significant increase in electricity consumption from 2030 onwards. Earlier work has already indicated that e-mobility is a pathway to reduce the dependence of Eastern European countries on Russian fossil energy imports, but at a relatively low intensity by 2030. The gradual replacement of the vehicle fleet in the Slovak Republic will cause a continuously faster transformation of fuel consumption in transport, to the detriment of fossil fuels (mainly petroleum products) and to the benefit of electricity consumption. For this reason, the above arguments for changes in its pricing also have a large potential impact on inflation, not only at the level of industrial prices but also at the level of the consumer basket of Slovak households.

Under the reference scenario (current parameters in EV mobility) and the gradual evolutionary transition of passenger cars to BEVs and PHEVs, the authors predict the annual electricity consumption of the Slovak Republic in 2035 at the level of approximately 192 GWh of additional electricity consumption, with the total annual consumption by BEVs and PHEVs to reach the level of 1.073 TWh in 2035. This means that either there must be a massive increase in energy efficiency in the Slovak Republic or additional sources of electricity generation will have to be implemented to meet the demand from the transport sector. Similar conclusions are also reached by [38], when analyzing the energy balance of the Slovak Republic and its prospective development with regard to decarbonization activities in the Slovak Republic and activities to reduce carbon emissions.

The ecological scenario, based on the assumption of an even faster transformation towards BEVs and PHEVs, foresees an annual growth in electricity consumption in the passenger car fleet of even 227 GWh of electricity in 2035. The total consumption of BEVs and PHEVs would thus be as high as 1.601 TWh in 2035, which implies the use of a natural gas-fired source (e.g. most of the annual production capacity of the Malženice power plant) or part of a new nuclear source in the Slovak Republic (Mochovce IV). The challenge for Slovak energy policy is the method of charging this fleet in 2035. Massive charging of BEVs and PHEVs in the afternoon/evening hours can place high demands on grid stability and thus on auxiliary services and an increasing integrated electricity price, which could again have a negative impact on the level of energy costs of automotive and industrial producers. A very important argument for supporting e-mobility in Slovakia is the low-emission nature of electricity production, which makes the Slovak vehicle fleet an ideal European candidate for a more revolutionary transition and transformation to BEVs.

In connection with the increase in e-mobility – whether at the level of the number of BEV/PHEVs in the Slovak Republic, but especially the production of batteries and the completion of BEV/PHEVs – a significant increase in electricity consumption in the Slovak Republic can be expected. In particular, new investors in battery production and electric vehicle assembly are likely to significantly increase electricity consumption in the Slovak Republic due to the circumvention of tariffs on imports to the EU. In connection with the growth of electricity consumption caused by e-mobility, the current topic at the level of the Government of the Slovak Republic for securing additional production capacity and stable electricity production itself is also gaining ground. A possible solution could be modular nuclear power plants (Westinghouse), but also an increase in the capacity of the Jaslovské Bohunice NPP, as they represent a stable and low-emission source of additional electricity. We note that the desired solution for additional power generation capacity is one that is close to existing or newly constructed power plants in order to minimize losses and minimize costs for the construction of new power facilities and the necessary infrastructure.

1.4 Modelling of changes in the technological mix in the automotive industry of the Slovak Republic on selected socio-economic and ecological indicators

The aim of the research and this part of the report is to outline the possibilities of modelling changes in the technological mix of the automotive industry in Slovakia as a result of the penetration of e-mobility on selected socio-economic and environmental indicators, using the IMPACTECH approach/model. The IMPACTECH_CZ model [39][2], was developed as a tool to assess the socio-economic and GHG emissions impacts of changes in the energy mix of the Czech Republic. It supplements this data with detailed information on employment and greenhouse gas emissions by branch in the electricity sector. It also adds detailed information on the impacts of capital investment, which will play a significant role in the event of a major energy transition given the expected need to adapt the energy infrastructure. The model allows to integrate forecasts of future developments of selected technologies. This tool is suitable for short to medium term analyses (5-to-10-year horizon), taking into account the ability of the model to integrate selected long term trends (technology development), but also the limitations of the model due to the methodology used in [40].

Methodology

When modelling changes in the automotive technology mix, we will rely on a combination of expert estimates of expected changes and their transfer into an input-output model to estimate the direct and indirect effects of these changes on selected socio-economic and environmental indicators. This process is outlined in the diagram below. Experts are expected to identify key changes in the automotive industry, future developments in the energy mix, as well as identifying scenarios for the introduction of new technologies in the automotive industry and other key sectors. These inputs will be used to model direct and indirect effects at the national economic and sectoral level through an input-output model.

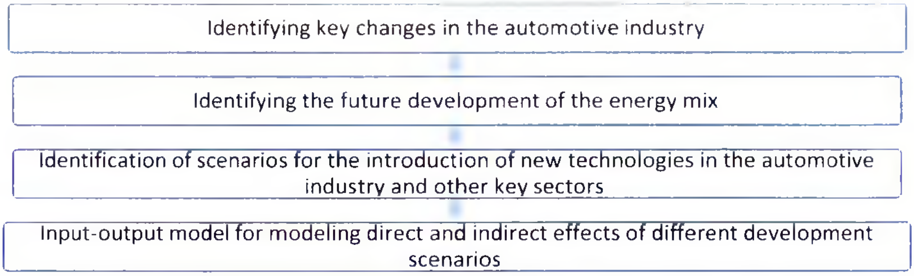
Identifying key changes in the automotive industry
Identifying the future development of the energy mix
Identification of scenarios for the introduction of new technologies in the automotive industry and other key sectors
Input-output model for modeling direct and indirect effects of different development scenarios

Fig. 1.10 Schematic of expert inputs to the input-output model, source: own elaboration

As an example of the change in the cost structure of car production, we present a comparison of the input structure of the most important components in the production of internal combustion engine vehicles compared to electric and hybrid vehicles. While in the production of cars with an internal combustion engine, the production of the engine and battery represents 13.5 %, so for electric motors and cars with a hybrid drive it is almost 25%. In addition, the e-drive system is included in the cost (6.2 % of the cost), which together represents approximately 31 % of the total cost.

---

[2] The software works with data from the input-output database EXIOBASE v3.6, which is available at https://zenodo.org/record/4588235#.YTYWvI4zaUk.

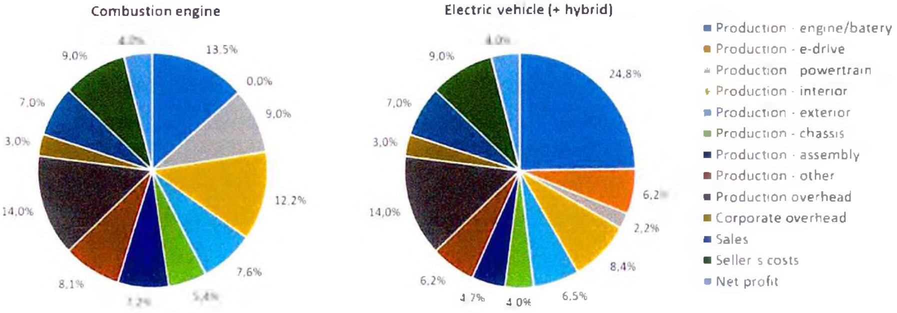

Fig. 1.11 Cost structure of car production by technology – what changes can be expected [40].

In modelling the scenarios, we can take inspiration from the four scenarios of decarbonization in the Czech Republic [40], which were as follows:

- Electrification/hydrogenation of production: preference for electrification of production processes and use of hydrogen-based technologies,
- Circular scenario: preference for recycling, secondary production and/or renewable materials (biomass, etc.),
- CCS (Carbon Capture and Storage) scenario: preference for technologies based on carbon capture, storage and utilization,
- BAU (Business as Usual) scenario: preference for current production methods.

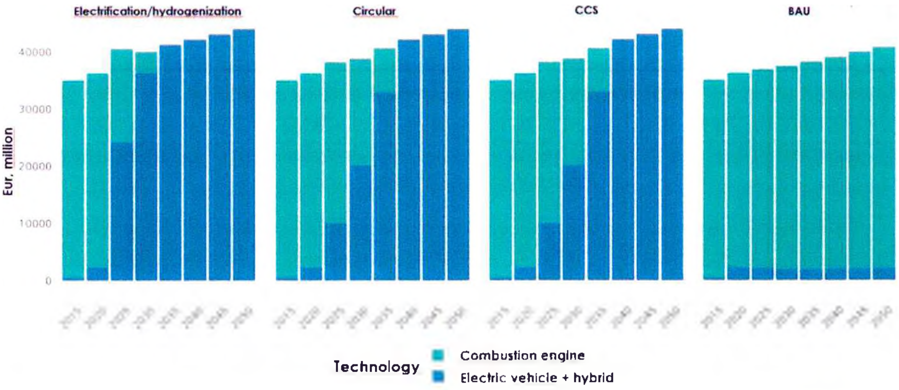

Fig. 1.12 Production scenarios by individual technologies in the Czech Republic – motor vehicle production [40].

In the case of modelling scenarios of motor vehicle production in the Czech Republic, the authors of the study [40] similarly based four scenarios, which differed in how fast the transformation of production towards electric and hybrid cars would take place. In the BAU (Business as Usual) scenario, the share of production of electric and hybrid cars remained fixed at the level from 2020. The fastest ramp-up of EV production is in the electrification and hydrogenation scenario, with more than 50 % of EV production in 2025 and 100 % of EV and hybrid production in 2035. The circular and CCS scenarios assumed a 100 % share only in 2040.

For modelling changes in the technology mix, we identified a combination of input-output analysis based on the FIGARO database, with detailed information supplemented from the EXIOBASE 3 database as the most appropriate method. This approach has several advantages but also limitations. Among the strengths of the FIGARO 2023 edition database is a much newer input structure. The latest available harmonized tables cover the year 2021. These tables are compiled by Eurostat using a harmonized methodology across all countries, with a detailed focus on European Union countries. For the EU countries, including Slovakia, this database can be extended relatively easily to include employment data or other socio-economic and environmental indicators that are reported in the NACE Rev. 2 sectoral classification. The EXIOBASE 3 database does provide symmetric input-output tables up to 2020, but these are only extrapolations from 2015 data based on the current evolution of aggregate variables. The structure of economies is thus fixed in a much older period. The advantage of EXIOBASE 3 may appear to be a much more detailed structure of inter-sectoral relationships. On the other hand, with such a detailed cross-sectoral structure of inputs, these are only estimates from the models. EXIOBASE 3 is not based on the original detailed supply and use tables to the extent that it is in its balanced and calculated form. Its use is thus more suited to the examination of direct and indirect linkages at the level of large economic groupings. However, the detailed material flow information from the EXIOBASE 3 database can serve as a useful source of information for extending the input-output tables in the FIGARO 2023 database. After comparison with data on the Slovak economy from other sources, and after experts have assessed the structure of the inputs, these data can be used for detailed modelling of various development scenarios.

The FIGARO tables are based on the new NACE Rev. 2 industry classification, in which the manufacture of motor vehicles, trailers and semitrailers is recorded in the sector C29. EXIOBASE 2 is based on the older NACE Rev. 1 classification of industries, and the motor vehicle manufacturing sector is numbered 34. Neither database provides a more detailed breakdown of this sector.

The sector C29 includes the manufacture of motor vehicles for the transport of persons or goods. This includes the manufacture of various parts and accessories for motor vehicles. This sector is divided into three parts: 29.1 Manufacture of motor vehicles, 29.2 Manufacture of bodies, trailers and semi-trailers, and 29.3 Manufacture of motor vehicle parts and accessories. Motor vehicle production includes the manufacture of passenger cars, the manufacture of commercial vehicles (such as vans, trucks, road tractors), production of buses, trolleybuses, production of motor vehicle engines, production of chassis for motor vehicles, and manufacture of other motor vehicles (snowmobiles, golf carts, etc.). Below we provide detailed examples of specific components and their classification within the NACE Rev. 2 classification, which is important for the creation of scenarios and their subsequent linking to the input-output model.

The manufacture of motor vehicles (C29.1) does not include (only those items are included that we consider relevant for our analysis):

- manufacture of electric motors (except starter motors), categorized as 27.11,
- manufacture of lighting equipment for motor vehicles, categorized as 27.40,
- manufacture of pistons, piston rings and carburetors, categorized as 28.11,
- manufacture of motor vehicle bodies, categorized as 29.20,
- manufacture of electrical parts of motor vehicles, categorized as 29.31,
- manufacture of parts and accessories for motor vehicles, categorized as 29.32,
- maintenance and repair of motor vehicles, categorized as 45.20.

Manufacture of parts and accessories for motor vehicles (29.30) includes 29.31 Manufacture of electrical and electronic equipment for motor vehicles, and 29.32 Manufacture of other parts and accessories for motor vehicles. Electrical and electronic equipment includes, for example, generators, alternators, spark plugs, ignition harness, electrical window and door systems, installation of purchased gauges in instrument panels, and voltage regulators. Conversely, the 29.31 category does not include:

- manufacture of batteries for vehicles, categorized as 27.20
- manufacture of lighting equipment for motor vehicles, categorized as 27.40
- manufacture of pumps for motor vehicles and engines, categorized as 28.13.

Manufacture of other parts and accessories for motor vehicles (29.32) includes the manufacture of various parts and accessories for motor vehicles such as brakes, gearboxes, axles, wheels, shock absorbers, radiators, mufflers, exhausts, pipes, catalytic converters, clutches, steering wheels, seat belts, airbags, doors, bumpers, car seats.

This class (29.32) does not include:

- production of types, categorized as 22.11,
- manufacture of rubber hoses and belts and other rubber products, categorized as 22.19,
- manufacture of pistons, piston rings and carburetors, categorized as 28.11,
- maintenance, repair and modification of motor vehicles, categorized as 45.20.

Data in the FIGARO database is available at the NACE Rev. 2 two-digit level, i.e. division level as C29, for a total of 64 sectors of the national economy, including 19 manufacturing industries. The examples of motor vehicle manufacturing components show that some important components are not part of the main industry C29 but belong to other manufacturing industries. These industries are mainly C22 Manufacture of rubber and plastic products, C27 Manufacture of electrical equipment and C28 Manufacture of machinery and equipment not elsewhere classified (n.e.c.). From the FIGARO tables, it is possible to identify the structure of motor vehicle manufacturing inputs (C29) at the NACE Rev. 2 2-digit level, broken down into domestic and imported inputs. Imported inputs are further disaggregated by country of origin for all EU countries and other major economies outside the European Union. For scenario building, one of the most important steps will be to differentiate the structure of inputs in the production of different types of vehicles, in particular between combustion engine vehicles and electric or hybrid vehicles. As Figure 2 shows, the biggest differences can be expected in electrical components, battery and other related accessories. In addition to the shift in the structure of inputs towards the sector C27, it will be necessary to examine changes in the structure of inputs in terms of import partners, but also in terms of the share of domestically produced inputs in Slovakia. A flowchart for the expert estimates is provided below.

Table 1.7

Expert estimate of the structure of inputs in the production of motor vehicles by engine type, source: own elaboration

NACE Rev.2 sector	Structure of motor vehicle production inputs from the FIGARO database	Expert estimation of the input structure in the production of internal combustion engine vehicles	Expert estimation of the input structure in the production of electric vehicles/hybrids
Sector C10 . Sector C33 . Other sectors			

For a detailed analysis of the environmental effects, it will be important to model changes in the technological mix of the energy industry and electricity generation in particular. The energy sector is captured in the input-output tables in section D, two-digit level, sector 35, and includes the supply of electricity, gas, steam and cold air. It is divided into three parts: 35.1 Electricity generation, transmission and distribution, 35.2 Gas generation, piped distribution of gaseous fuels, and 35.3 Steam supply and cold air distribution. The production of electricity itself is in sector 35.11. EXIOBASE 3 provides a detailed breakdown of electricity generation by source. Data from this database could be used to disaggregate the inputs in the FIGARO tables. Expert estimates of the future development of the energy mix could then be used to model impacts for selected socio-economic and environmental indicators. In Table 1.8, we provide an indicative template for inserting expert estimates.

Table 1.8

Template for inserting expert estimates of the future development of the energy mix, % representation of individual sources of electricity generation, source: own elaboration

Source of electricity	2020 – 2025	2030	2035	2040	2045	2050
Electricity generation from coal						
Generating electricity from gas						
Generating electricity from core						
Hydroelectric power generation						
Electricity generation from wind power plants						
Production of electricity from crude oil and other petroleum derivatives						
Electricity generation from biomass, biogas and waste						
Electricity generation from photovoltaic power plants						
Electricity generation from solar thermal power plants						
Electricity generation from tidal power plants						
Electricity generation from geothermal sources						
Electricity generation from other sources						

Source: Own elaboration.

Input-output analysis

Symmetric input-output tables broken down by industry x industry provide an overview of the economy in a given year, showing transactions between different industries and also within an industry. Input-output analysis allows modelling of different scenarios representing different energy transition options and the deployment of different technologies together with their environmental and socio-economic impacts, e.g. on employment. For a detailed explanation of the model and its variations, see [41]. If we use a multi-regional input-output model, we can track changes around the world through international trade linkages.

World input-output tables are based on national symmetric tables or, in other words, on their structure. They expand on their individual blocks to provide more detailed information on inter-sectoral relations. A simplified example of a multiregional table with two regions is shown in Fig.1.13

		Region A Branches 1 2 ……….n	Region B Branches 1 2 ……….n	Final demand	Total production
Region A	Branch 1 Branch 2 . . Branch n	Z		Y	X
Region B	Branch 1 Branch 2 . . Branch n				
Value added		E			
Extensions					

Fig. 1.13 Simplified example of a multiregional IO table with two regions, Source: own elaboration based on [40], [41].

In the multiregional model, the flow of intermediate inputs between countries (regions) and industries is captured in the intermediate consumption matrix **Z**. However, this matrix is composed of several sub-matrices that reflect either own intermediate consumption ($\boldsymbol{Z}^{11}$ and $\boldsymbol{Z}^{22}$on the main diagonal) or imported intermediate consumption (in the matrices $\boldsymbol{Z}^{21}$ and $\boldsymbol{Z}^{12}$off the main diagonal). The matrix can be displayed as follows:

$$\boldsymbol{Z} = \begin{vmatrix} \boldsymbol{Z}^{11} & \boldsymbol{Z}^{12} \\ \boldsymbol{Z}^{21} & \boldsymbol{Z}^{22} \end{vmatrix} \tag{3}$$

The z_{ij}^{11} element of the $\boldsymbol{Z}$ matrix represents intermediate consumption from the i sector from Region 1 (or Region A) in the j sector within the same Region 1 (A), thus representing domestic intermediate consumption. The matrices off the main diagonal ($\mathbf{Z}^{21}$ and $\mathbf{Z}^{12}$) reflect international trade in intermediate goods between regions. We can write the total production vector $\boldsymbol{x}$ as follows:

$$\boldsymbol{x} = \begin{bmatrix} x^1 \\ x^2 \end{bmatrix} \tag{4}$$

It captures output in Region 1 (x^1) and Region 2 (x^2) and we use it to calculate input coefficients within the matrix **A**, which represents the structure of inputs (both domestic and imported) per unit of output of the given sector. It can be expressed as:

$$\boldsymbol{A} = \boldsymbol{Z}\hat{\boldsymbol{x}}^{-1}$$

$$\mathbf{A} = \begin{vmatrix} \mathbf{A}^{11} & \mathbf{A}^{12} \\ \mathbf{A}^{21} & \mathbf{A}^{22} \end{vmatrix} \tag{5}$$

where $\hat{\boldsymbol{x}}^{-1}$ is the inverse diagonalised vector of total output. That is, it contains inverted values of the sectors' output on the diagonal and zeros everywhere else. The

a_{ij}^{12} element of the $\mathbf{A}^{12}$ matrix indicates the value of intermediate inputs from the i sector originating in Region 1 needed to produce one unit of total output in the j sector in Region 2.

$$\mathbf{y} = \begin{bmatrix} \mathrm{y}^1 \\ \mathrm{y}^2 \end{bmatrix} \tag{6}$$

The vector $\mathbf{y}$ of equation 4 contains the global final demand for goods originating in Region 1 (y^1) and Region 2 (y^2. For example, the vector y^1 contains the value of goods flows from Region 1 to domestic final demand y^{11} and final demand y^{12} in Region 2 (we formally write this as $\mathbf{y}^1 = \mathrm{y}^{11} + \mathrm{y}^{12}$). By definition, total commodity output in multiregional input-output tables is equal to the sum of intermediate consumption and global final demand:

$$\mathbf{x} = \mathbf{Ax} + \mathbf{y} \tag{7}$$

For an exogenously specified final demand y, the output can be rewritten in the form of a multiregional input-output model as follows:

$$\boldsymbol{x} = (\boldsymbol{I} - \boldsymbol{A})^{-1}\boldsymbol{y} = \boldsymbol{Ly} \tag{8}$$

where $(\boldsymbol{I} - \boldsymbol{A})^{-1}$ is the Leontief inverse matrix computed from the unit matrix $\boldsymbol{I}$ and the matrix of input coefficients $\boldsymbol{A}$. This is the key part of the model that captures the direct and indirect production of the commodity i in Region 1 or Region 2 (in rows) to satisfy the final demand for one unit of the commodity j coming from Region 1 or Region 2 (in rows). The model can be extended to more regions, but the basic principle explained simplistically for two regions still holds.

In line with [40], we also define the so-called employment intensity matrix $\boldsymbol{M}$ with elements m_{dj}, where the lower index d represents the 6 categories obtained by combining different levels of education (3 categories) and gender (2 categories).

$$\boldsymbol{M} = \boldsymbol{E}(\hat{\boldsymbol{x}})^{-1} \tag{9}$$

We can then model the effects of changes in the structure of inputs according to the selected scenarios. For example, the energy mix as well as the overall level of electricity generation depends on the projections for each country in the different scenarios. To ensure that the model correctly accounts for electricity generation, even if the base year electricity mix did not include a particular country's electricity source, we use the relevant columns of technical coefficients as well as employment intensities from another country. Substitutions are based on criteria of geographical proximity or similarity of economic structure. Using the example of the electricity generation sector(l), we can write the model according to [40] as follows.

We calculate the total output x_l^t of the electricity sector l in monetary units for each year t, assuming that it varies with proportionally with electricity production g_l in GWh between the modelled year t and the previous year considered in the analysis $(t-1)$ given the scenarios:

$$x_l^t = \left(\frac{g_l^t}{g_l^t}\right) * x_l^{t-1} \tag{10}$$

Since in the following steps we only need the output of the electricity sector l, we create a vector x^t, which will contain zeros and values from the vector x_l^t at the appropriate positions for the electricity sectors.

In the case of calculating the employment impacts of electricity generation, we will use data on total electricity production. To avoid double counting, we replace the rows of the electricity sectors in the A matrix with zero (for the modelled countries). The modified matrix (hereafter denoted as A') is used to derive the modified Leontief inverse matrix L', which is used in the calculations. The matrix A containing the coefficients of the intermediate inputs remains unchanged over time (and so does A'), assuming that the production technology does not change over time in the model, and hence the Leontief inverse matrix also remains unchanged. In this case, we only see the effects of the modelled changes within the electricity sector.

Finally, we calculate the employment impact for each year t, separately for each of the interacting effects (i.e. the impact of capital investment $Rk^{\,t}$ and the total change in electricity generation from each source $Rx^{\,t}$). We calculate the employment effects of electricity generation under each scenario for each year t:

$$Rx_d^t = \widehat{m'_d} L' x^t \tag{11}$$

To obtain the additional employment effects of capital investment (denoted as $Rk^{\,t}$), we need to proceed with a detailed fixed capital formation (GFCF) matrix with columns for each source of electricity K^t (specific to each model year t):

$$Rk_d^t = \widehat{m'_d} L' K^t \tag{12}$$

We can also extend the model to include ecological impacts, e.g. CO_2 pollution. The main advantage of input-output analysis is that it allows the effects to be taken into account when modelling changes in the technology mix of a selected industry through complex inter-industry linkages.

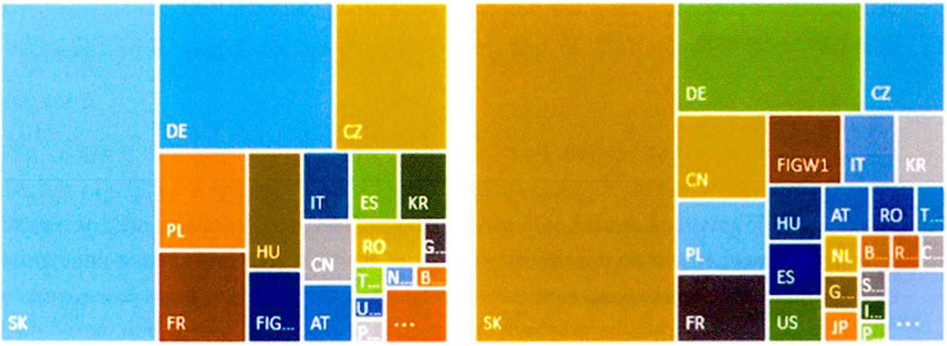

Fig. 1.14 Direct (left) vs. direct and indirect (right) structure of inputs of the Slovak automotive industry (C29) in 2020, source: own elaboration according to FIGARO (2022).

In Fig. 1.14, we illustrate the different structure of automotive inputs by country according to direct inputs and complex linkages. Directly, the automotive industry is among the industries with an above-average share of imported components, but indirectly, a number of firms operating in Slovakia are involved in the production chain of the automotive industry, and therefore the share of imported inputs in the complex chain is smaller than the share of direct imports. The main direct import partners include Germany, the Czech Republic, Poland, France and Hungary. China, for example, follows close behind. Taking into account the complex linkages in global value chains, China is the third most important supplier of components for the automotive industry after Germany and the Czech Republic. And that includes electronic components and chips, for example. We will be able to take this context into account and explore it when modelling different scenarios for the development of the technology mix.

Annex

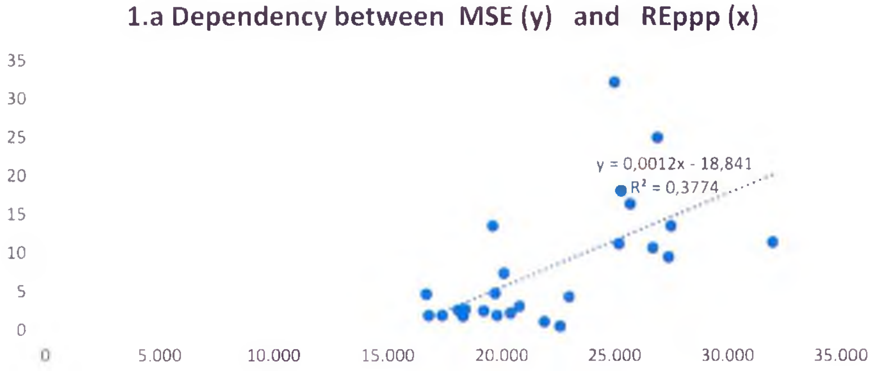
1.a Dependency between MSE (y) and REppp (x)

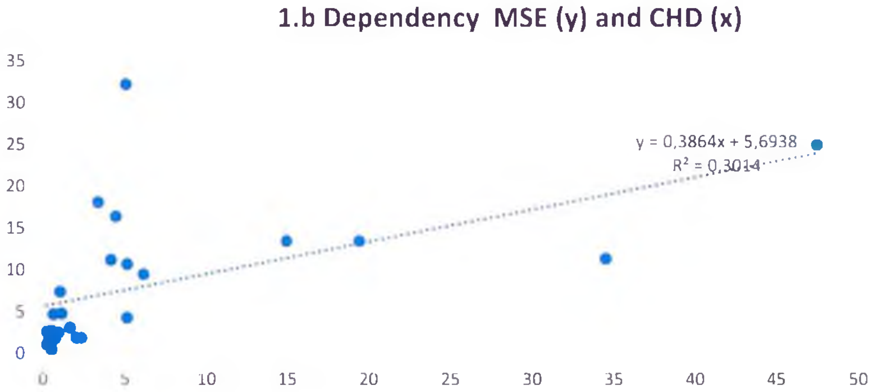

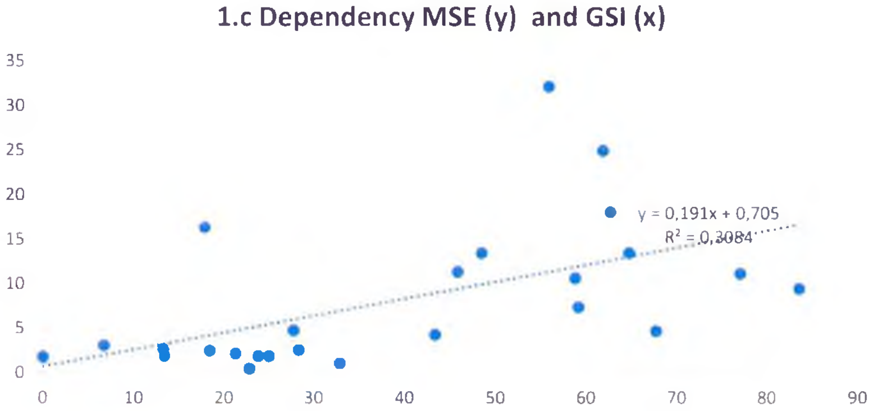

Source: own elaboration.

References

[1] European strategy for low-emission mobility (in Slovak), [11/11/2024], available on: https://ec.europa.eu/commission/presscorner/detail/nl/MEMO_16_2497

[2] Air Quality in Europe Report, EEA 2018. [11/11/2024], available on: http://www.eea.europa.eu/highliights/air-polution-still-too-high

[3] Annual Indicator Report Series (AIRS)—In Support to the Monitoring of the 7th Environment Action Programme 2017, [11/11/2024], available on: https://www.eea.europa.eu/airs/2017/environment-and-health/pdfStatic

[4] https://www.europarl.europa.eu/news/sk/headlines/society

[5] Rokicki, T, et al. 2021. Diversity and Changes in Energy Consumption by Transport in EU Countries. Energies, 14, 5414.

[6] IEA. *Key World Energy Statistics 2020*; OECD/IEA: Paris, France, 2020, [11/11/2024], available on: https://www.iea.org/reports/key-world-energy-statistics-2020/final-consumption#abstract

[7] 2. European Commission Climate Action. Road Transport.: Reducing CO2 Emissions from Vehicles, [11/11/2024], available on: https://ec.europa.eu/clima/policies/transport/vehicles_en

[8] Buekers, J., et al. 2014. Health and environmental benefits related to electric vehicle introduction in eu countries. Transp. Res. Part. D Transp. Environ. 2014, 33, 26–38.

[9] Messagie, M., et al. 2014. A Range-Based Vehicle Life Cycle Assessment Incorporating Variability in the Environmental Assessment of Different Vehicle Technologies and Fuels. Energies, 7, 1467–1482.

[10] Eltayeb, T.K. 2010. The examination on the drivers for green purchasing adoption among ems 14001 certified companies in malaysia. J. Manuf. Technol. Manag., 21, 206–225.

[11] Liao, F., Molin, E., van Wee, B. 2016. Consumer preferences for electric vehicles: A literature review. Transp. Rev., 37, 252–275.

[12] Ling, Z., Cherry, C.R., Wen, Y. 2021. Determining the Factors That Influence Electric Vehicle Adoption: A Stated Preference Survey Study in Beijing, China. Sustainability, 13, 11719.

[13] Rokicki, T., et. al. 2020. The Importance of Higher Education in the EU Countries in Achieving the Objectives of the Circular Economy in the Energy Sector. Energies 2020,

[14] Ochotnický, P., et al. 2023.Trends, main economic determinants of the e-mobility in the EU: Additional evidence and verification. Acta Montanistica Slovaca, 28, 4, DOI: 10.46544/AMS.v28i4.07.

[15] https://www.iea.org/commentaries/electric-cars-fend-off-supply-challenges-to-more-than-double-global-sales

[16] https://www.euractiv.com/section/electric-cars/news/electric-car-sales-gain-pace-despite-hurdles/

[17] Sriram, K.V., et. al. 2022. Factors influencing adoption of electric vehicles – A case in India. Cogent Engineering, 9, 1, 2085375, DOI: 10.1080/23311916.2022.2085375

[18] Rokicki, T., et al. 2022. Development of Electromobility in European Union Countries under COVID-19 Conditions. Energies 2022, 15, 9. DOI: 0.3390/en15010009.

[19] Javanmardi, E., et al. 2023. Evaluating the Factors Affecting Electric Vehicles Adoption Considering the Sustainable Development Level. World Electr. Veh. J., 14, 120. DOI: 10.3390/wevj14050120

[20] Noel, L., et a. 2020. Understanding the socio-technical nexus of Nordic electric vehicle (EV) barriers: A qualitative discussion of range, price, charging and knowledge. Energy Policy, 138, 111292. DOI: 10.1016/j. enpol.2020.111292.

[21] Coffman, M., Bernstein, P., Wee, S. 2017. Electric vehicles revisited: a review of factors that affect adoption, Transport Reviews, 37(1), 79-93.

[22] Kovárnik, R., Staňková, M. 2021. Determinants of Electric Car Sales in Europe. LOGI – Scientific Journal on Transport and Logistics, 12(1), DOI: 10.2478/logi-2021-0020

[23] https://top2023.elfa.sk/

[24] https://www.seva.sk/wp-content/uploads/2023/06/SEVS_VS_23.pdf

[25] Ferencikova, S., Krajcik, D., Zabojnik, S. 2023. The value of reverse knowledge transfer: Case of Austrian Bank subsidiary in Slovakia. Journal of Eastern European and Central Asian Research (JEECAR), 10(5), 764-772.

[26] Ochotnický, P., Hofreiter, M., Vojatasová, M. 2022. Basic macroeconomic frameworks for the development of the Slovak economy in 2022 and expectations of the business sector (in Slovak). [11/11/2024], available on: https://www.sopk.sk/tag/makroekonomika/

[27] Faiella, I., Mistretta, A. 2020. Energy costs and competitiveness in Europe. Bank of Italy Temi di Discussione (Working Paper) No. 1259.

[28] Faiella, I., Mistretta, A. 2022. The Net Zero Challenge for Firms' Competitiveness. Environmental and Resource Economics, 83(1), 85-113.

[29] Zábojník, S., Steinhauser, D., Král', P. 2022. E-mobility in Slovakia by 2030—End of oil dependency? IET Smart Cities, 4(2), 127-142.

[30] EUROSTAT. 2023. Database concering energies consumption and energy balace by industry. [11/11/2024], available on: https://ec.europa.eu/eurostat/databrowser/view/nrg_bal_c__custom_8637394/default/table?lang=en

[31] Morvay, K. 2022. Economic Development of Slovakia in 2021. Bratislava: Institute of Economic Research of Slovak Academy of Sciences.

[32] Ochotnický, P., Alexy, M., Kacer, M. 2020. Driving Forces of Total Factor Productivity in Europe I. Ekonomicky Casopis, 68(10), 1002-1020.

[33] Porter, M. The Competitive Advantage of Nations. New York: Harvard Business Review. [11/11/2024], available on: https://hbr.org/1990/03/the-competitive-advantage-of-nations

[34] Gonda, V. 2014. Strategy of competitiveness in the European Union (in Slovak). Determinanty formovania znalostnej ekonomiky v kontexte novej hospodárskej stratégie "Európa 2020", Bratislava: EKONÓM. 2014, 16-35.

[35] Lesáková, L., et al. 2017. Innovations in the activities of small and medium-sized enterprises in the Slovak Republic. Innovations in SME´s. Banská Bystrica: BELIANUM, 324 p.

[36] Baláž, P., Zábojník, S., Harvánek, L. 2019. China's Expansion in International Business: The Geopolitical Impact on the World Economy. London: Palgrave Macmillan, 335 p.

[37] Bureau, D., Fontagné, L., Martin, P. 2013. Energy and Competitiveness. Conseil d'analyse économique. 6, 1-12.

[38] Zabojnik, S., Hricovsky, M. 2021. Balancing the Slovak Energy Market After the Adoption of "Fit for 55 Package". In SHS Web of Conferences, 129, 05015. EDP Sciences.

[39] https://impactech.fss.muni.cz/

[40] Černý, M., et al. 2022. Employment effects of the renewable energy transition in the electricity sector: An input-output approach. ETUI Research Paper - Working Paper, 14.

[41] Miller, R. E., Blair, P. D. 2022. Input-Output Analysis: Foundations and Extensions. Cambridge University Press, 768 p.

2 Recycling of Laminated Glass – Research on Suitable Plate Material for the Line Scraper Module

2.1 Introduction

When separating the glass from the adhesive film, the biggest problem is separating the laminate film from the glass itself. These relevant facts led to the technological design of a processing line for bonded multilayer waste glass. The line itself consists of several separate modules; however, this chapter focuses on just one module, namely the scraper module. For the scraper module, the focus was specifically on the scraper module tools. The tool of the scraper module is a disc with attached plates made of hardox 500 steel. During the initial tests of the scraper module, we observed significant wear of the cutting interchangeable inserts, which was the main reason for the research on wear of the cutting plates. The research is built for a clear purpose, namely, to find out the most suitable surface treatment of the cutting plates, with the parameters of the cutting-edge roundness and the weight loss of the cutting plate as the wear criterion. Measurements of the main parameters were carried out on four different surface treatments, or on three surface treatments, and one cutting plate was uncoated. Wear measurements were carried out in time intervals in order to create a wear curve for the individual surface treatments of the cutting plates. The aim of the paper is essentially to compare the wear curves for the selected surface treatments with the clear objective of scientifically and experimentally determining which surface treatment is the most suitable for the particular application of the plates in the scraper module of a multilayer laminated glass separation line.

2.2 Design of the scraper module of the laminated glass processing line

The main, and therefore the working part of the scraper module of the multilayer laminated glass processing line, consists of working rollers. The working rollers are basically two shafts on which the working tools are mounted by means of a tongue. The working tools are mounted in bearing houses on the frame, which enables their rotary movement. The rotary movement is provided by two drives in the form of electric motors. The entire structure is interlocked by a frame with U-profiles. The distance between the working discs is ensured by a manual lever mechanism.

The main parts of the scraper module design are (Fig. 2.1):

- Frame – position 1
- Drive, electric motor – position 2
- Scraper rollers – position 3
- Working gap adjustment mechanism – position 4 [1].

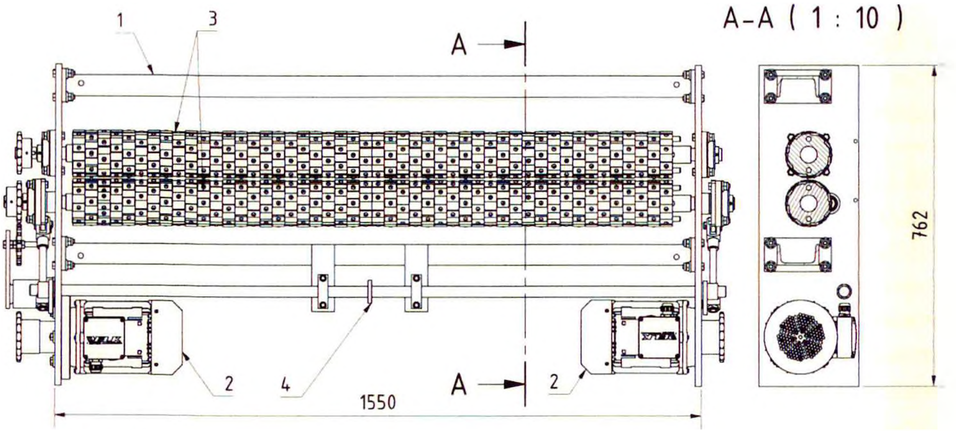

Fig. 2.1 Assembly drawing of the scraper module

There is a working gap between the scraper rollers, which is adjustable according to the thickness of the processed glass. This setting allows to ensure effective cleaning of the centre film of the multi-layer laminated glass. Since each of the working rollers has its own movement, it is possible to change the direction of rotation of the rollers and thus increase the efficiency of scraping the glass from the film if necessary [1].

The dimension and principle of the working gap and rotation principle is shown in the assembly section in Fig. 2.2

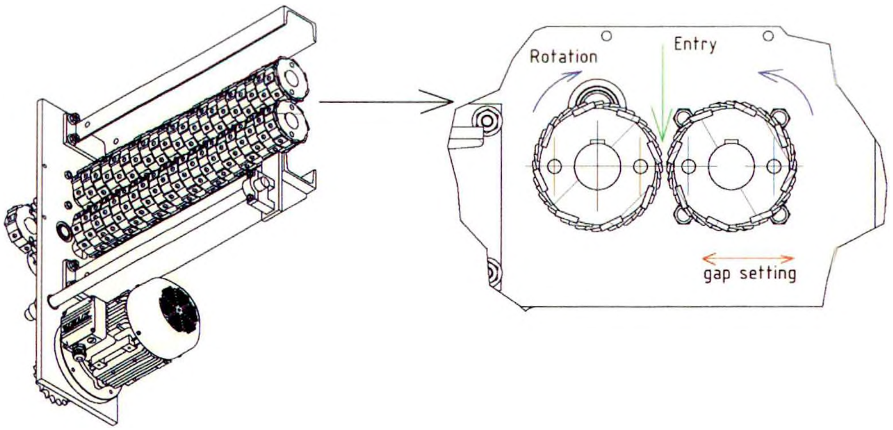

Fig. 2.2 Representation of the working gap in the assembly section

The scraper rollers are made up of scraper tools, specifically 96 pieces of discs mounted on a shaft. The scraper discs are made so that when they are mounted on the shaft, the cutting plates form a spiral (Fig. 2.3). The spiral shape ensures better separation of the glass from the foil.

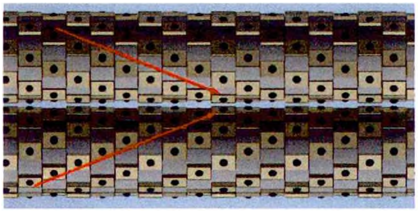

Fig. 2.3 Spiral placement of scraper discs

In order to provide or create a spiral effect from the scraper discs, it was necessary to produce 3 types of scraper discs. The difference is in the angle between the centre of the disc and the cutting plate seating area. The 10°, 25° and 40° discs are shown graphically in Fig. 2.4 [2].

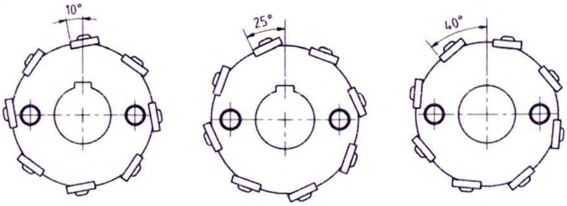

Fig. 2.4 Scraper disc design

The scraper disc assembly (Fig. 2.5), which is the working tool of the scraper module, consists of a disc body, a replaceable cutting plate, and an M5 metric screw.

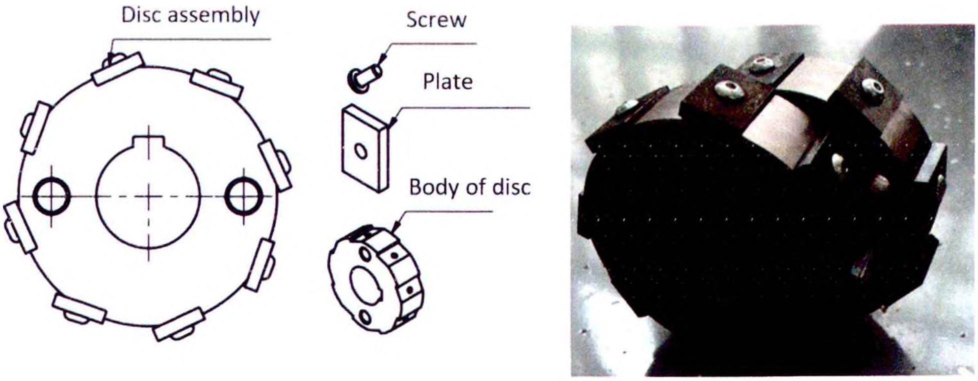

Fig. 2.5 Scraper disc assembly drawing and fabricated prototype

The replaceable plate is made of HADROX 500 material with a thickness of 5 mm. This type of material was chosen for better wear resistance, as the scraper plates are subject to considerable wear during the processing of waste glass. The location of the scraper discs in the assembly of the entire module is shown in Fig. 2.6 [2].

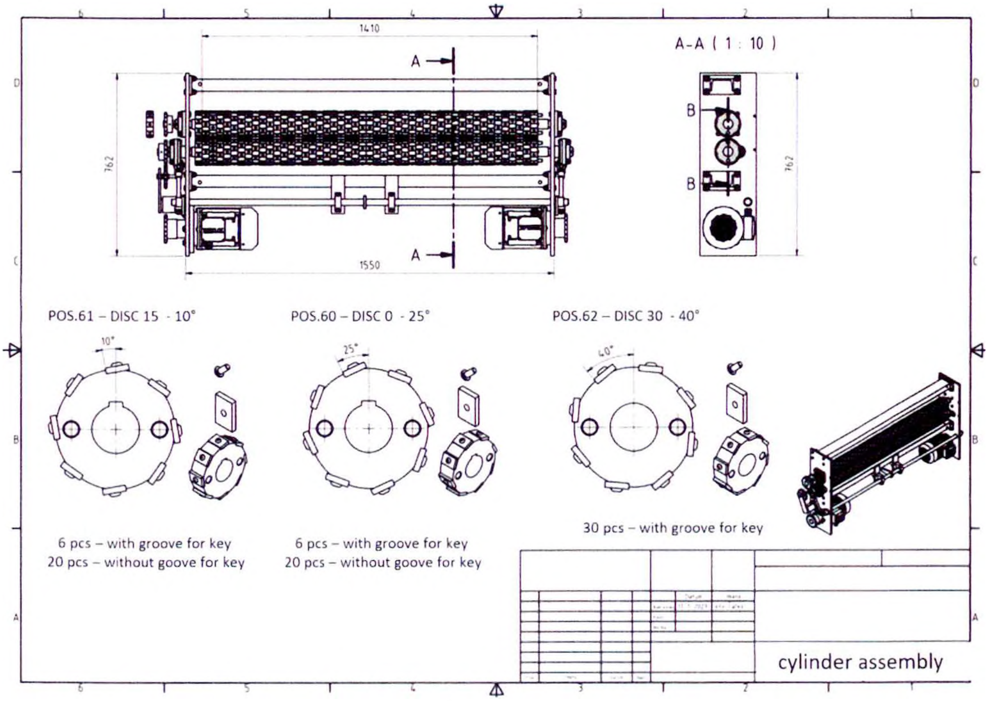
1410
A
A-A (1 : 10)
B
B
762
762
1550
A
POS.61 – DISC 15 - 10°
POS.60 – DISC 0 - 25°
POS.62 – DISC 30 - 40°
10°
25°
40°
6 pcs – with groove for key
20 pcs – without goove for key
6 pcs – with groove for key
20 pcs – without goove for key
30 pcs – with groove for key
cylinder assembly

Fig. 2.6 Assembly drawing of the scraper module

2.2.1 Plate design for the scraper module

As a tool for the scraper module, the plate was designed as a simple fired component. The tool, and therefore the plate for the scraper module, was also designed to fit into the overall context of the waste glass processing line. When designing the scraper tool, it was necessary to take into account aspects such as:

- manufacturability,
- economy,
- easy maintenance/replacement when worn,
- sufficient scraping of the glass from the foil [3].

Material design of the plate

When designing the material of the plate (HARDOX 500), the author also based his research on articles comparing the abrasive properties of selected steels. Analysis of the study Abrasion Resistance of S235, S355, C45, AISI 304 and Hardox 500 Steels Using Garnet, Corundum and Carborundum Abrasives, Fig. 2.8. [4].

In a published study titled Abrasion Resistance of S235, S355, C45, AISI 304 and Hardox 500 Steels Using Garnet, Corundum and Carborundum Abrasives [5], a comparison of the abrasive properties of selected steels is well performed.

The published study deals with the comparison of abrasion resistance for different steel types. The steel materials compared are listed in Tab.2.1.

Table 2.1
Vickers hardness for samples [4]

Material	Hardness HV
S235JR	128 ± 2
S355J2	155±5
AISI 304	211±7
C45	229±3
Hardox 500	521±15

The results of the analysed study can be factually interpreted in the graph shown in Fig. 2.9, where the effect of different abrasives on the wear of the investigated steel is shown. The above graph shows the weight loss of the material under the study while using different abrasives, such as garnet, corundum and carborundum. When analysing the results, the author concentrated on the abrasion resistance of the individual steels, as this parameter has a significant influence on the selection of a suitable material for the scraper plate. Another significant result of the analysed study is the dependence of the weight loss of steel on the hardness of the abrasive, due to the fact that the garnet material has a similar hardness to the glass that will enter the scraping process in his application. Examples of wear marks for different materials are shown in Fig. 2.7.

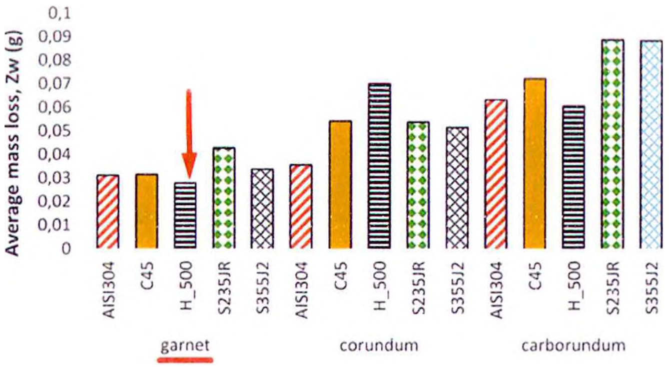

Fig. 2.7 Effect of different abrasives on the wear of steels (garnet, corundum and carborundum) [4]

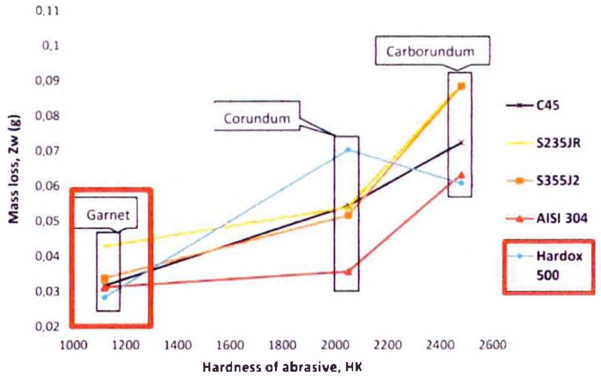

Fig. 2.8 Effect of abrasive hardness on the wear result [4]

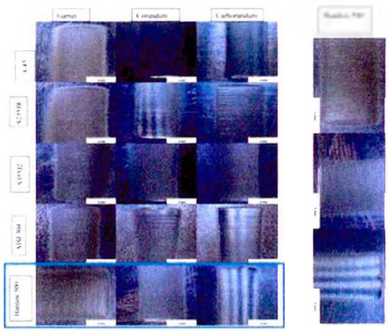

Fig. 2.9 Example of wear marks [4]

Design of the plate shape

Due to the large number of scraper plates, all of the above aspects had to be taken into account in the design of the plate. Basically, the chosen form of production by firing on the laser cutting machine ensured the aspects of manufacturability and also economy, since it is a simple technological production operation. Easy maintenance or replacement in case of wear and tear is ensured by a simple screw connection, and thus replacement is very simple and practical. The sharp edges created after the plate has been fired also ensure sufficient scraping of the glass from the middle film of the multilayer glass. The entire technological design of the production was also subjected to a simple analysis of the distribution of the plates on the sheet during the actual production. The distribution was analyzed in two versions, i.e.:

- distribution of plates on the sheet with gaps between the plates,
- distribution of plates on the sheet without gaps between the plates, common cut.

When comparing these two ways of plate distribution on the sheet, it was clearly shown that the common-section layout was definitely the preferable option. In addition to the plate distribution graphic itself, the above-mentioned non-stationary plans of the two variants also show two important economic factors - namely the production time and also the cutting length. When the plate is laid out on the sheet metal using common cuts, both parameters are clearly in better values.

It follows logically that with less production time as well as with a smaller cut length, the costs for the production of the plates are reduced. In the production of plates using the layout of manufactured parts by the method of common cuts, in addition to lower economic costs (production time and cutting length), the fact that the use of the common cut method almost completely minimizes the waste from the cut sheet metal is also important. The aspect of maximum elimination of waste from the used sheet metal is very important in the overall context of the proposed technology for the processing of bonded waste glass. Basically, the author wanted to avoid as much as possible the paradox that the design of the recycling technology would generate additional waste, which would also contradict the very principle of recycling. After considering all the aspects described above, the production documentation was elaborated, including cutting plans for the replaceable plate as a scraper tool for the scraper module of the waste laminated glass processing line.

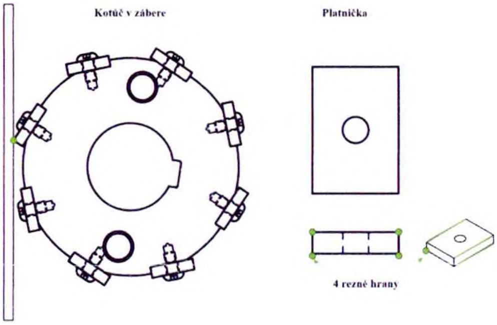

Fig. 2.10 Graphical representation of the plate cutting edges

A very important aspect in choosing the right shape was the possibility to achieve the maximum utilization of one plate. In the context of the nature of the plate engagement shown in Fig. 2.10, the plate so designed can be rotated sequentially after certain cycles. It is obvious that the plate designed in this way has up to 4 cutting edges.

2.3 Objectives and assumptions of the experimental research

After the initial tests on the scraper module were carried out, considerable wear was found on the scraper plates, despite the fact that the plates were made of Hardox 500 abrasion resistant material. The material selection and geometry of the plate is described in detail in the previous chapter. After the initial tests, the first measurements of the plate under the microscope were carried out. Measurements confirmed the wear of the cutting edge of the plate. The wear output in the form of measured edge curvature is shown in Fig. 2.11.

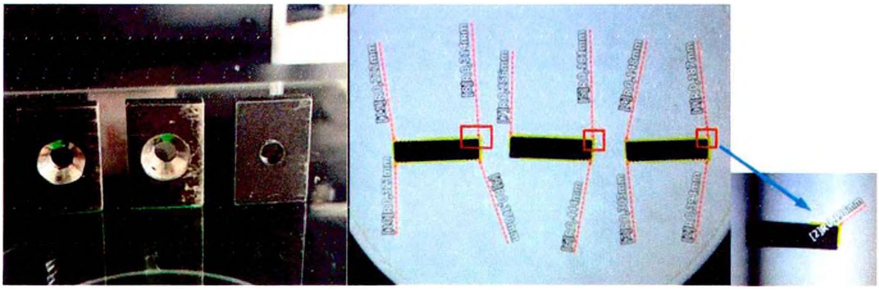

Fig. 2.11 Initial measurements of the cutting-edge curvature

After comprehensive analyses of the initial tests as well as after taking initial measurements, we came to a clear conclusion. The results of the analyses clearly showed the need to increase the wear resistance of the scraper plates. The main reason for the increased wear resistance of the plates is the large number of plates (700 pcs), and thus the frequent replacement of the plates for the scraper module. In the context of the entire glass processing line, this can be considered a significant disadvantage. The exchange process and the possible effects on the operation of the line as a whole are explained in the diagram shown in Fig. 2.12.

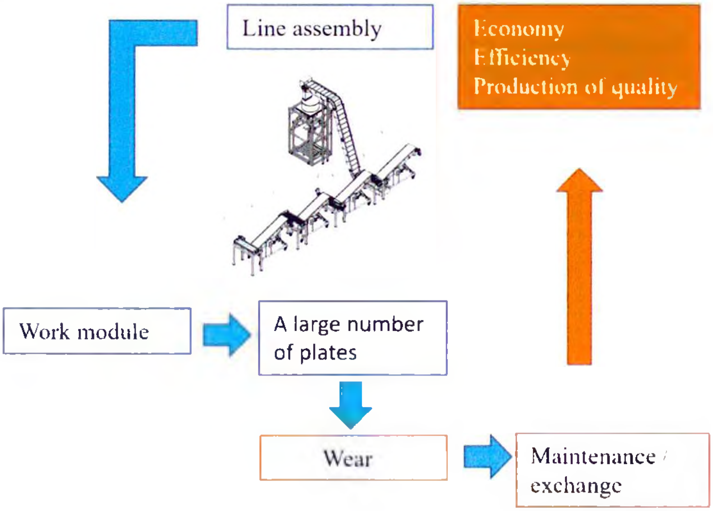
Line assembly
Economy
Efficiency
Production of quality
Work module
A large number of plates
Wear
Maintenance / exchange

Fig. 2.12 Diagram of the effect of wear of the plates on the line.

On the basis of the facts found, as well as after taking into account the issue of wear of the scraper plates in the context of the entire line, it was necessary to increase the wear resistance of the scraper plates. This could be approached in the following ways:

METHOD 1 – changing the plate material

METHOD 2 – designing the surface treatment of the plates while maintaining the Hardox 500 material

From the nature of scraper plate wear, as well as after considering the economics of both methods of increasing the wear resistance of the scraper plates, we decided to experimentally determine the appropriate surface treatment for a particular scraper application.

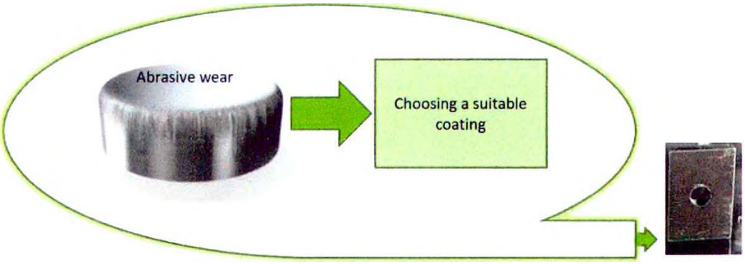
Abrasive wear
Choosing a suitable coating

Fig. 2.13 Nature of abrasive wear.

The aim of the experimental research was to carry out a wear analysis of the plates, both after the surface polishing treatment in the electrolyte and also an analysis of the PVD coatings suitable for the application. We discuss these theoretical analyses in detail in the next chapter. The output of the individual analyses is a specific determination of the measured quantities or a specific determination of the technological parameters of the applied surface treatment.

2.4 Analysis for the relevant investigation of wear of the plates in the scraper module

It was necessary to reflect on the right choice of analyses so that the output of the analyses would answer the basic questions (Fig. 2.14).

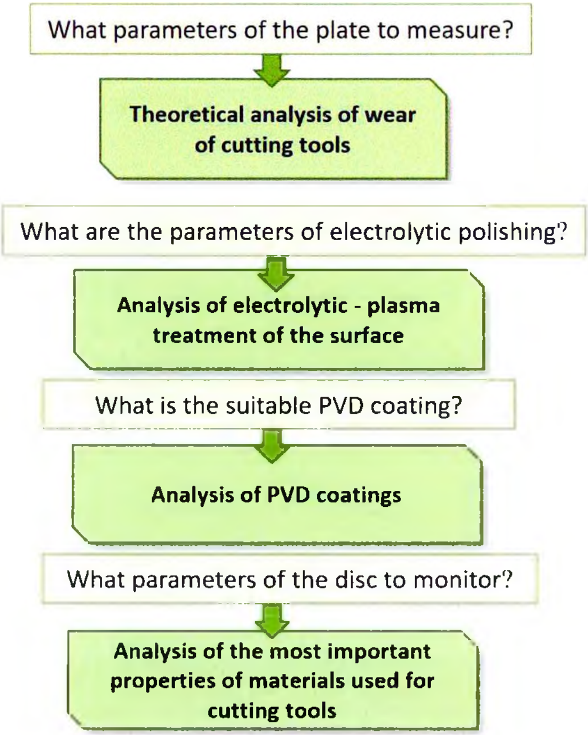
What parameters of the plate to measure?
Theoretical analysis of wear of cutting tools
What are the parameters of electrolytic polishing?
Analysis of electrolytic - plasma treatment of the surface
What is the suitable PVD coating?
Analysis of PVD coatings
What parameters of the disc to monitor?
Analysis of the most important properties of materials used for cutting tools

Fig. 2.14 Analyses needed.

The following analyses were developed for the entire research task in this particular section:

- theoretical analysis of cutting tool wear,
- analysis of electrolytic-plasma treatment of the scraper plate surface,
- analysis of PVD coatings for scraper plate application,
- analysis of the most important properties of materials used for cutting tools in machining.

The output of the individual analyses (Fig. 2.15 – Fig. 2.18) will be well-defined parameters (constants and variables). The outputs of the analyses are directly tie to the investigation of scraper plate wear in the application of scraping laminated glass from the foil.

Analysis of cutting tool wear theory

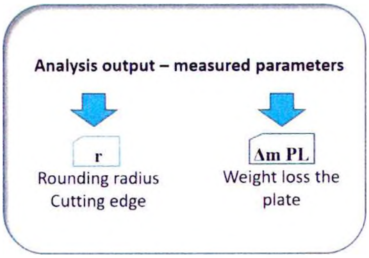
Analysis output – measured parameters
r
Rounding radius
Cutting edge
Δm PL
Weight loss the
plate

Fig. 2.15 Output of the cutting tool wear analysis.

Analysis of electrolytic-plasma surface treatment

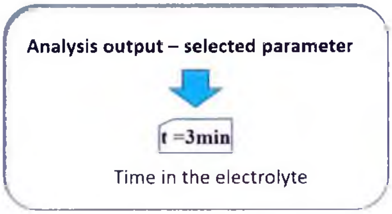
Analysis output – selected parameter
t =3min
Time in the electrolyte

Fig. 2.16 Output of the electrolytic-plasma surface treatment analysis.

Analysis of PVD coatings for scraper plate application

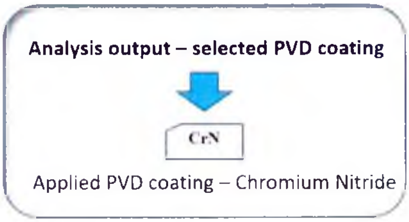
Analysis output – selected PVD coating
CrN
Applied PVD coating – Chromium Nitride

Fig. 2.17 PVD coatings analysis output.

Analysis of the properties of materials used for cutting tools in machining

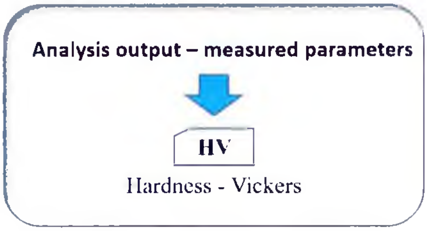
Analysis output – measured parameters
HV
Hardness - Vickers

Fig. 2.18 Output of the material properties analysis.

2.5 Experiment to determine the appropriate surface treatment for the scraper plate

The core of the experimental investigation was devoted to the scraper module of the laminated glass processing line. The equipment also includes replaceable plates, the wear measurement of which forms the principal part of the experiment.

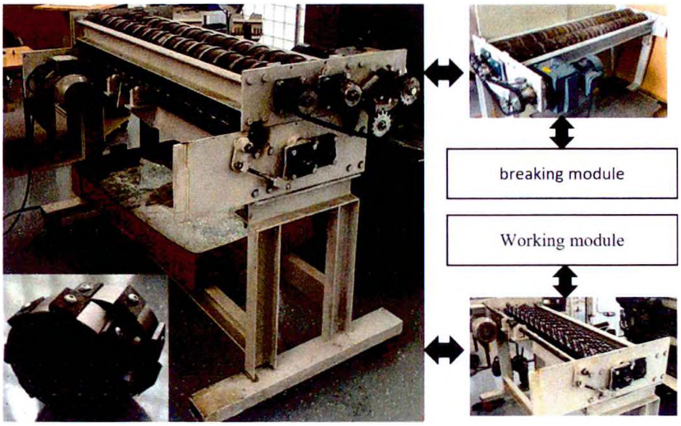
breaking module
Working module

Fig. 2.19 Measuring device – scraper module.

The apparatus on which the experiment was carried out consists of two modules (Fig. 2.19), namely a scraper module and a breaking module. The breaking module in this particular application serves the initial breaking and also acts as a holding device to ensure continuous feeding of the glass sample into the space where the actual glass scraping process takes place [5]. The scraper module is a device with discs to which scraper plates are attached by means of a screw. The scraper plates are arranged alternately on one disc so that no two samples of the same plate are in a row. They are also arranged so that in the case of four discs side by side in one diagonal line, all types of surface treatment are side by side. The best overall concept of distributing the experimental samples is shown in Fig. 2.20.

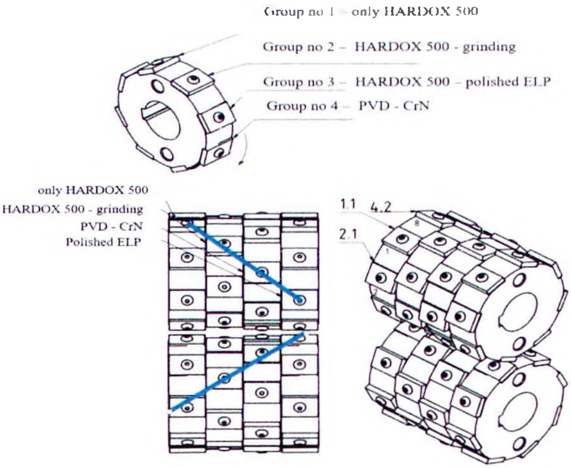
Group no 1 – only HARDOX 500
Group no 2 – HARDOX 500 - grinding
Group no 3 – HARDOX 500 – polished ELP
Group no 4 – PVD - CrN
only HARDOX 500
HARDOX 500 - grinding
PVD - CrN
Polished ELP
1.1
4.2
2.1

Fig. 2.20 Arrangement of experimental plates in a spiral.

The types of experimental plate samples are:

- **SET 1** – 16 pcs – Hardox 500, plates only fired without modification,
- **SET 2** – 16 pcs – Hardox 500, ground plates without surface treatment,
- **SET 3** – 16 pcs – Hardox 500, ground plates and surface finish plasma polishing im electrolyte,
- **SET 4** – 16 pcs – Hardox 500, ground and PVD coated CrN.

In the first step of the experiment, it was necessary to determine and define the values that willl change, and those that will be constant.

The constants of value in the experiment are:

- Device – scraper module and holder,
- Processed material – glass with a dimension of 1,200 × 250 mm × 10 mm,
- Plate material,
- The speed of the scraper module,
- Speed of the holder – feed into the working area,
- The gap between the rollers,
- Working cycle time (30 minutes),
- Number of working cycles: 4.

Changing parameters or plates surface treatment:

Surface treatment of the plates in the following variant

- 16 pcs – Hardox 500, plates only fired without modification (marked number 1)
- 16 pcs – Hardox 500, ground plates without surface treatment (marked number 2)
- 16 pcs – Hardox 500, ground and coated plates, plasma polishing in electrolyte (marked number 3)
- 16 pcs – Hardox 500, ground and PVD coated (marked number 4)

Pictures of sample plates with different surface treatment are shown in Fig. 2.21.

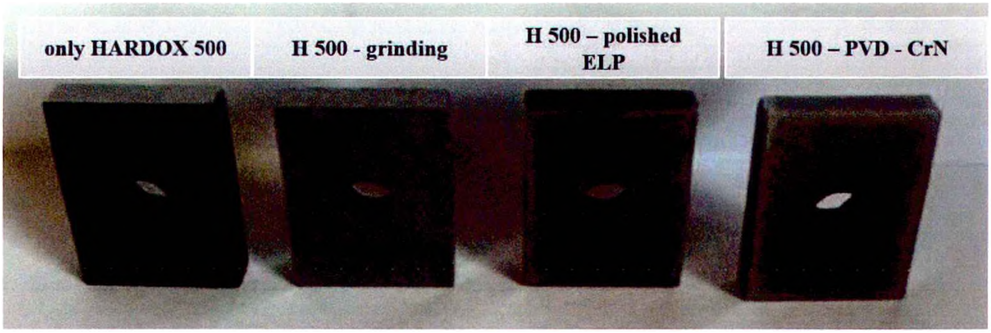

Fig. 2.21 Plates, samples of different surface treatments.

Measured quantities:

- Radius of curvature of the working edge of the plate after each working cycle,
- Weight of the plate after each working cycle,
- The hardness of the plate after each working cycle, the average value with five repetitions of the measurement,
- Measurement of the weight of the processed glass as a secondary parameter.

Detailed edge analysis of selected plates (one piece from each surface treatment):

- A more detailed analysis of the plate edge under the microscope represents secondary findings in the experiment, and for this reason will only be carried out before the first cycle – M0 on the selected plates and also at the end of the measurement after the M4 cycle on the same selected plates.

For the sake of clarity of the experimental procedure, the author considered it appropriate to present the entire plan of the experiment in a sequence of logically following points.

The resulting experimental procedure:

Phase M0 – measuring the radius of curvature, the weight of the plates, and the hardness of the plates on all 64 pieces of the experimental specimens, resulting in initial values of the measured quantities on all the experimental specimens. This also includes a more detailed microscope analysis of the edge of the plate.

Phase C1 – the first working cycle, i.e. scraping the glass with the scraper plates for 30 minutes

Phase M1 – repeat the measurement of radius of curvature, weight of the plates and hardness of the plates on all 64 pieces of the experimental specimens

Phase C2 – second working cycle, i.e. wiping the glass with the wiper plates for another 30 minutes

Phase M2 – repeat the measurement of radius of curvature, weight of the plates and hardness of the plates on all 64 pieces of the experimental specimens

Phase C3 – the third working cycle, i.e. scraping the glass with the scraper plates for another 30 minutes

Phase M3 – repeat the measurement of radius of curvature, weight of the plates and hardness of the plates on all 64 pieces of the experimental specimens

Phase C4 – the fourth working cycle, i.e. scraping the glass with the scraper plates for another 30 minutes

Phase M4 – the last measurement of radius of curvature, weight of the plates and hardness of the plates on all 64 pieces of the experimental specimens. This again includes a more detailed analysis of the edge of the plate under the microscope after all the working cycles.

Each working cycle C also includes the monitoring of secondary parameters, such as the measurement of the weight of the processed glass, as well as the number of processed glass specimens and the number of passes of the glass specimen through the working area. A graphical representation of the flow of the entire experimental investigation is shown in Fig. 2.22.

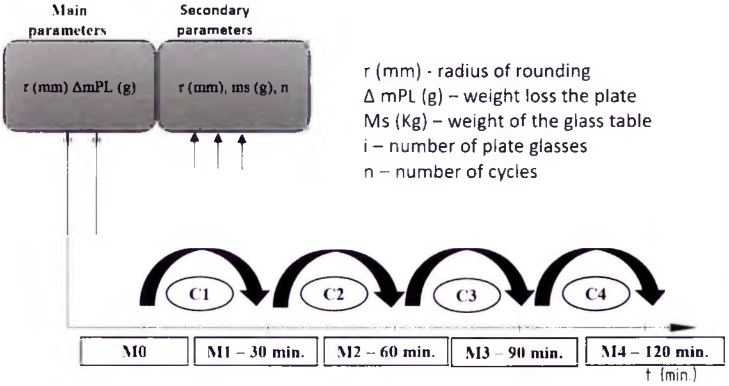
Main parameters
Secondary parameters
r (mm) ΔmPL (g)
r (mm), ms (g), n
r (mm) - radius of rounding
Δ mPL (g) – weight loss the plate
Ms (Kg) – weight of the glass table
i – number of plate glasses
n – number of cycles
C1
C2
C3
C4
M0
M1 – 30 min.
M2 – 60 min.
M3 – 90 min.
M4 – 120 min.
t (min.)

Fig. 2.22 Graphical representation of the experiment.

2.6 Experiment implementation and measured data for the fired plates

Based on the experimental plan, the course of the experiment as well as the measured data can be stated as follows:

M0 phase – the zero measurement before the application of the plates on the working disc, and thus it is the measurement of the radius of curvature (measurement A), the measurement of the weight loss (measurement B), and the measurement of the Rockwell hardness (measurement C) on the plates before the first working cycle C1. The M0 phase also includes a more detailed examination of the cutting edge and radius of curvature (D measurement) of a selected single plate from each surface treatment.

Measurement A – measurement of the radius of curvature of the working edge on all plates.

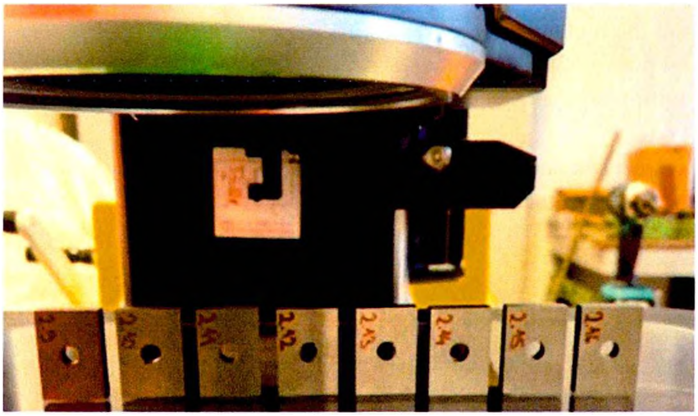

Fig. 2.23 Plates placed on the microscope worktable.

The plates were measured in sets of 8 plates, which means that the whole set of sixteen pieces was measured twice. All 16 radii of the working edge of the plates were measured in this way for all surface treatments. The result of this measurement phase, marked M0, will be the radii of curvature of the working edges for all 16 plates (Fig. 2.23).

Measurement B – measurement of the original weight of all plates before putting into the first working cycle. The measurement was carried out on a precision analytical scale with an accuracy of 0.0001 g (Fig. 2.24).

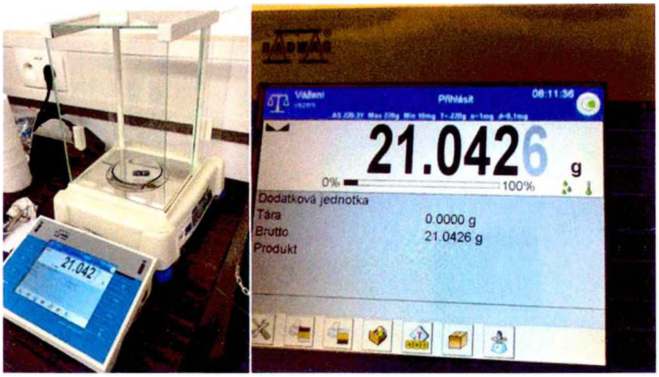
21.0426 g
0%
100%
Dodatková jednotka
Tára 0.0000 g
Brutto 21.0426 g
Produkt
21.042

Fig. 2.24 Graphical representation of the weight measurement process.

Measurement C – measurement of the hardness of all plates before starting the first working cycle. Rockwell hardness measurements were performed around the working edge of the plate 5 times, in order to find the average hardness of the plate and the statistical average of the five measurements (Fig. 2.25).

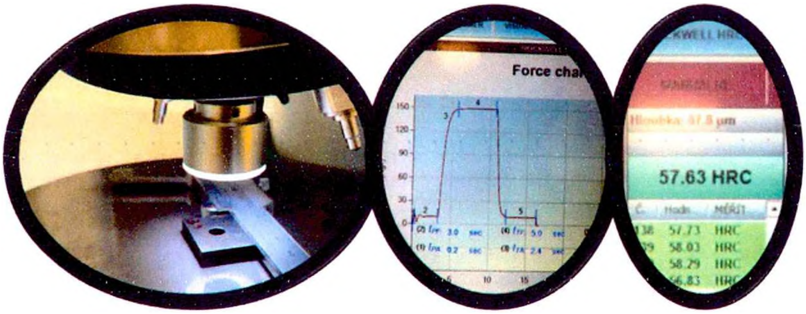
Force cha
57.63 HRC
57.73 HRC
58.03 HRC
58.29 HRC
56.83 HRC

Fig. 2.25 Graphical representation of the Rockwell hardness measurement process.

Tables of the resulting M0 measurement data – before the first cycle
The result of each section of an M-labelled measurement experiment is always a table of measured data, where all the basic measured data (raw data) are listed. In the resulting Tab. 2.2 are all specimens for the group fired plate – GROUP 1

Table 2.2

Measured data for the M0 measurement – Group 1 – fired piece.

Group no 1 – only HARDOX 500

Indication group sample	Radius (mm)	Weight (g)	Hardness M4 (HRC)					
	r4	m4	4 HRC1	4 HRC2	4 HRC3	4 HRC4	4 HRC5	Priemer HRC
1.1	1.063	21.0427	55.72	58.39	49.90	55.27	56.78	55.21
1.2	1.137	21.0775	57.88	56.28	56.43	56.28	56.71	56.72
1.3	0.951	21.0128	55.97	55.97	55.82	55.92	55.75	55.89
1.4	0.691	20.9981	54.62	56.18	56.83	55.88	55.83	55.87
1.5	0.632	21.0749	57.89	55.72	55.68	56.43	56.48	56.44
1.6	0.822	21.0233	57.39	56.68	53.71	55.22	55.76	55.75
1.7	0.679	21.0853	57.18	57.43	53.16	55.57	55.83	55.83
1.8	0.592	21.0447	56.33	54.87	56.73	57.94	56.48	56.47
1.9	1.130	21.0308	57.49	55.98	58.84	58.84	56.12	57.45
1.10	0.620	21.0315	56.53	58.29	55.87	57.43	57.02	57.03
1.11	0.558	21.0379	59.39	56.37	59.14	56.08	57.74	57.74
1.12	0.849	20.9936	57.08	57.73	55.72	56.83	56.85	56.84
1.13	0.405	21.0398	60.00	55.88	56.17	57.38	57.37	57.36
1.14	0.497	21.0119	54.21	56.58	56.68	54.32	55.44	55.45
1.15	0.637	21.0094	54.01	56.53	55.72	58.09	56.10	56.09
1.16	0.421	21.0971	55.97	58.24	57.58	56.68	57.13	57.12
mean	0.730	21.0382						56.45
median	0.658	21.0347						56.46

Phase C1 – the first working cycle, i.e. scraping the glass with the scraper plates for 30 minutes. The first working phase of the experiment, which took place over a period of 30 minutes, processed approximately 65 kilograms of glass in the form of 100 x 230 x 10 mm samples. The graphical progress of the cycle is shown in Fig. 2.26.

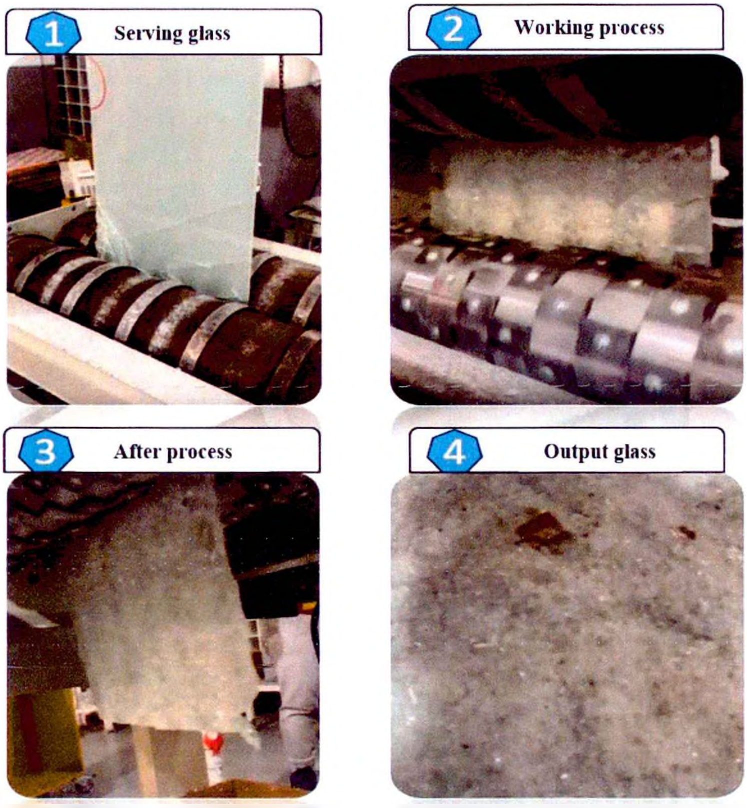

Fig. 2.26 Graphical representation of the C 1 working cycle process.

Phase M1 – repeated measurements of radius of curvature, weight of the plates and hardness of the plates on all 64 pieces of experimental specimens, essentially a repeat of phase M0, but without the analysis of the plates under the microscope.

Also, the result of this measurement phase M1, which represents the phase after the first working cycle, i.e. after 0.5 hours of the plate duty, are the tables of measured data, while again below the author will present the table only for GROUP 1 – fired plate

Phase C2 – the second working cycle, i.e. scraping of the glass with scraper plates, which took place over a period of 30 minutes and processed approximately 65 kilograms of glass in the form of specimens of 100 x 230 x 10 mm in size

Phase M2 – repeated measurement of radius of curvature, weight of the plates, and hardness of the plates on all 64 pieces of the experimental specimens

The M2 measurement phase is again a measurement, but after the second working cycle, which represents 1 hour of work. Likewise, the result of this measurement marked M2 are the tables of measured values; again, below the author will present the table only for GROUP 1 – fired plate.

Phase C3 – the third working cycle, i.e. scraping of the glass with scraper plates, which took place over a period of 30 minutes and processed approximately 65 kilograms of glass in the form of samples of 100 x 230 x 10 mm in size

Phase M3 – repeated measurement of radius of curvature, weight of the plates, and hardness of the plates on all 64 pieces of the experimental specimens

The M3 measurement phase is a measurement after 1.5 hours of plate duty. The result of this M3 measurement are tables of measured values; again below the author provides the table for GROUP 1 only – fired plate, and tables of measured values for the other groups for the M3 measurement are in Appendix 1. of this paper.

Phase C4 – the fourth working cycle, i.e. scraping of the glass with scraper plates, which took place over a period of 30 minutes and processed approximately 65 kilograms of glass in the form of specimens of 100 x 230 x 10 mm in size

Phase M4 – the last measurement of radius of curvature, weight of the plates and hardness of the plates on all 64 pieces of the experimental specimens. This again includes a more detailed analysis of the edge of the plate under the microscope after all the working cycles. This measurement is also the last measurement, and therefore the measurement will determine the final wear of the scraper disc.

The M4 measurement phase is the final measurement at the end of the plate working cycle or after 2 hours of work. The result of this measurement with the M4 marking are tables of measured values; again, below is the table for GROUP 1 – fired plate (Tab. 2.3).

Resulting tables of measured data for the M4 measurement – after all cycles

Table 2.3
Measured data for the M4 measurement – Group 1 – fired plate.

Group no 1 – only HARDOX 500								
	Radius (mm)	**Weight (g)**	**Hardness M4 (HRC)**					
Indication group sample	**r4**	**m4**	**4 HRC1**	**4 HRC2**	**4 HRC3**	**4 HRC4**	**4 HRC5**	**Priemer HRC**
1.1	1.063	21.0427	55.72	58.39	49.90	55.27	56.78	55.21
1.2	1.137	21.0775	57.88	56.28	56.43	56.28	56.71	56.72
1.3	0.951	21.0128	55.97	55.97	55.82	55.92	55.75	55.89
1.4	0.691	20.9981	54.62	56.18	56.83	55.88	55.83	55.87
1.5	0.632	21.0749	57.89	55.72	55.68	56.43	56.48	56.44
1.6	0.822	21.0233	57.39	56.68	53.71	55.22	55.76	55.75
1.7	0.679	21.0853	57.18	57.43	53.16	55.57	55.83	55.83
1.8	0.592	21.0447	56.33	54.87	56.73	57.94	56.48	56.47
1.9	1.130	21.0308	57.49	55.98	58.84	58.84	56.12	57.45
1.10	0.620	21.0315	56.53	58.29	55.87	57.43	57.02	57.03
1.11	0.558	21.0379	59.39	56.37	59.14	56.08	57.74	57.74
1.12	0.849	20.9936	57.08	57.73	55.72	56.83	56.85	56.84
1.13	0.405	21.0398	60.00	55.88	56.17	57.38	57.37	57.36
1.14	0.497	21.0119	54.21	56.58	56.68	54.32	55.44	55.45
1.15	0.637	21.0094	54.01	56.53	55.72	58.09	56.10	56.09
1.16	0.421	21.0971	55.97	58.24	57.58	56.68	57.13	57.12
mean	0.730	21.0382						56.45
median	0.658	21.0347						56.46

All the tables of measured values listed above contain measured data after specific working cycles, labelled M0, M1, M2, M3, M4. Each of the tables provides the values of each of the sixteen samples (1.1 to 1.16) of a given surface treatment. These are always specific values of r – radius of curvature of the working edge of the plate, m – weight of the plate, and Rockwell hardness values in five data for statistical evaluation.

Evaluation of measured data for fired plates – GROUP 1

All measured data obtained from the experimental investigations need to be thoroughly and factually analyzed. This part of the published paper represents a fundamental chapter of scientific investigation in terms of result and contribution. The author examines all the measured data in a comprehensive manner so that the entire evaluation process is in the context of the stated objectives of the paper. The aim of the research was to experimentally determine the appropriate surface treatment of scraper plates in the process of waste laminated glass processing. In order to achieve the most accurate results of the analysis of the measured data, we analyze the measured data in Excel. The analysis is divided according to the measured parameter into:

- evaluation of the parameter Increase in the radius of curvature of the working edge – fired plates,
- evaluation of the weight loss of the plates – fired plates.

For the evaluation of the individual groups of parameters, a source table is always provided, presenting the individual changes (increase in radius of curvature or weight loss of the plate), as well as the trend of the values for each specific plate. The evaluation of a given group includes a graph showing the average change in the measured parameter. The values given in the tables below are essentially always the measured values in the specific measurement M1, M2, M3 and M4 minus the original value measured in the measurement marked M0, which represents the increase in radius of curvature per working cycle. For the evaluation of the measurements, the same methodology was used as for the measured data. The above-mentioned facts are valid for the investigated parameters of the radius of curvature of the working edge and the weight loss of the plate.

Evaluation of the parameter Increase in the radius of curvature of the working edge

- GROUP 1 – fired plates

Table 2.4

Increase in radius of edge roundness for fired plates – GROUP 1.

Indication group sample	Increase in radius over time - only HARDOX 500 - GROUP no.1			
	M1 - 0.5 hour	M2 - 1.0 hour	M3 - 1.5 hour	M4 - 2.0 hour
1.1	0.173	0.323	0.377	0.821
1.2	0.394	0.515	0.602	0.807
1.3	0.258	0.356	0.522	0.651
1.4	0.063	0.102	0.181	0.394
1.5	0.219	0.314	0.372	0.431
1.6	0.237	0.329	0.426	0.635
1.7	0.074	0.234	0.289	0.349
1.8	0.167	0.282	0.306	0.335
1.9	0.233	0.257	0.596	0.882
1.10	0.200	0.276	0.323	0.385
1.11	0.040	0.060	0.080	0.246
1.12	0.088	0.319	0.470	0.594
1.13	0.072	0.140	0.153	0.160
1.14	0.124	0.152	0.173	0.243
1.15	0.057	0.203	0.213	0.305
1.16	0.071	0.108	0.147	0.169
mean	0.154	0.248	0.327	0.463
median	0.146	0.267	0.315	0.390
standard deviation	0.0981	0.1172	0.1642	0.2372

Fig. 2.27 shows the evaluation of all sixteen specimens with one group of surface finish, namely GROUP 1 plate fired, showing the progression of the increase in the roundness of the working edge radius over time. The graph (Fig. 2.27) has an origin at point zero, but this does not represent zero values. Starting at point zero means zero change in the value of the radii (zero radius increase) from their originally measured values in the MO measurement. On the y-axis are the values of the radius of curvature of the working edge, and on the x-axis is the time of taking the plates divided into half-hour intervals. The values of the radii of curvature always represent an increase after one working cycle. The measurement cycle ends after two hours, which also represents the edge radius evaluation phase. In the graphs (Figs. 2.27 and 2.28), the value of the average increase in wear from all sixteen plates of one particular group is always highlighted in red.

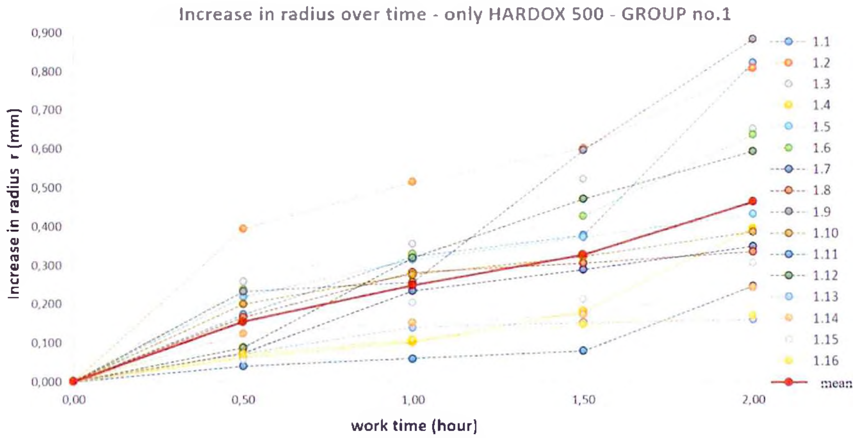

Fig. 2.27 Plate edge radius increase for fired plates – GROUP 1

Evaluation of the plate weight loss parameter

- GROUP 1 – fired plates

Table 2.5

Weight loss of fired plates – GROUP 1.

Indication group sample	weight loss the plate m(g) - only HARDOX 500 - GROUP no.1			
	M1-0.5 hour	M2 - 1.0 hour	M3 - 1.5 hour	M4 - 2.0 hour
1.1	0.0056	0.0119	0.0180	0.0376
1.2	0.0088	0.0168	0.0299	0.0431
1.3	0.0094	0.0197	0.0379	0.0510
1.4	0.0031	0.0069	0.0152	0.0279
1.5	0.0019	0.0066	0.0113	0.0142
1.6	0.0026	0.0107	0.0171	0.0293
1.7	0.0031	0.0085	0.0114	0.0195
1.8	0.0017	0.0081	0.0116	0.0173
1.9	0.0117	0.0234	0.0392	0.0649
1.10	0.0009	0.0051	0.0103	0.0148
1.11	0.0023	0.0042	0.0047	0.0067
1.12	0.0042	0.0104	0.0211	0.0413
1.13	0.0001	0.0032	0.0047	0.0086
1.14	0.0025	0.0072	0.0123	0.0224
1.15	0.0003	0.0106	0.0168	0.0318
1.16	0.0009	0.0030	0.0058	0.0065
mean	0.0037	0.0098	0.0167	0.0273
median	0.0026	0.0083	0.0138	0.0252
standard deviation	0.00346	0.00584	0.01066	0.01687

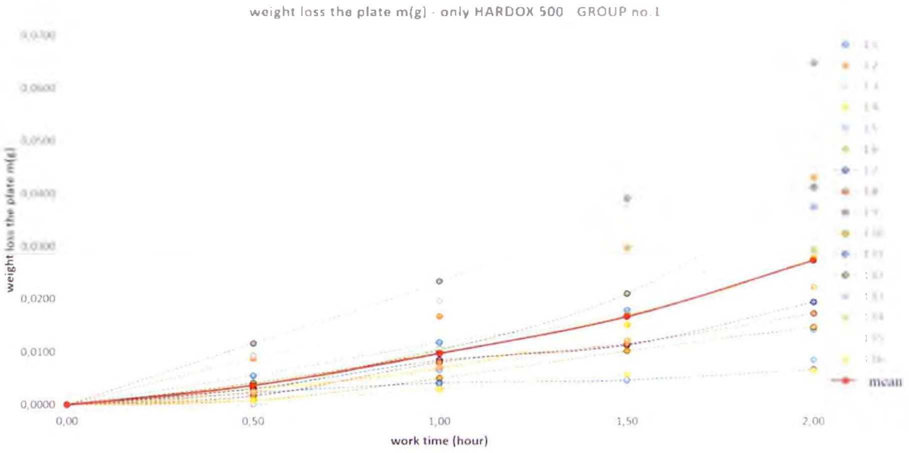

Fig. 2.28 Illustration of weight loss for fired plates – GROUP 1.

The above graph (Fig. 2.28) is an evaluation of all sixteen specimens with one group of surface treatment, namely GROUP 1 – fired plates, which shows the progression of the weight loss of the plates over time. Also highlighted in red on the graph (Fig. 2.28) is the value of the average weight loss from all sixteen plates of one particular group.

For the correct determination of the suitability of the surface treatment application for a given scraping glass from the film, the evaluation of the measurements includes not only the numerical processing of the measured data in the form of graphs, but also the optical inspection of the working edges of the plates. For a better comparison, the figures below show the edges before and after wear under a microscope, from which the changes on the edge of the plate before and after wear can be effectively compared.

- Fired plate, rounded working edge, marking 1.3.

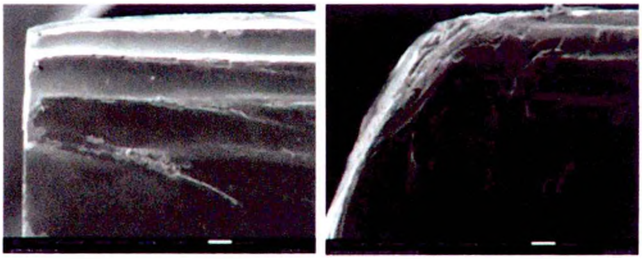

before wear – 100x after wear – 100x

Fig. 2.29 Comparison of a fired plate before and after wear.

Detailed examination of the working edge of the selected plates using an electron microscope (Fig. 2.29) also allows for an optical comparison of the change in the radius of curvature of the working edge of the plate - in this case the fired plates, and therefore group 1.

2.7 Conclusion

The experimental determination of the surface treatment itself is the main contribution of this phase of the UNIVNET project. In the design of the experiment, four types of surface treatment were chosen, namely the plate only fired without any treatment, the plate fired with a subsequent ground surface, a plate ground and polished by ELP method, and a plate with a PVD CrN (chromium nitride) coating. Technically speaking, the choice of these finishes can be seen as a better alternative to the base plate, which is just a fired sheet plate. For the relevance of the experimental results, the experiment needed to be properly set up and planned. The evaluation of the measured data clearly demonstrates the wear of the plates, which were only fired by laser cutting. In this particular paper, only the fired plates are evaluated – GROUP 1. In the next phase of the investigation, the data for all types of surface treatments used will be processed in the same way.

References

[1] Vermeulen, I. et al. 2011. Automotive shredder residue (ASR): Reviewing its production from end-of-life vehicles (ELVs) and its recycling, energy or chemicals' valorization. Journal of Hazardous Materials, 190, 8–27.

[2] N. Kanari, J.-L. Pineau, S. Shallari. 2003. End-of-life vehicle recycling in the European union, JOM 8, 15–19.

[3] Swain, B. et al. 2015. Recycling of waste automotive laminated glass and valorization of polyvinyl butyral through mechanochemical separation. Environmental Research, 142, 615–623.

[4] Dhaliwal, A. K., Hay, J. N. 2002. The characterization of polyvinyl butyral by thermal analysis. Thermochim. Acta, 391, 245–255.

[5] Tupý, M., et al. 2012. PVB sheet recycling and degradation. In: Achilias Dr., Dimitris (Ed.), Material Recycling: Trends and Perspectives. InTech, Europe, University Campus STeP Ri, Slavka Krautzeka 83/A, 51000 Rijeka, Croatia.

3 Traction Battery Dischargers

3.1 Introduction and definition of the analysis

Analytical expertise on 400 V and 800 V traction vehicle battery discharger of at least 30 A4 pages of standardized text, to include:

- Global situation (need, suppliers, available solutions),
- Situation in Slovakia (need, suppliers, available solutions).
- The need for this application (production, service, firefighters, ... other).

3.2 Motivational introduction and description of the need for a traction battery dischargers

The development of e-mobility in Europe is the subject of considerable development and investment. Several key factors are influencing the development:

Regulatory support: The European Union and its Member States support the transition to e-mobility through various regulations and directives, such as emission standards, CO_2 reduction targets and support for research and development of clean technologies following the commitments of the 2019 Green Deal. The main objective of this plan is to achieve carbon neutrality in the European Union by 2050.

Infrastructure investment: expanding charging infrastructure is key to electric vehicle (EV) adoption. European countries are investing in the development of a charging network that includes fast charging stations on key transport routes.

Technological progress: continuous battery development, such as improving capacity, lifetime and reducing costs, is essential for the development of e-mobility. Development in electric drives and energy efficiency are also contributing to the attractiveness of electric vehicles.

Economic incentives: many European countries offer various financial incentives such as subsidies, tax breaks or infrastructure benefits (e.g. bus lanes) to encourage the purchase of electric vehicles.

Environmental awareness: growing awareness of climate change and the need to reduce CO_2 emissions is motivating consumers and businesses to switch to more sustainable modes of transport, such as electric vehicles.

Growing EV range: car manufacturers are continuously expanding their EV portfolio, offering a wide range of models from small city cars to luxury and performance vehicles, including commercial vehicles.

These trends and supporting measures are expected to lead to a significant increase in the number of electric vehicles on Europe's roads in the coming years, with around 50 % of new cars sold by 2030 being electric. In the case of the Slovak Republic, the estimated trend is more moderate, at around 40 % (Fig. 3.1) [1]. As a result, this means that the industries concerned must adapt to the emerging requirements of e-mobility.

The subject of this study is the specific requirement for the application of discharging and bringing traction batteries from electric vehicles to a safe state. This requirement occurs in several possible areas, see Wikipedia.

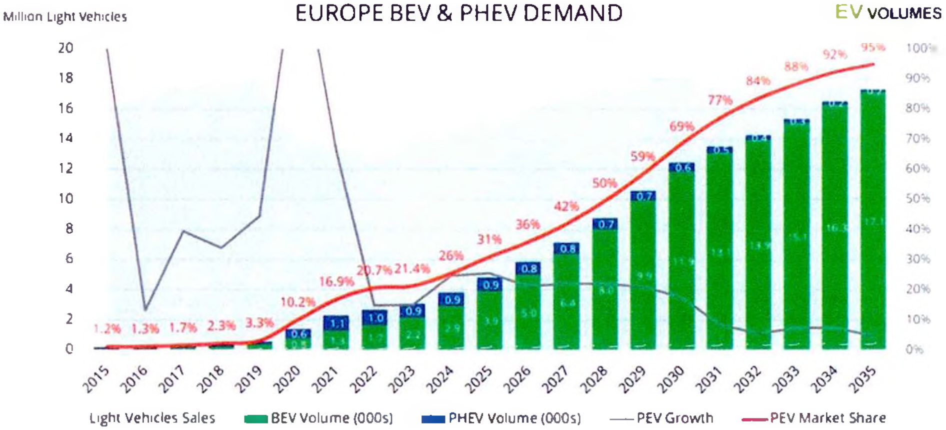

Fig. 3.1 Forecast of sales growth for electrified passenger cars and light commercial vehicles, source of EV volumes [2].

3.3 Using apps

3.3.1 Car service

Service providers specializing in electric vehicles may require special dischargers for traction batteries as well as batteries in order to safely maintain or repair electrified vehicles. Such a requirement is mainly addressed by safe disconnection of the high-voltage circuit instead of discharging the battery itself. The requirement to discharge the traction battery occurs at the moment the traction battery is replaced with a new one, and the original traction battery must be brought to a safe condition before further handling.

Discharging the traction battery with a discharger allows subsequent safe handling due to the high voltage of the traction batteries and minimizes the risks in case of accidental damage or incorrect handling. It is important that service workshops follow strict safety procedures. These safety practices are described in this analysis in the following chapters.

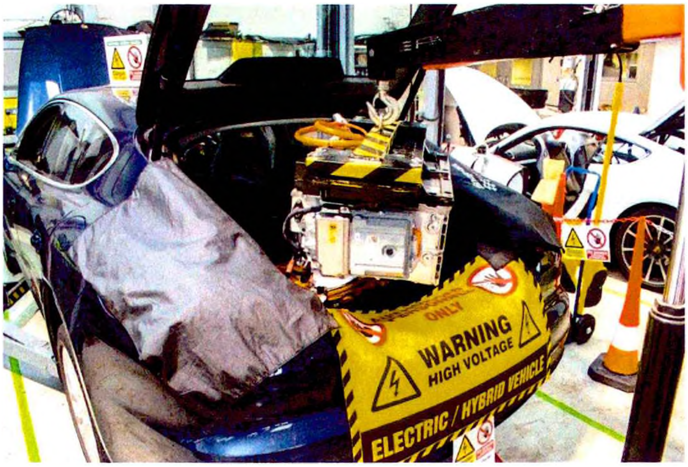

Fig. 3.2 Handling a high-voltage traction battery in a car service [2].

3.3.2 The basics of discharging

The purpose of a battery is to store energy and release it at the required time.

Discharging a battery is the process by which electrical energy is released from batteries to another device or system. Traction batteries are often used in electric vehicles, such as electric cars, electric scooters, electric bicycles and other electrically powered vehicles.

Discharge rate (DoD)

Lead acid batteries discharge at 1.75 V/cell, nickel batteries at 1.0 V/cell, and most lithium batteries at 3.0 V/cell. At this level, roughly 95 % of the energy is consumed and the voltage would drop rapidly with further discharges. To protect the battery from over-discharge, most devices prevent operation above a specified voltage value at the end of discharge.

The discharge/charge cycle is commonly understood as the complete discharge of a charged battery followed by a charge, but this is not always the case. Batteries are rarely fully discharged, and manufacturers often use the 80 % depth of discharge (DoD) formula to evaluate a battery. This means that only 80 % of the available energy is supplied and 20 % remains in reserve. Cycling a battery at less than full discharge extends its life, and manufacturers claim it is closer to field imaging than a full cycle, since batteries are usually charged with some reserve capacity.

There is no standard definition of what constitutes a discharge cycle. Some bike counters add a full count when the battery is charged. A smart battery may require 15 % discharge after charging, qualifying as a discharge cycle; anything less does not count as a cycle. The battery in the satellite has a typical DoD of 30 – 40 % before charging the batteries during the satellite day. The new electric car battery can only be charged to 80 percent and discharged to 30 per cent. This range gradually extends as the battery fades and provides the same range. Preventing full charge and discharge reduces the load on the batteries.

For the purposes of this expertise, we assume that the aim of battery discharge is to get the battery to as safe a state as possible so that it can then be recycled materially. This means minimizing the internal battery charge and achieving DoD levels up to 100 %. Please note that in this case the battery degrades and is therefore discharged to DoD 100 %; it is only suitable for batteries destined for material recycling or other material recovery or disposal (incineration, landfill).

If the battery is intended for second life, it is not recommended to discharge it to more than 80 % DoD, SoC residual charge 20 %. In this case, it is necessary to set the discharge cycle to the specified voltage. Fig. 3.3 Discharge curve below. The discharge curve is individual for each type of lithium battery.

The battery, even after discharging to 100 % DoD, i.e. until a complete short circuit on the battery, will contain residual charge, and after disconnection from the discharging device the residual voltage will reappear at the terminals.

Therefore, it is possible to:

- short-circuit the battery permanently,
- immerse the battery or modules in a salt bath where final discharge occurs.

When the battery is fully discharged, the battery goes into a so-called undercharge state, which can cause mechanical changes in the battery cells. Typically, this is so-called inflation. This phenomenon must be taken into account.

For the final state of discharge of the battery (lower voltage limit), the manufacturer's recommendations must always be followed.

In any case, the battery must be protected from dangerous contact after it has been discharged. This is the cover of the main connectors.

For the purposes of this expertise, we do not consider discharging using an individual connection to each battery cell or discharging using an original or external BMS.

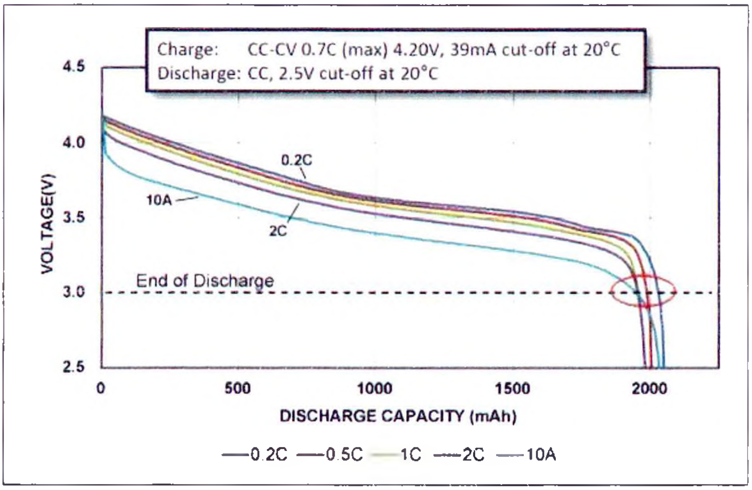

Fig. 3.3 Lithium battery discharge curves as a function of discharge current [3].

Traction battery discharger

The subject of this analysis is a device for intentional discharge of a 400 V or 800 V lithium traction battery.

Determining how the electrical energy from the batteries will be converted during the discharge process is critical to the design of a traction battery discharger. In electric cars, the electricity from the batteries is used to move the vehicle. In our case, the electricity must be safely and efficiently diverted away from the battery. There are currently two solutions, Fig. 3.4:

- the energy released from the battery is wasted in the resistance (resistance),
- regenerative use of battery power outside the device.

Option choice: a discharger with an energy dump in the resistor is suitable where it is a single-purpose device used, for example, as a one-time bringing of a battery to a discharged state to a pre-set voltage level, or DoD (discharge level). Regenerative discharge is used where discharging is part of cycling tests and it is important and economical not to waste the discharged energy.

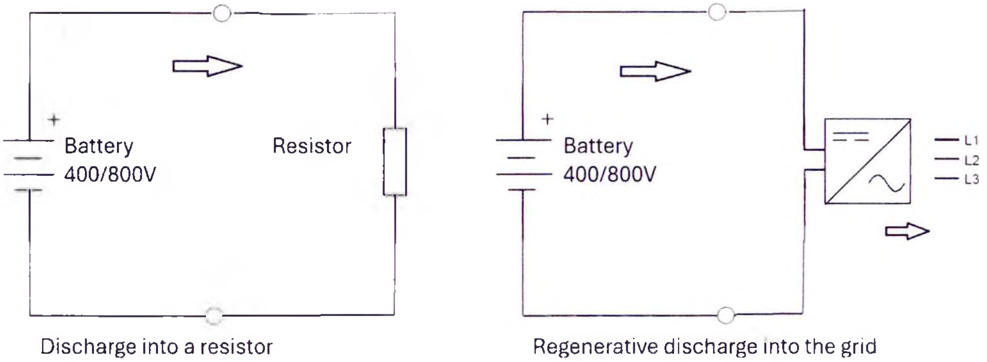
+
Battery
400/800V
Resistor
Discharge into a resistor
+
Battery
400/800V
L1
L2
L3
Regenerative discharge into the grid

Fig. 3.4 Methods of discharge in single-purpose and test equipment [3].

3.3.3 Types of discharge systems

Resistive discharge

The simplest way to discharge batteries consists of resistive elements that convert electrical energy into energy in the form of heat. They can simulate equivalent loads. They are usually designed in combination with a heat exchanger/cooling (to increase heat dissipation). The resistive discharge converts all the energy generated by the source into heat, allowing the battery to be tested at 100 % power. It is necessary to safely conduct the heat generated away from the equipment.

Benefits: simple design, cost effective and capable of working with a wide range of voltages.

Equivalent electronic load

Electronic loads are advanced devices designed to simulate battery loads in the real world. They offer precise control over discharge parameters. Batteries can be tested under a variety of static and dynamic conditions, including constant current absorption, voltage and power levels, as well as dynamically, where it is possible to change the way the instrument absorbs current, voltage and power based on pre-programmed test cases. Widely used in research, testing and development of battery systems for electric vehicles, renewable energy storage and other high-voltage applications.

Benefit: programmable, accurate and often equipped with safety features.

Test equipment

Specifically designed for battery testing and discharging, these devices provide a controlled environment for measuring battery performance and other parameters. It is a device that measures the capacity of a battery and examines its discharge curve. The discharge testing process involves discharging the battery at a constant current until it reaches a fully discharged state. During this

process, the battery voltage and current are measured at regular intervals and these measurements are used to calculate the battery capacity and its discharge curve.
Benefit: automated testing capabilities, data logging and accurate discharge profiling.
Due to the assignment of this expertise, in the following sections we will deal with the discharger corresponding to the type of resistive discharges, see Figure above, see Fig. 3.5.

The schematic diagram of the basic traction battery discharger to resistance/resistance is shown below:

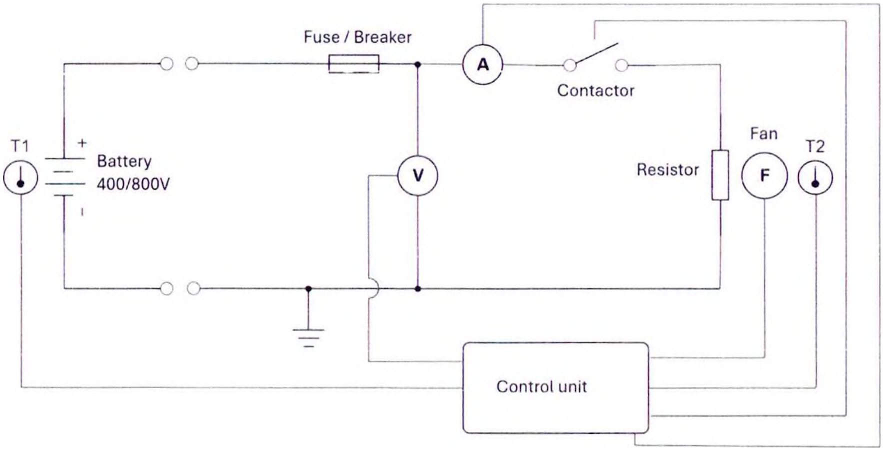

Fig. 3.5 Schematic diagram of the principle of the energy waste discharger [3].

3.4 Current status of discharger manufacturers in the world

Currently, there are a number of manufacturers on the market who supply equipment for discharging and testing traction batteries. It is possible to choose from a wide range of products that vary in range of functions and ease of use and, of course, price.

IBEKO Power AB (DV Power) – Swedish company, global supplier of test equipment and other related technologies, Fig. 3.6 [4].

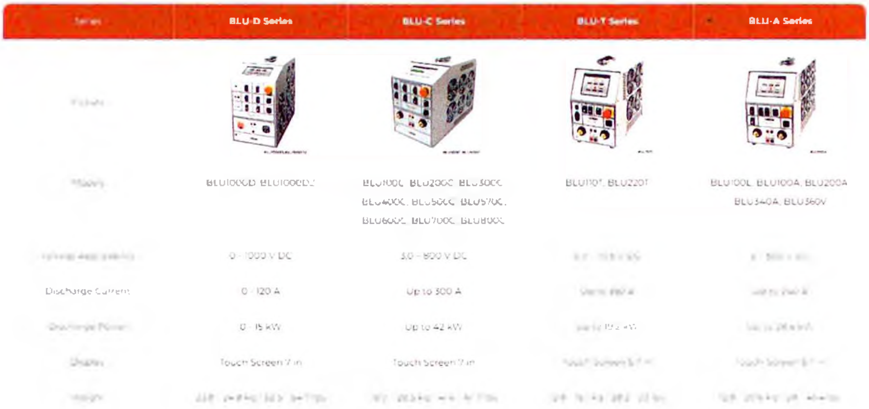

[illegible]	BLU-D Series	BLU-C Series	BLU-T Series	BLU-A Series
[illegible]	BLU1000D, BLU1000D2	BLU100C, BLU200C, BLU300C, BLU400C, BLU500C, BLU570C, BLU600C, BLU700C, BLU800C	BLU110T, BLU220T	BLU100L, BLU100A, BLU200A, BLU340A, BLU360V
[illegible]	0 - 1000 V DC	3.0 - 800 V DC	[illegible]	[illegible]
Discharge Current	0 - 120 A	Up to 300 A	[illegible]	[illegible]
Discharge Power	0 - 15 kW	Up to 42 kW	[illegible]	[illegible]
Display	Touch Screen 7 in	Touch Screen 7 in	[illegible]	[illegible]
[illegible]	[illegible]	[illegible]	[illegible]	[illegible]

Fig. 3.6 Discharge unit by IBEKO [4].

CHROMA – Chinese Taiwanese company, has a wide selection of regeneration systems and HW and SW simulations. Its equipment is widely distributed in Europe, Fig. 3.7 [5].

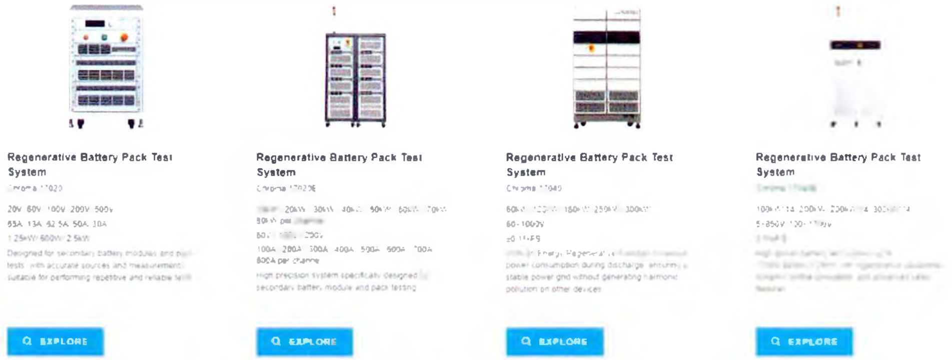

Regenerative Battery Pack Test System
Chroma 17020
20V 60V 100V 200V 500V
55A 13A 42.5A 50A 10A
1.25kW 600W 2.5kW
Designed for secondary battery modules and pack tests, with accurate sources and measurements, suitable for performing repetitive and reliable test
EXPLORE

Regenerative Battery Pack Test System
Chroma 17020E
[illegible] 20kW 30kW 40kW 50kW 60kW 70kW 80kW per channel
[illegible]
100A 200A 300A 400A 500A 600A 700A 800A per channel
High precision system specifically designed for secondary battery module and pack testing
EXPLORE

Regenerative Battery Pack Test System
Chroma 17040
60kW 120kW 180kW 250kW 300kW
60-1000V
±0.1% F.S
[illegible] Energy Regenerative [illegible] power consumption during discharge, ensuring a stable power grid without generating harmonic pollution on other devices
EXPLORE

Regenerative Battery Pack Test System
[illegible]
[illegible]
EXPLORE

Fig. 3.7 Discharge unit by CHROMA [5].

ARBIN – Chinese Taiwanese company supplying high-quality regenerative systems as EU standard, Fig. 3.8 [6].

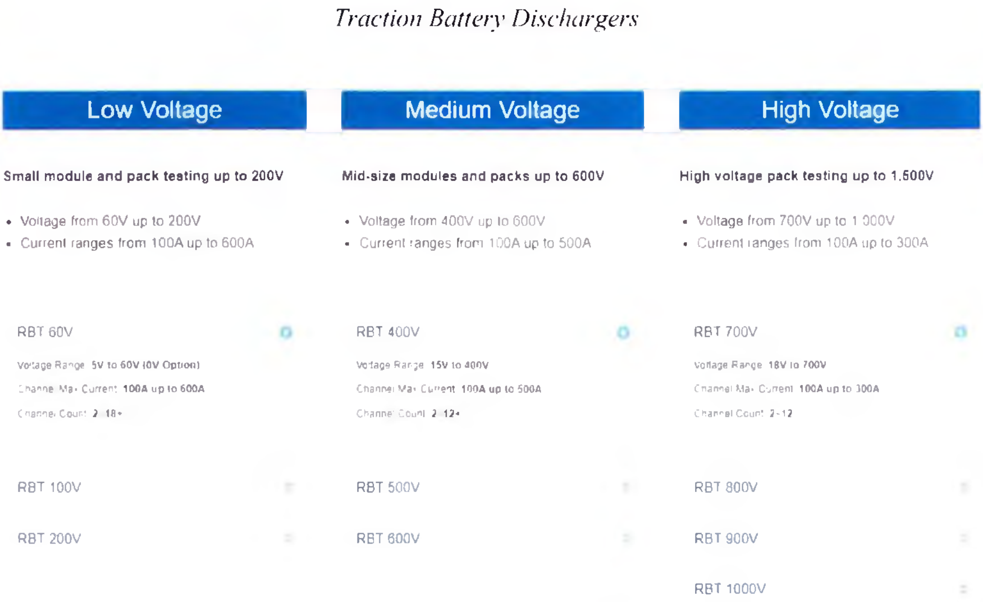

Traction Battery Dischargers

Low Voltage

Small module and pack testing up to 200V

- Voltage from 60V up to 200V
- Current ranges from 100A up to 600A

RBT 60V

Voltage Range 5V to 60V (0V Option)

Channel Max Current 100A up to 600A

Channel Count 2-18+

RBT 100V

RBT 200V

Medium Voltage

Mid-size modules and packs up to 600V

- Voltage from 400V up to 600V
- Current ranges from 100A up to 500A

RBT 400V

Voltage Range 15V to 400V

Channel Max Current 100A up to 500A

Channel Count 2-12+

RBT 500V

RBT 600V

High Voltage

High voltage pack testing up to 1,500V

- Voltage from 700V up to 1,000V
- Current ranges from 100A up to 300A

RBT 700V

Voltage Range 18V to 700V

Channel Max Current 100A up to 300A

Channel Count 2-12

RBT 800V

RBT 900V

RBT 1000V

Fig. 3.8 Discharge unit by ARBIN [6].

NI – US company, now merged with EMERSON
Regeneration Simulators for the Grid, Fig. 3.9 [7].

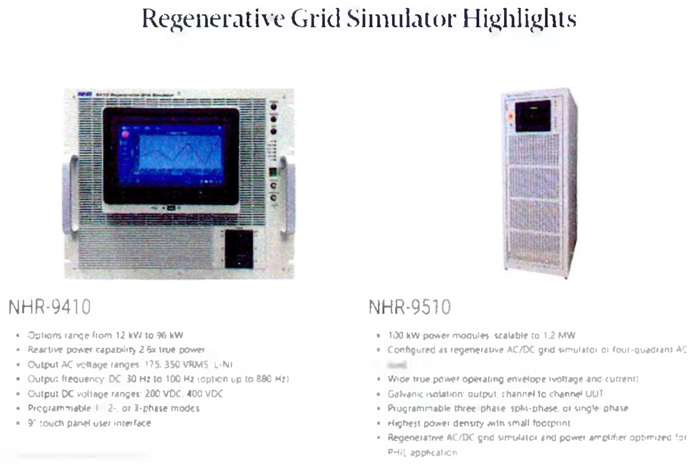

Regenerative Grid Simulator Highlights

NHR-9410

- Options range from 12 kW to 96 kW
- Reactive power capability 2.5x true power
- Output AC voltage ranges: 175, 350 VRMS (L-N)
- Output frequency: DC, 30 Hz to 100 Hz (option up to 880 Hz)
- Output DC voltage ranges: 200 VDC, 400 VDC
- Programmable 1-, 2-, or 3-phase modes
- 9" touch panel user interface

NHR-9510

- 100 kW power modules, scalable to 1.2 MW
- Configured as regenerative AC/DC grid simulator or four-quadrant AC load
- Wide true power operating envelope (voltage and current)
- Galvanic isolation: output, channel to channel, UUT
- Programmable three-phase, split-phase, or single phase
- Highest power density with small footprint
- Regenerative AC/DC grid simulator and power amplifier optimized for PHIL application

Fig. 3.9 Discharge unit by EMERSON [7]

CINERGIA – Spain, manufacturer of sieve and electronic dischargers, Fig. 3.10 [8].

GE&EL
Grid Simulator & Electronic Load (GE&EL)
GE&ELvAC/DC
The All-Terrain AC/DC Regenerative Converter
GE&EL+vAC
The All-in-one AC Regenerative Converter
cinergia

Fig. 3.10 Discharge unit by CINERGIA [8].

HDPOWER – Chinese company, a wide range of battery measurement and analysis products, both discharge and charge test equipment, Fig. 3.11 [9].

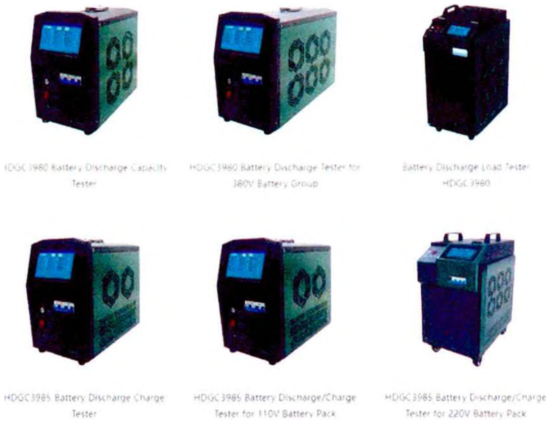
HDGC3980 Battery Discharge Capacity Tester
HDGC3980 Battery Discharge Tester for 380V Battery Group
Battery Discharge Load Tester HDGC3980
HDGC3985 Battery Discharge Charge Tester
HDGC3985 Battery Discharge/Charge Tester for 110V Battery Pack
HDGC3985 Battery Discharge/Charge Tester for 220V Battery Pack

Fig. 3.11 Discharge unit by HDPOWER [9].

AKTIF ELEKTROTEKNIK – German company, manufactures large resistance discharge lamps for a wide range of applications, Fig. 3.12 [10].

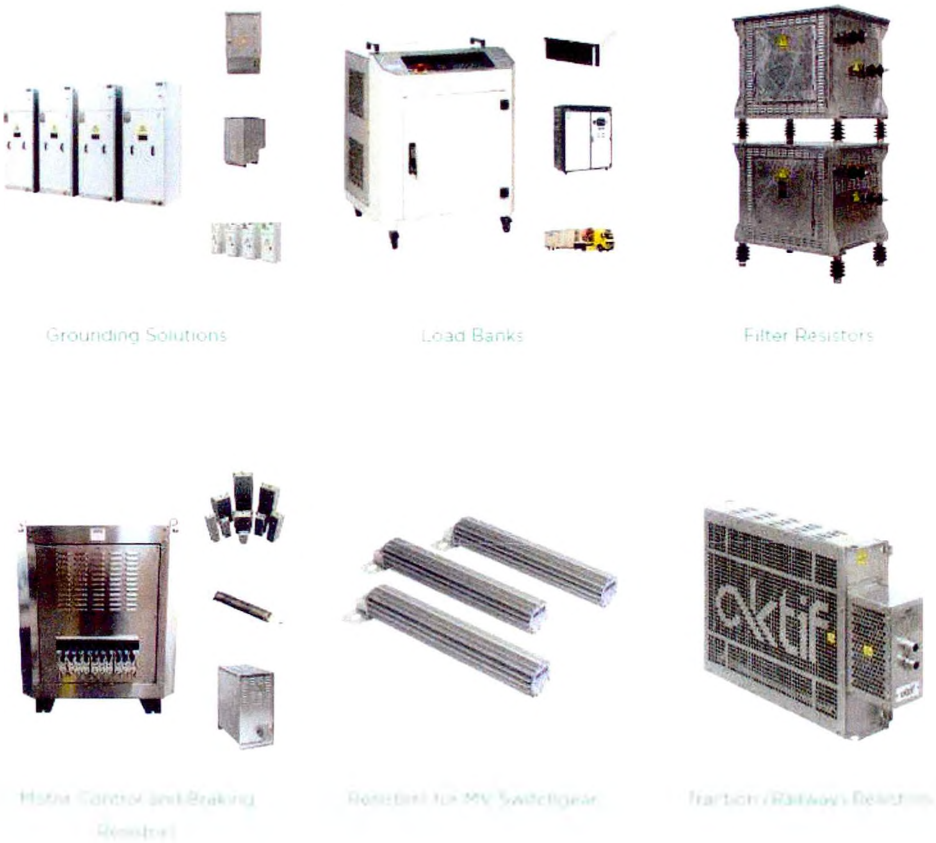
Grounding Solutions
Load Banks
Filter Resistors
Motor Control and Braking Resistors
Resistors for MV Switchgear
Traction (Railway) Resistors
aktif

Fig. 3.12 Discharge unit by AKTIF [10]

CADEX – Canadian company, manufactures all equipment related to battery testing, Fig. 3.13 [11], [12].

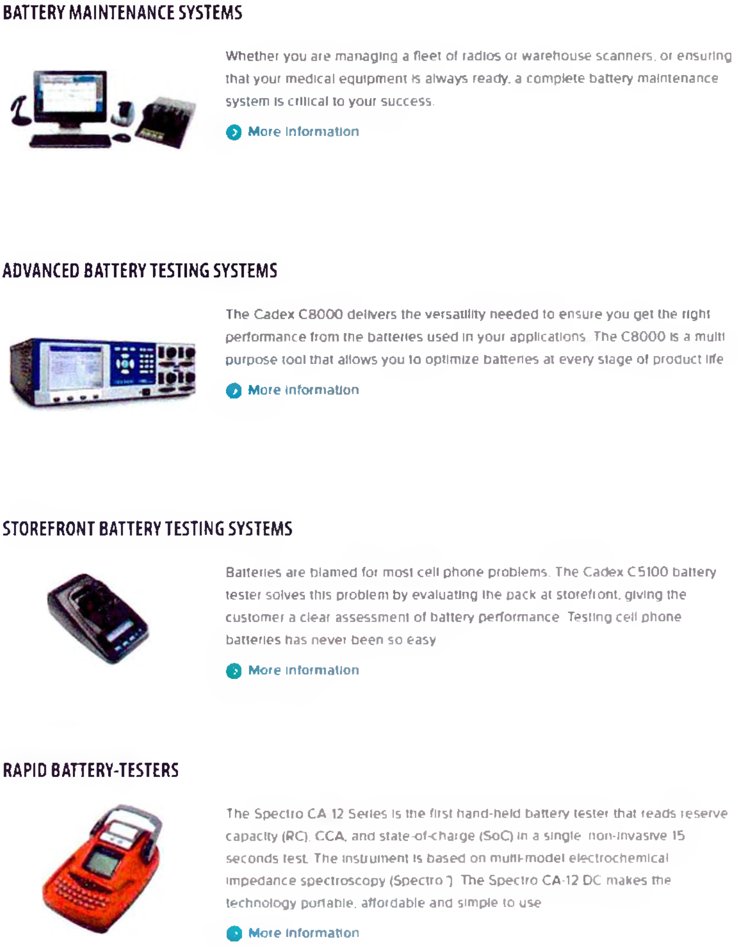

BATTERY MAINTENANCE SYSTEMS

Whether you are managing a fleet of radios or warehouse scanners, or ensuring that your medical equipment is always ready, a complete battery maintenance system is critical to your success.

More information

ADVANCED BATTERY TESTING SYSTEMS

The Cadex C8000 delivers the versatility needed to ensure you get the right performance from the batteries used in your applications. The C8000 is a multi purpose tool that allows you to optimize batteries at every stage of product life

More information

STOREFRONT BATTERY TESTING SYSTEMS

Batteries are blamed for most cell phone problems. The Cadex C5100 battery tester solves this problem by evaluating the pack at storefront, giving the customer a clear assessment of battery performance. Testing cell phone batteries has never been so easy

More information

RAPID BATTERY-TESTERS

The Spectro CA 12 Series is the first hand-held battery tester that reads reserve capacity (RC), CCA, and state-of-charge (SoC) in a single, non-invasive 15 seconds test. The instrument is based on multi-model electrochemical impedance spectroscopy (Spectro™). The Spectro CA-12 DC makes the technology portable, affordable and simple to use

More information

Fig. 3.13 Testing unit by HDPOWER [11], [12]

Slovácke strojírny, a.s., (MEP Postřelmov)
MEP Postřelmov is a traditional Czech manufacturer of electrical equipment and specialises in the production of resistive devices. Its devices are also used to discharge batteries, Fig. 3.14 [13].

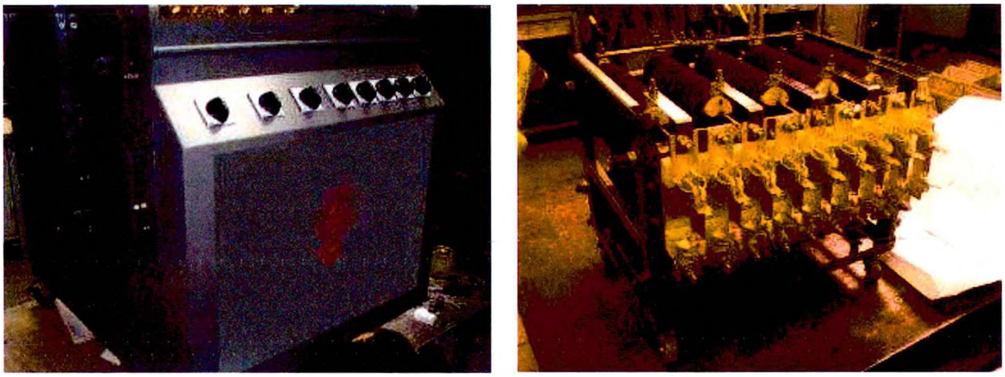

Fig. 3.14 Testing unit by Slovácké strojírny [13]

3.5 Current situation in Slovakia

A detailed analysis of the current situation in the Slovak Republic did not find any manufacturer offering its own solution for discharging or test equipment for traction batteries. There are trading companies that represent some of the world's manufacturers. Previous chapter.
Below are selected companies that have the know-how and facilities to develop and manufacture the discharge equipment as required by this expertise.

TESLA Liptovský Hrádok, a.s.
A company developing proprietary battery systems and having competence in the development and manufacture of battery discharge equipment [14].

ŽOS Vrutky a.s.
Traditional Slovak company with a rich history in the electrical industry. A company with its own development and products [15].

EVPÚ a.s.
Slovak company with an emphasis on research and development in electrical engineering and in several electrical engineering fields. The company has many years of experience in developing similar products [16].

IBG Slovakia, s.r.o
Czech Slovak company dealing with battery systems and related materials recycling, including a focus on batteries with a secondary life. The company has its own battery discharging facility in the Czech Republic for internal purposes [17].

ZTS Elektronika SKS s.r.o.
A company engaged in the development of custom industrial electronics and having experience in the development of test and laboratory equipment [18].

3.6 Discharge system requirements

For the purpose of this expertise, the performance requirements for equipment designed to discharge lithium traction batteries with a voltage of 400 V DC or 800 V DC were determined.

Functionality:
Discharging a traction battery is the process by which electrical energy is released from the batteries to another device or system. Traction batteries are often used in electric vehicles, such as electric cars, electric scooters, electric bicycles and other electrically powered vehicles.
In view of the requirement for a single-purpose device, ease of operation and favourable costs for the development and production of the device, the energy-wasting method in resistance (resistor) was chosen.
A resistive energy-wasting discharge device is suitable where there is a single-purpose device used, for example, as a one-off to bring a battery to a maximum safe state. This is the traditional way of discharging battery systems. This method is simple, and the construction of such a device is advantageous in terms of price and simplicity. The disadvantage is the necessity to provide heat dissipation, which is generated when the discharged energy is wasted in the resistor and the energy is not used for other purposes.

Basic features:

- Safe discharge (charge distribution) of lithium traction battery.

Secondary functions:

- 400 V DC or 800 V DC input voltage detection,
- measurement of voltage on the battery circuit,
- measurement of discharge power, current,
- resistance cooling control,
- detection of the end of the discharge cycle and stopping the discharge process.

Safety features:

- STOP safety button, discharge device and battery disconnect,
- reverse polarity protection,
- resistance overheat protection,
- discharged battery overheat protection,
- device overload protection,
- electric shock protection. Options, optional features:
- constant discharge power/current control,
- record of the discharge procedure.

Safety:

Ensuring safety when discharging traction batteries is critical as improper battery handling can lead to hazards and dangerous situations such as electric shock, short circuit, fire, explosion and chemical hazards.

In order to better understand the risks and hazards involved in the planned construction of the discharge facility, a risk analysis has been carried out; the chapters below and following specify the safety measures. Risk analysis is also an important part of the process of issuing a declaration of conformity and subsequent CE marking of a product before it is placed on the market. The hazard analysis identifies all potential hazards and risks that could arise from the normal use of the discharge equipment. Issuing a declaration of conformity and CE marking of the equipment is the sole responsibility of the future manufacturer and this risk analysis cannot replace the whole process.

3.7 Risk analysis for the design and construction of discharge facilities

Table 3.1

Risk analysis for design of discharge unit (e-Tech Systems Engineering s.r.o)

eTECH Sytems Engineering

Analysis of hazards and risks associated with discharge devices for traction batteries 400V DC/800V DC.

	New hazards	Type of hazards	Risk	Consequence
M	**Mechanical**	Mechanical damage to the battery	Short circuit and fire, short circuit explosion	Fire, explosion, injury
		Mechanical damage to the battery	Leakage of chemicals	Chemical burns, health damage, toxic fumes
		Mechanical damage to the battery	Creation of hazardous touch voltage risk	úraz elektrickým proudem
		Imperfect electrical connection (poor tightening, faulty connector)	Creation of contact resistance, sparking, etc.	Fire, ignition, malfunction
		Mechanical damage to the high-voltage wiring	Short circuit and fire, touch voltage	Electric shock, ignition
		Mechanical damage to high-voltage components	Short circuit and fire, touch voltage	Electric shock, ignition
		Ingress of water, moisture	Short circuit, touch voltage	Electric shock, short circuit
E	**Electrical risk**	Existence of hazardous touch voltage (up to 800V DC)	mproper handling	Electric shock
		Existence of hazardous touch voltage (up to 800V DC)	Failure to maintain insulation distance	Electric shock, arc flash, short circuit
		Existence of hazardous touch voltage (up to 800V DC)	Device malfunction, insulation failure	Electric shock, arc flash, short circuit
		Lossy electrical power, overload of electrical circuits	Occurrence of hot parts and risk of injury, burns, malfunctions	Electric shock, arc flash, short circuit
		Short circuit in electrical circuits	Fire, occurrence of touch voltage	
F	**Malfunction of the discharger**	Direct short circuit, unlimited discharge power	Battery damage	Short circuit, explosion, overheating, fire, mechanical damage
T	**Thermal shock, incorrect temperature**	Storage at low temperatures	Battery damage	Mechanical damage and short circuit, explosion, fire
		Storage at high temperatures	Battery damage	Mechanical damage and short circuit, explosion, fire
EM	**EMC risk**	Influence on the surroundings by electromagnetic radiation	Malfunction of electronic devices in the vicinity	Pacemaker, radio, influence on other devices
		Influence on other vehicle devices by electromagnetic radiation	Malfunction of electronic devices in the vicinity	Failure of other devices
V	**External influences**	Flooding, water ingress, condensation, fluid leakage into the device	Short circuit and fire, touch voltage	Electric shock, short circuit, fire, explosion
		Vibration during transport and handling	Short circuit and fire, touch voltage	Electric shock, short circuit, fire, explosion
		namrznuti a poškození vlivem nízké teploty	Short circuit and fire, touch voltage	Electric shock, short circuit, fire, explosion
		koroze a degradace materiálu	Short circuit, leakage of chemicals	Electric shock, short circuit, fire, explosion
CH	**Chemical risk**	Impact and damage from contact with toxic substances from the batte	Improper handling	Chemical burns, poisoning

3.8 Safety requirements

The risk analysis (Tab. 3.1) identifies the requirements for ensuring sufficient qualification of staff entering the processes concerned.

3.8.1 Operation of the discharging device

It is necessary to supplement the OHS training and to instruct the affected workers on the risks associated with handling the traction battery and the operation of the discharge equipment. Relevant information should be obtained from the safety data sheets or documentation relating to the batteries to be discharged.

In particular, information concerning the possible occurrence of high contact voltages, chemical substances, and associated risks in the event of mishandling or damage during handling, or where damage has previously been identified.

Updates to first aid rules: electric shock, chemicals, gases; see Emergency Response Rules. Safety Data Sheets.

3.8.2 Qualification and proficiency to operate unloading equipment falling under the definition of work on electrical equipment

The operation of discharge equipment falls under the category of work on electrical equipment. Work instructions and operating instructions for the equipment shall be established for activities involving the connection of the battery to the discharging equipment and the operation of the equipment. In particular, this area concerns the way in which the traction high-voltage battery is connected to the discharger.

WARNING: Even when the traction battery is disconnected from the discharger, residual voltage may remain at the battery terminals. Therefore, we recommend isolating the terminals from the battery after disconnecting the device to prevent accidental contact and short circuits, Fig 3.15, Fig 3.16.

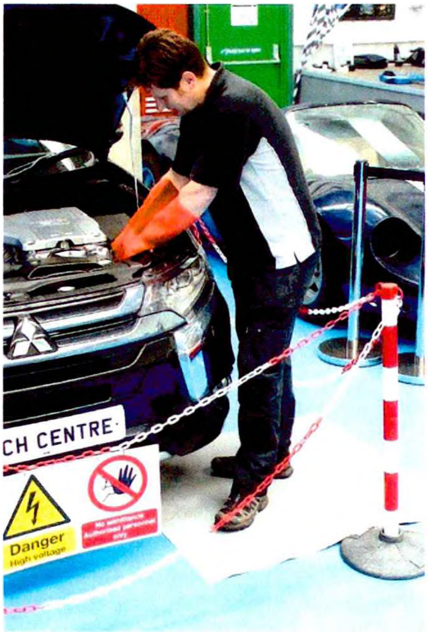
CH CENTRE
Danger
High voltage

Fig. 3.15 Maintenance work on EV with usage of protective gloves, source: archive e-Tech Systems Engineering s.r.o

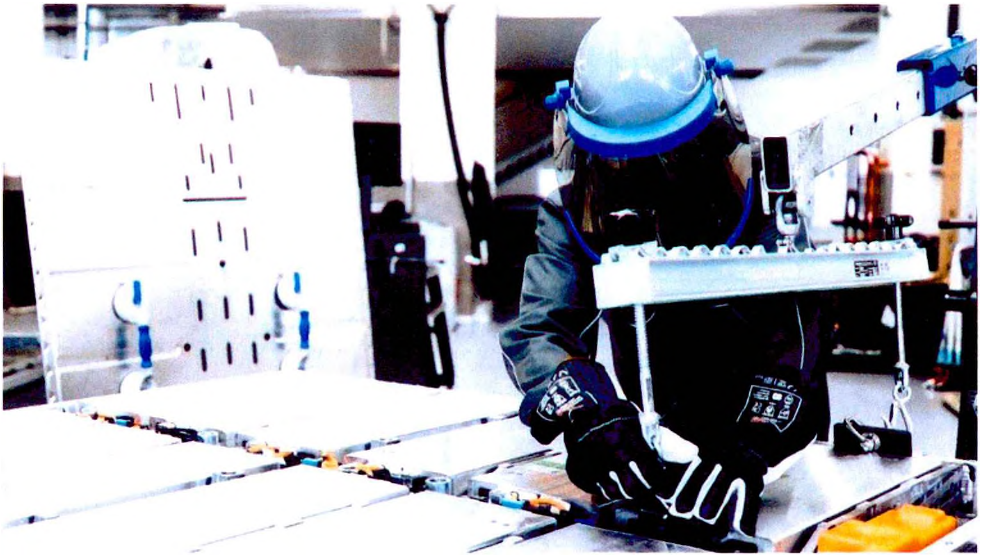

Fig. 3.16 Maintenance work on EV with usage of protective gloves and eye protection shield [3].

3.9 Design of the basic technical specification of the discharger (discharging into a resistive load)

3.9.1 Technical specifications

Table 3. 2

Technical specification of discharge equipment [13].

Discharger	
Battery discharge voltage range	300 – 800 V
Load	Resistance
DC voltage measurement accuracy	0.1 V
Discharging power	10 kW to 30 kW
Battery discharge protection	Minimum voltage, maximum current, maximum battery temperature
Safety features	STOP button, current protector, safety function
Infeed	220 V AC
Handling	mobile, on wheels
Use	Inner spaces

3.9.2 Typical discharge device design

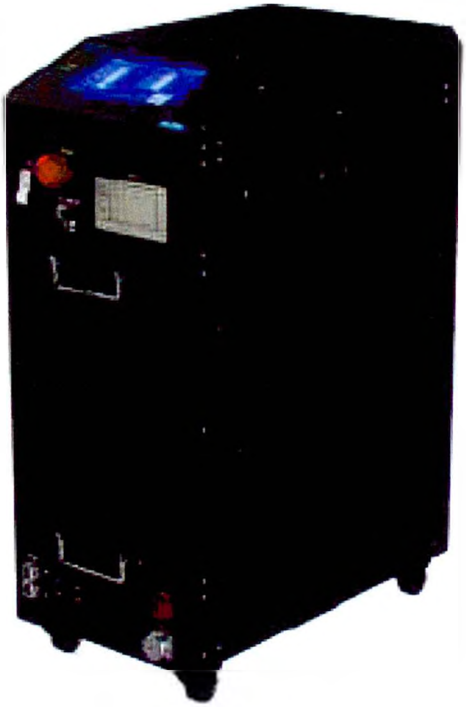

Fig. 3.17 Standard design of discharge unit [3].

3.9.3 Reference technical standards

As there is no specific technical standard for dischargers, a basic set of technical standards for the development and manufacture of discharge devices and the issuing of a Declaration of Conformity (CE) has been established. This range must always be confirmed by a qualified design engineer of the equipment manufacturer or competent authority.

ČSN EN 61439	Low-voltage switchgear
ČSN SK 60 664	Insulation coordination for equipment within low-voltage supply systems
ČSN SK 60 529	Degrees of protection provided by enclosures
ČSN EN 60 071	Insulation co-ordination: definitions, principles and rules

3.9.4 Service and discharge process [3]

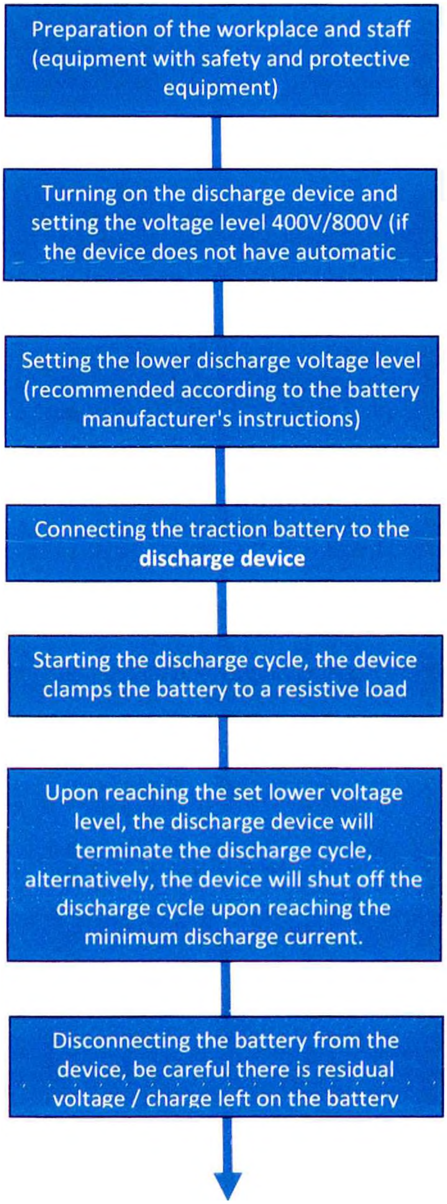

Preparation of the workplace and staff (equipment with safety and protective equipment)

Turning on the discharge device and setting the voltage level 400V/800V (if the device does not have automatic

Setting the lower discharge voltage level (recommended according to the battery manufacturer's instructions)

Connecting the traction battery to the **discharge device**

Starting the discharge cycle, the device clamps the battery to a resistive load

Upon reaching the set lower voltage level, the discharge device will terminate the discharge cycle, alternatively, the device will shut off the discharge cycle upon reaching the minimum discharge current.

Disconnecting the battery from the device, be careful there is residual voltage / charge left on the battery

3.9.5 Basic schemes of discharge equipment

Basic electrical diagram of the discharge device

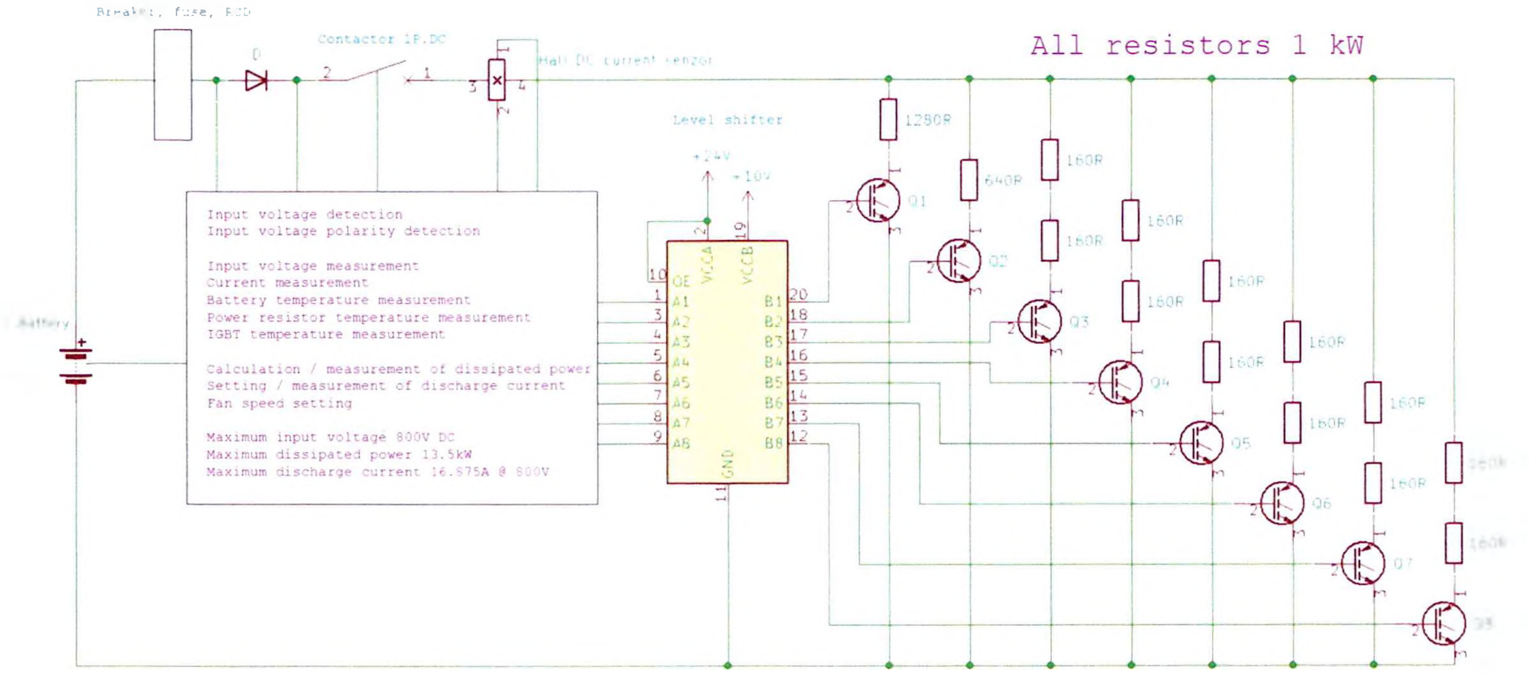
Breaker, fuse, RCD
D
Contactor 1P.DC
2
1
3
4
1
2
Hall DC current senzor
All resistors 1 kW
Level shifter
+24V
+10V
Battery
Input voltage detection
Input voltage polarity detection
Input voltage measurement
Current measurement
Battery temperature measurement
Power resistor temperature measurement
IGBT temperature measurement
Calculation / measurement of dissipated power
Setting / measurement of discharge current
Fan speed setting
Maximum input voltage 800V DC
Maximum dissipated power 13.5kW
Maximum discharge current 16.875A @ 800V
VCCA
VCCB
2
19
10 OE
1 A1
3 A2
4 A3
5 A4
6 A5
7 A6
8 A7
9 A8
B1 20
B2 18
B3 17
B4 16
B5 15
B6 14
B7 13
B8 12
GND
11
1250R
640R
160R
Q1
Q2
Q3
Q4
Q5
Q6
Q7
Q8

Fig. 3.18 Electric diagram of discharge equipment [3].

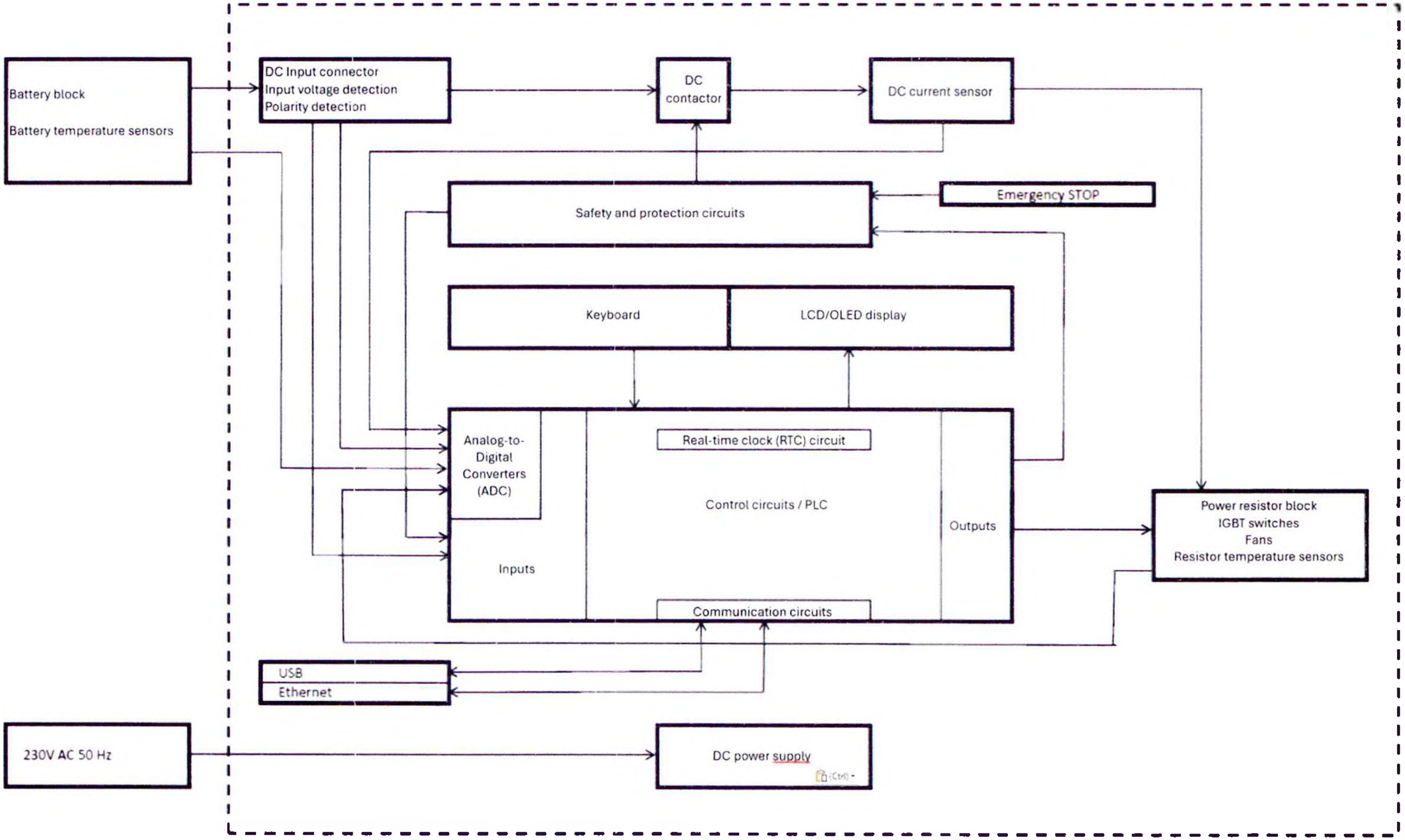
Battery block
Battery temperature sensors
DC Input connector
Input voltage detection
Polarity detection
DC contactor
DC current sensor
Emergency STOP
Safety and protection circuits
Keyboard
LCD/OLED display
Analog-to-Digital Converters (ADC)
Inputs
Real-time clock (RTC) circuit
Control circuits / PLC
Communication circuits
Outputs
Power resistor block
IGBT switches
Fans
Resistor temperature sensors
USB
Ethernet
230V AC 50 Hz
DC power supply

Fig. 3.19 Functional diagram of discharge equipment [3].

The basic design of the discharge device

Bill of materials	
Item number	Name
1	BOX
2	BRAKERS
3	TRACTION BATTERY INPUT
4	POWER INPUT
5	STOP BUTTON
6	DISPLAY

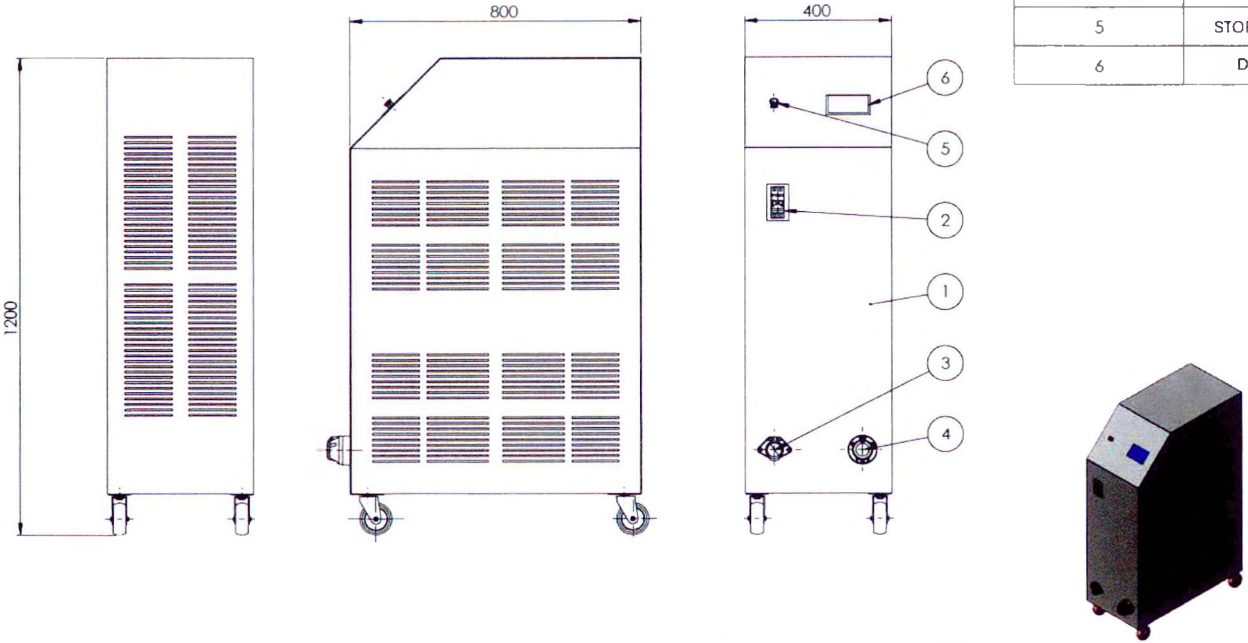

Fig. 3.20 Basic design discharge equipment [3].

3.9.6 Selection of key components

Load resistance, resistance: we recommend using traditional manufacturer resistors such as:

MEP Postřelmov, [19] :

GINO [20]:

Example of MEP Postřelmov resistive load implementation:

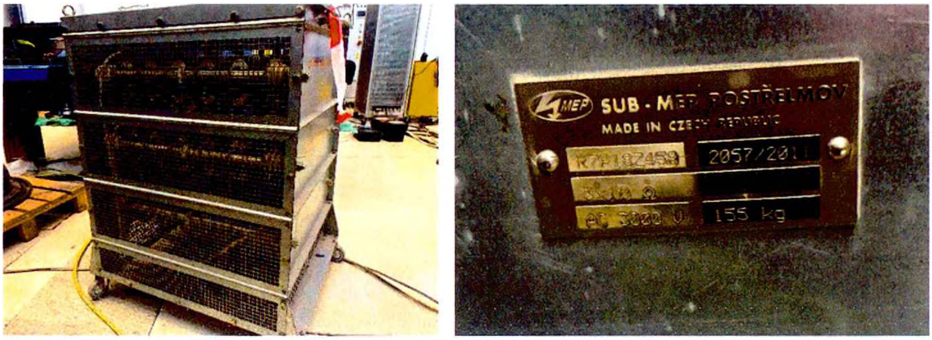
SUB - MEP POSTŘELMOV
MADE IN CZECH REPUBLIC
2057/2011
155 kg

Fig. 3.21 Source of specific components [19]

Control system:

We recommend using a basic industrial control system for automation and control of the discharge equipment, such as SIMATIC from SIEMENS or another industrial control system.

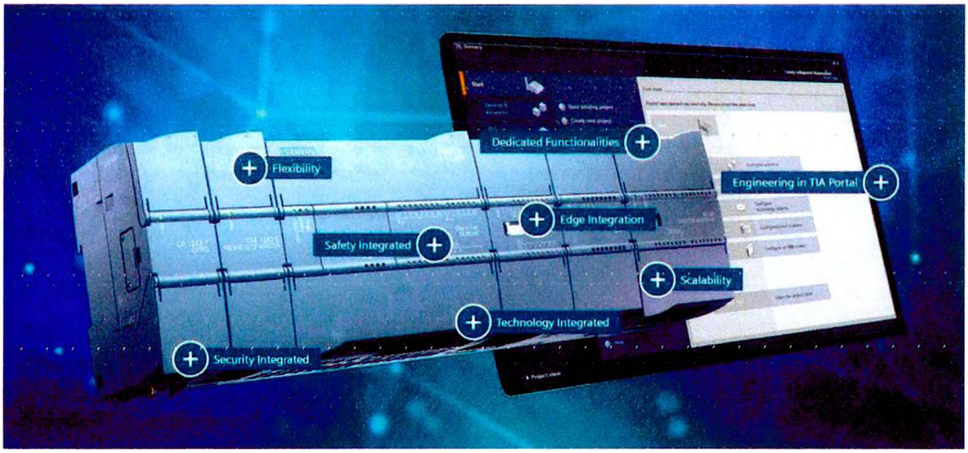
Dedicated Functionalities
Flexibility
Engineering in TIA Portal
Edge Integration
Safety Integrated
Scalability
Technology Integrated
Security Integrated

Fig. 3.22 Control system [21]

References

[1] Global EV Outlook 2023, IEA. International Energy Agency

[2] EV VOLUMES, Autovista Group

[3] archive e-Tech Systems Engineering s.r.o

[4] https://www.dv-power.com

[5] https://www.chromausa.com/applications/battery-test/

[6] https://www.arbin.com/battery-test-equipment/battery-test-product-series/rbt-series/

[7] https://www.ni.com/en/shop/power-electronics-test-systems/regnerative-grid-simulator-system.html

[8] https://cinergiapower.com/en/families

[9] https://www.hdpowertest.com/product/

[10] https://aktif.net/en/product-categories/power-resistors/

[11] https://www.cadex.com/products

[12] https://batteryuniversity.com/article/bu-1504-battery-test-analyzing-devices

[13] https://sub.cs/map-postrelmov/

[14] https://www.teslalh.eu/en/home

[15] https://www.zos-vrutky.sk/index_sk.html

[16] https://www.evpu.sk/

[17] https://www.ibg.cz/sk/kontakty

[18] https://www.elektronika.sk/profil-spolocnosti

[19] https://sub.cz/product-category/mep-postrelmov/mep-vyrobni-program/mep-odporove-pristroje/

[20] https://www.gino-ag.com/de/

[21] https://www.siemens.com/sk/sk/produkty/priemyselna-automatizacia/simatic-hmi.html

4 Development of Technology for the Recovery of Waste Foam into New Products

4.1 Introduction

Polyurethane (PUR) foams account for about 33 % of total polyurethane production. They are used for the production of seats in the automotive industry, mattresses, furniture, laminating textiles, for packaging purposes (impact protection), for the production of insulation and sealing strips. They are also used in the construction industry. The fact that they are commonly used both in industry and as consumables raises the issue of waste disposal and recycling. There is also the possibility of waste in the production, where it can reach up to 10 % of the total foam production. PUR can be used as foams, elastomers, varnishes, adhesives, elastic fibres or artificial leather. From these forms, the greatest demand is for foams. Soft foams are prepared exclusively in blocks. Their density ranges from 15 kg.m^{-3} to 70 kg.m^{-3}.

Hard foams are prepared in closed or open moulds. They are mostly used as insulation material in construction and engineering (pipes, refrigerators, cars), but also in aircraft as radar covers. This takes advantage not only of their good insulating capacity, but also of the hardness of hard PUR foams. Their hardness ranges from 10 kg.m^{-3} to 600 kg.m^{-3} [1].

Polyurethane foams are used in automobiles as seat fillers, armrests, roof upholstery, door trim, carpet pads, noise and vibration insulation for engine compartments etc.

The implemented project is focused on the efficient design of the treatment of PUR waste from old vehicles. As the output is to be an optimized design of the technology of material (or energy) recovery of waste - polyurethane foams, it is necessary to quantify the quantities of this problematic waste from old vehicles in the Slovak Republic. In 2022, 49,354 old vehicles were processed. Based on an average vehicle weight of 1400 kg and a percentage by weight of PUR foam (foam) in the car of 1.75%, it is possible to conclude that 1210 tonnes of this problematic waste will be generated from old vehicles in 2022 alone.

However, in terms of designing and optimizing a technology suitable for the treatment and recycling of such waste from old vehicles, two objectives need to be pursued:

- recycling of pure polyurethane foam from seats,
- recycling of polyurethane foam from other parts of the vehicle, which has an integral surface layer, i.e. PUR foam injected directly into moulded parts, upholstery with adhesive surface layer – textile, leather, artificial leather (armrests, door upholstery, roof, etc.).

A significant problem is the recycling of the polyurethane foam which has an integral surface layer. This problem is currently not addressed. At the same time, for the conditions and annual quantities of waste PUR foam from old vehicles in Slovakia, it is necessary to design and optimize a technology that would allow material recycling of both types of waste, which would allow to:

- process pure polyurethane foam from the seats,

- process polyurethane foam from other parts of the vehicle, which has an integral surface layer,
- process these two types of waste together,
- produce flat and shaped recycled products.

4.2 Characteristics of PUR foam

PUR foams have been used since the 1940s and are now a fundamental material with a wide range of applications in many industries. The reaction of isocyanates with alcohols produces so-called urethanes (Fig. 4.1). These are esters of carbamic acid [2].

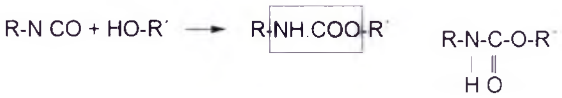

$$\mathrm{R{-}N\,CO + HO{-}R'} \longrightarrow \mathrm{R{-}}\boxed{\mathrm{NH.COO}}\mathrm{{-}R'} \qquad \mathrm{R{-}}\underset{\mathrm{H}}{\underset{|}{\mathrm{N}}}\mathrm{{-}}\underset{\mathrm{O}}{\underset{\|}{\mathrm{C}}}\mathrm{{-}O{-}R'}$$

Fig. 4.1 Scheme of the reaction of isocyanate with alcohol to form urethane.

Polyurethane foams should be distinguished in terms of mechanical properties into hard (e.g. refrigerator insulation, insulation in construction, insulation boards, sandwich building elements, etc.) and flexible (e.g. automotive seats, upholstery, mattresses, carpet pads, packaging material, etc.). Depending on which category a particular waste PUR foam falls into, it is possible to design a suitable technology for its subsequent processing and use. Possible examples of PUR foam applications are shown in Fig. 4.2.

 Car seats	 Mattress
 Consumables/packaging material	 Thermal insulation in construction

Insulation of refrigerators and freezers

Waste from production

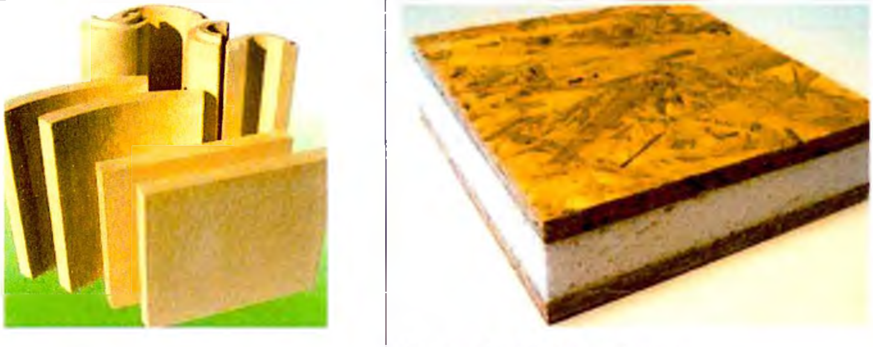

Shaped thermal insulation

Composite building elements

Fig. 4.2 Examples of the use of PUR foams – sources of waste.

4.3 Environmental impacts of recovery of PUR foams from old vehicles in Slovakia

Although the use of plastics in various industries is beneficial from an energy perspective (their production is less energy intensive, thus saving energy emissions), ecological (reducing emissions) and economic (saving raw material resources), it should not be forgotten that polymer materials are becoming a significant waste. Degradation processes release low molecular weight compounds that can be harmful to health or endanger the environment.

Waste PUR foams placed in landfills take up a huge volume. Without material and energy recovery, waste PUR foams from old vehicles alone would represent huge volumes of waste in landfills. The average density of PUR foams used in cars is about 30 $kg.m^{-3}$, with a weight of 1,210 tonnes in 2022, the volume of this landfilled waste would take 36,300 m^3. For the period 2014 to 2023, this waste from old vehicles alone, without further use, would amount to around 363,000 cubic meters.

The proposed technology of material recovery of PUR foam from old vehicles does not pose a risk to the environment, as there are no chemical reactions or pollution of the environment by solid dusts, liquids or gases.

4.4 Analysis of technological options for the recovery of polyurethane foams

The results of the status analysis showed that with regard to the total annual quantities of waste PUR foam from old vehicles, it is necessary to design and optimize a technology in Slovakia that that would allow for material recycling of both pure polyurethane foam from seats and recycling of polyurethane foam from other parts of the vehicle that have an integral surface layer. This problem is not currently being addressed.

Research, studies and testing have led to a number of areas and methods of recycling and using polyurethane that may be economically and environmentally feasible [3]. The four main categories [4] are: mechanical recycling, advanced chemical and thermo-chemical recycling, energy recovery, and recycling of the product itself (Fig. 4.3). Each method provides unique benefits that are particularly suited to specific applications or requirements [5, 6]. Mechanical recycling (i.e. material recycling) involves physical treatment, while in chemical and thermo-chemical recycling (i.e. raw material recycling) the waste is transformed into feedstock products or chemicals for the chemical industry. The energy recovery of this waste involves the full or partial oxidation of the material [7], the production of heat and power, and/or gaseous fuels, oils and coal, except for by-products such as ash which must be disposed of, [8]. Due to the typically long service life of products containing polyurethane, a fourth option – product recycling or so-called closed-loop recycling – is limited [9,10], as markets are changing rapidly and the concept of downcycling or open-loop recycling applies strongly to chemical-based products such as polyurethanes. Therefore, mechanical, chemical and thermo-chemical recycling and energy recovery are the only three ways to effectively recycle polyurethane [11].

Recycling of PUR foams

Mechanical recycling	**Chemical processing**	**Thermal-chemical processing**	**Energy recovery**
Recycling with re-bonding Adhesive pressing Forming under pressure Injection moulding	Hydrolysis Glycolysis Alcoholysis	Pyrolysis Gasification Hydrogenation	Incineration of municipal waste Fluid furnaces Rotary kilns Thermal degradation

Fig. 4.3 Overview of PUR recycling options [4].

Regardless of the recycling technology used, two factors play a key role in determining the technical and economic feasibility of recycling polyurethane materials:

a) increasing the density of the bulk polyurethane foams, enabling cost-effective transport from the collection point to the recycling plant,

b) size reduction of polyurethane products (mattresses, car seats, insulation boards, etc.) suitable for further processing in the selected recycling process.

4.5 Mechanical recycling

4.5.1 Disintegration of waste materials

An important and first step is to process the waste materials into smaller particles, which are then easier to process. This can be flakes, pellets or dust, depending on the type of PUR that is recycled. For polyurethane foams, recycling by grinding is used. The resulting dust can be reused as a filler in the production of new PUR foams. In other cases, waste material is shredded, [12]. The required fraction size for downstream processing of polyurethane ranges from particles smaller than 200 μm for reuse as fillers in polyurethane. The fine dust is further used in the recycling of polyurethane foams from car seats. For the production of fine powder, a two-roller mill is most commonly used. The essence of disintegration is a pair of cylinders rotating in opposite directions, each with a different circumferential velocity. The shear forces generated in the very narrow gap between the rollers turn the polyurethane foam into a fine powder with a typical particle size of less than 0.1 mm. This fine powder is sieved and stored in silos. It is then transported by screw conveyors and mixed with polyol. This mixture is conveyed to the mixing head, where it is reacted with isocyanate and then poured to form a flexible foam slab (Fig. 4.4). Up to 30 % recycled polyurethane powder can be added with this technology.

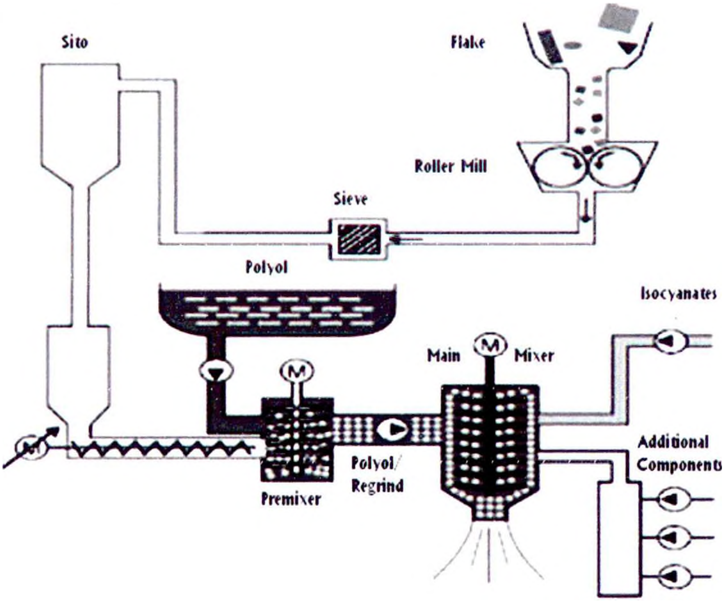

Fig. 4.4 Schematic of PUR recycling by regrinding.

For hard PU foams, particle sizes smaller than 85 micrometers can be achieved with ball mills. A crucial factor that limits the amount of waste PU foam recycled by grinding is the viscosity of the polyol and fine particle mixture that can be processed by the process equipment. In practice, it is possible to process a mixture of 15 wt% regranulate from grinding if MDI polyol is used, and up to 25 wt% if TDI polyol is used [5].

A major problem of grinding processes in waste treatment is their economics. Grinding waste PU foam to a size of less than 100 – 125 µm is no exception. However, one advantage compared to other (mineral) filling materials is that PU powder has a density like the new foam that is being produced. Overall, the recycling process with a recycled polyurethane mass fraction of 7 – 10 % in the new PU foam shows a cost saving of approximately 7.02 – 8.2 %, while the mechanical properties compared to 100 % new PU foam are almost unchanged [13]. Precision knife mills, pellet mills, impact disc mills or cryogenic grinding technologies are used in the disintegration of PUR waste foam.

Precision knife mills are special types of knife mills that have many static and rotating knives (Fig. 4.5). In these plants, screens are also used which are designed so that subsequent grinding of the cut material occurs in the chamber of the mill. Both flexible and rigid polyurethane foam materials are ground to particle sizes of less than 0.25 mm in this way. [12]

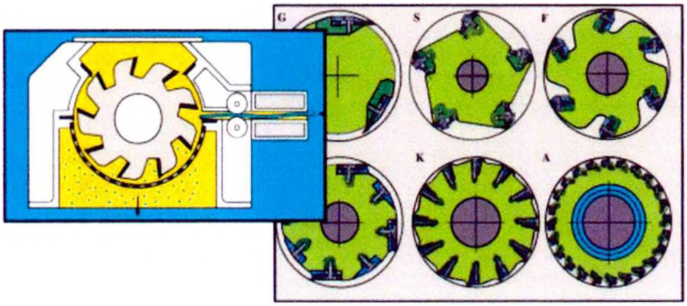

Fig. 4.5 Multi-knife rotors of precision knife mills.

Pellet mills use two or more metal rollers that push the processed material through a metal perforated matrix [12]. Depending on the type of foam technological conditions of the pelletising process, the product can be fine polyurethane powder or compact pellets. These pellets are suitable for energy use, as they suit the transport systems of combustion plants.

The impact disc mill disintegrates reaction-injected polyurethane waste (hard PU foams) in two stages. In the first stage, the material is granulated by a knife mill to a particle size of approximately 3 mm and then, in the second stage, the material is ground to powder by an impact disc mill (Figure 6). The typical output is a fine fractional composition, where up to 40 % is made up of particles smaller than 200 µm. Subsequently, the material is sorted through sieves and the larger fraction is returned to the grinding process.

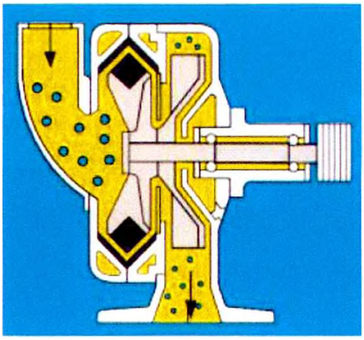

Fig. 4.6 Impact disc mill.

Cryogenic grinding. Due to the elastic nature of flexible polyurethane foams, grinding these materials to a fine fraction is often very difficult, especially when the material is heated during grinding. Therefore, it is very effective to cool this material below the embrittlement temperature, e.g. with liquid nitrogen.

Technologies for the fractional treatment of polyurethane foams are divided according to the type of PU foam (rigid, flexible). The type of effective technology, the achieved particle size fraction, as well as information on the manufacturers are given in Table 4.1.

Table 4.1
Available technologies for polyurethane fractionation

Type of polyurethane	**Size of particles [mm]**	**Technology**	**Manufacturer**	**Condition**
Hard PU foam	< 0.3	Precision knife mills	Pallmann	Prototype
	< 0.3	Pellet press	Kahl	Commercial
	< 0.2	Ball mill	Tecaro	Prototype
Flexible PU foam	< 0.3	Precision knife mills	Pallmann, Herbold, Alpine, Condus	Commercial
	< 0.3	Pellet press	Kahl	Prototype
	< 0.2	Shear extruder	Berstorff	Developed by
	< 0.2	Cryogenic grinding	Pallmann	Prototype
	< 0.2	High shear mixer	Silverson	Developed by
	< 0.1	Two-cylinder mill	Hennecke	Commercial
	< 0.1	Two-cylinder mill	Mobius Tech. Inc.	Commercial
	< 0.2	Impact disc mill	Pallmann	Prototype

In addition, recycled hard PU powder is an excellent material for absorbing oil spills [4]. Larger pieces are recovered for chemical processing or for energy recovery.

4.6 Known mechanical recycling methods

There are four basic methods of mechanical recycling: recycling with re-bonding, adhesive moulding, pressure forming, and injection moulding.

Recycling by bonding with the addition of a binder is one of the most widely used recycling processes. It has been in use for 30 years. It consists in a method of processing foam flakes obtained from recycling foam waste, e.g. by regrinding. The flakes are blown from the hoppers into the drum mixers. Here, the flakes are mixed with glue. The resulting mixture can be dyed and then compacted with a conveyor press. Stabilisation is carried out with the help of steam. With this procedure (Fig. 4.7) we can obtain new properties of PUR, e.g. higher density. The final stabilisation of the product is carried out by steam. The technology also includes high flexibility and wide variability in the mechanical properties of the finished products [12].

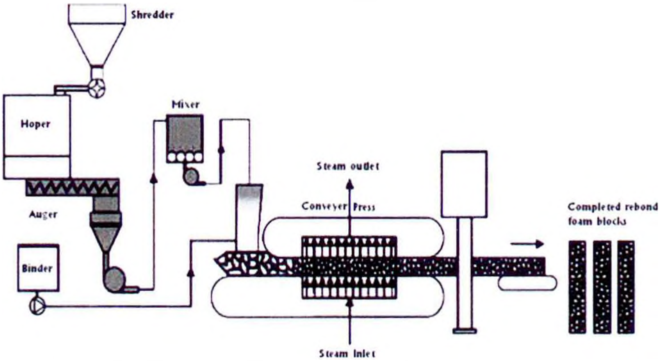

Fig. 4.7 Recycling scheme with re-bonding [12]

Adhesive moulding consists of layering polyurethane crumb and adhesive and then curing under the influence of temperature and pressure [10]. Moulded parts for the automotive industry, such as mats or spare tyre covers, are produced using this method. Adhesive moulding is applicable to many types of plastic waste and their mixtures. The crumbled PUR foam with a particle size of approximately 1 cm can be reassembled into a compact unit by the addition of MDI diisocyanate and subsequent compression moulding under temperature in the range of 100 – 200 °C and pressure of 3 – 20 MPa. The result is PU moulded parts, building boards with excellent water and moisture resistance, or insulation panels for use in new refrigerators and freezers. Waste PUR foam processed into blocks and then cut is used in carpet mats, parts of sports hall floors and furniture. Material recovery of the enormous amount of PU flexible foam (sponge) from old vehicles can satisfy a large part (in the USA, almost 50%) of the carpet underlay market, [5]. This recycling method is also very interesting for PUR foam from construction waste, but the processing method is more complicated and often impossible due to the flame retardants contained in this material [4].

Pressure moulding is a mechanical recycling technology which uses mainly reaction-injected polyurethanes as recycled raw material in moulds. It is possible to produce high-quality recycled products. The moulded parts contain 100 % recycled material. The processed waste is ground to fine particles and subjected to high pressures and temperatures to create a solid material that is ideal for many automotive applications. Pressure forming [14] involves forming polyurethane particles at temperatures and pressures high enough (180 °C, 35 MPa) to generate shear forces needed to melt and bond the individual particles together, without the need for additional binders. The technology focuses on the production of upholstery from the processing of polyurethane and polyurethanes obtained from old vehicles. It is suitable for the production of rigid and complex three-dimensional parts such as shaped pump and motor casings. Products produced in this way are particularly suitable for the automotive industry because they achieve high stiffness [5].

Injection moulding enables partial recycling of polyurethane. One method (Bayer high temperature pressing) processes granular polyurethane with a grain size of 250 to 1,000 µm at a temperature of around 180 °C and pressures greater than 35 MPa, making it possible to produce thermoformed products such as various automotive parts [15]. It consists in melting granulate from waste plastics, including the fine fraction of PU, in the extruder chamber by external heating and subsequent injection of liquid plastic into the mould. Injection can be done through a single extruder. Dual injection moulding with two (or more) extruders (Fig. 4.8) enables the recycling and reuse of waste thermoplastics and thermosets.

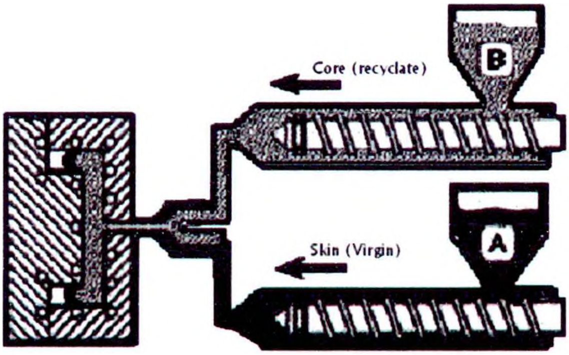

Fig. 4.8 Recycling and reuse of waste thermoplastics and thermosets by dual injection moulding [16].

The advantages of this technology lie in the increased mechanical properties of the product, in the higher surface quality, and in the possibility of any colour of the product.

4.7 Proposal of the appropriate technology for the stated project objectives

On the basis of an extensive analysis of technologies for the recovery of waste PUR foam, the technology for the formation of PUR recyclate under pressure will be further developed in detail for the above-mentioned project objectives as the only suitable and efficient technology meeting the requirements and satisfying the constraints, while allowing material recycling for the reuse of PUR in the automotive industry. This technology enables the recycling of pure PUR foams, as well as PUR foams with an integral surface layer. It enables the production of inherently flat insulating products, as well as shaped elements without the addition of binders or other chemical additives. The products find a wide range of applications due to their variability in shape, strength, density, etc. For the basic requirement of recycling PUR foams from old vehicles in Slovakia, pressure forming technology is highly investment efficient taking into account the quantities and diversity of this waste.

4.7.1 Detailed description of the technology

Pressed products contain 100 % recycled material. This pressure forming method, which primarily uses reaction-injected polyurethanes as recycled raw material in the moulds, is capable of producing high-quality recycled products. The recycled raw material is ground to fine particles and subjected to high pressures and temperatures to create a solid material that is ideal for many automotive applications. Pressure forming [14] involves forming polyurethane particles at temperatures and pressures high enough (180 °C, 35 MPa) to generate shear forces needed to melt and bond the individual particles together, without the need for additional binders. This technology focuses on the production of upholstery from the processing of polyurethane and polyurethanes obtained from old vehicles. Parts moulded from recyclate achieve guaranteed mechanical properties that may in fact be better than new polyurethane material. The technology is suitable for the production of rigid and complex three-dimensional parts, such as pump and motor casings. The method successfully utilises the recycling of reaction-injected polyurethanes in the production of automotive parts. The production of composite materials is not exceptional for this technology, e.g. by adding rubber granulate to recycled PU, aprons for cars or surfaces for athletic surfaces are produced. Also, a blend of 6 % recycled polyurethane and 15 % glass fibre can be used to make door panels and dashboards in cars. The recycling of polyurethane by compression molding with the product being a sandwich composite material also has great potential (Fig. 4.9). In this method, a layer of coarsely ground polyurethane waste (up to 30 % by weight of the product) is placed in the centre between reinforcing layers of glass fibres, which are covered on the outside with a layer of two-component polyurethane resin. Products produced in this way are particularly suitable for the automotive industry because they achieve high stiffness [5].

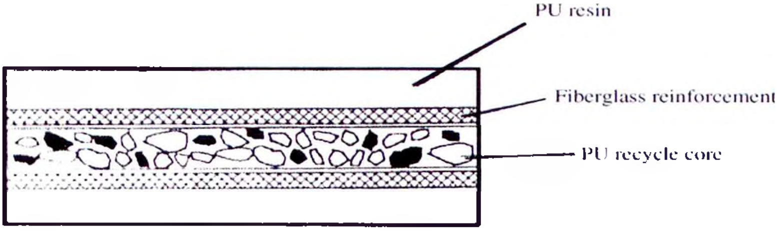

Fig. 4.9 Recycling of waste polyurethane by pressure forming into high stiffness sandwich materials [12].

4.8 Utilization of products from secondary raw materials

In the automotive industry, recycled polyurethane foam has great applications in soundproofing the bodywork and preventing vibration transmission. In addition to the excellent sound-insulating and damping properties, the thermal insulation properties of such products are also exploited. Compared to the new PUR foam, they have a higher density and hardness. In automobiles, they are used in the form of plates or belts as insulation to damp vibrations and transmit them to the cabin (e.g. engine compartment insulation, door insulation, etc.), Fig. 4.10.

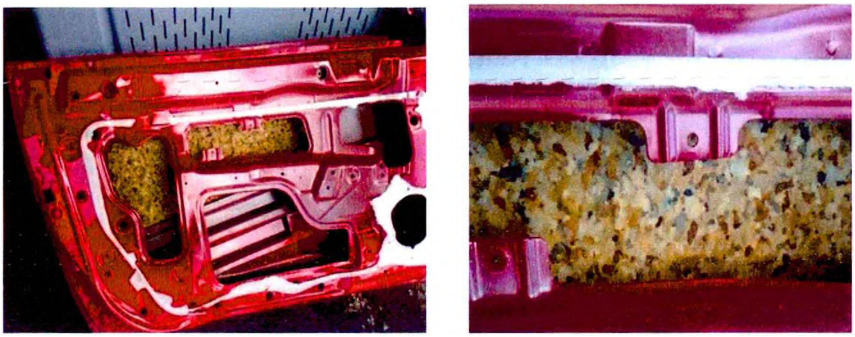

Fig. 4.10 Insulation for vibration damping in cars.

With the proposed technology of molding PUR recyclate under pressure, it is possible to produce other rigid and shape-complex moulded parts for the automotive industry, Fig. 4.11. Parts moulded from recyclate achieve guaranteed mechanical properties that may in fact be better than new polyurethane material.

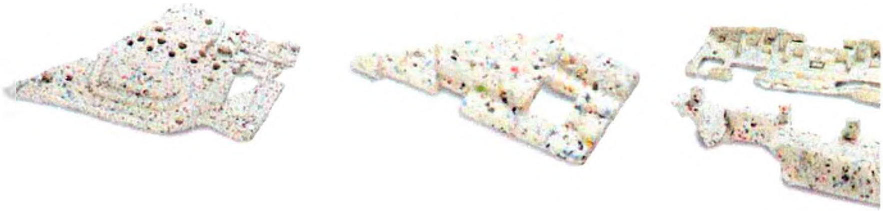

Fig. 4.11 Complex shaped parts from recycled PUR foam.

Thermal and acoustic insulation is used in the construction industry due to its excellent thermal and acoustic properties as an insulating element of walls or floors. This insulation is also suitable for soundproofing production halls. It can be produced either as plates, strips or blocks cut to the required thickness (Fig. 4.12). Due to its higher strength and density, which can be adjusted during recycling, it is also successfully used as a floor layer for sports halls.

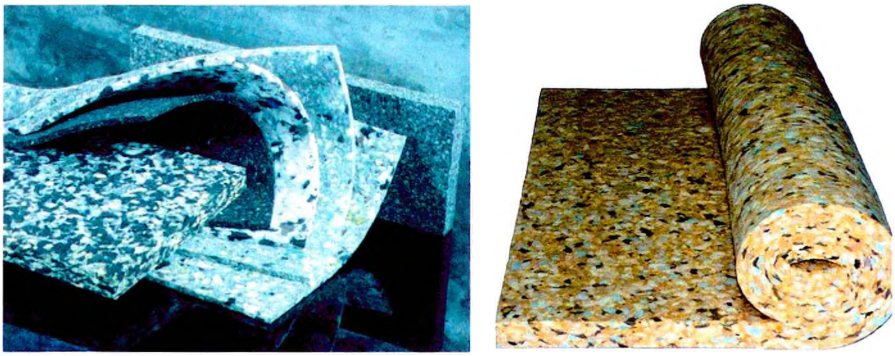

Fig. 4.12 Thermal and acoustic insulation in construction.

Impact noise insulation under parquet and laminate floors. This is the sound insulation of the floor (Fig. 4.13). It is this part of the floor that is often underestimated, made of unsuitable materials or implemented with inappropriate technology.

Conventional insulation, especially thermal insulation, has problems especially at low frequencies and cannot eliminate the noise sufficiently. Stamping, banging, walking are exactly the sounds at a low frequency. It is therefore very important to choose suitable material, effective even at low noise frequencies. The most important characteristic of a suitable impact noise insulation is elasticity. The higher the elasticity of the impact noise insulation, the better it eliminates noise, especially at low frequencies.

Benefits:

- effective reduction of impact noise (e.g. when walking),
- excellent acoustic properties,
- suitable insulation for the floors of living rooms of family or apartment buildings.

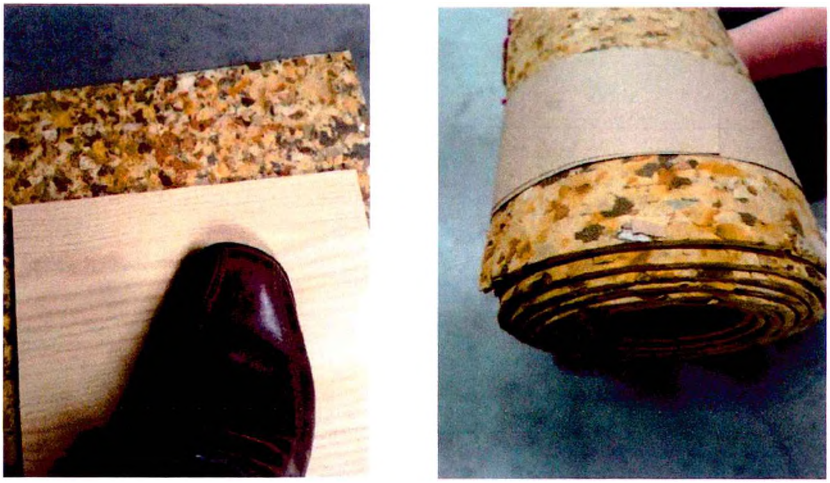

Fig. 4.13 Floor impact noise insulation

Carpet underlays give the carpet significantly increased walking comfort together with sound and thermal insulation. Recycled foam pads (Fig. 4.14) are made from recycled polyurethane foam, whereby using pressure and heat, this recyclate is compressed together to form a dense, flexible and lightweight pad with excellent impact noise comfort. These pads offer excellent thermal and acoustic insulation. The pads are recyclable, thus significantly saving the environment.

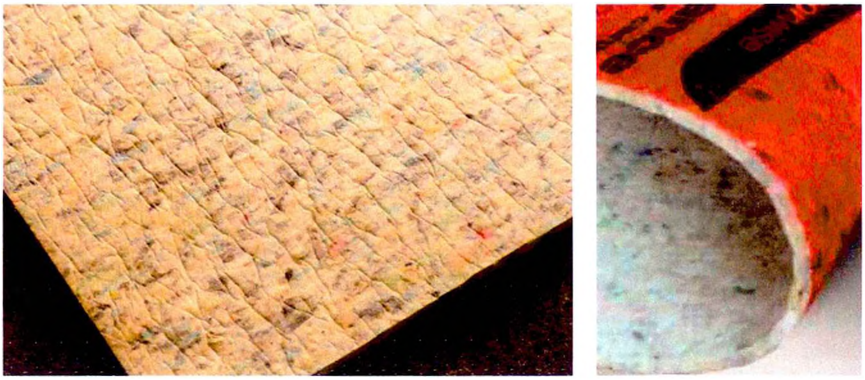

Fig. 4.14 Carpet pads.

Other applications of waste PUR foam recyclates

The products can also be installed in white goods (Fig. 4.15), in doors and windows (Fig. 4.16), in machines, in various equipment and in structures as an acoustic element with a noise absorbing function (Fig. 4.17). Thanks to its excellent thermal insulation properties, it can contribute to reducing the energy consumption of buildings. They can be recycled again and turned into the same or a completely new product.

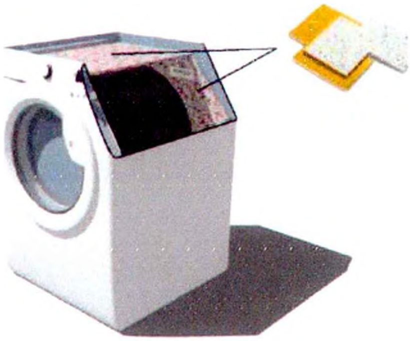

Fig. 4.15 Acoustic filler in white goods.

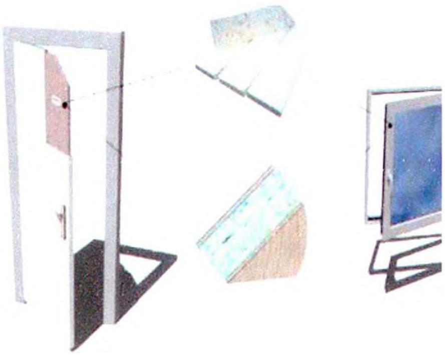

Fig. 4.16 Acoustic and thermal infill for door and window systems.

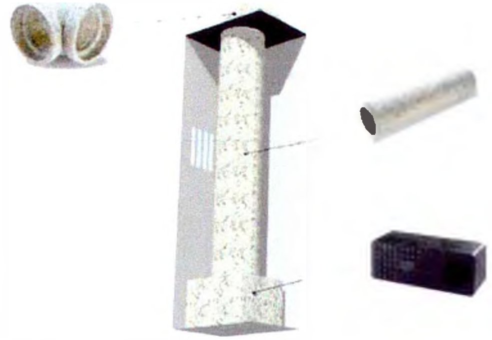

Fig. 4.17 Acoustic infill in exhaust and ventilation systems, thermal insulation of duct systems.

Products made from recycled PUR foam, thanks to their excellent thermal insulation properties, can contribute to reducing the energy consumption of buildings. Such products can be recycled and turned into the same or a completely new product again.

4.9 Experimental development and optimisation of the proposed technology

Within the experimental development of technology for the application of material recycling of waste PUR foams, especially from old vehicles, the aim is to define suitable (optimal) technological conditions for the production of shape-complex and precise elements.

Fig. 4.18 Acoustic infill in vehicle interiors and infill for car seats.

Based on the information from the analysis, we defined the compaction conditions of the PUR foam:

- compaction without the addition of a binder, at the temperature at which the flexible PUR foam softens, the edges of the individual flakes are melted and the interconnection of the particles can occur due to the action of pressure,
- in addition to size and shape, the 2D or 3D product must meet the required strength and density for the intended application,
- The fraction was undercut to 2.0 – 15.0 mm, Fig. 4.19.

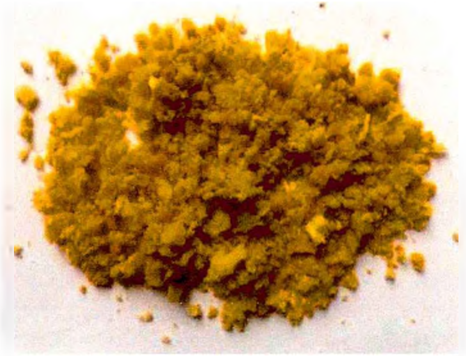

Fig. 4.19 Size fraction of the crushed PUR foam (2.0 – 15.0 mm).

The decisive technological parameters investigated in the experiments were the effect of pressing temperature, pressing force and endurance time. Proposed parameters of the verification experiment: pressing temperature: 200 – 300 °C, (200, 220, 250, 300) pressing force: 10 – 40 N, (10, 20, 30, 40) residence time at temperature under pressure: 10 – 25 minutes (10, 15, 20, 25) while we varied only one parameter at a time, the other parameters were unchanged during the experiments. The starting temperatures of the experiments were 200 °C, 10 N pressure and an endurance of 10 min.

4.10 Parameters affecting the quality of the moulding

The pressing temperature **has a decisive influence on the quality of the experimental samples.** At the lower limit of the pressing temperature (200 °C), compactness of the experimental sample occurred, but its strength and cohesiveness were minimal. The resulting moulding was virtually not joined at all, Fig. 4.20. Already at minimum tension, the test specimen failed. Upon closer analysis, we found that there was virtually no softening of the material and no melting of the flakes.

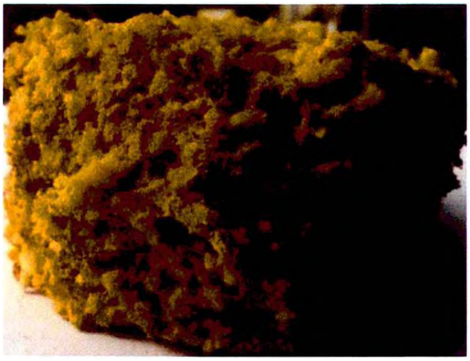

Fig. 4.20 Non-compliant moulding under inappropriate process conditions (150 °C; 2.0 MPa; 12 min endurance).

Already the increase in temperature to 250 °C degrees had a very significant effect on the increase in tensile strength of the test specimen. The experimental mouldings are cohesive, have a solid structure and hold their shape and volume, Fig. 4.21. The average density of the experimental samples is 1.2 g.cm^{-3}, which is a suitable density for these pressing methods.

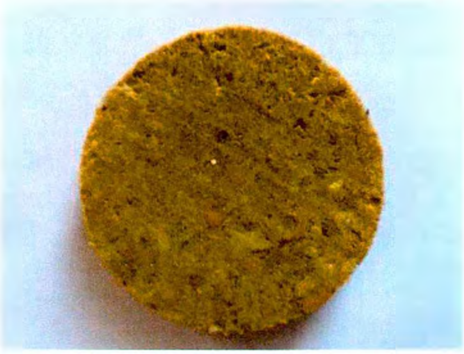

Fig. 4.21 Resulting moulded element at optimum process conditions (200 °C; 5.7 kPa; 12 min endurance).

Conversely, at 300 °C, there was significant toasting of the edges of the over crushed fraction. The second significant parameter is the **time of endurance**. Increasing the endurance time from 10 to 25 minutes had an effect on the cohesiveness of the examined samples.

On the contrary, preliminary experimental tests showed that the pressing force had the least effect on the strength of the test specimens. Even by increasing its value, we did not observe a significant increase in the quality of the experimental samples, Fig. 4.22. The magnitude of the pressing pressure has an effect on the density of the experimental samples.

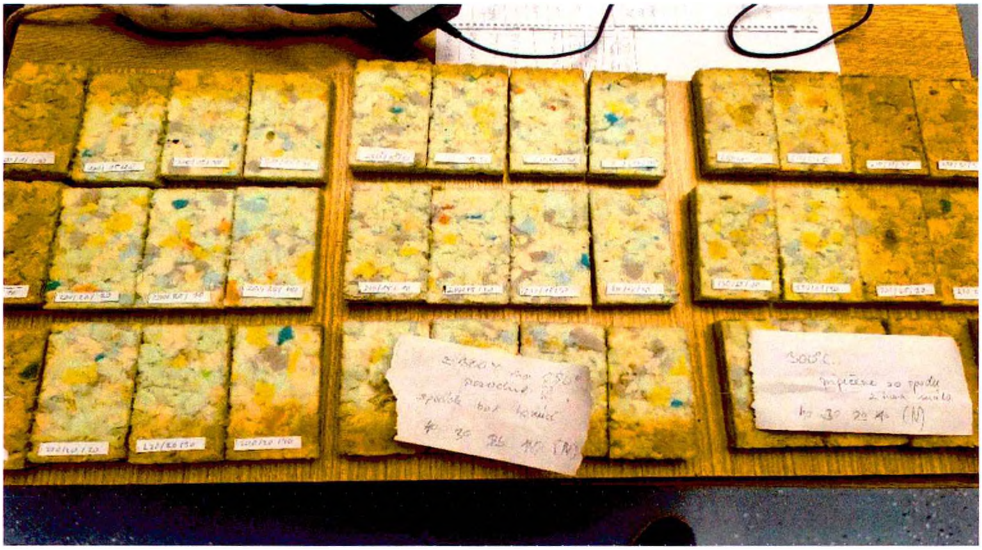

Fig. 4.22 Test specimens in the validation experiment.

4.11 Further research developments

It should be noted that these were only the first validation tests of the experimental samples. We will analyse, verify and repeat these tests very rigourously as needed. Testing of samples for tensile strength, flexural strength and determination of the required density for the mouldings is currently underway. Other parameters such as steam are likely to be added to the monitored parameters (temperature, pressure, endurance). The final results of these tests will be used in the definition of requirements and in the design of experimental equipment for the production of shape test specimens.

4.12 Conclusion

In conclusion, the proposed and verified technology for material recycling of waste PUR foam forming under pressure is suitable for the production of shaped precision elements with a wide application not only in the automotive industry under appropriate technological conditions. The excellent acoustic, damping and thermal insulation properties of this material implemented in the form of shaped elements predestine it for a wide range of applications in practice. This method of recovering waste polyurethane foam materials, not only from old vehicles, has a very positive economic and environmental effect.

References

[1] Liptáková, T., et al. 2012. Polymer construction materials (in Slovak). 1st ed. Žilina: EDIS, 190 p.

[2] Meekum, U., Kenharaj, R. 2002. Comparative study of polystyrene foam degradation in the open-air and artificial weathering exposure. The Arabian Journal for Science and Engineering, 27, 1C, 25–32.

[3] Howard, G.T. 2002. Biodegredation of polyurethane: a review. Int. Biodeterior. Biodegrad. 49, 245–252.

[4] Weigand, E. 1996. Properties and applications of recycled polyurethanes, In: J. Branderup, M. Bittner, G. Menges, W. Micheali (Eds.), Recycling and Recovery of Plastics, Hanser Publishers, Munich, Germany, 1996, section 7.10.

[5] Scheirs, J. 1998. Polymer Recycling, John Wiley & Sons, Chichester, 1998, chapter 10.

[6] Frisch, K.C., Klempner, D., Prentice, G. 1999. Advances in Plastic Recycling, 1st ed. Technomic Publishing Co (1 May 1999), 250 p.

[7] Troitsch, J. 1990. International Plastics Flammability Handbook, Hanser Publishers, Munich.

[8] Alliance for the Polyurethanes Industry. [15/06/2024]. Available on: <http://www.polyurethane.org/recycling>.

[9] DeGaspari, J. 1999. Mechanical Engineering Magazine (ASME) June 1999. Alliance for the Polyurethanes Industry. Available on: <http://www.polyurethane.org/recycling>.

[10] New Forecasts for Polypropylene, Polystyrene and Polyurethane, Gobi International, May 20, 2002.

[11] Huntsman Polyurethanes. [15/06/2024]. Available on: <http://polyurethanes.huntsman.com>.

[12] Zia, K.M. Bhatti, H.N. Bhatti, U.A. 2007. Methods for polyurethane and polyurethane composites, recycling and recovery: A review. Reactive & Functional Polymers, 67, 675–692.

[13] Stone, H., Villwock, R., Martel, B. 2000. Recent technical advances in recycling of scrap polyurethane foam as finely ground powder in flexible foam. Mobius Technologies, presented at Polyurethanes Conference, 2000, 7 p.

[14] Hulme, A.J. Goodhead, T.C. J. 2003. Mater. Proc. Technol. 139, 322–326.

[15] Held, S., Hicks, D.A., Hart, M. 1999. Proceedings of R'99 Recovery Recycling Re-integration, Geneva (Switzerland) February IV., 92–97.

[16] <http://www.warwick.ac.uk/atc/materials/recyclecentre/seminar/paper7>.

5 Material Recycling Perspectives of Discarded Lithium-Ion Automotive Batteries

5.1 Introduction

Current official doctrine proclaims that the earth is undergoing global climate change, which is significantly caused by human activity, mainly through the production of greenhouse gases such as carbon dioxide, methane, nitrous oxide and fluorocarbons, which are released from the combustion of fossil fuels, agricultural activity, industrial production and other human activities. Global warming is one of the most significant phenomena related to climate change, with significant negative impacts on the environment and human society. That is why there is currently a lot of pressure to reduce greenhouse gas emissions and switch to cleaner and more sustainable renewable energy sources. Other steps include, for example, improving energy efficiency, promoting low-carbon transport and agriculture, reducing waste and so on.

A very important segment of contemporary industrial society is the development and application of e-mobility in everyday life with the aim of reducing emissions, which is significantly influenced in particular by political decisions on a global scale, although these are not always entirely rational. As part of the rapidly expanding automotive sector, there has recently been a great deal of political pressure to reduce the use of internal combustion engines and replace them with alternative electric powertrains. The EU MEPs backed a proposal in June 2023 to ban the sale of new cars with internal combustion engines after 2035. This means that from this date, new cars and light commercial vehicles will have to meet the zero CO_2 emissions criterion. The Environment Council has also agreed on a more ambitious target to reduce these emissions by 55 %, or 50 % by 2030. In practice, the measure means banning the sale of petrol and diesel cars and switching to electric cars.

The power source for electric vehicles (EVs) and hybrid vehicles (HEVs) is currently lithium-ion traction batteries. These have an understandably limited lifespan. Current batteries in EVs last between 1,500 and 3,000 charge cycles, after which their capacity is expected to drop by about 30 % and LiA will be refurbished. Remanufacturing a LiA electric vehicle is a more cost-effective solution than immediate recycling. Manufacturers estimate that a reclaimed battery has a lifespan of an additional 10 to 15 years, dramatically extending the usefulness of batteries and reducing their overall carbon footprint. LiA can provide an additional 5 to 8 years of service, for example as energy storage for distribution system needs [1].

As such, the lithium-ion traction battery LiA is undergoing a very dynamic development, which is basically directed simultaneously in several directions, in particular design optimization, material optimization, simplification of operation, improvement of safety, reduction of economic intensity, versatility, possibilities of reuse and recycling at the end of service life, and so on.

In any case, after a certain relatively long period of time, the discarded LiA will have to be recycled. This longer time provides some advantages, as LiA material recycling is essentially a new phenomenon and LiA recycling capacity needs to be thoroughly studied, verified and built [2, 3]. Recycling of discarded LiA is an expected and necessary process due to the valuable constituent content as well as the hazardous nature of discarded LiA.

From the initial discovery of LiA´s in the 1970s through the 2019 Nobel Prize for their discovery, the use of LiA on a global scale has been increasing exponentially [4-7]. Depending on their increasing use, their production and recycling or disposal are becoming subject to political pressures, but also to environmental concerns [8, 9].

World supplies of metals without which LiA´s cannot exist, such as lithium, cobalt, nickel and other metals, are limited and unevenly distributed, while their extraction is energy and production intensive and polluting [10, 11]. More than 70 % of the world's cobalt production

comes from the Congo [12], with no other country producing more than 5 %. China and Mozambique produce 70 % of the world's natural graphite, an important material for LiA anodes [13].

The availability and exploitable natural resources are influenced by multiple, often unpredictable and uncontrollable influences, such as natural disasters, wars, or resource allocation decisions and ownership relationships. In the case of LiA this is particularly noticeable, especially in terms of lithium, cobalt and graphite. This is also the reason why these raw materials have been included in the list of critical raw materials for the European Union [14]. This also applies to the current military conflict in Ukraine. Ukraine is generally perceived as the breadbasket of Europe, but it has some of the world's largest reserves of titanium and iron ore, as well as untouched lithium deposits and extensive coal deposits. The total value of the raw materials is in the order of tens of billions of dollars. Here, too, one must look for a strong interest on the part of the parties and their allies in this conflict.

Resource scarcity and supply are particularly important given the relatively short lifespan of equipment, whether physical and/or marine depreciation, the drive for continued profit for manufacturers by "upgrading" to newer models of equipment, or the relatively frequent rapid end-of-life of LiA. The reality at present is that most of the discarded LiA´s end up in landfill, as there are still no economically viable ways to treat discarded LiA´s.

In February 2019, more than 5.6 million electric vehicles (EVs, HEVs) were registered globally, a 64 % increase from 2018 [15]. By 2040, global sales of all EVs, HEVs are projected at 58 % [16]. There are currently around 9,500 registered electric vehicles in Slovakia [17], which is only a third of the expected number. On the other hand, if a ban on the sale of internal combustion engine cars in the European Union after 2035 becomes a reality and only electric and hybrid vehicles are sold, the pressure to dispose of them at the end of their useful life will increase. Particular attention must be paid to the treatment of traction LiA due to the valuable constituents it contains as well as its hazardous nature.

In the European Union, LiA recycling is currently covered by Directive 2006/66/EC. This directive requires the recycling of fifty percent of the average weight of used batteries, including used LiA´s [18]. According to this Directive, lithium-containing e-cells are considered as other waste. However, this has now been surpassed, especially with regard to lithium-containing e-cells, as LiA were practically not used in 2006.

On 18 February 2024, regulation (EU) 2023/1542 of the European Parliament and of the Council of 12 July 2023 on batteries and waste batteries came into force, amending Directive 2008/98/EC and Regulation (EU) 2019/1020 and repealing Directive 2006/66/EC - Battery Regulation [19]. In this directive, the procedure for processing discarded LiA is significantly discussed and modified.

Material recycling of LiA is a challenging process, as LiA has a complicated structure that includes cathode, anode, electrolyte, separator and current collectors along with packaging materials and necessary electronics. According to the International Energy Agency, the EV-HEVs produced in 2019 contain up to 500,000 tons of LiA waste and the total amount of waste produced by 2040 could be up to 8 million tons [20].

The Paris-based agency has published a report on the role of critical materials in the clean energy transition. It states that a typical electric car requires six times more mineral inputs than a conventional vehicle. Nine times as many minerals are needed to build a wind power plant as for a gas power plant. If the old continent is to meet the Paris Agreement targets, this means quadrupling the requirements for minerals for clean energy production already by 2040. Such high demand raises legitimate questions about the availability and sustainability of raw material supply and production. The World Bank estimates that three billion tonnes of minerals and metals will need to be extracted by 2050, requiring the opening of 50 new lithium mines, 60 nickel mines and 17 cobalt mines. It is argued that the transition to clean fuels is more of a commodity transition than an energy transition. Given the huge demand and the short lead time, this will be a very turbulent period. It all points clearly to the fact that recycling of discarded LiA´s is an essential requirement of very high priority [20].

As one of the most significant challenges of the waste industry is the management of end-of-life traction LiA´s in the dynamically developing electric vehicle sector. They represent a potentially very dangerous waste, but, on the other hand, they are the source of very important materials that must be recycled with regard to their price and scarcity. It is not negligible that some components, such as cobalt, graphite, and lithium, contained in LiA belong among the critical raw materials for the European Union. Recycling of LiA is an important way to gain these critical raw materials, but, on the other hand, it is a complicated and demanding process, since it is a complex composite material and its character, as well as electrical and chemical properties, pose a serious risk in terms of safety and the protection of health.

5.2 Current state of the issue

The lithium battery is a rather complex system made up of different materials and operating at different levels, as shown in Fig. 5.1.

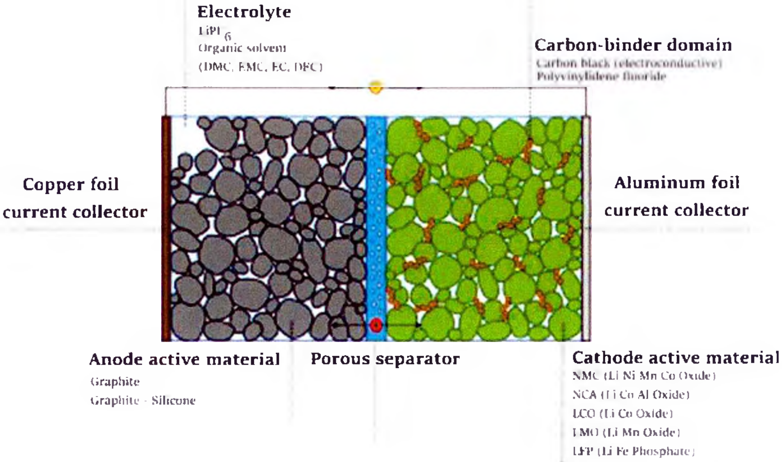
Electrolyte
$LiPF_6$
Organic solvent
(DMC, EMC, EC, DEC)
Carbon-binder domain
Carbon black (electroconductive)
Polyvinylidene fluoride
Copper foil current collector
Aluminum foil current collector
Anode active material
Graphite
Graphite - Silicone
Porous separator
Cathode active material
NMC (Li Ni Mn Co Oxide)
NCA (Li Co Al Oxide)
LCO (Li Co Oxide)
LMO (Li Mn Oxide)
LFP (Li Fe Phosphate)

Fig. 5.1 Schematic view of the main components of LiA [21]

The basic unit of LiA is a body consisting of a copper foil, representing the current collector, on which a porous anode material is placed consisting of graphite or silicon particles fixed with a binder. The space between the anode and cathode is separated by a polypropylene or polyethylene separator. The porous cathode is formed by an active material mixed with conductive carbon and a polymer binder polyvinylidene fluoride PVDF. The cathodic conductive collector is made of aluminium foil.

The porous electrodes and the separator are soaked with an electrolyte consisting of a $LiPF_6$ salt dissolved in a mixture of organic solvents, such as dimethyl carbonate DMC, ethyl methyl carbonate EMC, ethylene carbonate EC, cyclohexylbenzene CHB, and diethyl carbonate DEC) [22]. These materials are placed in layers hundreds of microns thick or less, often interleaved, and stored in a steel or aluminium casing or in a flexible casing wrapped with aluminium foil [23, 24].

The composition of the anode is essentially uniform and consists of graphite allowing intercalation of lithium [25]. The active anode material is bonded with a PVDF binder, allowing good adhesion to the current collector film [26].

In contrast to the anode, the composition of the cathode is more complicated due to conductive components such as soot and PVDF binder, different chemical composition of the cathode active material, which is due to the manufacturing processes and materials of the different manufacturers. Lithium cobalt oxide $LiCoO_2$ (LCO), lithium manganese oxide $LiMn_2O_4$ (LMO), lithium nickel manganese cobalt oxide $LiNi_xMn_yCo_{1-x-y}O_2$ (NMC), lithium nickel cobalt aluminum oxide $LiNi_xCo_yAl_{1-x-y}O_2$ (NCA) and lithium iron phosphate $LiFePO_4$ (LFP) are used as cathode active materials [27]. These differences are usually due to the use of individual cells in individual devices, such as smartphones, laptops, cameras, etc., hence their characteristics and, in turn, production costs.

For the EV and HEV segment, NMC cathodes are usually specified. They tend to have a different stoichiometry in the range of $LiNi_{0.33}Co_{0.33}Mn_{0.33}O_2$ and $LiNi_{0.5}Co_{0.3}Mn_{0.2}O_2$

to $LiNi_{0.6}Co_{0.2}Mn_{0.2}O_2$ and $LiNi_{0.8}Co_{0.1}Mn_{0.1}O_2$ in order to achieve various LiA properties [28].

The composition of LiA indicates the possibilities of obtaining valuable components by recycling this secondary raw material. Recycling makes it possible to recover valuable scarce metals, thus saving primary raw materials [29, 30].

Based on published experimental studies, it appears that recycling processes of discarded LiA start with pre-processing using physical-mechanical treatment procedures. These include the discharge of residual voltages, disassembly, reduction and sorting of the mainly pure components found in LiA as part of the composite structure. The next step is the application of physical or chemical processes, such as thermal or hydrometallurgical processes [31, 32].

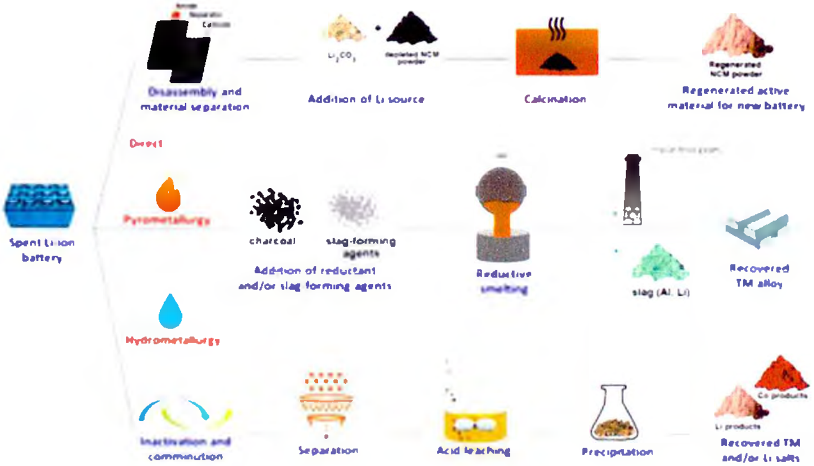
Anode
Separator
Cathode
Disassembly and material separation
Li_2CO_3
Depleted NCM powder
Addition of Li source
Calcination
Regenerated NCM powder
Regenerated active material for new battery
Direct
Spent Li-ion battery
Pyrometallurgy
charcoal
slag-forming agents
Addition of reductant and/or slag forming agents
Reductive smelting
slag (Al, Li)
Recovered TM alloy
Hydrometallurgy
Inactivation and comminution
Separation
Acid leaching
Precipitation
Co products
Li products
Recovered TM and/or Li salts

Fig. 5.2 Industrial treatment of discarded LiA at present [33]

Fig. 5.2 schematically illustrates the general sequence of industrial treatment of discarded LiA currently implemented by OnTo, Umicore and Recupyl in their recycling processes [33].

Historically, LiA recycling methods were initially developed through mechanical processing, where the results were an attempt to recover elemental copper, elemental aluminium and possibly plastics. From this perspective, these were relatively simple processes with a tail-end in which copper and aluminium were obtained by high-temperature smelting processes. However, it was obvious that particularly valuable components such as lithium, cobalt, and nickel also needed to be extracted, especially as their price was rising dramatically, as shown in Tab. 5.1, which shows that metal prices have recently risen dramatically, on average by as much as 100 per cent or more relative to 2020 [34]. The above data reflect the increase in the commodities monitored, especially metals, due to the global recession and economic crisis, and in 2022 the price of LiA waste, converted to pure metals, will reach more than three times the price in 2020. Undoubtedly, this was an interesting motivation for potential recyclers. Currently

(April 2023) prices are falling and have reached the 2021 level, which is still an interesting price level.

Tab. 5.1

Material composition of LiA in terms of prices of individual components

Component	Component percentage [%]	2020		2021		2022		2023		
		Component (price in US$/t)								
		price	price in LiA	price	price in LiA	Price	Price in LiA	Price	Price in LiA	Price portion [%]
Lithium (Li_2CO_3)	1(5.32)	8000	426	24800	1319	80250	4269	49100	2455	71
Cobalt	3	33965	1019	55755	1673	82000	2460	34500	1035	
Nickel	3	14554	437	19825	595	32445	973	24165	725	
Manganese	3	1667	50	7520	226	7039	211	6440	193	
Copper	9	6810	613	9860	887	10200	918	9080	817	29
Aluminum	35	1744	610	3076	1077	3214	1125	2356	825	
Graphite	8	500	40	970	78	1310	105	1400	112	
Steel	9	295	27	445	40	510	46	418	38	
Plastics	11									
Volatile components	8									
electronics	3									
cabling	2									
	together		**3222**		**5895**		**10107**		**6200**	

Tab. 5.1 shows that the LiA recycling processes used so far, aimed at obtaining mainly metals in the elementary form of copper, aluminium, etc., are relatively simple, but the financial benefit is only about one third of the total potential and represents about 30 % of the profit. Elements with a high price - lithium, cobalt, nickel etc. are bound into complex oxides externally in the active black mass and electrolyte and account for around 70 % of the possible gain. These components cannot be obtained by mechanical means, but only by physical-chemical means. While in the first case pyrometallurgical processing is mostly involved, in the case of extraction of components from compounds, hydrometallurgical methods are applied. Due to the continuous dynamic developments in LiA design and composition, recycling methods for LiA processing are quite difficult to optimize. Therefore, the possibilities of pyrometallurgical as well as hydrometallurgical recycling of LiA at the laboratory as well as semi-operational and industrial scale are continuously being investigated [35-37]. In both cases, the physical-mechanical pretreatment of discarded LiA is included in the process [36].

There are currently a number of scientific and technical publications on the possibilities of material recycling and often, due to the structural and material complexity of LiA, these are focused on certain specificities.

Fig. 5.3 graphically shows the evolution of LiA waste prices over the last period.

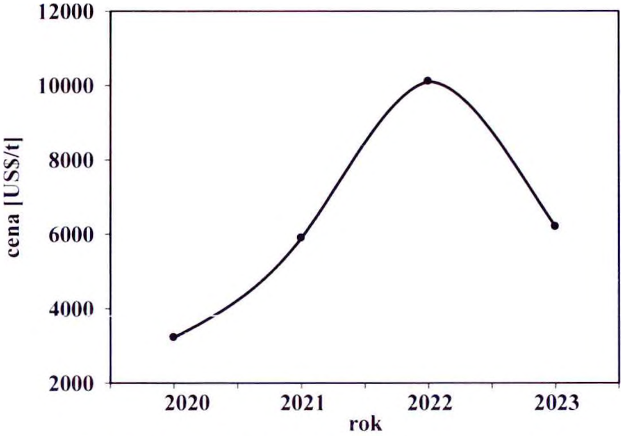

Fig. 5.3 Development of the LiA waste price

A draft general scheme for the treatment of end-of-life automotive LiA is shown in Fig. 5.4.

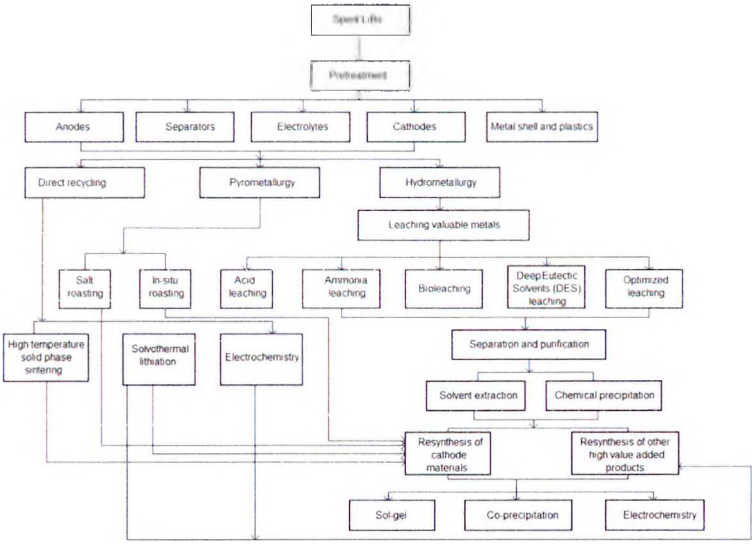
Spent LIBs
Pretreatment
Anodes
Separators
Electrolytes
Cathodes
Metal shell and plastics
Direct recycling
Pyrometallurgy
Hydrometallurgy
Leaching valuable metals
Salt roasting
In-situ roasting
Acid leaching
Ammonia leaching
Bioleaching
Deep Eutectic Solvents (DES) leaching
Optimized leaching
High temperature solid phase sintering
Solvothermal lithiation
Electrochemistry
Separation and purification
Solvent extraction
Chemical precipitation
Resynthesis of cathode materials
Resynthesis of other high value added products
Sol-gel
Co-precipitation
Electrochemistry

Fig. 5.4 Block diagram for the treatment of end-of-life automotive LiA [38]

The above scheme shows that several different procedures can be applied to the different steps of obtaining useful components. These need to be experimentally tested and optimised for specific types of discarded LiA.

Although formally classified as other waste in the Waste Catalogue [39], discarded LiA is potentially hazardous waste due to the explosivity, flammability, small particle size and toxicity of some of its constituents. A new Regulation of the European Parliament and of the Council on batteries and used batteries, repealing Directive 2006/66/EC and amending Regulation (EU) 2019/1020 [40], which should address some disputable issues, is currently in the process of being drafted and approved.

In any case, recycling of discarded LiA is a potentially environmentally hazardous as well as costly process [41].

5.3 Experimental part

Before the actual recycling procedure, it is necessary to take into account the fact that the electric cells in an EV or HEV are themselves designed in three groups as the electric cell itself, the battery module and the battery pack, as described in Tab. 5.2.

Tab. 5.2
Breakdown of batteries for automotive powertrain

Classification	Definition	View
battery cell [42]	A basic LiA unit, generating electricity by charging and discharging. It is made of cathode, anode, separators and electrolyte inserted into a rectangular aluminium housing.	
battery module [43]	Battery pack inserted in the frame in a precisely defined quantity to protect the cells from external shocks, vibrations or thermal shocks	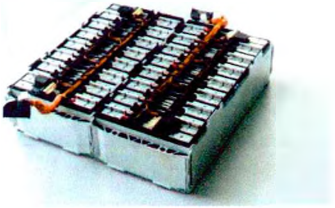
battery unit [44]	The final shape of the battery system installed in the EV/HEV. It is composed of modules and various control and protection systems including electronic control, cooling, etc. Usually contains 8 modules of 12 cells per battery	

The representation of the individual materials in each battery segment varies in this way, as the more robust an individual segment is, the more it contains other devices. The different amounts of components in LiA are due to the fact that the cells themselves are placed in cases, packaging, etc., while other electronic control and protection devices are present.

This fact significantly influences the economic calculations of recyclers, both in terms of investment and operating costs in relation to the size of the units processed and in terms of the expected yields and efficiencies of the recycling processes.

In this respect, the following procedures for the treatment of discarded LiA, or a combination thereof, are generally used:

- physical and mechanical pre-treatment
- pyrometallurgical processing
- pyro-hydrometallurgical processing
- hydrometallurgical processing

This order is also true historically – initially there was interest in obtaining the pure metals copper, aluminium iron, and since these are found in LiA in the elementary form, it was sufficient to apply physical and mechanical treatment procedures and then to remelt the pure metals after slight treatment (pressing, briquetting). The rest, however, was lost to waste. However, this residue contains very valuable components (Li, Co, Cr, etc.) which are usually of a hazardous nature due to the form of their presence. Therefore, gradually hand in hand with the progress of scientific research, more sophisticated pyro-hydrometallurgical and hydrometallurgical methods of their processing, or the processing of residues after physical-mechanical treatment, began to be applied in order to obtain these valuable components.

In the timeline, the scopes of the solution of this project dealt with theoretical study, material analysis, discharge of residual stresses, laboratory and semi-operational solution of LiA material recycling. In the first phase, the recycling and recovery of useful components, in particular metallic aluminium, copper, iron in elemental form, as well as active black mass and plastics contained in LiA were addressed. These metals are present in LiA in some quantity (Tab. 5.1), which on the basis of conventional economic analysis evokes a possible profit. These are recycled based on relatively simple recycling procedures.

However, discarded LiA´s also contain valuable metal components in the form of their complex compounds in the cathode, anode mass or electrolyte. These are mainly lithium, cobalt, nickel, manganese, but also graphite. The price of these components in their pure form significantly exceeds the prices of copper, aluminium, iron, etc. and therefore need to be recycled and recovered.

Therefore, the main focus of this project in the last year of solving was to focus on the treatment of black mass, but mainly on the design of a comprehensive treatment of discarded LiA´s in Slovak conditions.

After the residual voltages were discharged, the discarded LiA was crushed, and the resulting mixture was subjected to sieving. The individual grain size fractions obtained were also different at first glance. The presence of copper and aluminum particles, as well as plastic and black mass in the mixture, can also be observed by the naked eye.

Closer examination by optical microscopy (Fig. 5.5) may show the presence of golden red particles, which are represented by copper, grey to black particles, which are represented by either aluminium or plastic from the separators, both contaminated with black mass, and black mass itself, which is concentrated into fine grains. Likewise, the distribution of these particles into individual grain classes can be seen. Copper was mainly concentrated in the grain class +1 – 2 mm, aluminum in class +2 – 4 mm and separators in class +4 mm. However, the aluminum and separators are probably mixed, and there are more separators in the mixture with larger particles.

The finest particles are formed by black mass, and it was not possible to determine their form. Therefore, they were subjected to diffraction phase analysis.

The x-ray diffraction phase analysis has shown the presence of graphite and $LiNiO_2$, which represent the anodic and cathodic black mass (Fig. 5.6). It has been demonstrated that the "black matter" is not homogeneous material. Phase analysis pointed to the presence of carbon, $LiNiO_2$, $LiMn_2O_4$, or complex LiNiMn oxide.

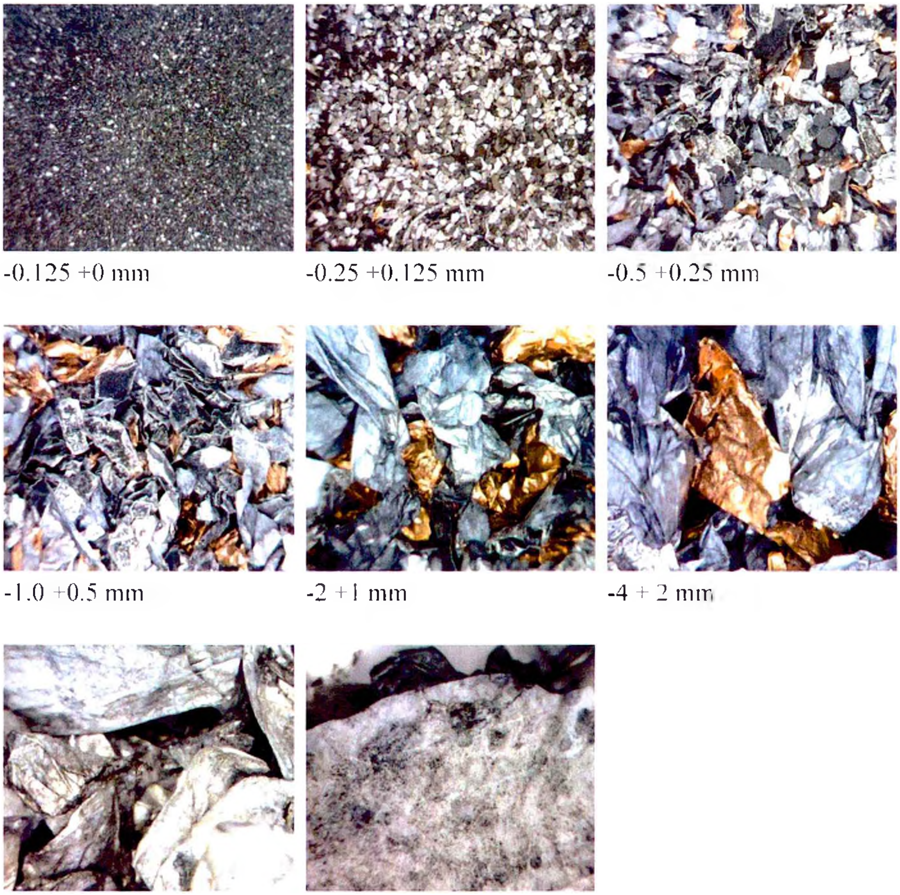

-0.125 +0 mm

-0.25 +0.125 mm

-0.5 +0.25 mm

-1.0 +0.5 mm

-2 + 1 mm

-4 + 2 mm

-6.3 +4 mm

+6.3 mm

Fig. 5.5 Detailed view of grain size fractions at 50x magnification

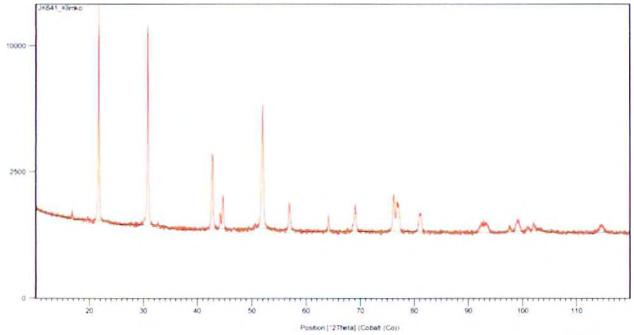

Ref. Code	Compound Name	Chemical Formula
01-088-1606	Lithium Nickel Oxide	Li.65 Ni1.08 O2
00-041-1487	Carbon	C
01-082-0322	Lithium Manganese Oxide	Li0.82 (Mn1.7 Li0.3) O4
96-153-3789	Li ((Mn1.5 (Ni0.44 Li0.06)) O4)	Ni3.48 Mn12.00 Li8.52 O32.00

Fig. 5.6 X-ray diffraction phase analysis of the black mass

On the basis of the different specific gravity masses of the basic components of copper, aluminium, black mass and plastic separators, these were experimentally separated from each other by gravity sorting. Relatively light aluminium is concentrated into a light fraction and heavier copper into heavier fractions. The separation of aluminum from copper can be achieved with high efficiency. Separators are very light and were separated into the lightest fractions.

There are two types of active black mass - anodic and cathodic. During the disintegration, it was shown that the anodic matter, represented by graphite, easily separates from the metal bearing material, but the cathodic matter, represented by complex lithium oxides, sticks to the aluminum cathode very firmly and is difficult or impossible to separate.

Overview of all products from sorting of crushed LiA through gravitational disintegration are shown in Fig. 5.7.

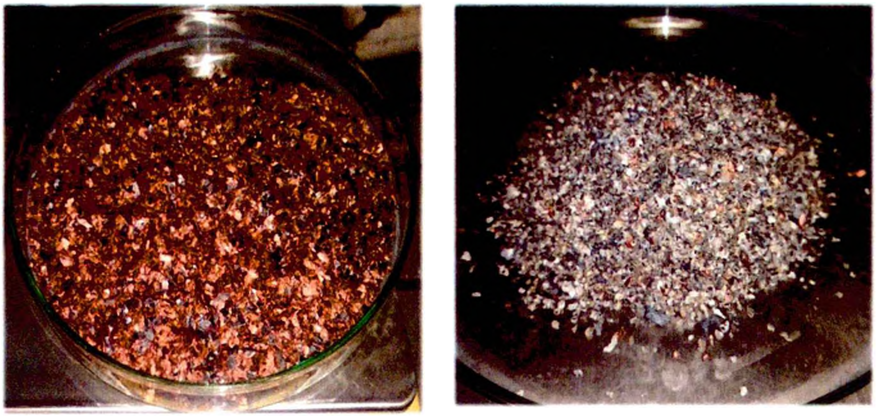

Cu concentrate Al concentrate

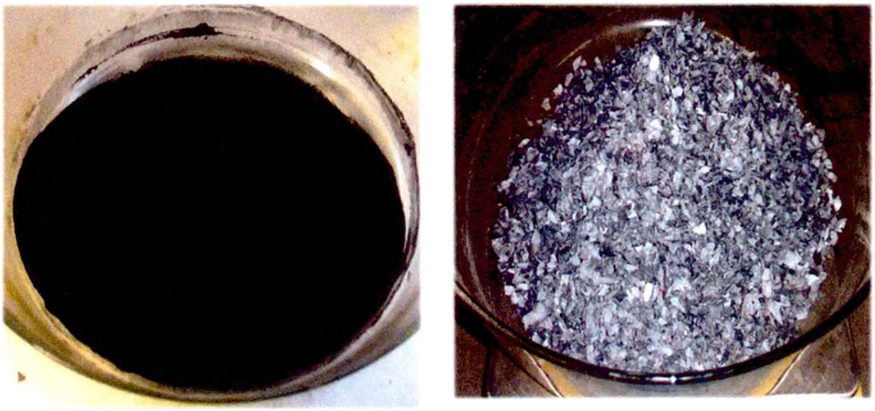

active black matter plastic separators

Fig. 5.7 Products of experimental LiA grit sorting.

The described procedures yielded metallic LiA components, represented by aluminium and copper in metallic form, plastic from the separators, and black mass of relatively high purity.

The materials obtained, metallic copper, metallic aluminium, plastic and black mass, are - in terms of functionality - the materials of construction in LiA, fulfilling the roles of current collectors, separators and the anode and cathode electrodes themselves. However, the elemental and phase composition of LiA (Fig. 5.8) indicates the presence of other elements in the form of compounds such as nickel, cobalt, manganese, but also titanium, silicon, tin, carbon and possibly others, whose presence in LiA is necessary for the progress of the required chemical reactions. This diversity is due to several influences. First of all, it is caused by dynamic development, where different materials have been investigated and explored to find the most advantageous composition in terms of LiA functionality, and from this point of view, upgrading to reach a higher level is a very fast process represented by the rapid turnover of LiA in devices.

Another reason is the still high price of LiA and, in an attempt to comply with commercial requirements, materials are being swapped for cheaper ones, but this is associated with lower performance, lower electrical capacity, lower lifetime and often lower safety.

Another consideration is the end use of LiA. In this respect, LiA is different when considered for use in EVs or HEVs, or in mobile phones, laptops, cameras, i.e. consumer electronics in general.

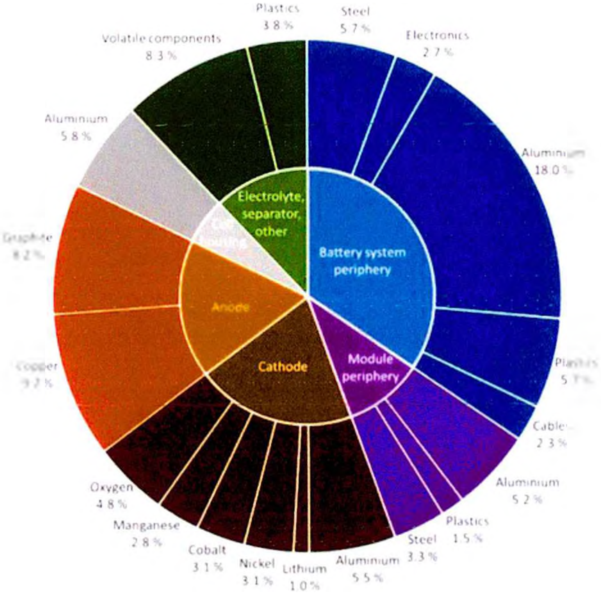

Fig. 5.8 Material composition of automotive LiA.

The individual compounds or salts are part of the cathode and anode mass or electrolyte, Tab. 5.3.

Tab. 5.3
The most common chemicals contained in LiA.

	salt
cathode	$LiNi_xMn_yCo_zO_2$, $LiNiCoAlO_2$, $LiMn_2O_4$, $LiFePO_4$, $LiCoO_2$
anode	$Li_4Ti_5O_{12}$, graphite, hard carbon, Sn-C alloy, Si-C

These compounds are present in LiA in different amounts and also in different forms. In their pure form, they have different, self-specific properties such as evaporation, melting and fusion points, reactivity, solubility in different solvents, etc. Obtaining them by simple mechanical or physical methods is not possible. Even lithium or phosphorus are unstable and extremely reactive in elemental form in air.

Therefore, in the last phase of the project, the possibilities of extracting mainly lithium, cobalt, nickel and also carbon for commercial reuse were investigated.

Previous work has studied the physical-mechanical treatment options for discarded LiA, and the proposed treatment scheme included a step of crushing the LiA, with the crushed material falling directly into the water to prevent ignition and combustion. Quite surprising was the finding that this water exhibited high pH values at pH = 13 and above. This meant that some of the lithium salts were readily soluble in water and went into a dissociated state. A simplified notation of the reactions is as follows:

$$LiNiO_2 + 2\ H_2O = LiOH + Ni(OH)_3$$
$$LiMnO_2 + 2\ H_2O = LiOH + Mn(OH)_3$$

The filtrate was filtered off and the homogeneous clear solution was evaporated and concentrated. After concentrating and evaporating the alkaline solution, a solid residue remained which was subjected to X-ray diffraction phase analysis, Fig. 5.9.

As a result, the solid residue is found to be composed of lithium carbonate with a small admixture of carbon with black mass. Since both hydroxide and lithium oxide are very relative substances, when the water was removed, it reacted immediately with air carbon dioxide to form lithium carbonate.

$$2LiOH + CO_2 \rightarrow Li_2CO_3 + H_2O$$

However, lithium does not transfer quantitatively to the aqueous solution; probably only a fraction of the lithium from the non-stoichiometric lithium compounds in LiA is leached. This is a variable amount and depends on the state of charge/discharge in the current cell. The rest of the insoluble lithium remains in the black mass and needs to be obtained by other means.

For the recovery of lithium, but also cobalt and nickel, a combined pyro-hydrometallurgical method was chosen. According to this approach, black mass pellets were prepared and subsequently melted to produce a metal alloy and a lithium-containing slag, which was processed hydrometallurgically.

The specific black material used was subjected to X-ray diffraction phase analysis, on the basis of which the presence of complex oxides of lithium manganese nickel oxide and carbon was determined as the majority components, as well as lithium nickel manganese oxide and cobalt manganese oxide in the form of $(Li_{0.91}Ni_{0.099})(Li_{0.099}Ni_{0.401}Mn_{0.5})O_2$, $LiNi_{0.5}Mn_{1.5}O_4$ and $Co_{2.2}Mn_{0.8}O_4$.

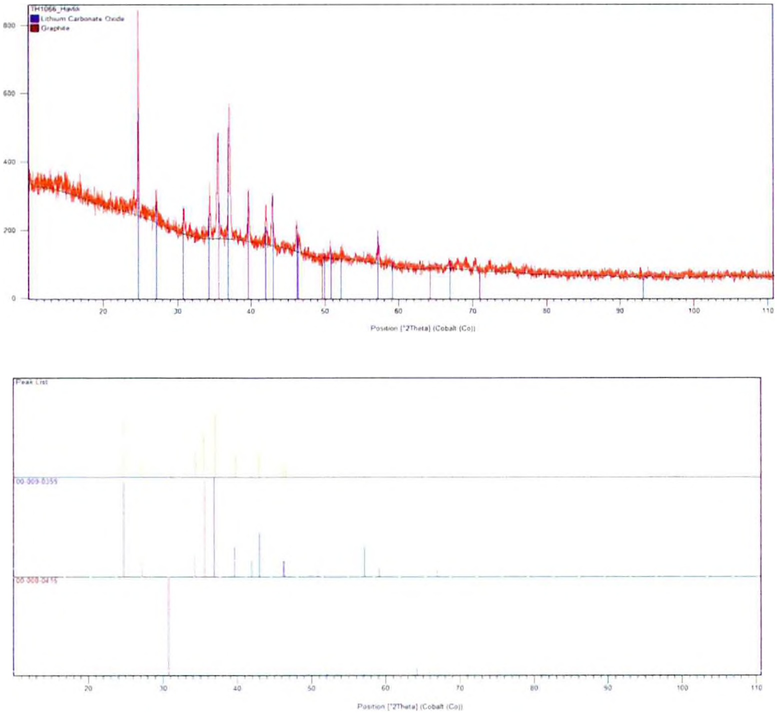

Ref. Code	Compound Name	Chemical Formula
00-009-0359	Lithium Carbonate Oxide	Li2 C O3
00-008-0415	Carbon	C

Fig. 5.9 Result of X-ray diffraction phase analysis of the solid residue after water evaporation.

This particular black mass was obtained from Accurec Recycling GmbH, Germany, on the basis of a direct cooperation with IME RWTH Aachen, Germany.

The aim was to pelletize the black mass, and to this end it was subjected to the pre-processing shown in the upper green part of Fig. 5.15.

The dismantling step involved manual removal of copper cables, steel cladding, plastics and electronic components. This was followed by a pyrolysis step in which residual voltages were discharged and the organic electrolyte evaporated. The pyrolyzed LiA proceeded to the mechanical processing steps of crushing and sieving to separate the coarse fraction from the fine fraction (<100) m containing black mass, which is pelletized in the next step. The black mass thus treated forms the raw material input for the electric arc furnace (EAF) for melting, Tab. 5.4.

Tab. 5.4

Composition of black mass, pre-prepared for pellet production.

Component	Composition of black mass [hm.%]										
	Co	Fe	Mn	Al	Cu	Si	Zn	Ni	Ag	Li	C
Table of contents	22.0	6.51	0.75	3.88	4.69	0.37	0.11	2.71	0.32	2.24	20.5

The results show, among other things, a high cobalt content compared to manganese and nickel.

In the next step, pellets were prepared for pyrometallurgical processing in the EAF. CuO and SiO_2 were added to the charge in the ratio Pellet: $CuO:SiO_2 = 5:4:1$, which served as slag-forming additives or, after reduction by the present carbon, as a non-ferrous metal collector.

After remelting and separation of the resulting slag from the metal alloy, the slag was homogenized by crushing and grinding. The metal impurities were removed by magnetic separation and the separated magnetic particles were further processed with the metal alloy obtained after melting in the EAF.

Table 5.5 shows the results of the chemical analyses of the recovered demetalised slag from the individual black mass pellet melting experiments.

Table 5.5

Chemical analysis of the slag from the individual EAF melting experiments.

experiment number	composition [hm%]								
	Li	Cu	Co	Ni	C	SiO_2	Al_2O_3	Fe_2O_3	Mn_3O_4
	analytical methods: ICP-OES, combustion, XRF								
1	5.53	0.23	0.09	0.01	0.029	56.2	22.0	0.52	2.25
2	5.18	1.4	1.44	0.05	0.035	53.4	20.2	2.25	2.23
3	5.84	0.39	0.41	0.05	0.120	49.7	27.1	0.67	1.69
4	6.24	0.40	0.25	0.03	0.285	46.5	30.2	0.22	0.84
5	6.77	0.35	0.07	0.01	0.238	43.1	32.2	0.31	2.12
6	7.40	0.10	0.06	0.01	0.184	41.8	33.4	0.14	0.70

Similarly, Tab. 5.6 presents the results of chemical analyses of metal alloys obtained from the same black mass melting experiments.

Tab. 5.6

Chemical analysis of alloy from EAF melting.

element	**Cu**	**Co**	**Ni**	**Fe**	**Mn**	**Si**	**Li**
[hm%]	66.1 – 65.0	20.2 – 19.9	2.83 – 2.68	8.05 – 7.69	0.58 – 0.55	3.18 – 3.10	0.074 – 0.070

In terms of the presence of lithium, it was found to be present in LiA in various forms, some of which tend to be variable depending on the charge/discharge state, LiA design, LiA designation, etc. Of course, these phases also have different properties and behave differently in the treatment of discarded LiA. In this case, at least the following lithium-containing phases were identified in the demetalised slag after pyrometallurgical processing: $LiAlO_2$, Li_2SiO_3, $LiAlSiO_4$, $LiAlSi_2O_6$, $LiAlSi_4O_{10}$, $Li_2Si_2O_5$ [45].

The slag obtained after melting in the EAF was crushed and ground, Fig. 5.10. The ground sample was subjected to magnetic sorting to reduce metallic impurities containing cobalt, copper, nickel and iron in the Li slag, Fig. 5.11.

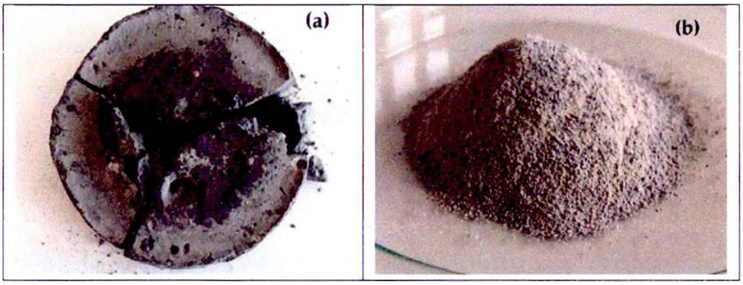

Fig. 5.10 Li slag from EAF: a) before mechanical pretreatment, b) after mechanical pretreatment (crushing, grinding, magnetic screening, sieving).

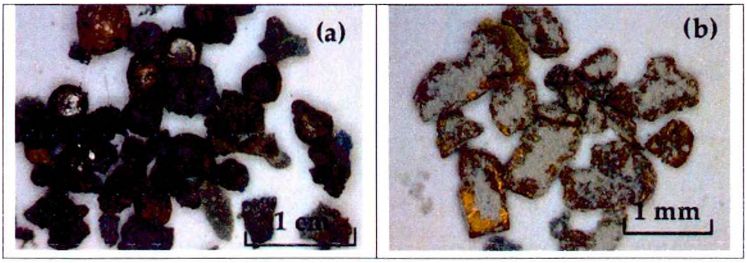

Fig. 5.11 Metal components obtained by magnetic sorting of Li slag a) after crushing, b) after grinding.

The chemical composition of Li slag and slag after mechanical pretreatment is given in Tab. 5.7.

Tab. 5.7

Chemical composition of Li slag and slag after mechanical pretreatment.

	Li	Co	Cu	Al	Fe	Si	Ca	Ni	Mn
Li slag	6.8	1.17	1.53	16.52	0.51	48.62	1.16	0.15	0.65
demetalised Li slag	6.96	0	0.11	16.40	0.20	51.10	1.26	0.01	0.88

X-ray diffraction phase analysis of this slag proved the presence of $LiAlSiO_4$ phases and Li_2SiO_3.

Other SiO_2-bearing phases were not identified by diffraction analysis, indicating that excess SiO_2 in the slag is present in amorphous form as $SiO_{2(am)}$.

Tab. 5.8 shows the potential reactions of the identified Li phases when reacted with sulphuric acid and the values of the changes in the standard Gibbs energy at 20 °C and 80 °C, i.e. ambient temperature and leaching temperature. The results clearly show that these reactions are thermodynamically possible, with reactions (5) and (6) showing the highest probability.

Tab. 5.8

Potential leaching reactions of the slag phase in H_2SO_4 and values of changes in standard Gibbs energy [46].

reaction		$\Delta G^o_{293.15}$ [kJ]	$\Delta G^o_{353.15}$ [kJ]
4	$2\ LiAlSiO_4 + 4\ H_2SO_4 = Li_2SO_4 + Al_2(SO_4)_3 + 2\ H_4SiO_4$	-274.727	-267.444
5	$2\ LiAlSiO_4 + 4\ H_2SO_4 = Li_2SO_4 + Al_2(SO_4)_3 + 2\ H_2SiO_3 + 2\ H_2O$	-300.098	-295.187
6	$2\ LiAlSiO_4 + H_2SO_4 = Li_2SO_4 + Al_2(SO_4)_3 + SiO_2 + H_2O$	-302.950	-295.722
7	$2\ LiAlSi_2O_6 + 4\ H_2SO_4 + 4\ H_2O = Li_2SO_4 + Al_2(SO_4)_3 + 4\ H_4SiO_4$	-216.581	-211.165
8	$Li_2SiO_3 + H_2SO_4 = Li_2SO_4 + H_2SiO_3$	-151.744	-141.622
9	$Li_2SiO_3 + H_2SO_4 + H_2O = Li_2SO_4 + H_4SiO_4$	-152.092	-142.666

Fig. 5.12 shows E-pH diagrams for Li-Al-S-Si-H_2O, Al-Li-S-Si-H_2O and Si-Al-Li-S-H_2O systems. Thermodynamic analysis confirmed the presence of lithium as Li^+ ion in acid leaching. Aluminium and silicon are thermodynamically stable even in the ionic form at pH > 4.

$Al_2O_3 * SiO_2$ precipitates at 80 °C. According to reactions (4), (5) and (6), three silicon phases (SiO_2, H_2SiO_3 and H_4SiO_4) are present in the leachate, and the thermodynamically most stable phase is H_4SiO_4.

For the hydrometallurgical treatment, based on preliminary considerations and system analysis, direct acid leaching in aqueous sulphuric acid solution at selected conditions of acid concentration, temperature and time was chosen. Fig. 5.13 shows a typical progression of kinetic leaching curves in a sulphuric acid solution.

Lithium is the most desirable element from LiA recycling. From this point of view, a high lithium leaching efficiency of almost 100 % was achieved already after 30 minutes even at ambient temperature, while the concentration of H_2SO_4 does not affect this process. As the leaching temperature increases, the process speeds up and therefore the time decreases.

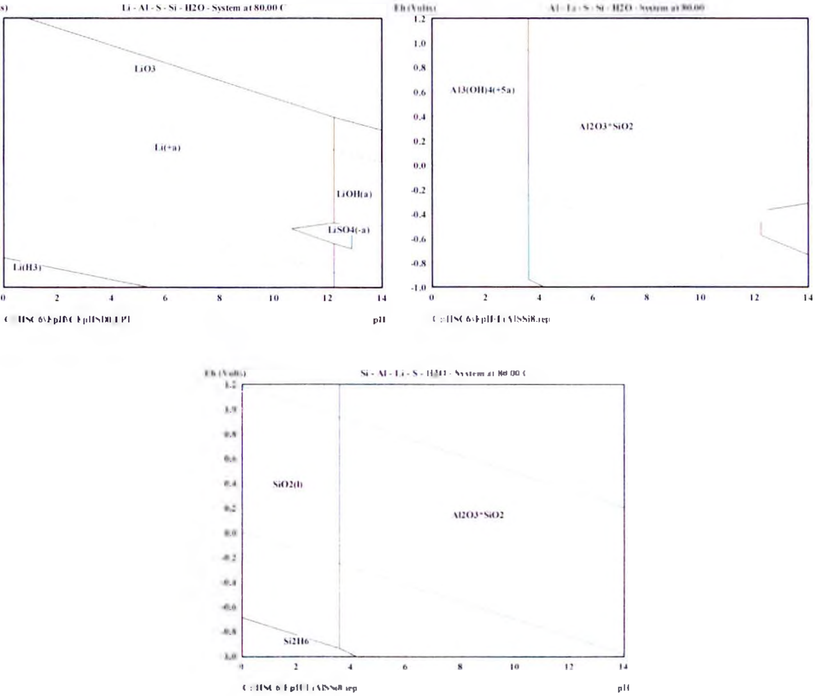

Fig. 5.12 E-pH diagrams for Li-Al-S-Si-H_2O, Al-Li-S-Si-H_2O a Si-Al-Li-S-H_2O systemsat 80°C.

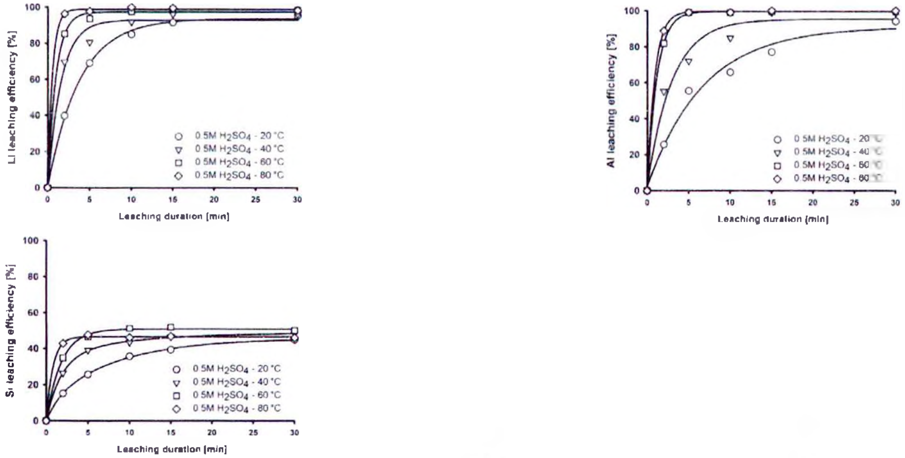

a b c

Fig. 5.13 Kinetic curves of leaching of a) lithium, b) aluminum, c) silicon in 0.5 M H_2SO_4 in the temperature range 20 to 80°C.

In addition to lithium, the leaching of aluminium and silicon has also been studied as they are present in relatively high amounts and in common phases with lithium. As regards aluminium, its yield increases slightly with increasing acid concentration, but also with increasing temperature; silicon leaches with an efficiency of up to 50 %. This corresponds to stoichiometric calculations, according to which approximately 50 % of silicon is present in the $LiAlSiO_4$ phase, which is leachable in H_2SO_4, and approximately 50 % in the SiO_2 phase, which is not leachable in H_2SO_4. From a thermodynamic point of view, leaching most likely occurs according to equations (4) and (9) with the formation of orthosilicic acid H_4SiO_4. When the leaching temperature changes, the leachability of Si changes, which may be related to the fact that, in addition to reaction (4), reaction (6) also takes place, in which solid SiO_2 and H_2O are formed instead of H_4SiO_4. In practical terms, this means that technically the result is essentially a solid gel-like substance (Fig. 5.14) which stops the process, makes sampling impossible, and collapses the experiment.

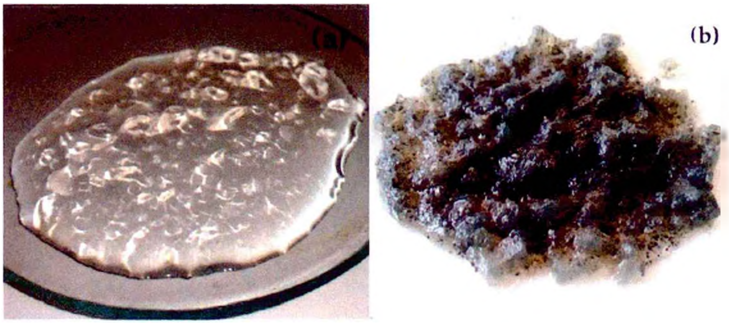

Fig. 5.14 Gel aggregates present in solutions after direct leaching of Li slag: (a) formed after filtration of the leaching residue; (b) formed before filtration with trapped leaching residues

For this reason, instead of traditional acid leaching in sulphuric acid, a method was chosen in which the slag was chemically decomposed and then neutrally leached in water. 50 g of slag and concentrated H_2SO_4 were used for chemical decomposition. Distilled water was then added, causing a violent exothermic reaction, decomposition of the phases present, and precipitation of the leached silicon from the resulting silicic acid in the form of $SiO_{2(am)}$. After decomposition, the mixture was leached in water with stirring without heating. In the above manner, a solution with a high lithium content with a leaching efficiency of Li above 90 % and aluminium with a leaching efficiency of Al above 70 % and a low silicon content with a leaching efficiency of Si up to 10 %, was gained. After filtering and separating the solution, the solid residue was washed in water, transferring an additional 8 % lithium into the solution. Thus, by leaching and subsequent washing of the solid residue, 98 % of lithium can be leached from the slag. The solution from the slag washing is reused in the next neutral leaching. The precipitated SiO_2 can be gravitationally separated from the solid residue after leaching and recovered separately. The solid residue after neutral leaching, washing and disintegrating should meet the conditions for its use in construction. The aluminum is removed from the resulting solution by precipitation with NaOH at $pH = 1 - 4$. Precipitation of lithium hydroxide only occurs at $pH > 12$. For this reason, sodium or ammonium carbonate is added to the solution, which causes the precipitation of lithium in the form of Li_2CO_3. Following filtration and drying, the commercial products $Al(OH)_3$ and Li_2CO_3 are obtained.

Fig. 5.15 shows a block diagram of the pyrometallurgical treatment of discarded LiA and the pyrometallurgical treatment of the black mass [47].

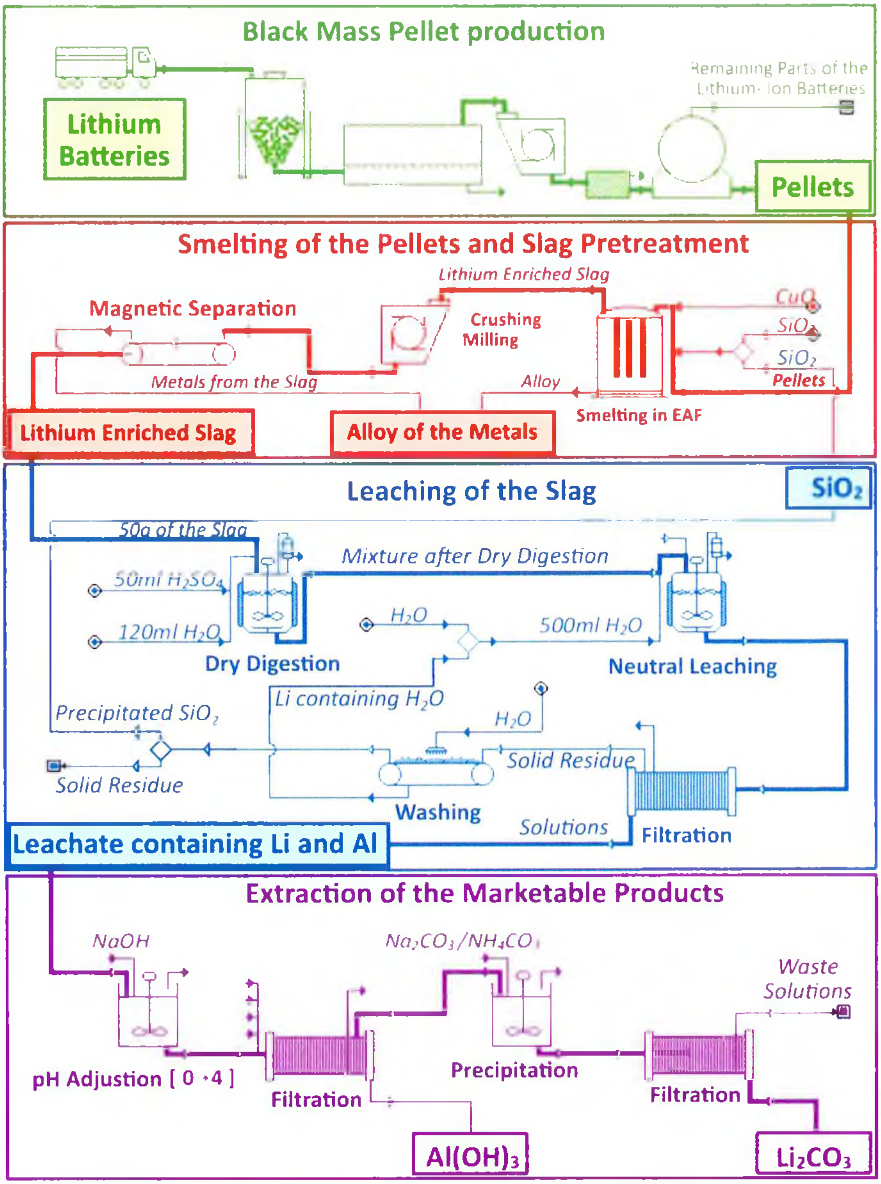
Black Mass Pellet production
Lithium Batteries
Remaining Parts of the Lithium-Ion Batteries
Pellets
Smelting of the Pellets and Slag Pretreatment
Lithium Enriched Slag
Magnetic Separation
Crushing Milling
CuO
SiO₂
SiO₂
Pellets
Metals from the Slag
Alloy
Smelting in EAF
Lithium Enriched Slag
Alloy of the Metals
Leaching of the Slag
SiO₂
50g of the Slag
Mixture after Dry Digestion
50ml H₂SO₄
120ml H₂O
H₂O
500ml H₂O
Dry Digestion
Neutral Leaching
Li containing H₂O
Precipitated SiO₂
H₂O
Solid Residue
Solid Residue
Washing
Solutions
Filtration
Leachate containing Li and Al
Extraction of the Marketable Products
NaOH
Na₂CO₃/NH₄CO₃
Waste Solutions
pH Adjustion [0 -4]
Filtration
Precipitation
Filtration
Al(OH)₃
Li₂CO₃

Fig. 5.15 Block diagram of the combined black mass processing method.

Other valuable components contained in LiA are mainly cobalt and nickel. These are concentrated into a metal alloy in the pyrometallurgical processing of ferrous matter (Tab. 5.7, Fig. 5.11). From the metallurgical perspective, these metals, even together with copper or iron, form essentially unlimited alloys, which practically excludes pyrometallurgical division on the basis of individual properties of these metals. Possible procedures, taken from the real field of non-ferrous metallurgy, are hydrometallurgical

– electrometallurgical procedures. In practice, this means the transfer of the components of a given alloy by leaching the individual metals in solution under specific conditions and their subsequent selective extraction by one of the known processes such as electrolysis, liquid extraction, ion exchange, crystallisation and the like.

These processes are very demanding and essentially require sophisticated metallurgical processes, and to be economically viable, large quantities of materials need to be processed, which recycling of discarded LiA does not meet.

Therefore, for the purpose of possible recovery of cobalt, nickel and also lithium, direct leaching of the black mass was chosen in this case [48].

Based on the thermodynamic study, the values of the changes in the standard Gibbs energy were determined - in this case ΔG^0 (Tab. 5.9) and E-pH diagrams were calculated to determine the stability regions of cobalt and lithium compounds in the Co-S-H_2O and Li-S-H_2O systems. The values of ΔG^0 were calculated for leaching temperature equal to 353 K, or 80 °C. The following chemical equations of selected cobalt and lithium compounds in sulphuric acid were considered.

Tab. 5.9

Leaching reactions of Co and Li components in black mass in H_2SO_4 and values of standard Gibbs energy changes [46].

reaction		$\Delta G^0_{353.15}$ [kJ]
10	$4\ LiCoO_2 + 6\ H_2SO_4 = 2\ Li_2SO_4 + 4\ CoSO_4 + 6\ H_2O + O_2$	-608.96
11	$Li_2O + H_2SO_4 = Li_2SO_4 + H_2O$	-306.69
12	$2\ Co_3O_4 + 6\ H_2SO_4 = 6\ CoSO_4 + 6\ H_2O + O_2$	-188.42
13	$Li_2CO_3 + H_2SO_4 = Li_2SO_4 + H_2O + CO_2$	-126.61
14	$CoO + H_2SO_4 = CoSO_4 + H_2O$	-114.12
15	$2\ Co_2O_3 + 4\ H_2SO_4 = 4\ CoSO_4 + 4\ H_2O + O_2$	-94.17

Negative values ΔG^0 determine the progression of chemical reactions from left to right. The more negative the value, the higher the probability of a given reaction.

The leaching experiments were carried out under laboratory conditions using sulphuric acid solutions with concentrations of 0.1, 0.5, 1 and 2 M H_2SO_4 at 20, 40, 60 and 80 °C, while the most effective results were achieved precisely at higher temperatures during 90 minutes of leaching.

The results obtained are shown graphically in Fig. 5.16.

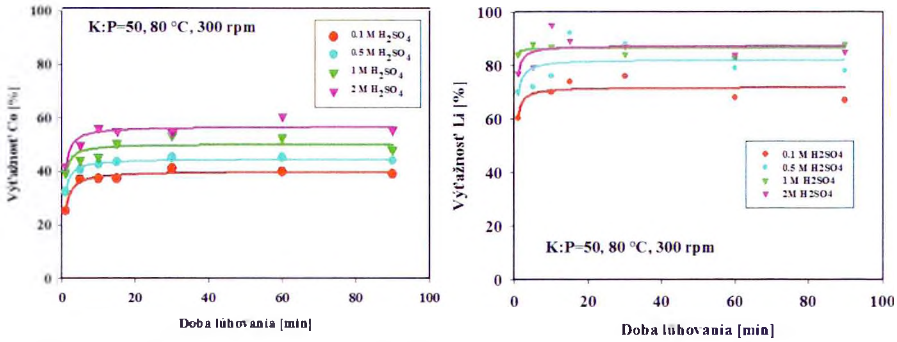

Fig. 5.16 Leaching kinetic curves for cobalt (left) and lithium (right) at leaching temperature 80 °C and individual concentrations of sulphuric acid

The results show that the yield of cobalt in H2SO4 leaching is lower, at 50-60%, and in a relatively short time of up to 15 minutes. Unlike cobalt, leaching of lithium is relatively progressive with higher extractions. The amount of cobalt passing into the solution depends on temperature and/or concentration of the leaching agent, but after 15 minutes the process slows down significantly or stops. Relatively high yields have been achieved for lithium.

The yield of cobalt to sulphuric acid solution was found to be at a lower level than expected. Therefore, it was suggested to use other leaching agents, e.g. HCl hydrochloric acid solution, for the following activities. At the same time, there is an expectation that as the temperature is further increased to near boiling point, the process will proceed much more rapidly.

The next logical step in the LiA processing procedure is to extract metals from solution as selectively as possible. As mentioned above, metals and hence cobalt and nickel can be selectively recovered from solution by any of the processes, such as electrolysis, liquid extraction, ion exchange, crystallisation and the like. The choice of the appropriate procedure depends on actual properties of the desired metals and their mutual affinities, concentration in solution, price, and so on.

In this case, the liquid extraction method was chosen. The paper focuses on the recovery of cobalt from the solution after leaching of black mass from discarded LiA in sulphuric acid solution by liquid extraction method. The effect of pH on extraction, precipitation and on the ratio of inorganic to organic phase was studied. At the same time, the effect of the ratio of inorganic to organic phase during extraction and the ratio of organic to inorganic phase during stripping from solution were studied.

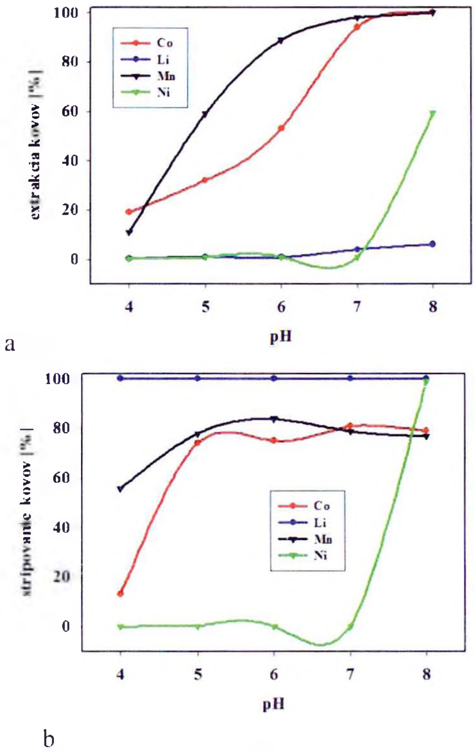

Fig. 5.17 Effect of pH on the efficiency of (a) extraction and (b) stripping of Co, Li, Mn and Ni.

The extraction was performed using a 0.1 M solution of Cyanex 272 extraction reagent at 20 °C for 15 minutes at A:O = 0.5. Stripping was carried out in a 2M solution of H_2SO_4 at 20 °C for 10 minutes at a ratio of O:A = 2.

Typical results of extraction and stripping curves are shown in Fig. 5.17.

The results show the following [49]:

The extraction and stripping efficiency of Co is not the same at the same pH. Therefore, it is necessary to extract at pH = 7 – 8 and after pH adjustment, stripping at pH = 6 – 7 will give more efficient results.

Another option is to use a more concentrated stripping agent higher than 2 M H_2SO_4. However, the disadvantage will be the subsequent dilution of the solution.

Mn, Ni and Li will also be co-extracted from the leaching solution along with cobalt depending on the pH. Nickel will remain in aqueous solution up to pH < 8. Therefore, the optimum pH = 7 at which the extraction efficiencies are Co = 90 % and Ni = 0 %.

The selective extraction of Co from the leaching solution after leaching of the LiA black mass with Cyanex 272 is limited by the presence of Mn, which co-extract at a certain pH together with Co, and its extraction is even higher than that of Co. The extraction efficiency of lithium is 0 – 10 %, so that under suitably chosen conditions selective extraction of Co and Li can be achieved.

It is not necessary to remove Ni prior to the extraction itself, and at the same time Ni is not selectively stripped from the solution as Ni extraction is virtually zero up to pH = 8.

An example of an already concrete procedure is the one tested at the URT FMMR and shown in Fig. 5.18. The proposed process is a combined process, in which the physical-mechanical sorting steps of metals present in the elementary form of copper, aluminium, steel and also plastics are applied in one process. These are further processed by individual, essentially pyrometallurgical procedures.

The separated black (active mass) is processed in a hydrometallurgical process in which the desired constituents lithium, cobalt, nickel and manganese are leached and these are selectively recovered by liquid extraction and recycled back into the cathode material. The anode carbon does not chemically react in the process and is reprocessed into anode material after separation of the metal components.

The system operates in a closed cycle with minimal waste generation.

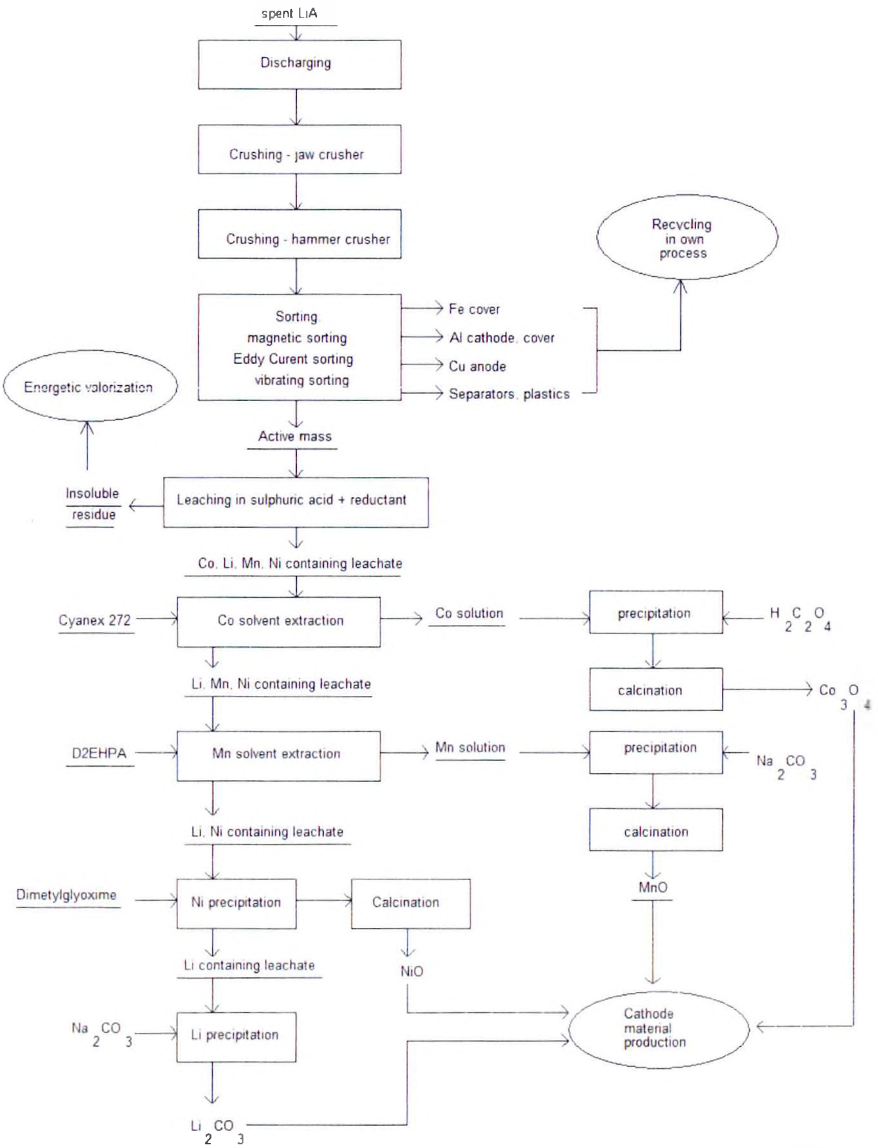
spent LiA
Discharging
Crushing - jaw crusher
Crushing - hammer crusher
Recycling in own process
Sorting
magnetic sorting
Eddy Curent sorting
vibrating sorting
Fe cover
Al cathode, cover
Cu anode
Separators, plastics
Energetic valorization
Active mass
Insoluble residue
Leaching in sulphuric acid + reductant
Co, Li, Mn, Ni containing leachate
Cyanex 272
Co solvent extraction
Co solution
precipitation
H2C2O4
calcination
Co3O4
Li, Mn, Ni containing leachate
D2EHPA
Mn solvent extraction
Mn solution
precipitation
Na2CO3
calcination
MnO
Li, Ni containing leachate
Dimetylglyoxime
Ni precipitation
Calcination
NiO
Li containing leachate
Na2CO3
Li precipitation
Cathode material production
Li2CO3

Fig. 5.18 Block diagram of the comprehensive treatment of discarded LiA [50]

5.4 Conclusion

The issue of material recycling of discarded LiA is currently focused in two directions, which are mainly determined by economic and technological aspects. The result is a philosophy whereby the path of least resistance has focused recycling activities on the recovery of metallic copper, metallic aluminium, metallic iron, plastics and ferrous matter through physical-mechanical recycling.

However, discarded LiA also contains other components, mainly metals in the form of compounds, especially Li, Co, Ni, Mn, Ti, graphite, etc., which are often scarce and their price is high. Therefore, the interest of researchers and recyclers is gradually being directed in this direction as well.

The presented results are part of a multi-year project of the University and Industrial Research and Education Platform of the recycling company UNIVNET, aimed at

the status and vision of recovery of selected types of waste, especially from the automotive industry of the Slovak Republic. Chronologically, the concept of the project's part aimed at the treatment of discarded LiA´s was initially focused on physical-mechanical recycling in order to obtain Cu, Al, black mass and plastics [51-54] and later on the physical-chemical processes of black mass treatment in order to extract the valuable components of LiA´s from their chemical compounds, such as Li, Co, Ni, Mn [55].

There are several ways of recycling and they depend on the overall context of the issue. In this case, the problem was solved by pyrometallurgical treatment of the black mass followed by hydrometallurgical treatment of the slag. In pyrolysis, the metals Co, Ni, Cu, Fe are concentrated into an alloy, whereas lithium is concentrated into slag. The slag is leached and the final commercial product Li_2CO_3 is obtained through individual steps. The other metals of interest - Co, Ni, Mn - can be obtained by hydrometallurgical processes of black mass leaching and subsequent selective extraction of metals from solution by liquid extraction, which has been confirmed experimentally.

The concept of a comprehensive treatment of discarded LiA, as shown in Figure 18, has been experimentally verified and offers a very promising solution.

The use of alkaline leaching media is also a separate chapter, which has not been discussed at all in the published results so far. Particular metals such as aluminium and heavy metals in general, including copper, cobalt, nickel and so on, are soluble in alkalis. In the framework of applied research, the optimized results of basic research must then be tested in a semi-operational and later in an operational scale. In this case, the economic analysis is the decisive factor, including in particular the factor of investment and operating costs and their return. It is clear that even the basic decision between the basic route to pyrometallurgical, hydrometallurgical or combined method depends heavily on the infrastructure, energy needs, logistics, environmental aspects and similar designed processes.

References

[1] European Commission, Study on the Critical Raw Materials for the EU 2023 – Final Report, [14/08/2024], available on: imap://th311qc@mail.tuke.sk:143/fetch%3EUID%3E/INBOX%3E57179?part=1.2&filename=Study%202023%20CRM%20Assessment.pdf&type=application/pdf.

[2] https://www.lithium-battery-factory.com/sk/automotive-lithium-ion-batteries/

[3] https://www.mojelektromobil.sk/elektromobil-baterie-nie-je-ekologicky/

[4] Ekberg, C., et al. 2020. Lithium-ion batteries – Current state of the art and anticipated developments. J. Power Sources, 479, 228708

[5] Kim, T., et al. 2019. Lithium-ion batteries: outlook on present, future, and hybridized technologies.Journal of Materials Chemistry A, 7 (7), 2942–2964.

[6] The Nobel Prize. The Nobel Prize in Chemistry 2019. [21/11/2011], available on: https://www.nobelprize.org/prizes/chemistry/2019/summary/

[7] Xie, J., Lu, Y.-C. 2020. A retrospective on lithium-ion batteries. Nat. Commun., 11(1), 2499.

[8] Philippot, M., et al. 2019. Eco-Efficiency of a Lithium-Ion Battery for Electric Vehicles: Influence of Manufacturing Country and Commodity Prices on GHG Emissions and Costs. Batteries, 5(1), 23.

[9] Notter, D. A., et al. 2010. Contribution of Li-Ion Batteries to the Environmental Impact of Electric Vehicles. Environ. Sci. Technol., 44 (17), 6550–6556.

[10] Farjana, S. H., Huda, N., Mahmud, M.A.P. 2019. Life cycle assessment of cobalt extraction process. Journal of Sustainable Mining, 18 (3), 150–161.

[11] Kaunda, R. B. 2020. Potential environmental impacts of lithium mining. Journal of Energy & Natural Resources Law, 38 (3), 237–244.

[12] USGS. Cobalt; 2019. [21/09/2024], available on: https://pubs.usgs.gov/periodicals/mcs2020/mcs2020-cobalt.pdf, October 2021

[13] USGS. Graphite (Natural); 2021. [14/06/2024], available on: https://pubs.usgs.gov/periodicals/mcs2021/mcs2021-graphite.pdf, October 2021

[14] Resilience in critical raw materials: mapping the path to greater security and sustainability (in Slovak), [15/06/2024], available on: https://eur-lex.europa.eu/legal-content/SK/TXT/PDF/?uri=CELEX:52020DC0474&from=EN

[15] Number of plug-in cars climbs to 5.6M worldwide; electrive.com; 2019. [17/11/2021], available on: https://www.electrive.com/2019/02/11/thenumber-of-evs-climbs-to-5-6-million-worldwide/

[16] Bloomberg NEF. Electric Vehicle Outlook 2021. [17/11/2021], available on: https://about.bnef.com/electric-vehicle-outlook/,

[17] https://autobild.pluska.sk/novinky/slovensku-jazdi-iba-9-500-elektromobilov-podpore-e-mobility-nas-predbehlo-aj-bulharsko

[18] European Parliament and Council Directive 2006/66/EC (in Slovak), 6 September 2006. [08/09/2024], available on: https://www.epi.sk/media/File/pdf/2006/299096f6-f710-4a98-bc12-38f7e2289243_pdf_DOC_1.pdf?attachment-filename=299096f6-f710-4a98-bc12-38f7e2289243_pdf_DOC_1.pdf

[19] Proposal for a Regulation of the European parliament and of the Council concerning batteries and waste batteries, repealing Directive 2006/66/EC and amending Regulation (EU) No 2019/1020 [24/08/2024], available on: https://data.consilium.europa.eu/doc/document/ST-5469-2023-INIT/en/pdf

[20] Stone, M. 2021. As electric vehicles take off, we'll need to recycle their bat teries ; National Geographi c, [13/12/2021], available on:

https://www.nationalgeographic.com/environment/article/electric-vehicles-takeoff-recycling-ev-batteries

[21] Zubi G., et al. 2018. The lithium-ion battery: state of the art and future perspectives, Renew. Sustain. Energy Rev. 89, 292–308, DOI: 10.1016/j.rser.2018.03.002

[22] Marcinek M. et al. 2015. Electrolytes for Li-ion transport - review, Solid State Ionics 276, 107–126, DOI: 10.1016/j.ssi.2015.02.006

[23] Herrmann C., et al. 2018. Sustainable Production, Life Cycle Engineering and Management, 2018. http://www.springer.com/series/10615

[24] Schroder R., Aydemir M., Seliger G. 2017. Comparatively assessing different shapes of lithium-ion battery cells, Procedia Manuf. 8, 104–111, DOI: 10.1016/j.promfg.2017.02.013

[25] Asenbauer, J., et al. 2020.The success story of graphite as a lithium-ion anode material-fundamentals, remaining challenges, and recent developments including silicon (oxide) composites, Sustain. Energy Fuels, 4, 5387–5416, DOI: https://doi.org/10.1039/ d0se00175

[26] Ellis B.L., Lee K.T., Nazar L.F. 2010. Positive electrode materials for Li-Ion and Li-batteries, Chem. Mater. 22, 691–714, DOI:10.1021/cm902696j

[27] Latini D., et al. 2022. A comprehensive review and classification of unit operations with assessment of outputs quality in lithium-ion battery recycling. Journal of Power Sources 546, 231979.

[28] Harper G. et al. 2019. Recycling lithium-ion batteries from electric vehicles. Nature, 575, 75–86, DOI:10.1038/S41586-019-1682-5

[29] Fan E., et al. 2020. Sustainable Recycling Technology for Li-Ion Batteries and Beyond: Challenges and Future Prospects. Chem. Rev., 120, 7020–7063. DOI: 10.1021/ACS.CHEMREV.9B00535

[30] Kim H.J., et al. 2020. A comprehensive review of li-ion battery materials and their recycling techniques. Electronics, 9, 1161. DOI: 10.3390/ELECTRONICS9071161

[31] Kim S., et al. 2021. A comprehensive review on the pretreatment process in lithium-ion battery recycling. J. Clean. Prod., 294, 126329, DOI: 10.1016/J.JCLEPRO.2021.126329.

[32] Metals and mining prices, https://www.fastmarkets.com/our-products/price-data/metals-and-mining-prices

[33] Lithium-Ion Battery Recycling - Overview of Techniques and Trends, ACS Energy Lett. 2022, 7, 712−719

[34] Metals and mining prices, [18/06/2024], available on: https://www.fastmarkets.com/our-products/price-data/metals-and-mining-prices

[35] Werner D., Peuker U.A., Mütze T. 2020. Recycling chain for spent lithium-ion batteries. Metals (Basel),10, 316. DOI:10.3390/MET10030316

[36] Yun L., et al. 2018. Metallurgical and mechanical methods for recycling of lithium-ion battery pack for electric vehicles. Resour. Conserv. Recycl., 136: 198–208. DOI: 10.1016/J.RESCONREC.2018.04.025

[37] Or T., et al. 2020. Recycling of mixed cathode lithium-ion batteries for electric vehicles: Current status and future outlook. Carbon Energy, 2, 6–43. DOI: 10.1002/CEY2.29

[38] Havlik T., Klimko J. 2022. Processing of spent automotive lithium batteries In: Smart technologies for waste processing from the automotive industry, Soos L. ed., Univnet, 86-102.

[39] Decree no. 365/2015 Coll. Ministry of the Environment of the Slovak Republic from November 13, 2015 establishing the Waste Catalog (In Slovak). [18/10/2024], available on: http://ekolamp.sk/wp-content/uploads/2016/06/vyhlaska-mzp-15-z365.pdf

[40] Regulation of the European Parliament and of the Council on batteries and used batteries, repealing Directive 2006/66/EC and amending Regulation (EU) 2019/1020 (in Slovak). [18/10/2024], available on: https://www.epi.sk/media/File/pdf/2020/4b5d88a6-3ad8-11eb-b27b-01aa75ed71a1_pdf_DOC_1.pdf?attachment-filename=4b5d88a6-3ad8-11eb-b27b-01aa75ed71a1_pdf_DOC_1.pdf

[41] Rahman A., Afroz R., Safrin M. 2017. Recycling and disposal of lithium batteries: An economical and environmental approach. IIUM Eng. J. 18, 238–252. DOI: 10.31436/IIUMEJ.V18I2.773

[42] Cell & chemistry, [03/11/2023], available on: https://electrichasgoneaudi.net/technology/battery/cell/

[43] Stellantis and the CEA collaborate on EV battery modeling, [03/11/2023], available on: https://evpowered.co.uk/news/stellantis-and-the-cea-collaborate-on-ev-battery-modeling/

[44] Battery Taxonomy: The Differences between Hybrid and EV Batteries, [03/11/2023], available on: https://www.caranddriver.com/news/a15345397/battery-taxonomy-the-differences-between-hybrid-and-ev-batteries/

[45] Sommerfeld, M., et al. 2020. A Combined Pyro- and Hydrometallurgical Approach to Recycle Pyrolyzed Lithium-Ion Battery Black Mass Part 1: Production of Lithium Concentrates in an Electric Arc Furnace, Metals, 10, 1069; DOI::10.3390/met10081069

[46] Roine, A. 2018. HSC Chemistry Thermodynamic Software; Outotec: Pori, Finland.

[47] Klimko, J., et al. 2020. A Combined Pyro- and Hydrometallurgical Approach to Recycle Pyrolyzed Lithium-Ion Battery Black Mass Part 2: Lithium Recovery from Li Enriched Slag – Thermodynamic Study, Kinetic Study and Dry Digestion, Metals, 10, 1558; DOI:10.3390/met10111558

[48] Takáčová Z., et al. 2016. Cobalt and lithium recovery from active mass of spent Li-ion batteries: Theoretical and experimental approach, Hydrometallurgy, 163, 9-17.

[49] Takáčová Z., Marcišová S., Havlík T. 2013. Solvent extraction of cobalt from leach liquor after leaching of the active mass of spent lithium accumulators, Metall, 67(10), 450-454.

[50] Takáčová Z. 2023. Recycling of metal-bearing components from used portable lithium batteries and accumulators, Habilitation thesis, FMMR TUKE.
[51] Havlik, T., Miškufová, A., Oráč, D. 2020. Material recycling of metal-bearing waste containing defined deficient metals into salable products Stav a vízie zhodnocovania odpadov z automobilového priemyslu SR., 2020, SPEKTRUM, Bratrislava, 285.
[52] Havlik, T., Miškufová A., Oráč, D. 2021. Material recycling of lithium automotive traction accumulators (in Slovak). Progresívne technológie zhodnocovania odpadov v automobilovom priemysle, Bratislava, SPEKTRUM STU, 120-143.
[53] Havlik, T., Miškufová A., Oráč, D. 2021. Industrial recycling End-of-life Electric Vehicles Litihium-ion Batteries. In: Analysis of the State, Forecasts and New Technologies of Waste recovery in the Automotive Industry. RAM-Verlag, Germany, UNIVNET STU, 93-110.
[54] Havlik, T., et al. 2022. Extraction of valuable components from the discarded lithium accumulators from electric vehicles. In: Smart technologies for waste processing from the automotive industry, 85-103.
[55] Havlik, T. 2023. Recycling of discarded car batteries: past, present, future (in Slovak), Proc. Int. Conf. TOP 2023, November 2023, Starý Smokovec

6 Analysis and Design of Innovative Material and Design Solutions for Noise Barriers Based on Recycled Materials

6.1 Introduction

Despite existing European and national legislation targeting noise control, public interest and concern over noise remains high. EU Directive 70/157/EEC on the determination and management of environmental noise aims to create a quieter and more pleasant environment for Europe's citizens within the framework of "Sustainable Development in Europe". The harmful effects of environmental noise are diverse and can manifest themselves in different ways. We can talk about health effects, quality of life effects, but also financial effects on the health of those affected [1].

In the European Union, around 80 million people are exposed to high noise levels that are unacceptable, often leading to sleep disruption and other adverse effects. Roughly 170 million people live in so-called "grey zones", where noise is very annoying and bothersome. Noise has become a serious problem especially in recent years due to the intensive development of industry and transport in 40 % of working and 60 % of non-working environments [2, 3]. In the EU countries, approximately 40 % of the population is exposed to traffic noise with an equivalent level exceeding 55 dB(A), and 20 % of the population is exposed to traffic noise with an equivalent level exceeding 65 dB(A) during the daytime [2-5]. At night, more than 30 % of the population is exposed to equivalent noise levels exceeding 55 dB(A), which has an extremely disturbing effect on e.g. human sleep [6, 7]. Transport is a significant environmental source of noise: road, rail and air traffic [8].

Traffic is a major environmental noise problem. In Europe, the first limits were set for transport. The most important is EU Directive 70/157/EEC limiting noise for vehicles. Since 2002, the EU has regulated noise emissions from rail transport. For air transport, the limits are mainly set at international ICAO (International Aviation Organization) levels. In the conditions of the Slovak Republic, the permissible values of the determining variables of noise in the outdoor environment are set by the Decree of the Ministry of Health of the Slovak Republic No. 549/2007 laying down details on permissible values of noise, infrasound and vibration, and on requirements for the objectification of noise, infrasound and vibration in the environment [5, 6].

The UNIVNET project team focused its activities in the given year on the analysis of current material and design solutions of noise barriers, summarization of the requirements placed on the used material, the structural and acoustic properties of noise barriers, and a design solution of the original noise absorber applicable to the noise barrier system. The researchers focused on the research of acoustic conditions on a selected section of the motorway, where the application of previously proposed modules of sandwich structures of noise barriers using recycled material from the automotive industry is assumed. The project authors also predict the next stages of the task.

6.2 Analysis of current material and design solutions for noise barriers

One of the current problems in the field of environmental protection is the increasing level of noise. Noise has a negative impact on the human body, affecting its activities and overall health. This problem is manifested not only in residential and industrial areas, but especially in the vicinity of traffic routes with automobile and railway traffic. Harmful acoustic impacts on people can be mitigated by appropriate design of noise protection measures in the form of noise barriers.

In addition to their primary role in environmental protection, noise barriers also have a secondary influence on the shaping of the space in which they are placed. Anti-noise screens (Fig. 6.1) also include noise reduction barriers (Fig. 6.2).

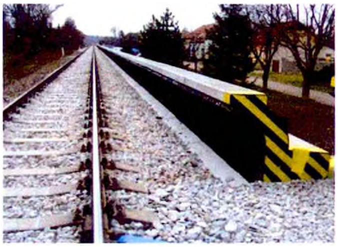

Fig. 6.1 Low noise barrier [19]

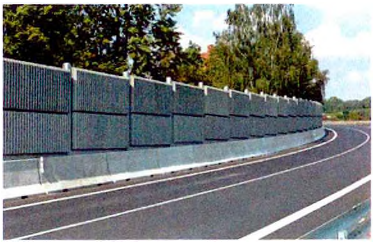

Fig. 6.2 Noise reduction wall [20]

The reduction of the sound level behind the sound barrier depends on the following factors: the acoustic properties of the noise reduction wall, dimensions of the noise reduction wall, position of the source, the noise reduction wall and the receiver, volume of traffic, road surface, condition and speed of vehicles, nature of the terrain between the road and houses, and weather conditions.

6.2.1 Criteria for the design and implementation of noise reduction measures

The decisive criterion for the design and implementation of noise reduction measures in the vicinity of the monitored road is the exceeding of the limit value of the determining variable for the individual reference time intervals, caused by traffic along the relevant section of the monitored road [9-11].

If, for the time interval and the area or location under consideration, the difference between the summed sound level value (equivalent A sound level) and the value of the determinant for road traffic noise (equivalent A sound level) as determined by the measurement or prediction for the road section under consideration is [10-12]:

- noise less than 3 dB, caused by traffic along the monitored section of the road, influences the acoustic situation in the evaluated place or area significantly, traffic along the monitored section of the road determines the noise load in its affected surroundings; through the implementation of appropriate noise reduction measures it is possible to achieve a significant reduction of the noise load in the monitored area;

- noise in the interval from 3.1 dB to 10 dB, caused by traffic along the monitored section of the road, influences the acoustic situation in the evaluated place or area; the implementation of noise reduction measures in the vicinity of the monitored road will affect the noise load in its affected surroundings;
- noise in the interval of 10.1 to 19.5 dB, caused by traffic along the monitored section of the road, influences the acoustic situation in the evaluated place or area minimally; the implementation of noise reduction measures in the vicinity of the monitored road will reduce the noise load in its affected vicinity minimally;
- noise greater than 19.6 dB, caused by traffic on the monitored section of the road, affects the noise load in the evaluated place or area insignificantly; implementation of noise reduction measures in the vicinity of the monitored section of the road will not affect the noise load in the affected area.

6.2.2 Categories of noise reduction measures

With respect to the solution principle of measures to reduce the noise burden from road transport, the noise reduction measures can be divided as follows [10-13]: urban-architectural, urban-traffic, transport-organizational and civil-technical.
Individual measures may be combined with each other. In most cases, civil engineering measures are used in the implementation of a specific road.

Urban-architectural noise protection measures

Urban-architectural noise protection measures are applied in the design of construction and reconstruction of residential buildings in the framework of spatial planning in an effort to achieve the least possible degradation of the urban environment by traffic noise.

The guiding principles of these measures are [11-13]:

- comprehensive design of residential complexes in terms of functional layout and, in relation to the transport system, with maximum application of the protection of quiet areas, if they are declared in accordance with the wording;
- appropriate dislocation of objects according to their purpose;
- appropriate layout of buildings;
- suitable height-oriented solution of the urban environment;
- appropriate architectural design of buildings;

Urban-traffic noise protection measures

The process of design and implementation of the transport system must ensure conditions for the reduction of noise pollution in the urban environment by following these principles [11], [13, 14]:

- optimize transport requirements;
- rationalize transport relations in the area under consideration;
- the communication system should be designed in a way to exclude transit traffic from the centre and residential areas;

- expressways and frequently used local roads, as well as flyovers or grade-separated junctions, to be routed away from residential and historic zones and areas with higher noise protection requirements;
- exclude the heavy traffic of goods from the vicinity of housing estates;
- concentrate the different types of traffic in the main routes with the possibility of creating noise reduction measures (observe the protection zones);
- routes of the roads need to be kept at a sufficient distance from buildings, with the protected outdoor space in front of the indoor protected space, or their planned construction, and at a sufficient distance from the outdoor protected space;
- create conditions for a preference for public transport in cities;
- transport areas such as car parks, rest areas and forecourts to be designed at a sufficient distance from residential, health, school and recreational areas;
- organize quiet zones in the centres of towns and housing estates, with the exclusion of car traffic and with the time limitation of vehicle entrances for supplies.

Traffic-organizational noise reduction measures

Restricting traffic by organizational and legislative measures generally always leads to a reduction in road performance. Nevertheless, this alternative is an effective and, in densely populated areas, the only feasible means of protection against road traffic noise.

This includes, in particular, the following measures [13-16]:

- speed limits for all vehicles or only for trucks;
- restricting the speed of vehicles at night;
- reducing traffic volume by banning trucks, establishing detours and designating one-way streets;
- improving traffic flow by coordinating signal-controlled intersections with a dynamic cycle, turning off traffic signals during the night;
- dedicating a special traffic lane for certain types of vehicles, e.g. buses;
- ingenious location of public transport stops and parking areas.

Construction-technical noise protection measures

If it is not possible to solve the reduction of the noise load in the vicinity of the monitored roads with the measures mentioned earlier, it is necessary to focus on the design of construction-technical anti-noise measures, while it is possible to consider the following measures: measures at the source of noise (rolling of road vehicle wheels in interaction with the road surface), measures on the noise propagation path and measures on buildings.

Measures at the noise source

The road layout interacting with moving vehicles has a significant contribution to the noise pollution (situation) in the vicinity of roads.

Suitable solutions that reduce the noise level of the noise source are [13, 15]:

- ensuring conditions for the smooth movement of vehicles;
- moderate longitudinal slope of the road level –higher gradients should be designed away from residential and protected buildings;
- implementation of covers, surfacing layers, pavement made of materials that generate less acoustic energy in interaction with the rolling of the wheels of road vehicles;
- routing of the road in the cut,
- deliberate use of the terrain configuration (e.g. when routing through a valley, the noise will hit the hillside and its reflection will virtually cover the entire unprotected valley area);
- routing in a tunnel (possibly also in an artificially created one, e.g. with a partial artificial cut and filling the upper part with soil), taking into account the increase in noise levels at the tunnel portals;
- routing through a gallery;
- routing on a bridge, viaduct or flyover.

6.2.3 Design, construction, material used and location of noise reduction barriers

A noise reduction wall consists of foundations, load-bearing and filling elements. Brick and block infills or blocks are fitted between columns of different profiles and materials and dimensioned in the structural calculation [17-20].

From the safety point of view, noise reduction barriers must respect the requirements of safety traffic on roads; another condition is sufficient stability, shape and dimensional stability, resistance to deformation, stone impact, wear, aging, etc.

Table 6.1 below describes the infill materials used, as well as showing realistic views of noise reduction barriers [17, 18].

Table 6

Noise reduction barriers according to the filling material used [17, 18]

Material	A realistic view of a noise reduction wall
concrete, reinforced concrete	
metal, metal with profiled sheet cladding	
aluminium	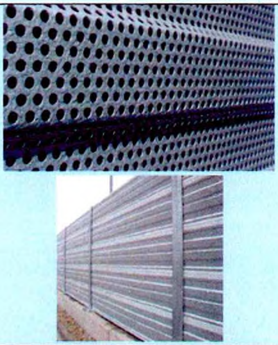
gabion	
bricks and blocks	

transparent material (safety glass, acrylics, polycarbonates, etc.)	
opaque recycled plastic with absorbent liner	
natural materials (chipboard, wood, all-wood with absorbent liner, cement chipboard)	
fully or partially green	
combined	

Table 6.2 shows and describes the geometric shapes of noise reduction barriers, which can be very diverse.

According to the principle of acoustic energy reduction, noise reduction barriers are divided into the following categories [21]:

- reflective,
- absorptive,
- combined.

Table 6.2

Schematic representation of the shapes of noise reduction barriers

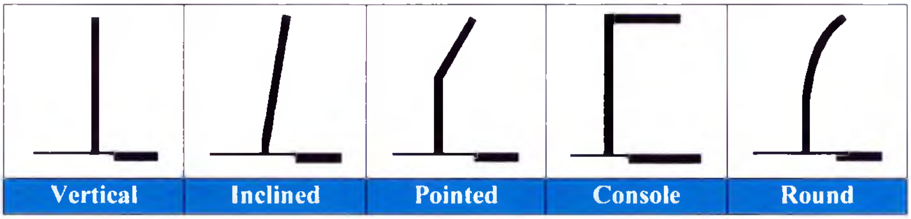

Reflective noise reduction barriers are made of hard materials that reflect sound. Absorption barriers are made of materials that absorb sound. Since no material has the property of merely reflecting or merely absorbing sound, the classification is made on the basis of which property is predominant.

The structure of barriers, or the classification of forms and structures, is not complex because in general noise reduction barriers are made of a small number of basic parts. The individual parts are the upper part, the middle part and the lower part.

The noise reduction wall also consists of the following structural parts [21]:

- the top edge that creates a silhouette against the background,
- the bottom edge that touches the substrate,
- the supporting or load-bearing structure,
- foundations, or lower construction

The choice of noise reduction barriers is determined by acoustic requirements, but technical and constructional characteristics, architectural appearance, road safety and stability of acoustic properties during their service life must also be taken into account. For each type of material there are many characteristics that can influence the appearance and design of the barriers. Durability is also an important factor of a noise reduction wall. A lifespan of 40 years is required, with maintenance only being considered after the twentieth year of construction. Exceptions are noise reduction barriers combined with vegetation, which require ongoing maintenance.

Absorptive noise reduction barriers are almost always opaque. Reflective noise reduction barriers can be opaque or transparent.

Transparent barriers allow a full or partial view through the barrier. Various methods are used to reduce transparency (etching, foil bonding, surface staining, etc.). Transparent barriers require more frequent cleaning, unless surface treatments are applied to prevent dirt build-up and ensure self-cleaning by rain.

A noise reduction barrier needs to be designed as a whole, including consideration of the terrain configuration and the inclusion of embankment or cut slopes, earth banks and retaining or frame walls.

It may consist of a uniform surface (a single material), but elements under the wall, especially the substrate or terrain, makes a complete noise barrier [21].

Location of the noise reduction wall

The screening effect of a noise reduction wall is most effective when it is placed as close as possible to the road. If a roadside design cannot be implemented due to terrain constraints, the wall can also be placed at the receiver if it is located in an isolated group of houses. The suitability of this solution must be examined with regard to the ownership relations of the area where the noise reduction wall will be implemented [22-24].

The rule that the noise reduction wall should be placed as close as possible to the source or receiver does not apply if the road is in a cut or if they are separated by a terrain elevation. In this case, it is best to place the noise reduction wall at the top of a slope or a cut.

The noise load on the receiving side is most affected by the traffic stream furthest away from the noise reduction wall. Simply increasing the height will not change the dominant effect of the noise on the receiving side caused by the furthest traffic stream. Raising the noise barrier to eliminate this impact may result in unacceptably high walls. In such situations, it may be advantageous to use a second noise reduction barrier, placed between the traffic lanes, as the two barriers are placed as close as possible to the two noise sources – see Fig. 6.3. This technique allows the overall height of the noise reduction wall to be minimized and is particularly beneficial for roads with a central reservation, and situations where the receivers are located above road level.

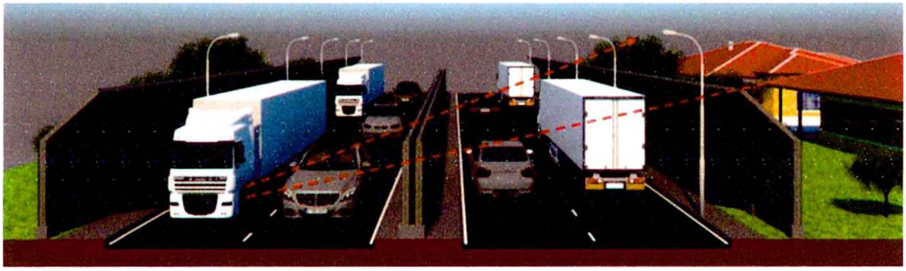

Fig. 6.3 Applied noise reduction wall between two traffic lanes to improve protection

Length of a noise reduction wall

Sound scattering does not only occur at the top of the noise reduction wall, but also at the ends of the wall. Therefore, the overall noise reduction of a noise reduction wall depends not only on its height and location between the noise source and the receiver, but also on its length (Fig. 6.4).

Sound that is scattered at the ends of the noise reduction wall is of less importance than sound scattered at the top edge, because this path of travel will still be favored by the absorptive effect of the terrain. If there is sufficient space and it is necessary to reduce the noise load in a smaller area or even in a limited area, the length of the noise wall can be reduced by bending its ends away from the road (Fig. 6.4).

Material properties

Noise generally propagates in all directions (Fig. 6.5). Effective noise protection requires comprehensive and high-quality consideration in the project documentation, specifically in a site-specific noise study. The project documentation must meet the noise protection criteria, and it is therefore important that the design of the solution is based on the analysis of the noise study. The result of the noise study is a noise map that graphically shows the distribution of noise in the area using isophones.

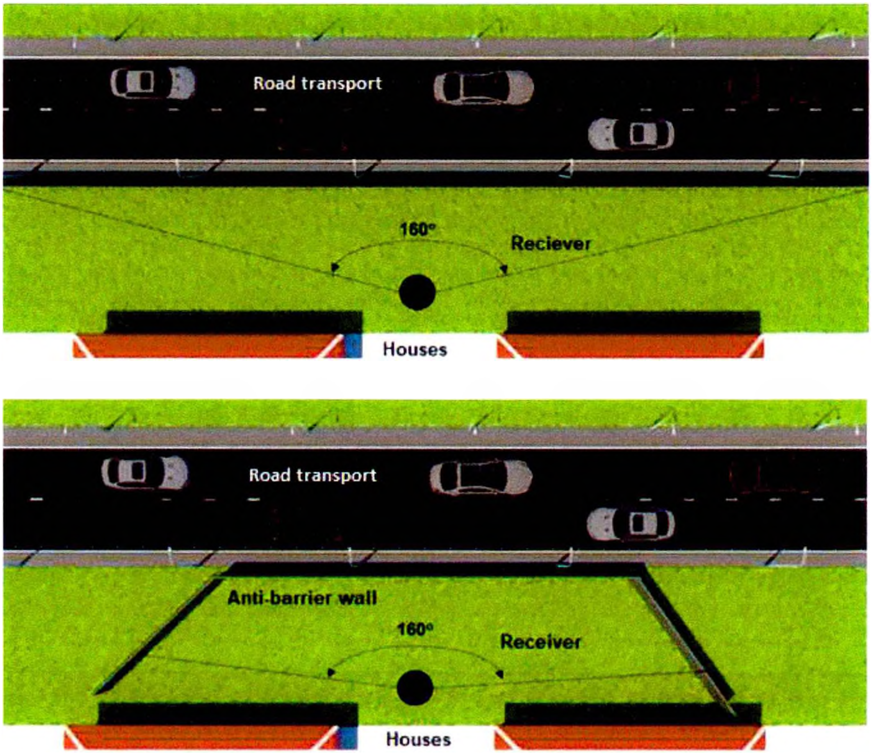

Fig. 6.4 Reducing the length of the barrier by bending the ends away from the road

One of the measures to comply with the permissible limits of noise levels is the construction of noise reduction barriers. The extent and parameters of these barriers result from the calculations of the noise study.

In general, the materials of which noise reduction barriers are made are divided into two basic groups:

a) **noise reflective materials** – do not transmit sound, but reflect it into the space (often preferred in areas outside residential zones),

b) **noise absorbing materials** – the material absorbs sound (these materials are used most often in urban areas). The most popular are sandwich panels with sound insulation.

a) Reflecting noise reduction barriers

With a reflective wall, the noise is reflected and further propagated into the space. Reflected noise is noise spreading from an imaginary source located at the same distance from the wall as the source, but on the opposite side of the road.

Even if the imaginary source is further away from the receiver than the real source, it must be taken into account and the need for shielding of an imaginary noise source must be verified. For tall vehicles, noise reflections between vehicle objects and the parallel wall are generated and can be reduced by the acoustic properties of the wall. The reduction of the acoustic properties of the reflective wall when any vehicle passes along significantly affects the increase in peak noise levels (the distance between the vehicle and the wall does not matter), to which the equivalent noise level L_{Aeq} is sensitive. The acoustic properties of the wall are restored by applying a noise-absorbing layer, even if the vehicle object is higher than the wall.Figs. 6.6, 6.7 and 6.8 show the direction of propagation of sound waves using reflective noise reduction barriers.

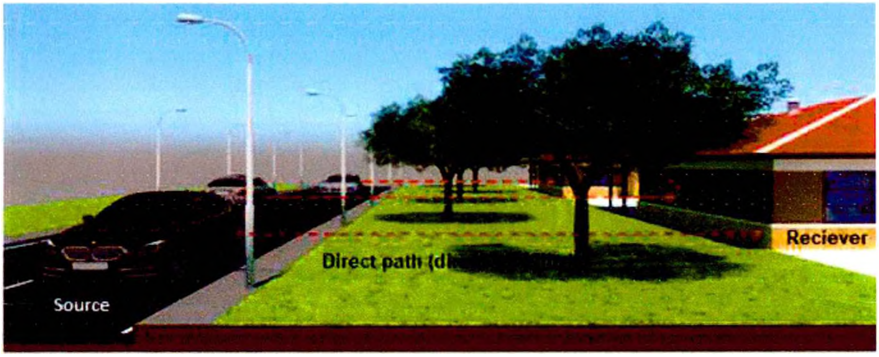

Fig. 6.5 Direction of propagation of sound waves without a reflective noise reduction wall

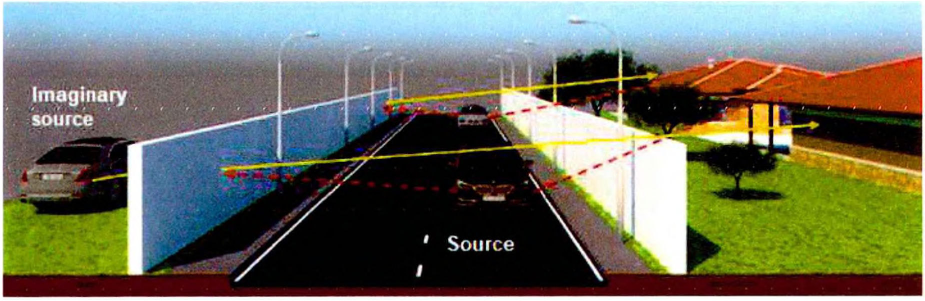

Fig. 6.6 Direction of propagation of sound waves using a reflective noise reduction wall

b) Barriers with absorbent treatment

The trend nowadays is to use sound-absorbing barriers as much as possible (Fig. 6.9), which absorb sound as close as possible to the noise source. Especially in cities, it is required that noise be minimised rather than reflected further into space. There are two main groups of sound absorption mechanisms used in noise absorbing barriers. Most absorptive barriers have a permeable layer of material to counteract the incoming noise. The flow resistance of the porous material causes the acoustic energy of the sound waves to dissipate inside the material and is eventually transformed into thermal energy. Here we are talking about sandwich stacked infill panels. The mechanism of the second group is based on the Helmholtz resonator principle, where the incoming sound wave enters a series of cavities in the wall through small holes or narrow openings where it is absorbed. The strongest absorbent materials, such as mineral wool, are protected and enclosed in a shell (casing) with the perforated surface exposed to sound. These casings can be made of wood, steel, aluminium, ceramic or recycled plastic.

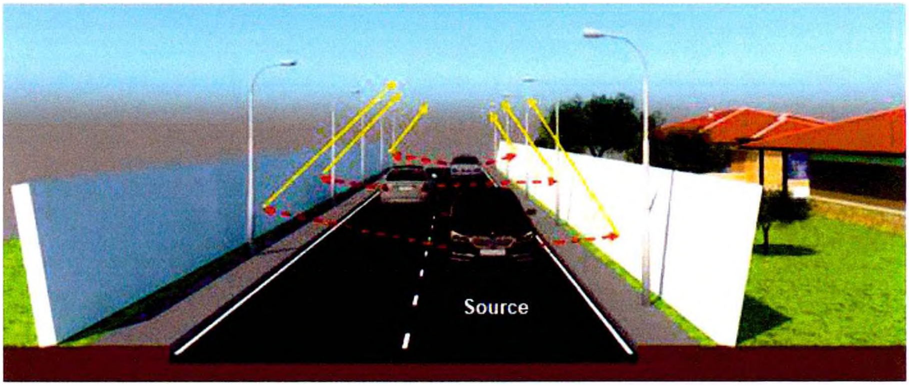

Fig. 6.7 Direction of propagation of sound waves using a reflective noise reduction wall

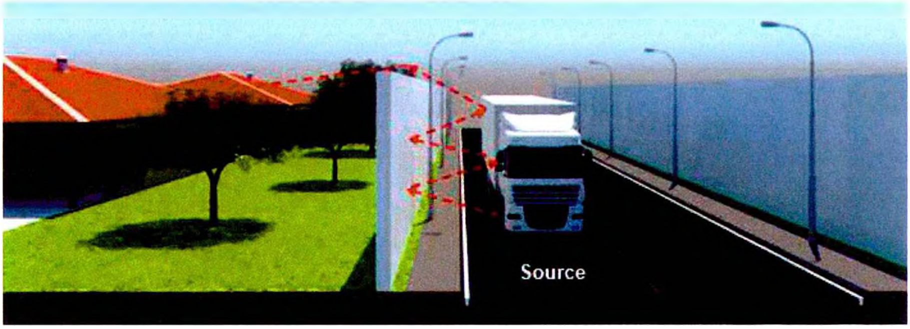

Fig. 6.8 Multiple reflections between a barrier and a high vehicle

Noise protection wall height reduction

The overall performance of a vertical wall is generally controlled by the sound scattering at its upper edge. These features can be improved by additional devices (Table 6.3).

There are currently a number of suitable solutions available on the market for additional devices to reduce road traffic noise. The effect of the device primarily depends on the diffracted (scattered) energy.

In general, they include sound-absorbing elements (Fig. 6.10), such as: barriers with multiple diffraction edges, phase-interference devices (e.g. octagonal reducer), bulb-and-nozzle (pear-shaped) moulds, Y-, T-shaped barriers and cylindrical heads.

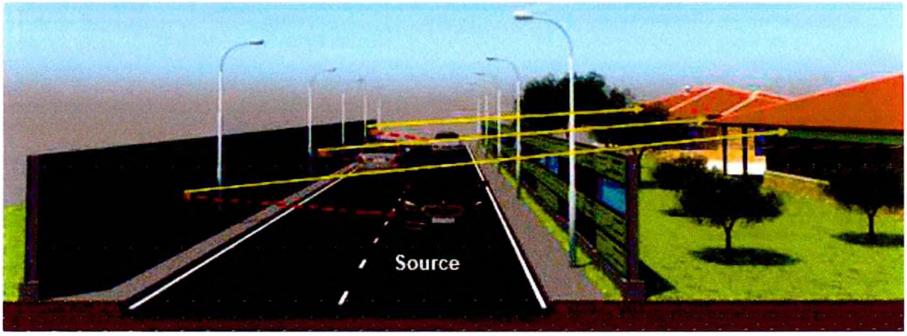

Fig. 6.9 Direction of sound propagation by reflection from a sound-absorbing wall.

Table 6.3 Schematic diagram of different noise reduction wall designs

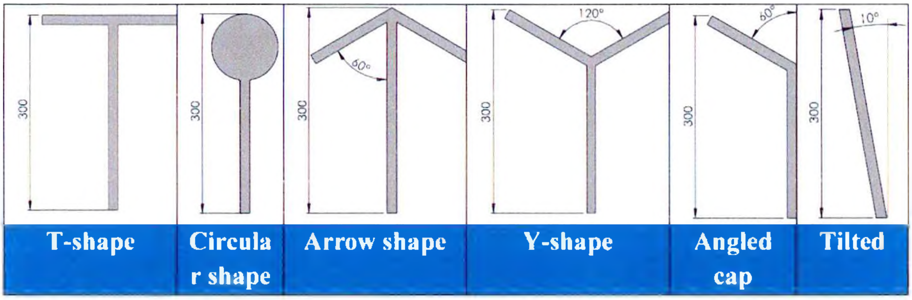
300
300
300
300
300
300
60°
120°
60°
10°
T-shape
Circular shape
Arrow shape
Y-shape
Angled cap
Tilted

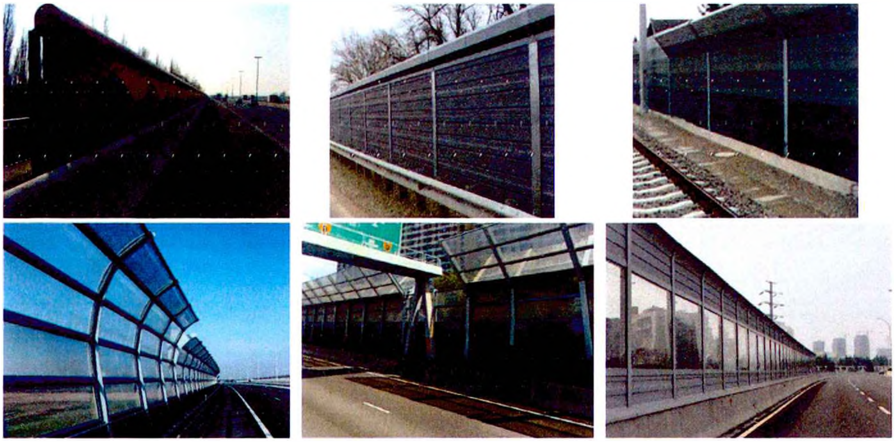

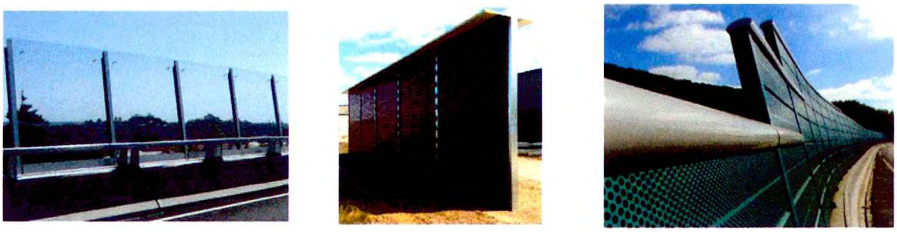

Fig. 6.10 Different shapes of noise reduction barriers.

The effectiveness of the wall depends on its structural elements, the material, as well as the effective height, length and location of the wall in the terrain. The less visible the source from the receiver (angle of coverage), the higher the so-called effective obstacle height, and the deeper in the sound shadow area the location under consideration, the higher the wall efficiency.

In open country, earth bank protection can be used. Earth banks should be designed as noise protection if excessive material from road construction can be used. However, they require more space – both the footprint of the land and the barriers, but on the other hand they have lower maintenance costs, their lifespan is not limited, and they adapt well to the environment once vegetation is planted.

Verification of acoustic properties of noise reduction barriers

The test methods for determining the acoustic performance of wall reduction barriers (NRB) for the purpose of their categorisation are given in STN EN 1793-1 and STN EN 1793-2. These standards specify laboratory test methods for the determination of airtightness and sound absorption for the purpose of NRB categories. Both procedures make it possible to determine for a NRB a single numerical quantity calculated using a standardised spectrum of traffic noise (see STN EN 1793-3) and to assign it, according to the observed value of the parameter under consideration, to one of the categories according to the categorisation given in STN EN 1793-1 and STN EN 1793-2.

For existing NRBs, their insertion loss is determined by measurement according to STN ISO 10847. Attenuation and absorption (reflective) properties are determined according to STN EN 1793-5 (absorption properties), or STN EN 1793-6 (attenuation properties). Following the procedures given in these standards, it is possible to obtain data similar to laboratory tests according to STN EN 1793-1 and STN EN 1793-2. The diffraction properties of existing NRBs shall be determined in accordance with STN EN 1793-4.

The real effect of NRB in terms of reducing the noise load in the affected vicinity of the road under consideration can only be determined by measuring the determinant of road traffic noise, the equivalent A sound level, at the point of reception or another defined location [25], [26], [27], [28]. The procedure is given in [29].

The entire NRB and the individual structural elements of the NRB shall meet the acoustic and non-acoustic performance requirements in accordance with [25].

Verification of the effect of the NRB on the reduction of noise load in the affected area by calculation using mathematical modelling shall be carried out according to the procedure set out in [29].

6.3 Requirements for the material, construction and acoustic properties of noise reduction barriers

When selecting materials for noise reduction barriers, the aggregate properties of the selected materials, their durability, longevity and, in some cases, safety characteristics must be taken into account. The following requirements prior to the construction and installation of noise reduction barriers shall be taken into consideration: fire resistance, shrinkage, UV protection, vandalism, shatter resistance – destruction resistance, surface finish, adhesives, binders, sealants, material ability to block sound transmission (STC), recyclability, cost, cleaning, light reflectivity, climatic constraints, structural strength and toxicity.

Concrete

Concrete (Fig. 6.11) is one of the most common and versatile building materials. It is a mixture made from a combination of Portland cement, coarse and fine aggregate and water, and may also contain specific additives to modify the rate of curing, aeration, strength, flow and porosity. Concrete intended for the construction of NRBs must in all cases exhibit a high degree of resistance to freezing aggressive environmental effects and the effects of thawing salts. The quality of concrete for structural parts made of plain concrete, reinforced concrete or pre-stressed concrete shall meet the requirements specified in [26], while the elements must be designed for the relevant aggressive environment, depending on the location of use, by incorporating the different environmental impact grades according to STN EN 206+A1. The concrete cover on the steel reinforcement shall meet the corrosion protection requirements of [26] and STN EN 1992-1-1. Concrete parts or their components that will be in contact with soil and ground moisture must be isolated. The shape, dimensions and grade of concrete shall be determined by the relevant project documentation or manufacturer's delivery conditions approved by the client.

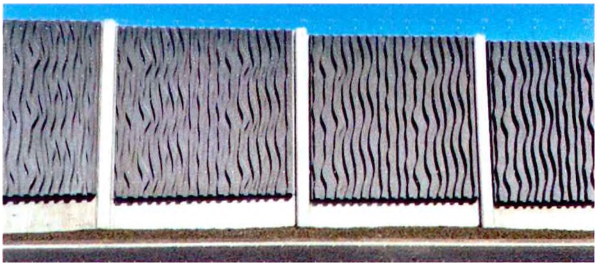

Fig. 6.11 Concrete noise reduction barrier

The main advantage, for example in reinforced concrete barriers, is its superior acoustic parameters, high durability, and quick and easy installation. The barriers have a self-cleaning effect due to their porous structure and are therefore completely maintenance-free.

Steel

Steel is the cheapest and most common of all metals used in construction. It consists of a mixture in varying proportions of iron ore, carbon and small amounts of other metals, depending on the desired physical properties. The material quality of the steelwork for the noise reduction barrier components shall be in accordance with the design documentation and meet the requirements in [27] and STN EN 1993-1-1. The steel plates used for the construction of a NRB shall be at least 1 mm thick. Steel structures shall be protected against corrosion due to atmospheric effects and chemical defrosting agents depending on the service life of the steel structure, the degree of corrosive aggressiveness of the atmosphere, the required service life of the protection, and the location of the protection application. Corrosion protection shall be carried out in the manner specified in the project documentation and in accordance with [27].

Light metals

Of the light metals, only aluminium alloys (Fig. 6.12), which are suitable for statically stressed structures, may be used for NRBs. Structural parts made of light metals shall not be permanently in direct contact with concrete, copper alloys, copper or other materials with which they react chemically on contact. The quality of the materials used for the light metal noise barriers shall comply with the requirements specified in the design documentation and the relevant STN EN 1993-1-1. Materials shall be suitable for statically stressed structures.

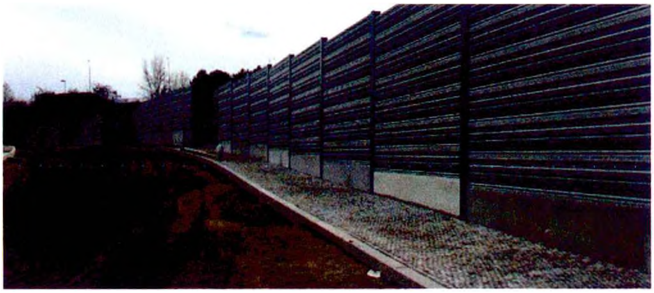

Fig. 6.12 Aluminium noise reduction barrier

Wood

Wood (Fig. 6.13) on the NRB must be marked by species and grade. It must be dry, pest-resistant and treated with hygienically sound wood preservatives. The required service life of the NRB timber elements is at least 25 years. Most wooden NRBs are made from pressure preserved wood, plywood and glued laminated timber. The quality of the material used for the wooden parts of the noise reduction barriers must comply with the requirements of the project documentation and the relevant STN EN 1995-1 1+A1 in terms of type, quality class, durability, and possibility of disposal. Wooden constructions must be deeply impregnated against rot, mould and wood-boring insects with products that have a certificate of approval in terms of hygienic safety. Wooden noise reduction barriers are often used when the barrier is required to blend in as much as possible with the surrounding nature. However, their disadvantage is their short service life and low resistance to mechanical effects of the packed material and the pressure exerted by winter and summer road maintenance equipment.

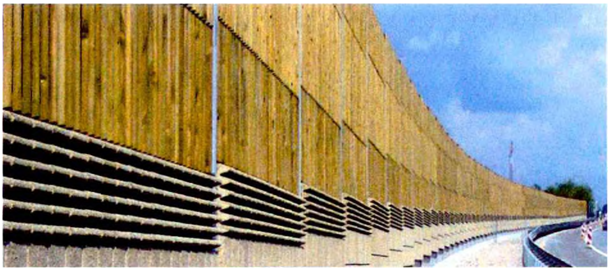

Fig. 6.13 Wooden noise reduction barrier

Glass

Transparent material of at least 12 mm thickness should be used for the construction of glass NRBs (Fig. 6.14). If the guide posts are more than 2 m apart, the transparent material shall be at least 15 mm thick. When using transparent materials, the effect of dangerous light reflections must be taken into account, which can also be a potential hazard for drivers (risk of glare) depending on local conditions. NRBs made of transparent materials are also dangerous for flying birds and therefore silhouettes of birds of prey are placed on the barriers.

The material quality of the glass barrier elements must comply with the requirements of the relevant STN EN 12150-1. The glass shall be safety glass of the thicknesses prescribed in the project documentation and shall be free from defects, such as visible depressions, edge notches or scratches. The type of glass used must be clearly specified in the project documentation.

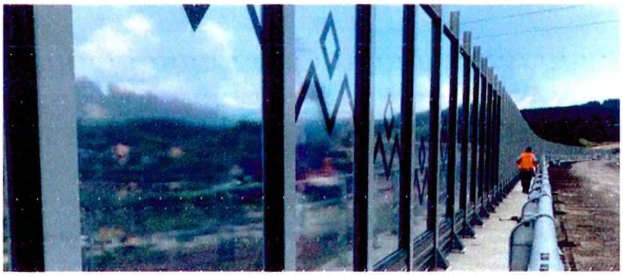

Fig. 6.14 Transparent noise reduction barrier

Plastics and recycled plastics

The plastics (Fig. 6.15) used for the NRB shall be resistant to ultraviolet and infrared radiation. Colored plastics must be colored permanently. Plastics must be resistant to damage by micro-organisms, fungi, rodents, etc. Combustion must not produce toxic gases in concentrations that endanger human health and the environment [24]. The required service life of the NRB plastic elements is at least 25 years. The quality and durability of the materials used for the plastic parts of the NRB shall comply with the requirements of the project documentation and the relevant STN 64 0011. They must be equipped with protection against ultraviolet and infrared radiation and environmental aggressiveness, while their physical-mechanical properties must not be compromised.

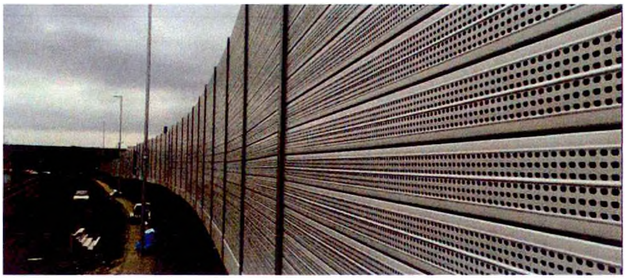

Fig. 6.15 Plastic noise reduction barrier

Bricks

The quality of the masonry and bonding materials used for the construction of a NRB must comply with the requirements of the design documentation and the relevant STN EN 1996-1-1+A1. They must be resistant to the effects of water, frost, environmental aggressiveness and chemical defrosting agents. When using perforated bricks, the barrier must be designed so that water does not enter the channels. Masonry elements shall be sufficiently durable to withstand relevant environmental exposure conditions over their expected service life. The mortar in the masonry shall be sufficiently durable to withstand relevant micro conditions of environmental exposure over its service life, and shall not contain ingredients which may have a detrimental effect on the properties or durability of the mortar or on adjacent materials.

Recycled rubber

The individual parts of a NRB made of recycled rubber (Fig. 6.16) shall fully comply with the acoustic and non-acoustic performance requirements of STN EN 14388. Rubber noise reduction barriers can be designed and implemented taking into account the circumstances. They help to elegantly address various constraints arising from local conditions and the requirements of the client. Recycled rubber panels are made from a mixture of recycled rubber granulate and a colorless or colored polyurethane binder. Used tyres dominate the rubber waste stream, and there is an effort to use this type of material as a usable product.

6.3.1 Selected data on NRBs in the Slovak road network

Table 6.4 provides data on the length of the constructed NRBs in the territory of the Slovak Republic.

6.3.2 Selected NRB parameters

Test methods for determining the acoustic properties of NRBs for the purpose of their categories are given in STN EN 1793-1 and STN EN 1793-2. These standards specify laboratory test methods for the determination of airtightness and sound absorption for the purpose of NRB categories. Both procedures make it possible to determine for a NRB a single numerical quantity calculated using a standardised spectrum of traffic noise (see STN EN 1793-3) and to assign it, according to the observed value of the parameter under consideration, to one of the categories according to the categorisation given in STN EN 1793-1 and STN EN 1793-2.

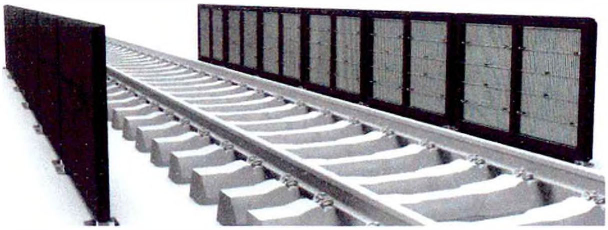

Fig. 6.16 Rubber noise reduction barrier

Table 6.4
Information on NRBs in the Slovak Republic (as of 1 January 2023)

Class	Used material	Total section in km	Partial section in km
Class I road	Wood	39.487	6.836
	Glass		5.212
	Plain concrete		0.788
	Reinforced concrete		16.880
	Brickwork		3.577
	Stone masonry		0.203
	Steel		1.497
	Plastic		4.469
	Gabions		-
	Other		0.025
Class II road	Wood	2.261	0.693
	Glass		0.406
	Plain concrete		-
	Reinforced concrete		-
	Brickwork		0.196
	Stone masonry		0.899
	Steel		-

	Plastic		0.067
	Gabions		-
	Other		-
Class III road	Wood	2.443	0.075
	Glass		0.098
	Plain concrete		-
	Reinforced concrete		2.061
	Brickwork		0.006
	Stone masonry		0.052
	Steel		0.151
	Plastic		-
	Gabions		-
	Other		-
Highways	Wood	146.407	3.995
	Glass		45.319
	Plain concrete		5.949
	Reinforced concrete		38.416
	Brickwork		20.028
	Stone masonry		3.025
	Steel		21.269
	Plastic		4.237
	Gabions		2.291
	Other		1.878
Expressways	Wood	101.672	-
	Glass		13.897
	Plain concrete		2.109
	Reinforced concrete		54.985
	Brickwork		2.713
	Stone masonry		1.466
	Steel		24.961
	Plastic		0.990
	Gabions		0.551
	Other		-
		292.270 km	

For existing NRBs, their insertion loss is determined by measurement according to STN ISO 10847. Attenuation and absorption (reflective) properties are determined according to STN EN 1793-5 (absorption properties), or STN EN 1793-6 (attenuation properties). Following the procedures given in these standards, it is possible to obtain data similar to laboratory tests according to STN EN 1793-1 and STN EN 1793-2. The diffraction properties of existing NRBs shall be determined in accordance with STN EN 1793-4. The real effect of the NRB in terms of reducing the noise load in the affected vicinity of the road under consideration can only be determined by measuring the determinant of road traffic noise, the equivalent A sound level, at the point of reception or another defined location [23]. The procedure is given in [7]. The entire NRB and the individual structural elements of the NRB shall meet the acoustic and non-acoustic performance requirements in accordance with [3]. Verification of the effect of the NRB on the reduction of noise load in the affected area by calculation using mathematical modelling shall be carried out according to the procedure set out in [7].

Sound absorption STN EN 1793-1:2017

This European Standard specifies a test method for the qualification of sound absorption values of road traffic noise reduction equipment (determination of internal values). It does not apply to the determination of losses (external value) which are not related to the product itself, e.g. dimensions of the barrier, quality of construction work or site-related influences such as ground surface impedance, urban-morphological situation, etc. The test involves measuring the sound absorption values of the equipment measured under diffuse sound field conditions; the resulting evaluation is intended to assist in the selection of equipment for specific road noise protection applications. The result of the test is intended to assist in the selection of a NRB for a particular application case on the relevant road. The test is carried out according to STN EN ISO 354: 2003. The NRB sound absorption categories are given in Table 6.5.

Table 6.5

NRB sound absorption categories

Category	Sound absorption [dB]	Characteristics
A0	Not specified	-
A1	< 4	low-absorption barriers
A2	4 – 7	partially absorbent barriers
A3	8 – 11	absorbent barriers
A4	> 11	high-absorption barriers

Sound insulation STN EN 1793-2:2018

Road noise barriers shall provide sufficient sound insulation so that the sound passing through the barrier is insignificant compared to the sound propagating through the top of the barrier. This European Standard specifies a test method for the determination of the airborne acoustic impermeability of noise barriers intended for use in reverberant locations such as tunnels, deep cuts or noise reduction barriers.

This document specifies a laboratory method for the determination of the air-tightness values of road noise barriers at reverberation points. It includes the assessment of the internal properties of noise barriers that can be assembled inside the test room, as described in EN ISO 10140-2 and EN ISO 10140-4. The NRB airtightness categories are given in Table 6.6.

Table 6.6
NRB airtightness categories

Category	Sound absorption [dB]	Characteristics
B0	Not specified	-
B1	< 15	soundproof barriers
B2	15 – 24	adequately soundproof barriers
B3	> 24	perfectly soundproof barriers

6.4 Design solution of the original damper applicable to the noise reduction barrier system

Mutual cooperation of the Faculty of Mechanical Engineering of the Technical University in Košice (Slovak Republic), the company Ochrana životního prostředí s.r.o, Prague (Czech Republic) and Wavebreaker AB (Sweden) brings a new type of damper to reduce unwanted traffic noise based on a patented innovation (Fig. 6.17). The basic technical parameters of the damper are given in Table 6.7 and the dimensions of the basic damper module are given in Fig. 6.17.

The design solution allows passively emitting "counter-noise – anti-noise", which reduces noise on the receiver side.

Table 6.7
Technical parameters of the damper

Noise reduction:	3 – 7 dBA (rail, road noise)
Width:	50 cm
Height:	0.2 m above the barrier
Weight:	approx. 8 kg/pc = 16 kg/m
Construction:	2 modules
Material:	Polypropylene, HD polyethylene
Maintenance:	The material generally requires no maintenance
Delivery:	Ready for mounting on the noise reduction barrier
Durability:	Lifetime of the material in the original colour up to 50 years

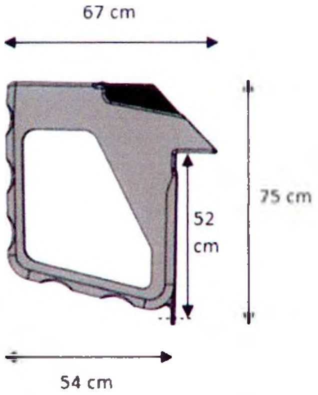

Fig. 6.17 Dimensions of the module

The principle used is one that has been known since 1866 (Fig. 6.18). On the basis of the simulations carried out, it is possible to predict noise reduction up to 7 dBA. It is a lightweight product with negligible impact when mounted on existing noise barriers.

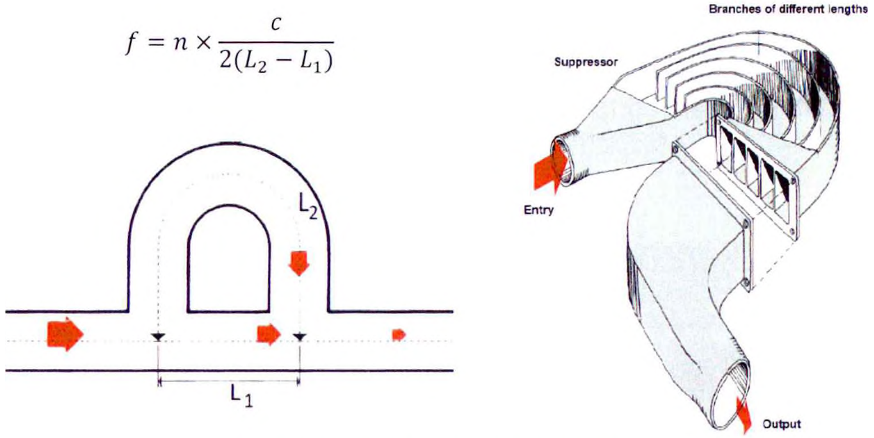

$$f = n \times \frac{c}{2(L_2 - L_1)}$$

Fig. 6.18 Basic principle of a damper

The damper consists of an acoustic insert and an acoustic box, which together radiate sound waves that meet the direct sound that passes over the damper and the noise barrier. This creates acoustic interference and reduces noise in the frequencies that are most disturbing, annoying, etc. It is a completely passive damper and does not need any electrical power to operate. It can be applied to both existing noise barriers and newly constructed noise barriers.

The damper consists of three basic modules (Fig. 6.19), which can be combined as required to form

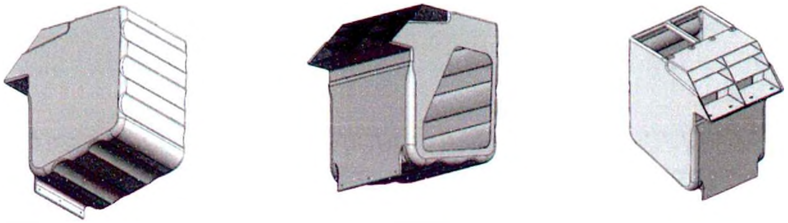

a) leftmost module b) centre module c) rightmost module

Fig. 6.19 Damper modules

of unlimited length (Fig. 6.20). The proposed design and material solution predicts easy assembly and disassembly on already existing or newly built noise

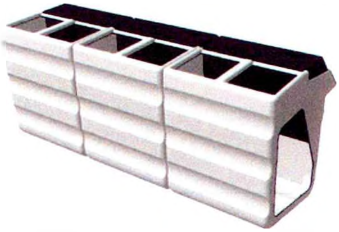

Fig. 6.20 View of the module assembly

reduction barriers (Fig. 6.21). It contains no metal parts and can be presented as a lightweight product with negligible impact on the noise barrier. The material used for the production of individual modules is assumed to be HD-polyethylene and polypropylene. Selected technical parameters of the possible material to be used are given in Table 6.7.

Table 6.6
Technical parameters of the possible material used

HD-polyethylene is a thermoplastic with good chemical resistance and low water absorption.		**Polypropylene is a thermoplastic with good chemical resistance and low water absorption.**	
Tensile strength:	20 MPa	**Tensile strength:**	30 MPa
Melting point:	135 °C	**Melting point:**	165 °C
Fire characteristics:	HB (UL94)	**Fire characteristics:**	HB (UL94)
UV resistance:	high	**UV resistance:**	high

The product could meet today's environmental requirements, and it can be manufactured from 100 % recycled plastic from the automotive industry. It can be recycled again at the end of its life cycle. The standard color is assumed to be dark grey black. Other color versions according to customer requirements are not excluded.

Fig. 6.22 shows the outputs of a simulation carried out on the propagation of the sound disturbance field at a frequency of 1,000 Hz, which is typical for traffic noise, assuming no applied damper (Fig. 6.22 (a)) and provided that a damper is applied (Fig. 6.22 (b)). The simulations performed predict the possibility of noise reduction in the range of 3 – 7 dB.

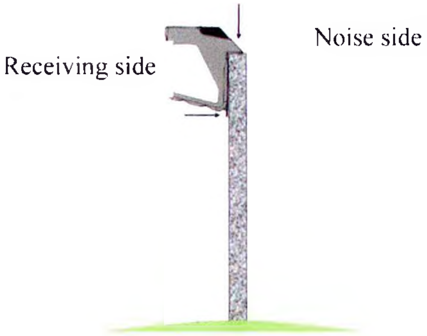
Noise side
Receiving side

Fig. 6.21 Design of the damper location

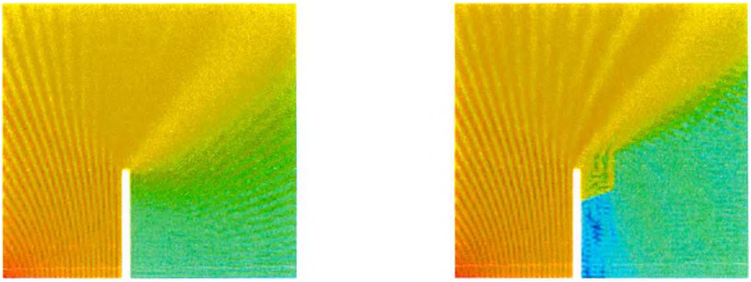

a) Without sound damper

b) With sound damper

Fig. 6.22 Simulation of the propagation of a sound disturbance field (frequency 1,000 Hz).

The benefits of the presented damper can be considered as the positive benefits presented in Fig. 6.23.

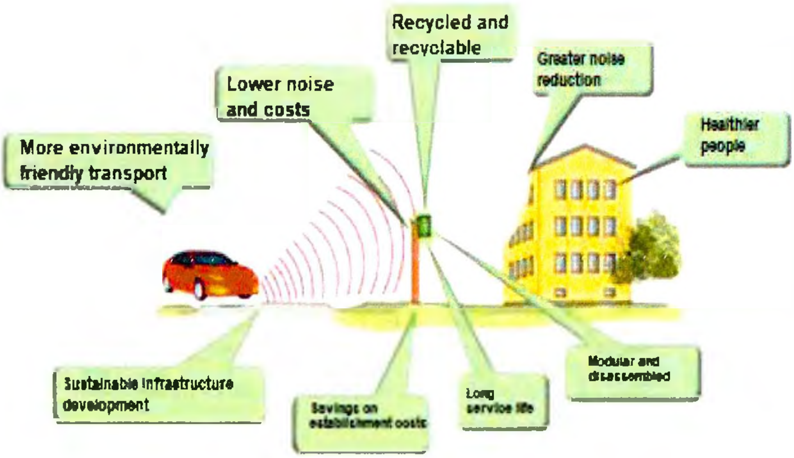
Recycled and recyclable
Greater noise reduction
Lower noise and costs
More environmentally friendly transport
Healthier people
Sustainable infrastructure development
Savings on establishment costs
Long service life
Modular and disassembled

Fig. 6.23 Positive aspects of the presented damper

6.5 Investigation of acoustic conditions on a selected motorway section

Description of the monitored site

The D2 motorway section (Fig. 6.24) in the vicinity of Jarovce runs west of Jarovce, which is

the city part of Bratislava, Bratislava V district. This is the section from the D2/D4 motorway junction in the direction of the border crossing Čunovo (SR) – Rajka (HU).

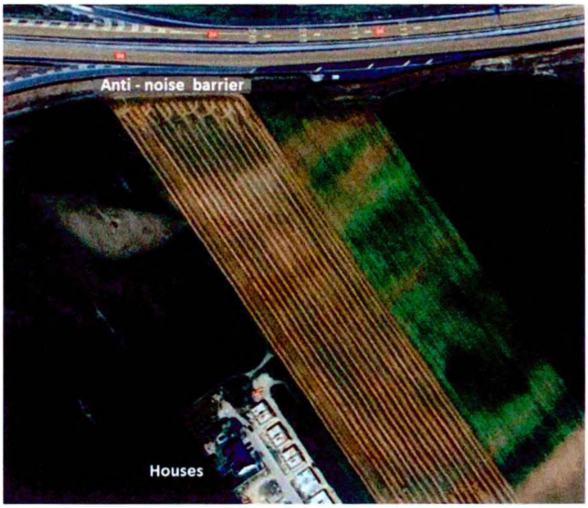

Fig. 6.24 Motorway section D2 in the vicinity of Jarovce

The motorway section runs through flat terrain, surrounded on both sides by agricultural land. The motorway section under consideration runs in full profile with a maximum permissible speed of 130 km/h. In the northern direction in this part of the motorway section there is the Jarovce motorway junction, which connects the motorway section in question with the following section of the D4 motorway, which connects the border crossing Bratislava – Jarovce (SR) – Kittsee (AT) with the Jarovce intersection and continues on in the direction Bratislava – Rača. Local road no. III/1020 from Jarovce leads over the motorway section D2 Jarovce. The surface of the section is made of asphalt.

North of Jarovce there is agricultural land, behind which there is the local road no. III/1020 and the D4 motorway. To the east and south of Jarovce there is agricultural land. To the west of Jarovce there is agricultural land, the section of the D2 Jarovce motorway in question, beyond which there is agricultural land and the SK – AT state border.

The given section was selected for the assessment on the basis of repeated measurements before and after the construction of the noise reduction barrier (NRB). Based on these measurements, it is possible to assess the effectiveness of the constructed NRB.

The M1 measurement site (Table 6.7) was chosen in a field near Kožušnícká Street in Jarovce, at a distance of approximately 346 m east of the axis of the D2 Jarovce motorway section. On Kožušnícká Street there are family houses. In the direction between the assessed section of the D2 Jarovce motorway there is agricultural land, the construction of new family houses, and a local road along Kožušnícká Street. In the eastern and south-eastern direction, there is a development of family houses with adjacent plots of land.

Noise reduction barrier

The object deals with the construction and foundation of noise reduction barriers, which consist of two branches

Tab. 6.7

Measurement site M1 – Jarovce, near Kožušnícká Street.

Measurement		**Stage 1 of noise monitoring prior to NRB construction**		**Stage 2 of noise monitoring prior to NRB construction**		**Comparison of stages 1 and 2 difference in**
Reference time interval	**Permissible value** [dB]	$L_{\mathrm{Aeq,Tref}} + U$ [dB]	**Evaluation**	$L_{\mathrm{Aeq,Tref}} + U$ [dB]	**Evaluation**	
Day (06:00 – 18:00)	60	52.6 + 1.8	**Not exceeded**	50.4 + 1.8	**Not exceeded**	+ 1.8
Evening (18:00 – 22:00)	60	52.3 + 1.8	**Not exceeded**	51.4 + 1.8	**Not exceeded**	- 0.9
Night (22:00 – 06:00)	50	52.5 + 1.8	**Exceeded**	52.3 + 1.8	**Exceeded**	- 0.2

Measurement		**Stage 3 of noise monitoring during NRB construction**	
Reference time interval	**Permissible value** [dB]	$L_{\mathrm{Aeq,Tref}} + U$ [dB]	**Evaluation**
Day (06:00 – 18:00)	50	49.4 + 2.3	**Not exceeded**

Measurement		**Stage 4 of noise monitoring during the 1st year of NRB operation**		**Stage 5 of noise monitoring during the 1st year of NRB operation**		**Comparison of stages 4 and 5 difference in [dB]**
Reference time interval	**Permissible value** dB	$L_{\mathrm{Aeq,Tref}} + U$ [dB]	**Evaluation**	$L_{\mathrm{Aeq,Tref}} + U$ [dB]	**Evaluation**	

Measurement		**Stage 1 of noise monitoring prior to NRB construction**		**Stage 2 of noise monitoring prior to NRB construction**		**Comparison of stages 1 and 2** difference in
Reference time interval	**Permissible value** [dB]	$L_{Aeq,Tref}$ + U [dB]	**Evaluation**	$L_{Aeq,Tref}$ + U [dB]	**Evaluation**	
Day (06:00 – 18:00)	60	49.0 + 1.8	**Not exceeded**	45.4 + 1.8	**Not exceeded**	- 3.6
Evening (18:00 – 22:00)	60	48.4 + 1.8	**Not exceeded**	44.4 + 1.8	**Not exceeded**	- 4.0
Night (22:00 – 06:00)	50	45.5 + 1.8	**Not exceeded**	47.9 + 1.8	**Not exceeded**	+ 2.4

NRB 1 and NRB 2. These are further subdivided into smaller sections where the noise reduction barrier had to be moved back to take account of fixed obstructions.

The classification and basic parameters of NRB:

- **NRB1**
  - Barrier length: 1,604 m.
  - Height of the barrier from the top of the pile: 5.27 m.
- **NRB2**
  - Barrier length: 138.00 m.
  - Barrier height: 5.27 m.

Along the proposed noise reduction barrier, existing safety devices will be maintained. Noise reduction barriers must meet the acoustic requirements and architectural appearance: NRB supporting structure – self-supporting columns, fill of NRB – one-sided absorbent panels 125 mm thick, double-sided absorbent panels 125 mm thick in sections 1H, 2A, 2B and corrosion protection of the steel parts must meet the requirements of long-term durability.

The purpose of the noise reduction barrier is to reduce the sound level from traffic in the adjacent inhabited parts of the road. The NRB must meet acoustic and static requirements and also fulfil an aesthetic function. The above also implies the characteristics of the noise reduction barrier, the construction of which consists of steel HEB columns, between which are inserted one-sided and two-sided absorbing panels. The noise reduction barrier is installed in such a way that its construction does not interfere with the deformation depth of the guardrail. Since the NRB forms a barrier to the rushing air, which can cause a sudden change in dynamic pressure under wind loading on a short stretch of roadway and endanger the stability of vehicles, the beginning and end of the barrier is stepped.

In places where the portals of the traffic signs are mounted, the noise reduction barrier is offset from the base NRB by 1.50 m and in one case by 1.15 m. The basic NRB is discontinued at this point. The offset NRB overlaps the discontinued barrier on both sides by 3.0 m. There are 3 escape exits on the NRB1 route. An escape route will be located within these areas.

From the above measurements before and after the construction of the NRB (Fig. 6.25 and Fig. 6.26), it is evident that after the construction of the NRB there was a reduction in equivalent noise levels at each reference time interval of between 3 and 7 dB at the selected measurement location (Fig. 6.27 and Fig. 6.28).

Fig. 6.25 View of the measurement site before the construction of the NRB

Fig. 6.26 View of the measurement site after construction of the NRB

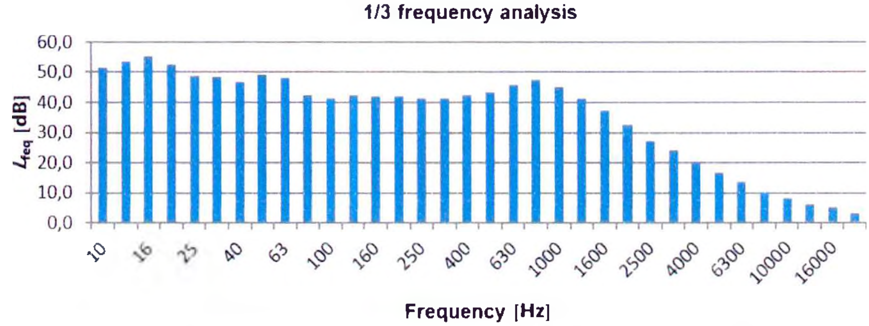

Fig. 6.27 Third-octave frequency spectrum – before construction

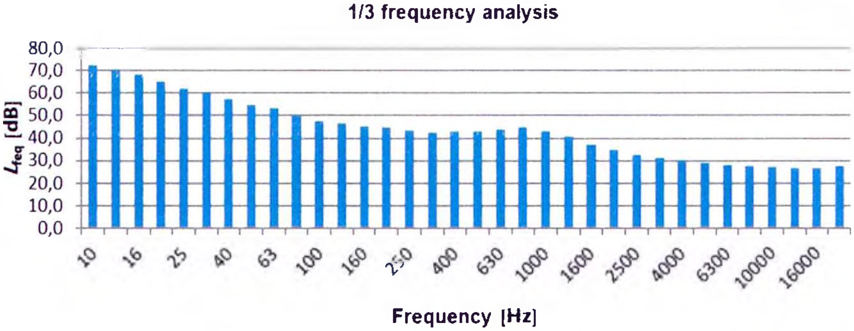

Fig. 6.28 Third-octave frequency spectrum – after construction

6.6 Conclusion

The UNIVNET 2023 research project team focused on the analysis and design of innovative material and construction solutions for noise reduction barriers. It focused on criteria related to the design and implementation of noise reduction measures. Emphasis was placed on the analysis and research of the structures, the buildings, the materials used, as well as the placement of the noise reduction barriers in the space. Research on the properties of the materials used was also of interest. The requirements for the material, construction and acoustic properties of the noise reduction barriers were summarised. The project developers, together with their foreign partners, present a design solution for a noise damper applicable to existing as well as newly designed noise reduction barriers. It is an original technical solution fully accepting the principles of environmental sustainability. The aim of the project researchers is to build on the research of the UNIVNET project in the years 2020 to 2022 and to produce and apply the designed damper to the original solutions of noise reduction barriers using material from recycled automotive components after their service life proposed by the researchers. In the year under assessment, noise analyses were also carried out on a selected section of the motorway before and after the implementation of the noise reduction barrier. In the coming period, it is foreseen to apply just such noise reduction barriers, which could be described as environmentally sustainable.

References

[1] EEA Report No 22: Environmental noise in Europa – 2020. European Environmental Agency, Luxembourg, 2020, 100 p.

[2] Clark, C., Paunovic, K. 2018. WHO environmental noise guidelines for the European region: a systematic review on environmental noise and cognition, International Journal of Environmental Research and Public Health. 2018, 15(2), 1-285. DOI:10.3390/ ijerph15020285.

[3] Clark, C., Paunovic, K. 2018. WHO environmental noise guidelines for the European region: a systematic review on environmental noise and quality of life, wellbeing and mental health, International Journal of Environmental Research and Public Health. 2018, 15(11), 1- 240. DOI:10.3390/ijerph15112400.

[4] Dreger, S., et al. 2019. Social inequalities in environmental noise exposure: a review of evidence in the WHO European region, International Journal of Environmental Research and Public Health. 2019,16(6), 1- 240. DOI:10.3390/ijerph16061011.

[5] Decree MZ SR N. 549/2007 (in Slovak), MZ SR, 2007.

[6] McCarth, N. 2021. Where Neighborhood Noise Is Problematic in Europe. Statista, 2021.

[7] Uptake and impact of the WHO Environmental noise guidelines for the European Region: experiences from Member States. Word Health Organization, 12 p., 2023.

[8] European Commission. 2020. Commission Directive (EU) 2020/367 of 4 March 2020 amending Annex III to Directive 2002/49/EC of the European Parliament and of the Council as regards the establishment of assessment methods for

harmful effects of environmental noise. OJ. 2020; L 67:132–6 (https://eur-lex.europa.eu/eli/dir/2020/367/oj).

[9] European Commission. 2021. Communication from the Commission to the European Parliament, the Council, the European Economic and Social Committee and the Committee of the Regions. Pathway to a healthy planet for all: EU action plan: "Towards zero pollution for air, water and soil". Brussels: European Commission (COM (2021) 400 final;https://eur-lex.europa.eu/legal content/EN/ALL/?uri=COM%3A2021%3A400%3AFIN).

[10] European Commission. 2022. Report from the Commission to the European Parliament, the Council, the European Economic and Social Committee and the Committee of the Regions. First "zero pollution" monitoring and outlook. "Pathways towards cleaner air, water and soil for Europe". Brussels: European Commission (COM(2022) 674 final; https://eur-lex.europa.eu/legal-content/EN/TXT/PDF/?uri=CELEX:52022DC0674).

[11] European Commission. 2023. Report from the Commission to the European Parliament and the on the Implementation of the Environmental Noise Directive in accordance with Article 11 of Directive 2002/49/EC. Brussels: European Commission (COM/2023/139 final;https://eurlex.europa.eu/legalcontent/EN/TXT/?uri=COM%3A2023%3A139%3AFIN).

[12] EEA. 2021. Exposure of Europe's population to environmental noise [website]. In: European Environment Agency/ Indicators. Copenhagen: European Environment Agency (https://www.eea.europa.eu/ims/exposure-of-europe2019spopulation-to)

[13] EEA. 2022a. Health impacts of exposure to noise from transport [website]. In: European Environment Agency/Indicators. Copenhagen: European Environment Agency (https://www.eea.europa.eu/ims/health-impacts-of-exposure-to-1)

[14] EEA. 2022b. Noise pollution and health. In: Zero pollution monitoring assessment [web report]. Copenhagen: European Environment Agency (https://www.eea.europa.eu/publications/zero-pollution/health/noise-pollution).

[15] EEA. 2022c. Additional information on health impacts from transport noise at EU level. In2017. Copenhagen: European Environment Agency (https://www.eea.europa.eu/data-and-maps/figures/additional-information-on-health-impacts).

[16] Peeters B, Nusselder R. 2019. Overview of critical noise values in the European Region. Copenhagen: European Network of the Heads of Environmental Protection Agencies (Report No. M+P.BAFU.19.01.1; https://epanet.eea.europa.eu/ reports-letters/reports-and-letters/ig-noise_critical-noise-values-in-eu.pdf/view).

[17] Types and properties of anti-noise walls (in Slovak). [14/09/2024], available on: https://cbmont.sk/druhy-vlastnosti-protihlukovych-stien/

[18] Principles of designing noise barriers (in Slovak). 2023. [14/09/2024], available on: https://www.asb.sk/stavebnictvo/realizacia-stavieb/zasady-navrhovania-protihlukovych-stien

[19] Low noise barrier. 2023. [14/09/2024], available on: https://intertechplus.cz/produkty/dopravni-site/nizka-protihlukova-clona/

[20] Anti-noise barrier barrier (in Czech). 2023. [14/09/2024]. Available on: https://www.mcvelox.cz/clanek/5/kontakty.html

[21] Design and assessment of anti-noise measures for roads. 2021. [14/09/2024]. Available on: https://www.ssc.sk/files/documents/technicke-predpisy/tp/tp_052_2021.pdf

[22] TP 052. 2021. Design and assessment of anti-noise measures for roads, MDV SR: 2021

[23] Technical report 2017-02 state of the art in managing road trafic nosie: noise barriers. 2017. Conférence Européenne des Directeurs des Rautes - Conference of European Directors of Roads, January 2017.

[24] Act of the NR SR no. 355/2007 Coll. on the protection, support and development of public health and on the amendment of certain laws, as amended (in Slovak).

[25] TD 051. 2021. Use, quality and evaluation system of anti-noise walls (in Slovak), MDV SR: 2021.

[26] TKP 15. 2018. Concrete structures in general (in Slovak), MDV SR: 2018.

[27] TKP 20. 2014. Steel structures (in Slovak), MDVRR SR: 2014.

[28] TKP21. 2013. Protection of constructions against corrosion (in Slovak), MDVRR SR: 2013.

[29] TP 066. 2021. Determining the noise load caused by road traffic (in Slovak), MDV SR: 2021.

7 Mechanical-Physical and Ecotoxicological Properties of New Wood-Plastic Composites

7.1 Introduction

In the current era, in which we are faced with an ever-increasing need to use natural resources efficiently and to address environmental challenges, new perspectives are opening up in the field of materials research. One innovative approach is to redirect our attention to the use of waste materials. Instead of these materials ending up in landfills or in nature, we are witnessing an impressive shift towards their use in a beneficial context. This approach not only reduces the environmental burden, but also opens the door to innovation and the creation of materials with exceptional properties. By using waste materials, we are not only creating a more sustainable community but are also discovering various improvements in environmentally responsible material creation that can open the way to new and better solutions for the future.

Plastic is one of the most widespread and useful materials in our daily lives. Its use in a variety of industries, from food packaging, textiles, healthcare, automotive and electronics, has brought a number of benefits in terms of practicality, durability and lightness. Although plastic is a versatile material, it is also becoming a source of significant environmental problems. The problem with plastic waste lies mainly in its excessive use and the failure to manage it effectively. Plastic production is often linked to oil extraction and greenhouse gas emissions, which worsen the environment. In addition, a large amount of plastic waste in many cases ends up in landfills, in the oceans or in illegal dumps instead of being recycled or treated efficiently. In an effort to respond to the growing threat of the environmental impact of plastic waste, exceptional progress has been made in recent years. Plastic waste can be transformed and recycled into new forms of materials that offer unique properties and applications. These materials can be used in advanced technologies, including 3D printing, the creation of plastic panels, or the development of innovative textile materials. One new approach is to combine plastic waste with wood to create new wood composites that combine the advantages of both materials. The plastic adds weather resistance, the wood component adds strength and a natural look. This material opens the door to innovations in the construction and automotive industries, as well as in the production of furniture and other consumer materials. Using a combination of plastic waste and wood is not only an environmentally friendly solution, but also represents a technological advance in creating materials with improved properties.

7.2 Automotive industry

The automotive industry is one of the main producers of industrial waste [1]. As technology advances and the economy grows, so does the demand for motor vehicles. People are also increasingly prone to regularly replace their vehicles, whether due to technical developments or personal preferences. This results in more waste, which contributes to various environmental problems. Going forward, green and sustainable initiatives are expected to be the dominant aspects of reverse logistics in the automotive industry [2]. Across Europe, between 8 and 9 million tonnes of waste are generated each year from the disposal of vehicles. On 24 May 2000, the European Parliament and the Council adopted a Directive entitled "Technical Directive 2000/53/EC on end-of-life vehicles". This Directive requires EU Member States to strengthen their end-of-life car recycling measures, increase vehicle recycling rates, effectively reduce the environmental impact of vehicles, and achieve sustainable development in the automotive industry [2].

7.3 Plastics in the automotive industry

Plastics are often used in the exterior parts of vehicles, including bodywork, gaskets, wheel covers, sealing strips, bumpers and mudguards, as well as in interior parts such as instrument panels, dashboards, door panels, steering wheels, seats and related parts, including dashboard cladding and decorative elements. Plastics are also used in components located under the bonnet of the vehicle, such as sensors, ignition systems, parts of fluid systems, electrical wiring and resonators [3], [4]. For parts of the vehicle that are not part of the vehicle's structure, such as front and rear bumpers and other parts of the interior, plastics make up around 20 – 25 % of the vehicle's total weight [5]. Two main types of plastics are used in the automotive industry: engineering thermoplastics and high-performance thermoplastics. The choice between the two depends on the specific purpose and the desired properties of the plastic. Engineering thermoplastics, also known as technoplastics, belong to the category of thermoplastics with improved mechanical properties. These plastics have a strength that allows them to compete with metals and ceramics, meaning they can be used for the same purposes. Their improved properties include a higher modulus of elasticity, less deformation on cooling and higher impact resistance. Car bumpers are an ideal example. Engineering thermoplastics are also able to maintain their dimensions and mechanical properties at extreme temperatures above 100 °C or below freezing [6].

Engineering plastics are highly durable materials with excellent thermal and mechanical properties compared to conventional plastics. Despite their higher price than conventional plastic products, their advantages lie in their amorphous or crystalline nature, manifested in good strength, toughness, rigidity, light weight and good resistance to heat, chemicals, wear and abrasion. These properties allow easy processing into different forms. Engineering plastics are widely used in the electrical and electronics industries as well as in transportation applications, where they can effectively replace metal components due to their light weight and metal-like properties. Within the industrial sectors, transport is one of the most prominent sectors for the use of engineering plastics [7]. Vieyra et al. [8] reports that the automotive industry has started to use plastics virtually from its inception. Thanks to their light weight, flexibility and many other good properties, plastic materials have become the ideal choice for the automotive sector. Their use allows to reduce the overall weight of vehicles and improve energy efficiency. Engineering plastics occupy a place in this context in the field of high-performance non-renewable materials. They represent a higher segment with advanced properties compared to conventional plastic materials. Unlike conventional plastics, engineering plastics have more distinctive technical and performance characteristics. Thanks to these properties and the high standards, they meet, they can be reused after recycling with minimal loss in quality.

Plastic components used in cars have a potential adverse environmental impact if the waste produced is not managed effectively. These plastic materials have evolved from common decorative parts to important structural and functional components. In addition, materials have shifted from simple plastics to more advanced plastic alloys and composites with improved mechanical properties and impact resistance. In this context, plastics such as polypropylene, polyurethane (PU), polyethylene, polycarbonate (PC), polyvinyl chloride (PVC), polyphenylene oxide (PPO), polyformaldehyde (POM), polyamide (PA), acrylonitrile-butadiene-styrene (ABS) and thermoset composites play a major role. In addition, thermoplastic polyesters such as polybutylene terephthalate (PBT) and polyethylene terephthalate are often used [9].

Table 7.1 lists the types of polymers used in the different parts of the car.

Table 7.1

Types of polymers in car parts (adapted from Vieyra et al. [8]).

Component	Polymer type
Bumpers	PS, ABS, PT/PCB, PP, PA, PU
Seats	ABS, PA, PP
Dashboards	ABS, PC, ABS/PC, PP
Fuel systems	POM, PA, PTB
Electric components	PBT, PA
Headlights	PC, PTB, ABS
Upholstery	ABS, PU
Eheel covers	ABS

7.4 Use of waste plastics from the automotive industry

Compared to the recycling of commodity plastics, engineering plastics stand out for their properties and high performance characteristics, which allows them to be used efficiently even after recycling [10]. In general, the recycling of these materials is a challenge because the automobile at the end of its life is a complex material resulting from metallurgical, chemical and plastic transformation processes that create significant added value. It is clear that current technologies cannot ensure that all plastic materials in cars are fully recycled and achieve maximum recovery for these recycled materials [11].

Several recycling options are used for automotive plastics:

- reuse, which is carried out as a direct installation of recycled components in a new vehicle;

- remanufacturing or refurbishment, which is a way of repairing plastic parts;
- mechanical recycling, where plastic car parts are heated and reprocessed into a new product with a similar use;
- chemical recycling, which means the conversion of plastic materials into monomers that can be re-polymerized and used to produce primary resins or their petrochemical products, which are usually liquids or gases;
- energy recovery, where plastic waste is incinerated to produce energy in the form of heat, steam and electricity [12].

Research is currently focusing intensively on the use of waste plastics from cars as a promising resource for a variety of applications. Efforts are focused on finding efficient ways of recycling and new technologies to transform this waste into sustainable and valuable materials.

Farzana a Sahajwalla [13] represent a new approach to the production of silicon carbide (SiC) using waste glass and plastics from automobiles. This innovation brings two significant benefits: it transforms non-metallic automotive waste into valuable resources such as refractories containing SiC, while reducing the industry's reliance on conventional raw materials such as silica and coke, often used in the production of silicon and carbon.

Rajagopal et al. [14] explored the use of waste printed circuit boards and automotive plastics in the production of sustainable composite panels. The resulting panels, with a wide range of potential applications, were comparable to medium density fibreboard (MDF). Experimental results of measurements of mechanical and physical properties showed that the combination of the two waste products produced a panel with improved properties. This sustainable approach to waste recycling has the potential to reduce landfill waste and create materials for construction and domestic applications.

In further research in the field of creating wood-plastic composite material from waste plastics from cars and macadam shells, it was shown that this use of waste materials could be a solution to environmental pollution and would also have economic benefits. Additionally, this composite material exhibited good physical and thermal properties [15].

Liu et al. [16] represents a new recycling approach that uses automotive shredded waste plastics to produce lightweight aggregates. This innovative process improves the physical properties of the lightweight aggregate, such as bulk density and porosity, while the addition of 2 % plastic to the clay composite leads to a significant improvement in its properties. Products made from this lightweight and porous aggregate are suitable for thermal insulation and use as substrates in soilless cultivation. This approach can not only reduce the volume of automotive waste plastics in landfills, but also provide an alternative to conventional additives in the production of building composite materials.

Particleboard composites are wood-based materials where the wood particles used in production can come from a variety of woods, including logs or waste parts such as offcuts and shavings from lumber. This approach allows the efficient use of different types of wood or waste materials, for example from plywood production. The entire manufacturing process involves the application of a binder resin to dry wood particles, which are then subjected to pressure and heat, allowing for a joint that provides the strength and integrity of a particleboard composite. These panels have a wide range of applications in the construction or furniture industry, offering durability and stability with the advantage of using different types of wood [17]. In the current era of modern technology and high product quality, new wood materials are being developed. These products appear in various forms or combinations with other materials to achieve environmental benefits and improved performance of the resulting products [18]. As a result, there is an interest in joining wood and plastic, which represents a significant development in the field of composite materials. This trend is particularly evident in the production of wood-plastic composites, which use a combination of wood fibres or particles and plastic polymers. The advantages of combining wood and plastic create an attractive alternative to traditional materials, with the possibility of efficient recycling and reduced unwanted environmental impact.

Since the last century, the world has seen a proliferation of products made from waste plastics, such as carpets, decorations, baskets, park benches and plastic lumber. One way of using waste plastic is wood-plastic composites [19]. Wood Plastic Composites (*WPC*) are innovative materials that combine the advantages of wood and plastic to create a new balanced material with excellent strength and durability. These composites represent a sustainable alternative to conventional building materials and combine ecological considerations with exceptional technical properties. Their use is now expanding in a variety of industries, from construction to furniture manufacturing.

Wood plastic composites combine wood materials in the form of powder, flour or fibres with thermoplastic polymers. The manufacturing process involves mixing wood fillers with the desired melt, forming pellets and then shaping them by pressing, injection or extrusion to achieve the desired properties and aesthetics of the resulting products [20]. The wood flour used is affordable, making it a simple and effective material for the production of polypropylene composites. Integrating wood flour into a polypropylene matrix not only reduces the cost of composite materials but can also improve their mechanical properties [21].

According to the results of various research, wood plastic composites have great potential. Waste and recycled thermoplastics, which are among the main components of municipal waste, are a promising source for the production of wood plastic composite materials [22].

These primary components include mainly high-density polyethylene (HDPE), low-density polyethylene (LDPE/LLDPE), polypropylene, polyethylene terephthalate (PET), polystyrene and polyvinyl chloride (PVC) [23], which are used in large quantities in the automotive industry.

Wood plastic composites are defined as materials in which the matrix is plastic, and wood fibres are incorporated. As reported by Wolcott [24], a wood plastic composite consists of polymers, most commonly polypropylene, polyethylene or polyvinyl chloride, wood fibre, a bonding agent and other additives such as various lubricants, dyes, flame retardants or antimicrobials. Production involves mixing wood particles with a thermoplastic matrix and subsequent extrusion or injection moulding. The polymer matrix usually has a processing temperature below the wood degradation temperature [25].

For example, in the work Klímek et al. [26], wood plastic composite boards containing up to 30 % polyethylene terephthalate flakes were assessed in terms of physical and mechanical properties. It was shown that the decrease in mechanical properties could be successfully minimized by pretreating the PET flakes with air plasma, as the samples with 30 % by weight of plasma-treated PET achieved the same internal bond strength as the control specimen of pure wood. In terms of physical properties, the swelling of particleboards with PET flakes was lower compared to spruce particleboards.

Wood plastic composites have the appearance of wood but can be processed like plastic. Compared to solid wood, they have a longer life, lower maintenance requirements, and can be used as building material, for the production of automotive parts or furniture [27].

The combination of wood and plastic creates a material in which both substances contribute their useful properties to create an improved final product. This process allows for synergistic use of the individual components, with none of them losing their individual characteristics, while at the same time avoiding a complete blending of the materials [28].

7.5 Particleboard containing plastic filler

Our research focused on the production of single and three-layer particleboards containing plastic/rubber filler from recycled material from the automotive industry and evaluating its properties in order to determine the suitability of using these composites in interior applications.

7.5.1 Material used for the production of single and three-layer particleboards with plastic/rubber content

Waste wood particles from spruce logs, processed in Kronospan s.r.o. (Zvolen, SR), were used for the production of three-layer wood composites with the addition of waste plastics and rubber from cars. The particle sizes for the centre layer of the particleboards ranged from 0.25 to 4.0 mm, and the particle sizes for the surface layer ranged from 0.25 to 1.0 mm. The particles were dried to a moisture content of 5 %. The single-layer particleboards were prepared by the same procedure as for the centre layer of the three-layer particleboards.

The waste plastic was delivered from VOLKSWAGEN SLOVAKIA, a.s. and ALUEX s.r.o., Zvolen. The companies supplied plastic, specifically painted bumpers, unpainted bumpers and fuel tanks from scrapped cars. The painted and unpainted bumpers are made of polypropylene plastic material and the fuel tanks are made of polyethylene plastic material. The materials were cut into smaller parts and cleaned. Subsequently, small particles (granulate) were produced from the material in the workshops of the Technical University in Zvolen, using a plastic crusher from Profing (type DP 11 – 240/350) and a sawdust and chip extractor from Holzmann (type ABS 1080).

Granulate made from waste tyres (SBR: styrene butadiene rubber) and from a mixture of waste gaskets and carpets (EPDM: ethylene propylene diene) were also used as additional synthetic polymers. The granulate from waste rubber and tyres from scrapped cars was provided by AVE SK-Kechnec, plant Slovakia.

The plastic/rubber granulate, fraction from 1 mm to 4 mm, was separated using a Retsch analytical sieving device (type AS 200 digit cA).

As a binder, Kronores CB 1100 F urea-fomaldehyde (UF) adhesive (solids content 67.1 %, viscosity 460 mPa.s, condensation time 55 seconds, pH value 8.6) was used in the composite material with waste plastic. The adhesive mixture contains ammonium nitrate NH_4NO_3 (47 %) as hardener and paraffin emulsion (30 %). The weight composition of the material used for the production of 6 pieces of three-layer particle-board is given in Table 7.2.

The wood plastic composites were prepared by conventional technology, which is first cold pre-pressing of particle mats to 1 MPa and subsequent hot pressing under pressure with a laboratory press CBJ 100-11, TOS (Rakovník, former Czechoslovakia).

Table 7.2

Mass composition of six pieces of three-layer particleboard containing plastic/rubber granulate from cars.

Material	**Chips (g)**	**Adhesive (g)**	**Paraffin emulsion (g)**	**Hardener (g)**	**Granulate (g)**
Surface layer	4.355	675	94	28	0
Centre layer	5.774	644	106	55	642

The surface layer was produced by mixing waste wood chips and adhesive mixture in a laboratory application drum. The centre layer was made of waste wood chips, shredded plastic granulate and adhesive mixture, and these ingredients were thoroughly mixed in a laboratory application drum. A surface mixture of 396 g was applied to the mould where it was evenly distributed. The surface layer was coated with 1,110 g of the centre layer and finally again with 396 g of the surface layer. The mixture was placed in a hydraulic precompressor for about 2 minutes. Pre-pressing will be followed by hot pressing at pressing pressures of 20 MPa, 10 MPa and 5 MPa at different time intervals. The total pressing time will be 5 minutes at 230 °C.

Table 7.2
Labelling of single-layer particleboard samples containing waste plastic from cars.

PB-1	Single-layer particleboard without filler
L10	PB with 10 % granulate from painted bumper
L15	PB with 15 % granulate from painted bumper
L20	PB with 20 % granulate from painted bumper
N10	PB with 10 % granulate from non-painted bumper
N15	PB with 15 % granulate from non-painted bumper
N20	PB with 20 % granulate from non-painted bumper
P10	PB with 20 % granulate from fuel tank
P15	PB with 15 % granulate from fuel tank
P20	PB with 20 % granulate from fuel tank

Table 7.3
Labelling of three-layer particleboard samples containing waste plastic/rubber from cars

PB-3	Three-layer particleboard without filler
LN 10	Particleboard with 10 % granulate from painted bumpers
NN10	Particleboard with 10 % granulate from non-painted bumpers
PN10	Particle board with 10 % granulate from fuel tanks
T10	Particleboard with 10 % granulate from tyres
TK10	Particleboard with 10 % granulate from a mixture of sealants and carpets

This process produced single and three-layer particleboards with waste plastic/rubber, with a given percentage of filler. The labelling of particleboards containing plastic/rubber granulate from cars is given in Tables 7.2 and 7.3.

Analysis of the wood material used

Preliminary analysis of the main components of spruce wood, which will be used in the production of particleboards, has been carried out. Wood constituents such as holocellulose, cellulose, hemicelluloses, lignin and extractives were analysed. The analysis is important because it provides information about the composition of the wood at the molecular level.

Samples of Norway spruce *(Picea abies* L. Karst.) were disintegrated into sawdust and fractions ranging in size from 0.5 mm to 1.0 mm were used for chemical analyses. According to ASTM D1107-21 (2021), the extractables were determined in a Soxhlet apparatus with a mixture of absolute ethanol and toluene for analysis (Merck, Darmstadt, Germany) (2:1, v:v). The duration of extraction was 8 hours with 6 cycles per hour. Lignin content was determined according to Sluitera et al. (2008), cellulose according to Seiferta (1956) and holocellulose according to Wise et al. (1946). Hemicelluloses were calculated as the difference between the holocellulose and cellulose contents.

Measurements were performed in four repetitions per sample. The results are presented as a percentage of wood dried in the furnace. The results of the spruce wood analysis are presented in Table 7.4.

Table 7.4

Results of spruce wood analyses

Sample	Extractives (%)	Lignin (%)	Cellulose (%)	Holocellulose (%)	Hemicelluloses (%)
1	1.59	24.45	45.7	82.74	37.06
2	1.57	24.51	45.72	82.76	37.02
3	1.58	26.44	45.72	82.39	36.67
4	1.58	26.42	45.69	83.11	37.42
Average	1.58	25.43	45.71	82.75	37.04

7.6 Analysis of thermophysical properties of single-layer particleboards containing plastic

Before the actual measurement of the thermal properties of particleboards (PB) with automotive waste plastic, it was necessary to weigh the test bodies, measure the dimensions (thickness, width, height) and determine their density. Two test bodies were measured for each sample type. From the measured values, the average values were calculated, from which we further calculated the volume and density of the samples. Bodies were weighed on RADWAG laboratory scales and their dimensions were measured with a digital caliper. Each dimension was measured at four points. The average characteristics found are presented in Table 7.5.

Table 7.5

Measurement characteristics of PB samples with waste plastic from cars

Sample	Weight (g)	Average thickness (mm)	Average height (mm)	Average width (mm)	Volume (cm^3)	Density ($kg.m^{-3}$)
P10-1	91.78	15.10	104.44	98.13	154.71	593.15
P10-2	92.49	14.98	100.73	104.74	158.03	585.26
P15-1	90.01	15.05	102.04	98.72	151.61	593.70
P15-2	84.11	15.13	102.06	96.74	149.41	562.92
P20-1	87.60	15.08	102.19	97.26	149.86	584.52
P20-2	81.35	15.14	101.52	101.92	156.65	519.33
L10-1	98.89	15.22	110.49	109.01	183.26	539.63
L10-2	92.91	15.17	110.75	109.24	183.50	506.30
L15-1	97.43	15.35	103.27	104.49	165.58	588.28
L15-2	93.91	15.30	104.39	104.65	167.08	562.02
L20-1	96.42	15.23	105.60	103.41	166.26	579.91

L20-2	88.44	15.17	102.63	103.08	160.45	551.18
N10-1	83.02	15.11	104.16	100.77	158.57	523.55
N10-2	96.27	15.11	104.22	102.20	160.88	598.37
N15-1	91.52	15.21	100.95	104.25	160.05	571.83
N15-2	96.52	15.16	103.87	104.91	165.14	584.48
N20-1	106.80	15.22	107.13	104.30	170.06	628.00
N20-2	94.41	15.26	101.19	104.14	160.81	587.11

The thermal-physical properties (thermal conductivity, thermal diffusivity and specific heat capacity) were determined by the non-destructive TPS (Transient Plane Source) or also "Hot-disk" method. The TSP method can be used to measure thermal conductivity, temperature conductivity, and specific heat capacity for anisotropic materials in a short time. With the TPS method, there is no need to recalibrate or use standard samples. The TSP method uses a sensor that is placed between two test bodies of one sample. The sensor is coated with a thin polymer that provides chemical resistance and also makes it possible to measure electrically conductive materials. The measurements were repeated ten times. The mean values and standard deviations were calculated from the measured values.

Table 7.6

Measured average thermal conductivity values of PB with waste plastic from cars.

Sample	**Thermal conductivity $\lambda = [W \cdot m^{-1} \cdot K^{-1}]$**	**Standard deviation**
PB-1	0.104	0.0050
P10	0.156	0.0032
P15	0.156	0.0041
P20	0.148	0.0025
L10	0.144	0.0043
L15	0.154	0.0056
L20	0.153	0.0042
N20	0.149	0.0022
N20	0.149	0.0033
N20	0.156	0.0042

Table 7.6 shows the average thermal conductivity values for each sample type. For the particleboard samples with plastic content from fuel tanks and painted bumpers, it is evident that the thermal conductivity was highest at a filler content of 15 %. When the filler content was increased to 20%, it again tended to decrease. For PBs containing plastic from non-painted tanks, the sample with a filler content of 20 %. Compared to PBs without filler, the thermal conductivity increased for all types of fillers. The thermal conductivity of spruce wood is on average 0.126 $W \cdot m.^{-1} \cdot K^{-1}$ [29]. It can be stated that depending on the measured values from 0.144±0.0032 $W \cdot m.^{-1} \cdot K^{-1}$ to 0.156±0.0042

W·m.$^{-1}$·K^{-1}, the plastic filler present in the PB has an influence on increasing the thermal conductivity of this material.

Table 7.7
Measured average values of thermal diffusivity of PB with waste plastic from cars

Sample	Thermal diffusivity a = [mm^2·s^{-1}]	Standard deviation
PB-1	0.12	0.0040
P10	0.16	0.0069
P15	0.15	0.0085
P20	0.17	0.0044
L10	0.18	0.0141
L15	0.16	0.0126
L20	0.16	0.0097
N20	0.18	0.0051
N20	0.13	0.0080
N20	0.15	0.0090

The thermal diffusivity, shown in Table 7.7, ranged from 0.13±0.008 mm^2·s^{-1} to 0.18±0.0141 mm^2·s^{-1} for PB samples containing plastic. According to the International Materials Database, the thermal diffusivity value for spruce wood is 0.24 mm^2·s^{-1}, from which we can find that the waste plastic from automobiles in all types of samples reduced the average value of thermal diffusivity.

Table 7.8
Measured average values of specific heat capacity of PB with waste plastic from cars.

Sample	Specific heat capacity c = [J·K^{-1}·kg^{-1}]	Standard deviation
PB-1	1,454	87
P10	1,682	39
P15	1,815	57
P20	1,494	39
L10	1,651	144
L15	1,675	66
L20	1,621	55
N20	1,610	28
N20	2,137	37
N20	1,815	55

The specific heat capacity averaged from 1,494±39 J·K^{-1}·kg^{-1} to 2,137±37 J·K^{-1}·kg^{-1}. The International Materials Database gives a specific heat capacity for spruce wood of 1,255 J/K.kg [29]. Czajkowski et al. [30] report values for oriented strand board (OSB) and low-density fibreboard (LDF), where the results of the specific heat capacity measurements ranged from J·K^{-1}·kg^{-1} to 1,450 J·K^{-1}·kg^{-1} for LDF and averaged 1,550 J·K^{-1}·kg^{-1} for OSB. Therefore, we can say that for our samples, the plastic significantly affected the specific heat capacity of these materials, which may be due to the fact that the average value of the specific heat capacity of the plastic material used (polypropylene PP) is 2,000 J·K^{-1}·kg^{-1}.

7.7 Analysis of the physical properties of particleboards containing plastic and rubber

The densities of each sample were calculated according to EVS-EN 323 (2002). For each three-layer particleboard, measurements were taken on six specimens. The principle of the measurement is to determine the density of individual samples of one type of particleboard and then to calculate the average value.

The results of the density values are shown in Table 7.9. Based on the values, it can be concluded that the average density of each type of PB ranged from 0.69 to 0.72 g.cm^{-3}. These density values are typical for conventional single-layer and three-layer PBs.

Table 7.9

Average density of three-layer composites

Sample	Density (g.cm^{-3})
PB	0.70 ± 0.03
LN10	0.72 ± 0.02
NN10	0.71 ± 0.03
PN10	0.72 ± 0.03
T10	0.70 ± 0.04
TK10	0.69 ± 0.02

Water absorption and thickness swelling after 2 and 24 hours were calculated according to EVS-EN 317 (2005). For each particleboard, measurements were taken on eight samples. The basic principle is to add the samples to a water bath (Nüve BM 402), then measure their thickness and weight after 2 and 24 hours.

Table 7.10

Average values of water absorption and swelling of a three-layer PB

Sample	Water absorption (%)		Thickness swelling (%)	
	2 hours	24 hours	2 hours	24 hours
PB-3	13.16	42.53	5.22	17.50
LN10	11.75	41.61	5.08	18.08
NN10	10.81	36.87	5.53	16.82
PN10	12.68	41.89	4.75	16.79
T10	14.73	43.58	5.26	18.40
TK10	16.39	47.22	6.53	21.68

The results of the physical tests, presented in Table 10, show that the average thickness swelling after 24 hours for particleboards with plastic/rubber filler ranged from 16.79 % to 21.68 %. STN EN 312 (2011) specifies a requirement for chipboards with a thickness of 18 mm of 14 % thickness tension for boards for use in wet environments. In the case of our measurements, we obtained higher values. Since the wood particles are responsible for the swelling, from the perspective of the observed properties, it would be advisable to increase the proportion of plastic/rubber filler in the PB.

7.8 Analysis of mechanical properties of wood composites containing plastic and rubber

EVS-EN 319 (2005) was used as the standard for the determination of tensile strength (TS). For each particleboard, measurements were taken on eight samples. The basic principle is to load and then record the tensile stress at the point of the specimen break. A Shimadzu AG-IC laboratory testing machine was used to measure the samples.

The EVS-EN 310 (2005) standard was used to determine the flexural strength, specifically the modulus of rupture and modulus of elasticity (MOR, MOE). Six samples were measured for each particleboard. The principle is to load and then record the bending stress when the specimen breaks. A Shimadzu AG-IC laboratory testing machine was used to measure the samples.

Screw resistance torque (SDT), namely tightening torque (SeT) and pulling torque (StT) were also measured on the specimens. For each particleboard, measurements were taken on eight samples. The principle of the test is to screw the bolt into the specimen and then record the torque while turning the bolt without resistance.

The results of the tensile strength, modulus of rupture and modulus of elasticity and torque of the bolt are given in Table 7.11. Based on the values, it can be concluded that the average tensile strength ranged from 0.30 to 0.52 MPa, the average modulus of rupture ranged from 10.50 to 12.44 MPa, the average modulus of elasticity ranged from 2,079.07 to 2,204.39 MPa, and the average tightening torque ranged from 0.37 to 0.46 N.m and the average pulling torque from 1.29 to 1.44 N.m.

Table 7.11

Average values of tensile strength (TS), modulus of rupture (MOR), modulus of elasticity (MOE) of wood composites and screw resistance torque (SDT) (tightening torque (SeT) and pulling torque (StT))

Sample	TS (MPa)	MOR (MPa)	MOE (MPa)	SDT (N.m)	
				SeT	StT
PB-3	0.52	12.44	2204.39	0.46	1.44
LN10	0.40	11.24	2088.01	0.37	1.29
NN10	0.49	10.50	2056.28	0.42	1.30
PN10	0.42	11.96	2203.88	0.37	1.31
T10	0.30	11.57	2079.07	0.37	1.35
TK10	0.33	11.49	2131.36	0.44	1.38

Based on the results obtained (Table 7.11), it can be concluded that the values of tensile strength and flexural strength decreased for the PB containing plastic filler, however, according to the standard STN EN 312 (2011) for general purpose boards for use in dry environments, the prescribed flexural strength value for particleboards with a thickness of 18 mm is 10.0 N.mm^{-2}. The resulting flexural strength values of the PB with 10 % plastic/rubber content reached the values specified by the standard. For tensile strength, the standard specifies a requirement of 0.24 N.mm^{-2} at a thickness of 18 mm, which was also achieved in all specimen types.

7.9 Ecotoxicological testing of single-layer PBs containing plastic

Plastics, which are durable and slow to biodegrade, pose a risk to the environment, including entering the food chain [12], [31]. Ecotoxicological biological tests assess the potential toxic effects of waste at the molecular level down to the ecosystem level. Ecotoxicity, a hazardous property of waste, results from its toxic effect on the environment. This article focuses on the reuse of plastic waste as a substitute for wood in particleboard and the assessment of its environmental impact using ecotoxicological tests [32], [33].

Preparation of aqueous infusions

Demineralized water adjusted to pH 3 was used for the preparation of aqueous infusions. The volume of water in which the samples were leached was calculated according to the procedure derived from Hybská and Samešová [34] and TNI CEN/TR 17105 (2017). The samples were leached in glass containers for 24 hours. The particleboard was removed, and the infusion was used for testing.

Determination of pH and chemical oxygen demand

A combined electrode apparatus was used to determine the pH: pH meter, type InoLab Level 1, WTW Germany and STN EN ISO 19396-1 (2017). The method of determination is based on STN ISO 15705 (2005).

Ecotoxicological testing

To assess the effects of substances dissolved in aqueous infusions from the woodchip samples, we performed preliminary tests: a growth inhibition (stimulation) test on *Lemna minor* and an acute toxicity test on *Daphnia magna*. The growth inhibition (stimulation) test on *Lemna minor* evaluates the toxic effects of substances on freshwater plants. It is a standardized test OECD 221 (2006) with the test organism *Lemna minor* according to STN EN ISO 20079 (2008). The acute toxicity test on *Daphnia magna* is most commonly used to assess the toxic effect of substances in the aquatic environment. The immobilization of the organism is evaluated. The organisms used must not be older than 24 hours according to EN ISO 6341 (2012) and OECD 202 (2004).

Ecotoxicity test results achieved

Determination of pH and COD

COD (chemical oxygen demand) serves as an indicator of organic water pollution. In our study, aqueous infusions from particleboard samples used in different environments were simulated to assess their impact on surface water. The COD values in the control samples, which were pure particleboard, exceeded the legal limit 50 times according to the Slovak Government Regulation amending Slovak Government Regulation No. 269/2010 Coll, laying down requirements for achieving good water status. Interestingly, as the proportion of waste replacing wood increased, the content of organic matter extracted into water decreased, probably due to the poor solubility of the plastics used in particleboard. The pH values also varied, with the addition of waste plastics leading to higher pH values. Specifically, the sample containing 20 % of the painted bumper granulate had the lowest COD values. This trend has been consistent in infusions from automotive waste rubber-containing boards [35].

Table 7.12

Chemical oxygen demand and pH of particleboard samples containing plastics.

	N10	**N15**	**N20**	**L10**	**L15**	**L20**	**P10**	**P15**	**P20**	**PB**
COD mg/l	1,305	1,209	1,112	1,499	1,209	919	1,450	1,401	1,450	1,655
pH	5.16	5.02	5.02	5.09	5.05	4.96	4.85	5.02	5.01	3.66

Lemna minor growth inhibition test

The preliminary test with *Lemna minor* test organisms is negative if the growth inhibition is < 30 % compared to the control sample, and positive if the growth inhibition is ≥ 30 %.

Table 7.13

Representation of growth inhibition in *Lemna minor*.

Sample	Iμ, %				number of repetitions
	Average	Standard deviation	-95.00 %	95.00%	
L10	81.56	3.10	73.60	89.52	6
L15	78.57	1.88	73.74	83.40	6
L20	74.06	4.61	62.22	85.90	6
N10	70.08	2.77	62.96	77.20	6
N15	68.87	2.67	61.99	75.74	6
N20	64.54	4.72	52.41	76.68	6
P10	83.40	4.09	72.88	93.92	6
P15	73.09	2.96	65.47	80.70	6
P20	64.05	2.98	56.40	71.71	6

The use of plastic waste in the board reduces growth inhibition. In the clean plate sample, the inhibition was 79.18 %. There is a difference in inhibition of approximately 10 % between the tested samples with painted and non-painted bumpers %. The sample with 10 % fuel tank waste content had the highest growth inhibition. *Lemna minor* has been successfully used for several years as a test organism to assess the toxic effects of chemicals, as confirmed by the study of Hybská et al. [35], where the use of *Lemna minor* to assess the toxicity of infusions from waste tyres was confirmed.

Daphnia magna acute toxicity test

A *Daphnia magna* pre-test result is negative if < 50 % mortality or immobilization occurred during the test. The test is positive if mortality or immobilization is ≥ 50 % compared to the control sample. The number of immobilized individuals was evaluated after 24 hours and 48 hours, the % immobilization after 48 hours is recorded in Table 7.14.

Table 7.14

Immobilization (in %) *Daphnia magna* after 48 hours.

	L10	**L15**	**L20**	**N10**	**N15**	**N20**	**P10**	**P15**	**P20**
	70	60	65	60	80	70	55	70	55
	60	75	75	55	65	55	50	65	65
	70	50	75	70	75	65	35	65	65
	52	80	72	75	70	55	25	80	80
Average	**63**	**66**	**72**	**65**	**73**	**61**	**41**	**70**	**66**

The data (Table 7.14) show that % immobilization increases with increasing proportion of waste plastic in the board. The test result was positive (immobilization ≥ 50 %), except for the infusion from the board with 10 % fuel tank content (41.25 %). There was an increase in immobilization in the infusion with a higher proportion of waste in the board. In a study by Hybská et al. 2023 [35] the toxicity of a board with a rubber waste substitute was tested, where all immobilization determinations were also positive.

Linthner et al. [36] monitored the toxicity of 26 plastic products made from 5 types of plastics that were leached in deionized water and tested for acute toxicity to *Daphnia magna*. All infusions from soft PVC and epoxy products were found to be toxic and none of the infusions from polypropylene, ABS (acrylonitrile butadiene styrene) and rigid PVC products showed toxicity. Toxicity was mainly caused by hydrophobic organics and metals were the main cause of toxicity in one infusion (release of metals was also confirmed by chemical analysis).

The study by Hybska et al. [33] was aimed at assessing the ecotoxicological impact of waste tyres on the environment. They found that the most sensitive test organism was *Daphnia magna*. Furthermore, the effect of particle size of the waste material was found to have a significant effect on ecotoxicitySamples containing tyre parts with a size of < 1 mm showed higher toxicity than samples with a particle size > 3 mm.

Studies by Wika et al. [37] recommend the use of the toxicity test method with the test organism *Daphnia magna* as a basis for environmental labelling of automotive types.

It follows that *Daphnia magna* is one of the frequently used test organisms because of its sensitivity. *Lemna minor* is also a sensitive test organism for aquatic environments. *Lemna minor* is a more readily available aquatic plant and its care in the laboratory is also easier than providing laboratory rearing of *Daphnia magna*.

7.10 Economic demand from the point of view of calculations of the innovated product – three-layer PB with plastic content

In the framework of the design of a comprehensive model for the assessment of the economic intensity of the production of an innovative product (three-layer PB with plastic content), in addition to the application of dynamic economic indicators for the evaluation of the efficiency of the investment project concept, the specific intention is to present the design and comparison of possible modifications of the conversion calculations. The given design of the comparison should be supported by a practical decision-making tool using software support. The purpose is to find an answer to the research question of whether by comparing the methodological procedure of the traditional markup calculation, it is possible to expect a change in the selling price of classic three-layer PB vs. PB with plastic content. Another intent is to modify and apply an alternative method of calculating machine hour rates to determine a more accurate selling price differential.

The concept of the investment project of the technological line for the production of wood plastic boards provides a variable methodological procedure for the evaluation of the effectiveness of the investment even at a certain level of risk. The process line consists of components: drum chipper, shredder, dryer, vibrating panel, forming machine, pre-press machine, hot press machine, panel turning machine, edge processing saw, grinder (estimated investment of € 700,000, with an annual capacity of 15,000 m^3/year). The economic evaluation of the project efficiency in all parameters of dynamic indicators (net present value, profitability index, internal rate of return and payback period) showed positive values. One of the most important areas influencing the successful implementation of the intended project for the production of PBs with plastic content is the determination of the selling price and its comparison with the market price of the alternative product (classic raw three-layer particleboard). The gross conversion calculation can be determined through the most commonly used surcharge calculation technique using a standard calculation formula for industrial enterprise conditions. The structure of the calculation formula is essentially uniform in theory and practice with minimal modifications [38], [39], [40], [41], [42]. The initial object of comparison in the area of calculations was a three-layer raw particleboard (thickness 16 mm), produced by pressing technology. It is a large-area material designed for a variety of applications in dry environments (according to STN EN 312 boards type P1), but especially to produce furniture and interior furnishings. Starting from the real conditions of production of such a product, but maintaining some anonymity of the producer's data, it is possible to present in Tab. 7.15 the basic structure of the calculation (raw PB) and its quantification per 1 m^3 of product.

Table 7.15

Traditional markup calculation for a conventional three-layer PB.

Calculation item – three-layer PB (classic product "K")	**Calculation unit (€/1 m^3)**
K1 Material costs (chips, fraction 0.25 – 1 mm, 0.25 – 4 mm)	62.15
K2 + Material costs (adhesive + additives)	10.10
K3 + energy (water, electricity, gas)	28.07
K1 – K3 **Direct production costs (excluding labour costs)**	100.32
K4 + production costs (50 %)*	36.13
K5 + administrative and sales costs** (20 %)	20.06
K1 – K5 **Total product cost**	**156.51**
K6 + profit margin (15 %)	23.48
Offer price excl. VAT	**180.00**

* The costing basis for production overheads (including labor costs) is direct material costs

** The basis for other overheads is direct production costs

In the case of the investment plan for the production of a three-layer PB with plastic content (Innovative product "I"), it is possible to consider the substitution of material costs in the amount of 10 % of the share of plastic granulate (this is waste plastic from vehicle bumpers at the end of the life cycle, supplier Volkswagen Slovakia). In the context of the comparison of the traditional methodological procedure of the mark-up calculation for the classic product (marking of the calculation items "K"), the following changes to the calculation items for the innovative product "I" can be considered (Table 7.16).

Table 7.16

Traditional markup calculation of the innovative product three-layer PB with the addition of plastic

Calculation item – three-layer PB with plastic content (upgraded product "I")	**Calculation unit** (€/1 m^3)
I1 Material costs (chips, fraction 0.25 – 1 mm, 0.25 – 4 mm) (0.9 x K1)	55.94
I1 + Material costs (plastic, fraction 1 mm – 4 mm)	1.65
I2 + Material costs (adhesive + additives) (K2 = I2)	10.10
I3 + Energy (water, electricity, gas) (K3 = I3)	28.07
I1 – I3 **Direct production costs (excluding labour costs)**	5.76
I4 + Production overhead (55 %) (K4 x 0.1)	37.23
I5 + Administrative and sales overhead** (20 %) (K5 x I5)	19.15

I1 – I5 **Total product cost**	**152.14**
I6 + Profit margin (15 %)	22.82
Offer price excl. VAT	**175.00**

*Surface treatment would increase the level of selling prices by about 50 % but without affecting their differentiation

Based on the more detailed structure and documents of the investment project, it is therefore possible to consider the material cost item with the need for 90 % of the chips from item K1. The remaining 10 % share of material costs in the form of plastic additive will be based on the market price of 1,500 €/t of granulate, including transport and within the recipe with consumption of 1.1 kg of plastic granulate per 1 m^3 of PB. Other items of material costs, energy, but also administration and sales overheads, will be essentially identical (irrelevant) cost items in both options considered. The process of incorporation of plastic additives, its storage and the increased preparation time required can be considered from 10 % increase in production overheads (depreciation, wages, maintenance), which will be reflected in an increase in the production overhead mark-up to 55 %. The quantification of the mark-up costing of the innovated product to determine its selling price is presented in Table 7.16.

It is clear from the presented calculation that if the assumptions are confirmed and the cost structure is fundamentally unchanged within the defined capacity, as well as if the original idea of a profit premium is maintained (15 % cost profitability at the level of the industry average), the level of the market price for a calculation unit of 1 m^3 of PB with plastic content could be € 175 excl. VAT. Compared to the classic product of raw three-layer PB listed on the market, it is a possible price drop of 5 €/m^3, which would have the potential to create a competitive advantage. However, if the original price of €180/m^3 is maintained, this would be an increase in the profit margin of the upgraded product by €5 per calculation unit, which at the considered capacity of 15,000 m^3/year would mean a potential increase in profit of €75,000. However, the limiting and certain risk factor for these assumptions is the fulfilment of the production capacity plan and its overall market sales to potential customers. This can only be done provided that the required physical-mechanical properties of the innovated product are met within the requirements of STN EN 312, comparable studies of the product's impact on the environment through LCA analysis, increased marketing sales support, and the aforementioned invariability of the structure of input costs (material, energy, labor costs and overheads of a variable nature), as well as the utilization of the installed capacity. When these conditions are met, the innovative product, a three-layer wood plastic board with plastic content, is competitive on the market and its use is quite wide-spectrum in the field of furniture production and interior furnishing.

However, there are also some disadvantages and inaccuracies associated with the use of the type of calculation formula and the mark-up methodology. The use of the averaging principle is dominant, using monetary scheduling bases allocating a share of overhead costs to the product price, and also a static picture of cost levels that does not respond to the dynamics of changes in input conditions [43]. Therefore, it is possible to find innovative alternative costing approaches in theory, and increasingly in practice. The innovative methodological procedure for determining the final price of the product is based on an attempt to calculate the selected direct and especially overhead costs as accurately as possible by means of special cost items – machine hour rates (MHR). The structure of the modified calculation formula, adapted from the authors [44], [45], [46], is as follows:

Material costs of a wood raw material (chips)
+ Material cost of a plastic component (HDPE + additions)
+ Wage cost rate per machine hour (WCR/MH)
+ Energy cost rate per machine hour (ECR/MH)
+ Calculation depreciation rate per machine hour (CDR/MH)
+ Technology maintenance rate per machine hour (TMR/MH)
= Full cost of production
+ Other corporate overheads (OCO)
= Total product cost
+ Profit margin
= Offer price excl. VAT

To determine the proposed machine hour rate entries in the costing, consideration is given to using the following methodological procedures for determining MHR (Table 7.17):

Table 7.17
Procedure for the calculation of the items for the calculation of the machine hour rates

Wage cost rate per machine hour (WCR/MH)	WCR/MH = wage costs/scheduled time pool MH
Energy rate per machine hour (ER/MH)	ER/MH = rated power of the machine × Ø % electrical capacity utilization × rate per unit of energy
Calculation depreciation rate per machine hour (CDR/MH)	CDR/MH = (acquisition cost of technology/(lifetime × planned time fund MH))
Technology maintenance rate per machine hour (TMR/MH)	TMR/MH = (acquisition price of technology × annual maintenance rate)/planned time fund MH)
Mark-up for other overheads (OCO – %)	OCO = (other corporate overheads)/(direct wages) ×100

The quantification of cost items for the determination of MHR depends greatly on the technologization of production (its components), the determination of the need for machine installed capacity, and the amount of each group of overheads (labor, energy, depreciation, maintenance, or rent). They are currently in the process of being estimated and allocated to the costing process. Only after their accurate quantification will it be possible to compare the selling price levels of the conventional and the innovative product with the intention of even more accurately quantifying the difference in selling price levels and potential cost savings.

The effect of using the MHR calculation is not only in eliminating the inaccuracies of the surcharge calculations (their static nature and the use of the principles of averaging principle), but mainly in the fact that such a design gives the possibility of a very quick reaction and flexible adjustment of changed conditions of the input calculation. These are mainly changes in the tariff for the technological part of energy consumption, or the inflationary impact on changes in material and labour inputs for production or maintenance, but also investment costs expressed in the item depreciation. The calculation procedure is therefore an ideal tool for flexible and reasoned decision-making, but it must also be based on accurate input information contained in the investment project.

7.11 Conclusion

In this phase of the project, selected physical and mechanical properties of single and three-layer particleboard (PB) with plastic content from end-of-life cars were evaluated. Based on the results obtained, we can conclude that the thermal-physical properties achieved are slightly worse if compared to PBs without plastic filler, but this does not mean that they cannot be used as part of building structures. The evaluation of water absorption and swelling of a 3-layer PB with plastic/rubber content shows that the lowest values of water absorption after 24 hours were found for PBs containing non-painted bumpers, and the lowest swelling values after 24 hours for PBs containing fuel tanks. In terms of these observed properties, it can be concluded that the properties of the plastic-containing PBs were comparable to those of conventional PBs. Higher values of water absorption and swelling were found for the PBs containing tyres and the mixture of carpets and seals.

Based on the evaluation of the mechanical properties, tensile strength (TS), modulus of rupture (MOR), modulus of elasticity (MOE) and screw resistance torque (SDT) of three-layer PBs with plastic/rubber content, it can be concluded that for TS, comparable values to those of unfilled PBs were obtained for particleboards with 10 % of non-painted bumpers. For the other sample types, the values of this strength were lower. In the case of MOR, we obtained comparable results to PBs for most samples. For MOE, the best results were found in PBs containing fuel tanks. Within the observed bolt resistance moment, lower values can be observed for the specimens containing plastic/rubber. Among the studied PBs with fillers, the best values (SDT) were obtained for the PBs containing a mixture of carpet and sealers.

Several biological tests were used for ecotoxicological testing. In the *Lemna minor* growth inhibition test, growth inhibition exceeded the thresholds for suitable samples. In the test assessing *Daphnia magna* immobilization, the percentage of immobilization increased with a higher proportion of plastic waste in the particleboard. The test results were positive for all samples. Testing of aqueous infusions from experimental samples revealed the most significant effect on the growth rate of *Lemna minor* and immobilization of *Daphnia magna*. The results suggest that biological tests are a suitable tool for assessing the environmental impact compared to the results obtained when testing infusions from particleboard without replacing the wood with plastic. The results measured as chemical oxygen demand (an indicator of total organic matter content) confirm that with increasing plastic the content of organic matter in the aqueous infusions decreases with increasing plastic content in particleboards compared to particleboards without wood substitution. The best methods to limit the release of plastics into the environment are reduction, reuse and, above all, recycling. Due to the widespread use of particleboards in interior and exterior applications, the recycling of automotive plastic waste as a substitute for wood in particleboard is a current method of use. A study by Keskisaari et al. [47] aimed at comparing the economic viability of particleboard confirmed the economic benefits of using recycled plastics as a substitute for wood in particleboards. Therefore, the use of plastic waste as a partial substitute in particleboards is a suitable approach. The results obtained from the experiments complement the safe use of particleboards made with wood substituted by plastic waste from the automotive industry compared to pure particleboards.

Based on the results obtained, we can conclude that PBs have good strength and physical properties and can therefore be used for various applications, e.g. for the production of furniture or in the construction industry.

References

[1] Zhang, X., et al. 2023. A comprehensive review of reverse logistics in the automotive industry. IEEE Access. 2023, 11, 47112–47128. DOI:10.1109/access.2023.3273591

[2] Prasanth, S.M., et al. 2021. Application of biomass derived products in mid-size automotive industries: A review. Chemosphere. 2021, 280, 130723. DOI: 10.1016/j.chemosphere.2021.130723

[3] Adeniyi, A., et al. 2016. Chapter 2 - Thermoplastic-Thermoset Nanostructured Polymer Blends. V: Sabu, T., Shanks, R., Chandrasekharakurup, S. (eds). Design and Applications of Nanostructured Polymer Blends and Nanocomposite Systems. Boston: William Andrew Publishing, Micro and Nano Technologies, s. 15–38. DOI: 10.1016/B978-0-323-39408-6.00002-9

[4] Imre, B., Pukánszky, B. 2013. Compatibilization in bio-based and biodegradable polymer blends. European Polymer Journal. 2013, 49(6), 1215–1233. DOI: 10.1016/j.eurpolymj.2013.01.019

[5] Bellmann, K., Khare, A. 1999. European response to issues in recycling car plastics. Technovation. 1999, 19(12), 721–734. DOI:10.1016/S0166-4972(99)00081-4

[6] Chauhan, V., Varis, J., Kärki, T. 2019. The potential of reusing technical plastics. Procedia Manufacturing. 2019, 39(502–508). DOI: 10.1016/j.promfg.2020.01.407

[7] Vieyra, H., et al. 2022. Engineering, Recyclable, and Biodegradable Plastics in the Automotive Industry: A Review. Polymers. 2022, 14(16), 3412. DOI:10.3390/polym14163412

[8] Zhang, H., Chen, M. 2014. Current recycling regulations and technologies for the typical plastic components of end-of-life passenger vehicles: A meaningful lesson for China. Journal of Material Cycles and Waste Management. 2014, 16. DOI:10.1007/s10163-013-0180-3

[9] Awaja, F., Pavel, D. 2005. Recycling of PET. European Polymer Journal. 2005, 41(7), 1453–1477. DOI: 10.1016/j.eurpolymj.2005.02.005

[10] Froelich, D., et al. 2007. State of the art of plastic sorting and recycling: Feedback to vehicle design. Minerals Engineering. 2007, 20(9). Selected papers from Material, Minerals & Metal Ecology '06, Cape Town, South Africa, November 2006, 902–912. DOI: 10.1016/j.mineng.2007.04.020

[11] Guo, W., et al. 2022. A sustainable recycling process for end-of-life vehicle plastics: A case study on waste bumpers. Waste Management (New York, N.Y.). 2022, 154, 187–198. DOI:10.1016/j.wasman.2022.10.006

[12] Farzana, R., Sahajwalla, V. 2015. Novel recycling to transform automotive waste glass and plastics into SiC-bearing resource by silica reduction. Journal of Sustainable Metallurgy. 2015, 1(1), 65–74. DOI:10.1007/s40831-014-0004-2

[13] Rajagopal, R.R., et al. 2016. Sustainable composite panels from non-metallic waste printed circuit boards and automotive plastics. Journal of Cleaner Production. 2016, 144. DOI: 10.1016/j.jclepro.2016.12.139

[14] Cholake, S., et al. 2017. Composite panels obtained from automotive waste plastics and agricultural macadamia shell waste. Journal of Cleaner Production. 2017. DOI: 10.1016/j.jclepro.2017.03.074

[15] Liu, P., et al. 2017. Lightweight expanded aggregates from the mixture of waste automotive plastics and clay. Construction and Building Materials. 2017, 145, 283–291. DOI:10.1016/j.conbuildmat.2017.04.009

[16] Owodunni, A.A., et al. 2020. Adhesive application on particleboard from natural fibers: A review. Polymer Composites. 2020, 41(11), 4448–4460. 1548-0569. DOI:10.1002/pc.25749

[17] Horta, J.F., Simões, F.J., Mateus, A. 2017. Study of wood-plastic composites with reused high-density polyethylene and wood sawdust. Procedia Manufacturing. 2017, 12, International Conference on Sustainable and Intelligent Manufacturing, RESIM 2016, 14-17 December 2016, Leiria, Portugal, s. 221–229. DOI: 10.1016/j.promfg.2017.08.026

[18] Meikle, Jeffrey L.. 1997. Material Doubts: the Consequences of Plastic. Environmental History [online]. 1997, roč. 2, č. 3, s. 278–300. ISSN 1084-5453. Dostupné na: doi:10.2307/3985351

[19] Gogoi, R., Manik, G. 2021. Mechanical properties of wood polymer composites. 2021, 113–136. DOI:10.1007/978-981-16-1606-8_6

[20] Haque, Md., et al. 2018. Melt-viscosity and mechanical behaviour of polypropylene (PP)/wood flour composites: Effect of pulverization of wood flour with and without water. Advanced Industrial and Engineering Polymer Research. 2018, 2. DOI: 10.1016/j.aiepr.2018.11.001

[21] Kazemi N.S. 2013. Use of recycled plastics in wood plastic composites – A review. Waste Management. 2013, 33(9), 1898–1905. DOI: 10.1016/j.wasman.2013.05.017

[22] Chanda, M., Roy, S.K. 2006. Plastics Technology Handbook. 4. vyd. Boca Raton: CRC Press. DOI:10.1201/9781420006360

[23] Wolcott, M. P. 2001. Wood–Plastic Composites. V: BUSCHOW, K.H.J., CAHN, R.W., FLEMINGS, M.C., ILSCHNER, B., KRAMER, E.J., MAHAJAN, S., VEYSSIÈRE, P. (eds). Encyclopedia of Materials: Science and Technology. Oxford: Elsevier, 9759–9763. DOI:10.1016/B0-08-043152-6/01772-1

[24] Andersone, I., et al. 2012. Handbook of wood chemistry and wood composites, 2nd Edition. Rowell, R. M. (ed.), Routlege, Taylor and Francis Group.

[25] Klímek, P., et. al. 2016. Utilization of air-plasma treated waste polyethylene terephthalate particles as a raw material for particleboard production. Composites Part B: Engineering. 2016, 90. DOI: 10.1016/j.compositesb.2015.12.019

[26] Clemons, C. 2002. Wood-plastic composites in the United States: the interfacing of two industries. Forest products journal. 2002, 52(6),10-18, [cit. 28.11.2023]. Dostupné na: https://www.fs.usda.gov/research/treesearch/8778

[27] Jayamani, E., Balakrishnan, V. 2021. Thermal properties and flammability of wood plastic composites. 2021, 161–178.DOI:10.1007/978-981-16-1606-8_8

[28] Properties of building materials and thermal insulation (in Slovak), [3/5/2023], Available on: https://www.semargl.sk/vlastnosti-stavebnych-materialov-a-tepelnych-izolacii/

[29] Czajkowski, L., et al. 2016. Thermal properties of wood-based panels: specific heat determination. Wood Science and Technology. 2016, 50, 537–545. DOI:10.1007/s00226-016-0803-7

[30] Hallack, E., et al. 2022, Systematic Design for Recycling Approach – Automotive Exterior Plastics. Procedia CIRP, 2022, 105, 204-209, DOI: 10.1016/j.procir.2022.02.034

[31] Fargašová, A. 2009. Ekotoxikologické biotesty. Bratislava: Perfekt, 2009.

[32] Hybská, H., Samešová, D., Lobotková, M. 2021. Ecotoxicological effects of the leachate from the waste tires on the environment. Waste forum. 2021, 166-175.

[33] Hybská, H., Samešová, D. 2014. Processes of treatment and purification of water: instructions for exercises (in Slovak), Technical University in Zvolen, 2014.

[34] Hybská, H., et al. 2023. Ecotoxicological tests of the particleboards containing rubber waste. Wood research. 2023, 68(4), 758 – 767. DOI: 10.37763wr.1336-4561/68.4.758767

[35] Lithner, D., et al. 2012. Comparative acute toxicity of leachates from plastic products made of polypropylene, polyethylene, PVC, acrylonitrile-butadiene-styrene, and epoxy to Daphnia magna, Environmental science and pollution research. 2012, 19(5), 1763-1772. DOI:10.1007/s11356-011-0663-5

[36] Wik, A., Dave, G. 2005. Environmental labeling of car tires - toxicity to Daphnia magna can be used as a screening method. Chemesphere. 2005, 58, 645-651.

[37] Ekbatani, M., Sangeladji, M. 2011. Traditional vs. contemporary managerial/cost accounting techniques differences between opinions of educators and

practitioners. The International Business & Economics Research Journal. 2011, 7(1). DOI: 10.19030/iber. v7i1.3213

[38] Potkány, M., Krajčírová, L. 2015. Calculations and budgets (in Slovak). Technical University in Zvolen, 2015. 197 s.

[39] Coenenberg, A.G, Fisher, T.M., Günther, T. 2016. Kostenrechnung und Kostenanalyse. 9., Überarbeitete Auflage. 2016, Stuttgart: Schäffer-Poeschel Verlag. 950 s.

[40] Popesko, B., Papadaki, Š. 2016. Modern methods of cost management: how to achieve effective spending of costs and their reduction (in Czech). 2nd, updated and expanded edition. Prague: Grada Publishing, 263 p.

[41] Král, B. et. al. 2018. Managerial accounting (in Czech). 4th expanded and updated edition, Prague: Management Press, 2018. 792 p.

[42] Popesko, B. 2013. Costing methods utilization in Czech enterprises. International Journal of Entrepreneurial Knowledge. 2013, 1(1). DOI: 10.15759/ijek/2013/v1i1/53755

[43] Ostermann, R. 2010. Basiswissen Internes Rechnungswesen: Eine Einführung in die Kosten- und Leistungsrechnung. Herdecke; Witten: W3L, 2010. p. 304.

[44] Mumm, M. 2015. Kosten- und Leistungsrechnung: Internes Rechnungswesen für Industrie- und Handelsbetriebe. Berlin: Springer Gabler, 2015. p. 343.

[45] Wöltje, J. 2016. Kosten-und Leistungsrechnung. Freiburg: Haufe Lexware, 2016. p. 456.

[46] Keskisaari, A., Kärki, T. 2018. The use of waste materials in wood-plastic composites and their impact on the profitability of the product, Resources, Conservation and Recycling. 2018, 134, 257-261. DOI: 10.1016/j.resconrec

Standards used:

ASTM D1107-21: 2021. Standard Test Method for Ethanol-Toluene Solubility of Wood. 2021. West Conshohocken, PA, USA: ASTM International.

EVS-EN 323/2002: Wood-based panels. Determination of density.

EVS-EN 317/2005: Particleboards and fibreboards. Determination of swelling in thickness after immersion in water.

EVS-EN 319/2005: Particleboards and fibreboards. Determination of tensile strength perpendicular to the plane of the board.

SEIFERT, V.K. 1956. About a new method for rapid determination of pure cellulose. *Papier*, s. 301–306.

SLUITER, A., HAMES, B., RUIZ, R., SCARLATA, C., SLUITER, J., TEMPLETON, D., CROCKER, D. 2008. Determination of structural carbohydrates and lignin in biomass, in: Laboratory Analytical Procedure (LAP). *National Renewable Energy Laboratory*. 2008.

STN EN 312: 2011. Chipboards - Specifications.

WISE, L.E., MURPHY, M., D'ADDIECO, A.A. Chlorite holocellulose, its fractionation and bearing on summative wood analysis and on studies on the hemicelluloses. *Paper Trade Journal*. 1946, 122, 35–44.

TNI CEN/TR 17105: 2017. Construction products – Assessment of release of dangerous substances – Guidance on the use of ecotoxicity tests applied to construction products; European community for standardization: Brussels, Belgium.
STN EN ISO 19396-1: 2017. Paints and varnishes — Determination of pH value, Part 1: pH electrodes with glass membrane.
STN ISO 15705: 2005, Water quality. Determination of the chemical oxygen demand index (ST-COD). Small-scale sealed-tube method
OECD 221: 2006. Lemna sp., Growth Inhibition Test, DOI: 10.1787/9789264016194
STN EN ISO 20079: 2008. Water quality. Determination of the toxic effect of water constituents and wastewater on duckweed (*Lemna minor*). Duckweed growth inhibition test (ISO 20079:2005)
EN ISO 6341: 2012. Water quality, Determination of the inhibition of the mobility of *Daphnia magna Straus* (*Cladocera, Crustacea*), Acute toxicity test; International Organization for Standardization: Geneva, Switzerland.
OECD 202 I.: 2004. Daphnia sp., Acute Immobilisation Test, DOI: 10.1787/9789264069947

8 Energy Recovery/Disposal of Waste Sludge from the Automotive Industry

8.1 Introduction

Industrial waste sludge can be categorized as industrial waste, which is generated in various production processes. The industrial waste category includes, for example, product residues, furnace dust, slag, ash and sludge. Most industrial waste comes from three types of industries: metallurgical, non-metallurgical and food processing. Industrial waste can vary from sector to sector depending on the raw materials used, the production processes and the output products. In the waste catalogue, industrial waste can be classified in both category N (hazardous waste) and category O (other waste) according to its type and composition.

Industrial sludge is essentially a suspension of a solid with a liquid. In solving this research task, the research team focused on the recovery of industrial sludge from the automotive industry, where it is possible to identify various types of sludge that are associated with different phases of automotive production and components, maintenance of production lines or dismantling. In this solution of the research task, the aim was to assess the possibility of energy utilization of sludge arising in the production of cars, specifically in the process of production of car bodies at the Volkswagen Slovakia a.s. production plant in Bratislava. According to the waste catalogue, the sludges generated here belong to the hazardous waste category, waste catalogue number 06 05 02 – sludges from on-site treatment of liquid waste containing hazardous substances. It is currently managed under category D1 – disposal by landfill or surface disposal (e.g. landfill). If the research task is successfully solved, the management of this waste could move from waste disposal to waste recovery, for example into the category R1 – use mainly as fuel or for other energy recovery, R2 – solvent recovery or regeneration, R3 – recycling or recovery of organic matter not used as solvents (including composting and other biological transformation processes, including gasification and pyrolysis, which use components as chemicals) or other recovery.

8.2 Waste sludge treatment

Sludges generated in industrial processes are particularly burdened by high humidity, so the primary process of their treatment is dewatering and drying. The technological process of drying is ecologically and energetically demanding, also due to the amount of sludge produced in the technological process. For example, municipal sewage sludge or paper mill sludge has a very high output moisture content, coming out of the process with a moisture content of approximately 70 to 80 %. For further processing, e.g. for energy use, but also for transport, it is advisable to dry them to an output moisture content of 10 to 20 %. For easier transport and handling, the treated sludge can then be pressed into pellets or briquettes, with the addition of suitable additives (e.g. biomass, used oils, etc.) to increase the energy content.

Sludge dewatering and drying technologies:

- mechanical moisture separation based on the principle of external forces such as gravity, centrifugal forces, etc. Examples of applications are high-speed counter-rotating centrifuge (good dewatering results, low resulting moisture content of the trapped solid phase), gravity settling (high moisture content of the trapped solid phase) etc.;
- mechanical separation of moisture by pressure – pressing: the most used method in practice, by which we are able to process large hourly quantities of waste sludge even
- with high liquid content, with a relatively low energy input and therefore with low economic costs (good dewatering results, low final moisture content of the captured solid phase);
- separation method based on different particle size – filtration, particles with size larger than the free space between the material forming the filter medium; as the filter medium fills, the so-called "filter medium" is formed. Filtration can be surface filtration (particles are trapped only on the surface of the filter) or bulk filtration (particles are trapped on the surface of the filter in the entire volume of the filter material); the method reliably separates a large amount of solid phase from the sludge, but with a high resulting moisture content of the trapped solid phase;
- chemical moisture separation processes – the possibility of complete separation of moisture from sludge; technologies are based, for example, on processes of absorption, adsorption and ion exchange – collectively referred to as sorption; a technology not widely used in the treatment of waste sludge, mainly because of its high moisture content and large quantity: it is used in the chemical industry rather than in waste management.
- technologies based on the action of heat – mostly used for sludge drying, the technology is energy and therefore economically expensive; by using waste heat from another technological process, it is possible to achieve a more favorable energy and economic balance;
- combination of the above-mentioned methods into one technological unit – by suitable combination of the above-mentioned methods it is possible to achieve up to zero resulting moisture content of the solid phase captured from the waste sludge.

To remove large quantities of liquid from sludge, the most commonly used technology is mechanical separation by pressing, the equipment used is called a sludge press. A sludge press is a device used to separate solid particles from turbid suspensions using pressure and filtration. In filtration, the flow of the polluted fluid occurs most often through a non-moving porous layer of material that has the ability to trap particles of the suspended solid phase. The fluid that flows through the filter and around the trapped particles is called the filtrate, and the layer of particles trapped on the filter partition is referred to as the filter cake.

The sludge suspension is either transported directly to the sludge treatment plant or the sludge preparation processes are carried out beforehand. Depending on the nature of the suspended solids and the suspension itself, there are specifics of the process that may take place prior to the actual separation of the liquid phase:

- settling – using a settling vessel, natural sedimentation separates the individual components based on the difference in densities and settling velocity; this phase is used to separate larger suspended particles;
- thickening – change of concentration, serves to effectively reduce the volume of pumped sludge into the dewatering device – the sludge settling tank, either by evaporating part of the liquid phase (most often by free evaporation or by the use of waste heat from another technological process), or by dilution by adding a certain amount of the liquid phase – for significantly thick suspensions (especially for facilitating transport, e.g. through a pipeline system);
- crystallization – a flocculant (organic or polymeric) is added to the reaction vessel by a dosing pump and by proper stirring, clusters of solid particles – also called flakes – are formed in the sludge.

After the preparatory processes, the sludge suspension is transported to the sludge tank, where pressure is created, which forces the liquid to pass through the filter medium, on which solid particles are trapped, thus creating the so-called "filter cake". This actually separates the solid and liquid phases.

According to the basic construction and principle of operation, the devices – sludge presses can be divided as follows:

- threaded presses,
- band presses,
- chamber presses,
- membrane presses,
- frame presses.

The capacity and performance of the different types of sludge presses depend on the size of the filter area, the dimensions of the filter plates, the volume of the filter chambers and their thickness. This process can achieve a final moisture content in the furnace of up to 5 %. Operation can be continuous or intermittent – discontinuous.

8.2.1 Threaded sludge press

The threaded sludge press (sometimes also referred to as screw press) is an efficient and energy-effective, low-energy-consumption device for continuous sludge dewatering. The most common design is with slow-running conical screw valves (screw turns below 1 rpm). The main technological part is the screw with sealing rubber slats and the sieve, which is interchangeable for dewatering different types of sludge (with different sieve mesh sizes). The screw has variable pitch and slats that act as a self-cleaning moving filter. The solid phase of the slurry is trapped on the sieve, the sieve must be rinsed and this is possible even without interrupting the dewatering process. The model of the threaded sludge press is shown in Fig. 8.1. An example of a threaded sludge press in partial disassembly is shown in Fig. 8.2.

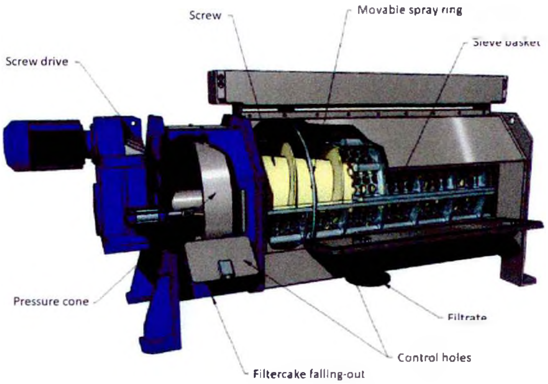

Fig. 8.1 Model of a screw sludge press (IEA Press)

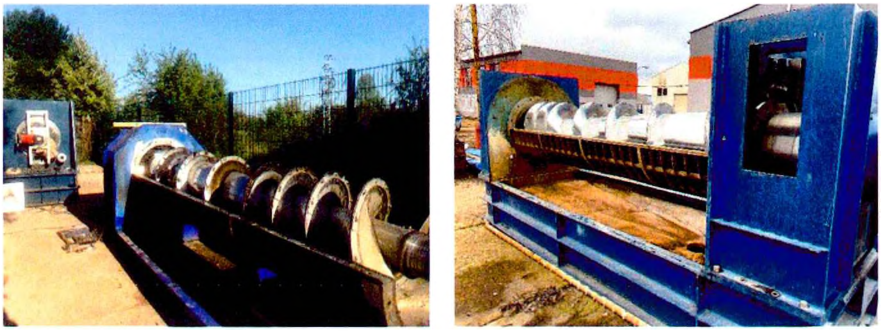

Fig. 8.2 Threaded sludge press (IEA Press)

8.2.2 Band sludge press

The band sludge press (Fig. 8.3) is a device with reliable performance, stable operation, high final dewatering, low energy consumption, suitable for continuous operation. The device is also suitable for operation with uneven fluctuating loads in sludge management. The principle and operation of the band sludge dewatering unit can be divided into four important stages: pre-treatment of the input sludge, gravity dewatering, pressurized dewatering in the wedge zone, and press dewatering. The most common design is with two upper and lower tensioned filter bands that are bent into an S-Shape over a series of regularly arranged cylinders. The sludge layer is compressed by the tension of the filter belt itself and by the geometry of the roller arrangement so as to create a shear force that displaces the capillary water from the sludge layer and to obtain a filter cake with a high solids content, thereby achieving the actual dewatering of the sludge. Principle of operation of the band sludge press:

- pre-treatment of the input sludge – this type of sludge treatment plant has higher requirements for flocculation effect in the input sludge,
- gravity dewatering – sludge is uniformly fed into the filter belt; on the surface of the belt a sediment is formed by removing the free liquid – the primary filter cake and it is subsequently moved forward with the filter band. The main function of this technological step is to remove the free liquid, reduce the liquidity of the sludge and prepare it for further extrusion,
- low/medium pressure dewatering in the wedge zone – by entering the sludge band into the wedge-shaped zone, the sludge is further dewatered,
- high-pressure press dewatering – the filter cake is repeatedly compressed and sheared around the press cylinder by means of upper and lower filter bands; this process removes a large amount of capillary moisture (Fig. 8.4)

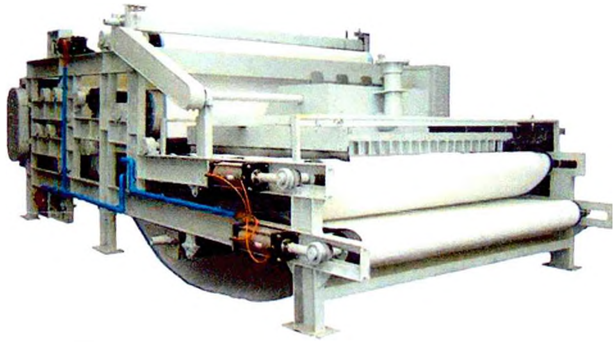

Fig. 8.3 Band sludge press (www.filterpressmachine.com)

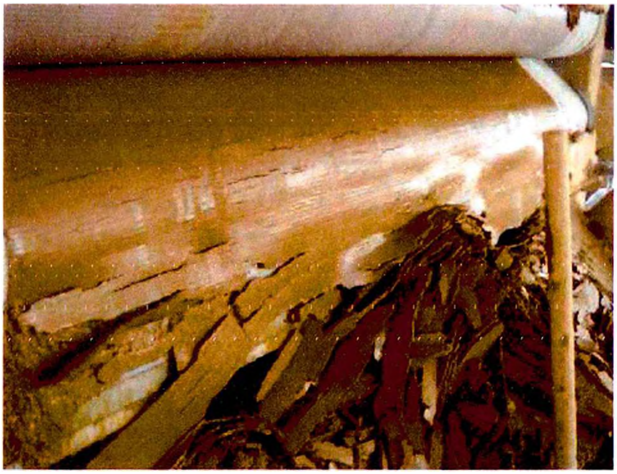

Fig. 8.4 Output of the band sludge press (www.filterpressmachine.com)

8.2.3 Chamber sludge press

Chamber sludge presses are one of the most widely used types of sludge presses due to their high dewatering efficiency, low energy and operating demands, high modularity, which makes it possible to adapt them to any technological process (they are usually custom-made according to customer requirements). The working space consists of filter chambers made of detachable filter plates, which have a recess in the flat part with a drainage system for the filtrate inlet and outlet. The filtrate outlet can be made as open or closed. The total recess depth of the two adjacent filter plates determines the thickness of the resulting filter cake, which ranges from 10 to 50 mm. Chamber filter plates are most often made of polypropylene. The working pressure is from 16 bar in the standard design, up to 30 bar in special designs (some up to 60 bar). Sludge presses usually come with the possibility of manual or automatic closing of the filter plates; the filter plates are mounted either on side clamps or with upper suspension. An example of a chamber sludge press is shown in Fig. 8.5. The design with side connecting rods or bolts is a simpler design, the design with a top beam ensures free access to the filter battery, it has a solid construction for harsh operating conditions (Fig. 8.6).

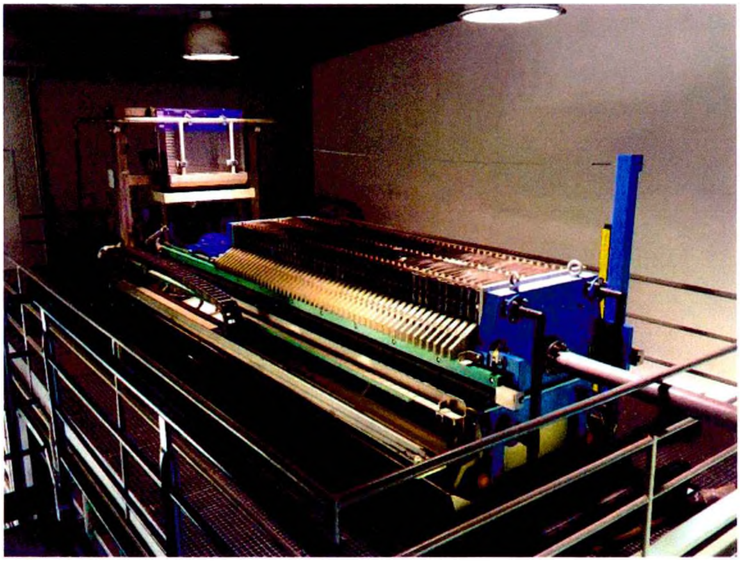

Fig. 8.5 Chamber sludge press with side connecting rods (Envites)

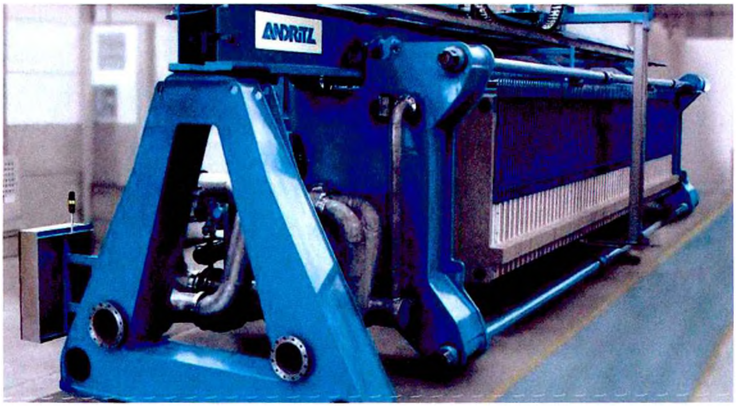

Fig. 8.6 Chamber sludge press with upper suspension – beam (Andritz)

8.2.4 Membrane sludge press

The membrane sludge press uses a workspace with filter plates with a flexible movable membrane. The membrane serves to compress and wring out the filter cake. This results in higher dewatering, i.e. lower moisture content of the resulting filter cake than in the case of a chamber sludge press. Materials for membranes include polypropylene, synthetic rubber (e.g. NBR, EPDM), or thermoplastic elastomer (TPE). Special materials are also available, such as PVDF. The membrane is impermeable and compresses the filter cake in the chamber after the filtration process is complete. Liquid or gas (compressed air) is used as the medium for compressing the membranes. In order to ensure maximum protection of the membrane press, special safety systems are used for different membrane compression media. The boost pressure can be up to 30 bar, and in special cases it can be even higher.

8.2.5 Frame sludge press – sheet filter

The chambers of this type of sludge press are formed by combining polypropylene filter plates and frames, a system with alternately aligned metal or plastic plates and frames. Filter fabrics (sheets) are inserted between the plates, which are grooved on both sides to allow the filtrate to flow over them. The frames and plates are pressed together to form filter chambers into which the filtered suspension is fed and the filter cake accumulates. In the corners of the frames and plates there are openings forming two channels in the system, one of which feeds the suspension or washing liquid into the filter chambers, the other drains the filtrate. This creates chambers from 5 to 40 mm thick, depending on the thickness of the frame. Frame callouses are suitable for pre-coating filtration, for example, which is used in the beverage industry for clean filtration. Conventional frame sludge presses are designed for operating pressures up to 6 bar.

8.2.6 Sludge press accessories

Due to the different requirements and different applications of sludge presses in industrial processes, the presses are produced in a modular design with a large number of optional components, the systems are designed for semi-automatic and automatic operation. The basic accessories for chamber, membrane and frame sludge presses are systems for single or chain plate sorting, or a system for rapid plate sorting for the mining industry or ejection frames, a shaker or scraping device, drip dampers and a spraying device for filter membranes.

8.3 Methods of recovery of industrial sludge

In many cases, the technologies used in the sludge management of a particular industrial plant predetermine how sludge can be effectively recovered. This statement implies that we choose specific technologies in sludge management based on the characteristics of the industrial process (sludge generated, its quantity, chemical composition, physical properties, etc.), but also on how we want to ultimately evaluate the sludge.

In EU countries, we can observe different ways of dealing with industrial sludge, also depending on local conditions, such as legislation. For example, treated and stabilized sludge from waste water treatment plants (WWTPs) can be directly applied to land (this is the most common use of sewage sludge in Estonia, Bulgaria, Spain and Ireland), composted (this is the most common use of sewage sludge in Cyprus, Finland and Hungary), incinerated or otherwise used for energy by other thermal methods (this is the most common use of sewage sludge in Austria, Germany, Belgium and the Netherlands), or landfilled (this is the most common use of sewage sludge in Malta and Romania). In general, the management of this type of sludge in Europe could be summarized as being disposed of by incineration, energy recovery or composting in countries where legislation is stricter. On the other hand, in countries where legislation is more relaxed, people choose the cheapest possible solutions – direct land application or landfilling.

For industrial sludges from other industries, the recovery is more challenging, either in terms of legislation or the chosen technology. The most commonly used method of energy recovery is in industrial waste incinerators or cement kilns.

8.3.1 Landfill

A landfill is a place with waste disposal facilities where waste is permanently deposited on the surface of the ground or directly into the ground. It can also be defined as an engineering structure, or a structure with an environmental designation that minimises the negative environmental impact of the disposed waste. Landfills are usually created on the site of abandoned or disused quarries, mines and pits. When selecting a suitable site, several criteria are taken into account, such as the protection of nature, landscape, groundwater and cultural heritage in the area, hydrogeological and engineering-geological conditions and others. It is the most used method of waste disposal in the Slovak Republic. In 2020, there were 111 legal and more than a thousand illegal landfills in Slovakia. Waste is landfilled without any further use of its potential (for example, energy or material); currently the conditions for using landfills are becoming more and more strict, and in the near future landfilling will be prohibited.

8.3.2 Incineration and co-incineration

Incineration is a thermal treatment of waste with access to oxygen, which can produce usable energy that can be considered renewable in some sense. During incineration, organic matter from waste sludge is rapidly oxidized with excess oxygen (or generally with excess combustion air) at high temperatures above 750 °C to produce mainly CO_2 and water vapour, together with other gaseous emissions (depending on the composition of the input fuel, the setting of the combustion process, e.g. CO, SO_x, NO_x, etc.), the main product of combustion is the aforementioned recoverable heat and another by-product is the solid residue – ash and fly ash. The combustion process reduces the mass and volume of the waste sludge (depending on the ash content of the input fuel), safely destroying micropollutants (except heavy metals) in the sludge.

As mentioned above, sludge usually contains a significant amount of moisture, which needs to be removed by appropriate technology before incineration. According to available literature sources and practical experience, the optimum moisture content of the fuel is considered to be 20 %. Depending on the type of sludge, its physical-chemical properties (especially calorific value and heat of combustion) and its processing, we often need a greater amount of energy to dry it to the optimum moisture content than we subsequently extract from it by incineration.

Incineration of waste sludge can be implemented as:

- direct incineration – for sludges with suitable properties for energy recovery, in particular with high energy content (calorific value), high content of volatilised combustible substances, low ignition temperature, high combustion temperature, etc,
- co-incineration with other fuels – for sludges that are more difficult to ignite, for example because of the need for high ignition temperature, long residence time and for sludges with lower calorific value. These sludges can be co-incinerated with gaseous fuel on the grate, directly mixed with solid or liquid fuel, or form mixes with a suitable solid fuel (e.g. sawdust) to form fuel pellets or briquettes. Such a method is applicable for energy recovery in, for example, thermal power plants, industrial and municipal waste incineration plants or cement and lime plants, in order to replace part of the conventional fuel. Cement and lime plants in Slovakia annually consume hundreds of thousands of tonnes of alternative fuels, most of which are solid alternative fuels (SAF) produced from waste and waste sludge. SAF in these plants replaces the use of conventional fuels such as coal and fuel oil, the combustion of which produces significantly more CO_2 emissions. SAF is a raw material produced from waste; the waste used to produce it is most commonly categorized under waste catalogue number 19 12 12 – other wastes, including mixed materials from mechanical treatment of waste other than those listed under 19 12 11 or 19 12 10 – combustible waste (fuel from waste). Cement kilns operate at temperatures in excess of 1,400 °C, with long flue gas residence times, thus achieving perfect waste disposal and maximum utilization of energy and ash. The advantage of burning SAF in cement plants is that these plants can recycle the residual ash which, due to its similar chemical composition, replaces part of the feedstock, limestone or clay. This ash thus becomes part of the product (clinker), which is the basic raw material in cement production.

Advantages of incineration and co-incineration:

- obtaining usable thermal energy,
- maximum reduction of the mass of the waste sludge volume, this parameter is indicated by the characteristic – ash content of the fuel,
- chemical neutralization and decomposition of sludge components by the action of an oxidizing agent and high temperature, under ideal conditions to produce neutral CO_2 and water vapour,
- elimination of odours that would arise from the spontaneous uncontrolled breakdown of waste sludge molecules (depending on the chemical composition of the sludge).

Disadvantages:

- waste sludges with high moisture content during combustion cause problems such as delayed ignition, different and uneven temperatures in different parts of the combustion chamber, lowering of the actual combustion temperature (due to the high evaporation heat of the water contained in the fuel); the sludge must therefore, as already mentioned, be significantly dewatered and then additionally dried, which represents an extra energy cost and often the sludge combustion has a negative energy balance;
- incineration of waste sludge can produce emissions of hazardous gases (dioxins, furans, sulphur and nitrogen compounds, possibly heavy metals, etc.), in which case flue gas treatment technology must be supplemented by technologies for capturing and neutralizing hazardous gas emissions,
- solid residue from incineration – ash and fly ash may also contain potentially toxic substances (especially in the form of heavy metals) and therefore its final treatment is usually by landfill.

Combustion products:

- Energy: waste sludge can in some sense be considered as a renewable energy source – assuming that nowadays industrial waste sludge is mostly disposed of in landfills without exploiting its energy potential. The problem with extracting energy from sludge is, as already mentioned, that we need to dry it considerably, which means that we have to expend energy first in order to be able to extract it by combustion. For example, according to [1], in most cases the incineration of sewage sludge comes out with a negative energy balance. However, the advantage of generating energy from sludge incineration is that it produces significantly lower greenhouse gas emissions than fossil energy production. For the same amount of energy produced, sludge produces 58 % fewer emissions than natural gas and 80 % fewer emissions than coal and fuel oil [2].
- Ash and fly ash: depending on the chemical composition of the incoming waste sludge, the ash and fly ash from incineration may contain different recoverable liquids, but also hazardous substances that pose a threat to the

environment (in particular heavy metals such as nickel, lead, cadmium, chromium, etc.). Organic pollutants are destroyed by combustion, but heavy metals remain in the ash and fly ash or, if not captured, are released into the air (e.g. toxic Pb, Cd). The content of hazardous substances depends on the type, quantity and composition of the sludge and on the setup of the incineration process itself [3]. There are technological processes for recovering e.g. heavy metals or other important elements from ash, but nowadays these processes are still more costly than their direct extraction in nature and subsequent processing. Neutralized and ash cleaned of undesirable elements and additives is also usable as an additive in various building materials (cement, masonry materials, etc.) [3].

Legislation: the process of incineration of waste sludge is governed by the Waste Act, under which it is considered as energy recovery of waste by activity R1 – use mainly as fuel or for energy recovery in other ways, provided that the energy generated is further used.

8.3.3 Pyrolysis and gasification

In the pyrolysis and gasification process, the waste sludge is treated at temperatures above 350 °C, without air access for pyrolysis or with limited air access for gasification, in order to obtain synthesis gas, condensate and solid residue. The advantage of these technologies over incineration is the recovery of other products that have other uses, for example they can be processed into fuels or in the chemical industry. Synthesis gas is most often used for energy purposes; the heat is used to heat the pyrolysis or gasification reactor or to dry the feedstock. Condensate, also called pyrolysis oil, contains condensed higher hydrocarbons from synthesis gas; it is usable either directly as fuel or for the production of synthetic noble fuels – gasoline, diesel, kerosene, etc., or by processing in the chemical industry to produce completely different materials. The solid residue contains a high proportion of solid carbon and can also be used for energy purposes, for example in thermal power plants and heating plants. In general, pyrolysis and gasification greatly reduces the weight and volume of sludge, safely destroying the vast majority of micropollutants, pathogens and organisms in it. The advantage of pyrolysis and gasification treatment of waste sludge is that, with the right process, we can largely immobilize heavy metals in the waste sludge that remain in the solid residue [4], [5] and also get rid of large amounts of microplastics [6], for example.

Advantages of pyrolysis and gasification

- significant reduction in the volume and weight of the treated waste sludge,
- destruction of pathogenic substances and organisms or pharmaceuticals,
- significant destruction of plastics and microplastics,
- stabilization of heavy metals, their binding in the solid residue,
- lower unwanted emissions of environmentally harmful gases compared to combustion,

- the possible recovery of thermal energy from the products of pyrolysis and gasification,
- the possible recovery of other products such as liquid and gaseous fuels,
- complete odour removal.

Disadvantages:

- tar may be produced during the pyrolysis and gasification process,
- the solid residue from pyrolysis and gasification may contain toxic elements, which can cause environmental problems if disposed of incorrectly,
- equipment for pyrolysis and gasification of waste sludge is not widely used and therefore there is no practical experience with such treatment.

Products of pyrolysis and gasification:

- Synthesis gas: also referred to as "syngas" from waste sludge treatment, it consists mainly of carbon monoxide, carbon dioxide, methane and hydrogen gas. Depending on the composition of the incoming waste sludge, other lower hydrocarbons may also be present which have not condensed under cooling conditions. All components of synthesis gas (except CO_2) can be converted into heat energy, or it can be used as a feedstock in the production of chemicals. It can be used as a substitute for conventional fuels (natural gas or other fossil fuels) whether in the process of drying waste sludge, in the heating of a pyrolysis reactor, in industrial processes or, for example, in cogeneration (for the combined production of electrical and thermal energy). Another new use of synthesis gas is to directly power hydrogen fuel cells; hydrogen is simply captured from the synthesis gas, purified and refined for use in fuel cells [7].
- Pyrolysis oil: formed by cooling, i.e. condensation, of synthesis gas, it is a liquid usually dark brown in color with a characteristic odour. It is a multicomponent mixture that can be separated into its individual components by fractional distillation and treated to obtain, for example, gasoline and diesel fuel, fuel oil, etc. or by processing in the chemical industry to obtain completely different new materials which are normally produced from crude oil. Pyrolysis oil and fuels produced from it are suitable for combustion in boilers and furnaces, diesel engines and combustion turbines in cogeneration of electricity and heat.
- Solid residue: it is mainly composed of carbon, its adsorption properties are similar to activated carbon, it has a high surface porosity, a wide microstructure, effective water retention capacity, and therefore in its pure form has a wide application in industry. The only disadvantage of this material is that it also contains other substances that are bound in it after pyrolysis, such as the aforementioned heavy metals [8], so its disposal is largely by landfill. Depending on the composition of the incoming waste sludge, the solid residue after the pyrolysis process is approximately 8 to

15 % of the original weight, effectively eliminating the volume and weight of the waste sludge. The other components, liquid and gaseous, are recovered either energetically or by other means. As the main component of the solid residue is carbon, energy recovery by combustion is also possible.

Legislation: the process of pyrolysis of sewage sludge is governed by the Waste Act, under which it is considered as recovery R3 – recycling or recovery of organic substances not used as solvents (including composting and other biological transformation processes).

8.4 Measurement of moisture and calorific value of waste sludge

First of all, it should be mentioned that the sludge dealt with in the research task is generated during the technological processes in the paint shop, so some of them also have a high energy value, as they contain substances that are commonly present in the processes used for the surface treatment of car bodies. The classification of sludge as waste varies and some of it is classified as hazardous waste, its disposal by methods other than incineration is costly, not to mention the legislative procedures. In this case, the main task of sludge disposal in combustion processes is to neutralize the sludge; the energy value of some sludge is not negligible and is comparable to common solid fuels such as wood or coal. Thus, some of the sludges can not only be thermally treated in incinerators but can also positively influence the energy balance of the incinerated mixture by their energy value.

The analysis was preceded by sampling of the paint shop at the Volkswagen car plant in Bratislava, where the plants where the individual sludges are produced were inspected and the technology for sludge treatment prior to removal was also important – sludge dewatering on the sludge settling tanks. The main problem with these waste sludges is the large amount of water that needs to be removed, not because they need to be heat treated, as currently this waste is not heat treated, but because of the consistency of the waste and the ease of transport. The sludge is thus modified by various processes into a solid rather than a liquid form, e.g. a solid slurry that forms clumps and holds its shape.

8.4.1 Sample preparation prior to laboratory testing

The samples were taken during a site visit to the paint shop where they are generated and were taken from the containers in which the sludge is taken for disposal, i.e. they were in exactly the condition in which they would be taken to the incinerator in the event of thermal treatment. The samples were taken in a simple form – scooped into a labelled plastic bag and properly sealed, not only for transport reasons, but also so that they would not lose the moisture with which they would be taken to the incinerator, so that the measurement results would reflect reality.

The preparation of the samples was subsequently carried out in the laboratory of the Department of Power Engineering of the University of Žilina. In order to determine the calorific value of the samples, they had to be dried to standard at 105 °C on a drying balance Fig. 8.7, where the moisture content of each sludge was also measured in weight percent.

8.4.2 Fuel moisture measurement

Measurement procedure:

1. Samples shall be prepared on disposable trays intended for the drying scale. First, an empty tray is placed in the scale and its mass is reset to zero so that only the net mass of the sample is counted.
2. The sample is then spread over the surface of the tray in as thin a layer as possible, so that drying takes place thoroughly and in a short time.
3. The sample tray is placed in the drying tray, the scale records the net weight of the sample and the drying program of the scale is started.
4. Drying is carried out at the standard recommended temperature of 105 °C (a temperature high enough to remove water from the sample but low enough not to lose the volatile part of the combustible material contained in the fuel).
5. The scale stops drying when the sample weight stops decreasing – this process happens automatically because the scale is equipped with an algorithm that evaluates when the sample is dry enough.
6. After the drying process has stopped, the scale calculates the moisture content in weight percent of the original sample loaded into the scale before the drying process.

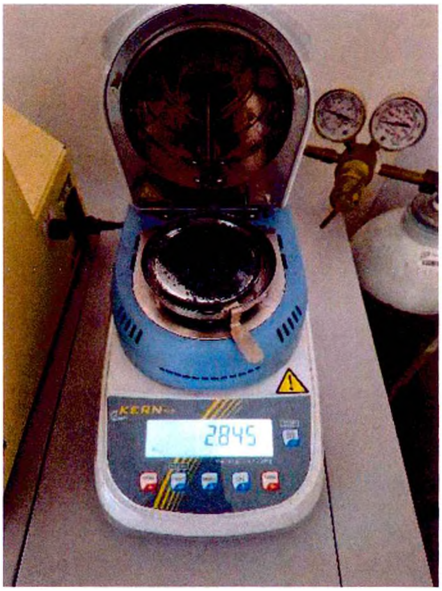

Fig. 8.7 Sample ready for drying in the KERN drying scale

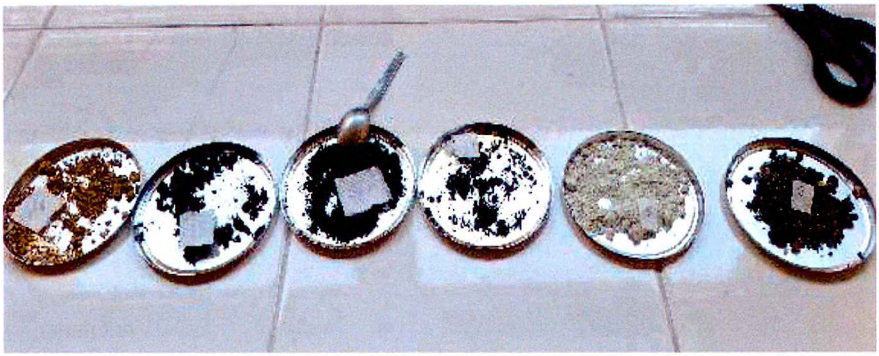

Fig. 8.8 Prepared dried samples, ready for weighing prior to calorific value determination

Table 8.1
Moisture measurement of waste sludge samples

Sample marking	**Moisture content in % by weight**
Sludge 1+2	7.78
Sludge 3	12.20
Sludge 4	19.71
Sludge 5	20.01
Sludge 6	6.94
Sludge X	8.88

The samples were consecutively labelled with numbers and the last sample with the letter X; this sample represents a mixture of waste sludge that was from the cleaning of the shipping containers, the sample therefore contained all samples 1 to 6. From the measurements, the moisture contents of each sample were obtained; a representative selection of the measured values for each sample are shown in the following Table 8.1. The results of the moisture assessment show that the waste sludge from the production is left sufficiently dewatered and is suitable for subsequent energy recovery (the recommended maximum moisture content for e.g. firewood 20 %).

8.4.3 Measurement of waste sludge calorific value

The calorific value of each sample (Fig. 8.8) was measured immediately after sample preparation by drying to ensure that the measurement was as little affected as possible by ambient moisture. Calorific value measurements were carried out on a LECO AC500 calorimetric combustion heat measuring device (Fig. 8.9).

The LECO AC500 calorimeter is an automatic calorimeter for measuring the calorific value of liquid and solid fuels. The device contains not only the calorimeter itself, but also a computer with a keyboard, a calorimetric cylinder – a small, pressurized container with a sample container and an ignition resistance wire, an oxygen cylinder, a sample preparation device, and a device for automatic filling and flushing of the pressure container with oxygen. This calorimeter is developed to measure the calorific value of various organic substances such as coal, coke, fuel oil and other solid and liquid substances containing organic combustibles. The calorific value of a substance is determined from the combustion of a sample in the controlled environment of a pressurized container, and the heat released from combustion is directly proportional to the calorific value. The sample is placed in the environment of the combustion vessel – pressure container, where it is ignited. This vessel is immersed in the water environment of the calorimeter, to which the heat from the combustion vessel – pressure container is transferred, and the temperature of this water is measured by an electronic temperature probe with an accuracy of 1.10^{-4} °C every 6 seconds. The device also performs correction of the heat supplied by the ignition wire.

Measurement procedure:

1. Before each measurement, it is necessary to clean the calorimetric cylinder – pressure container with water, to remove residues after samples from the previous measurements and remove the combustion container, which must be cleaned to ensure that no sample residues from previous measurements remain in it.
2. We dry all the parts that will be put into the calorimetric cylinder.
3. Then we pour 10 ml of distilled water into the bottom of the container.
4. We check the patency or condition of the filters that trap impurities from the water in the calorimeter.
5. Then we fill a measuring cup with the exact amount of distilled water that the calorimeter pump will push out. The exact amount of water is ensured by making an overflow on the dipstick and, when the dipstick is full, the unnecessary amount overflows into the overflow of the calorimeter.
6. This precise amount of water is poured through the three-way valve of the calorimeter into a removable stainless-steel container in which the pressure container containing the sample to be measured will be nested.
7. We clean the container in which the sample is to be weighed of coarse dirt with a brush designed for this purpose. Then we rinse and dry the container – not with a cloth that can leave lint.
8. A sample weighing 0.8 to 1.2 g is weighed into the container thus prepared.
9. A resistance wire (Fig. 8.10) is inserted, which ignites the sample in the oxygen atmosphere of the measuring cylinder.
10. The calorimetric cylinder is hermetically sealed with the sample.
11. Then the closed calorimetric cylinder space is flushed with pure oxygen to remove atmospheric air.
12. After the flushing is completed, the calorimetric cylinder is filled with oxygen by an automatic pressurizing device (Fig. 8.11).
13. We place the calorimeter cylinder in the calorimeter in the previously prepared water bath and connect the ignition electrodes (Fig. 8.12).
14. The exact net mass of the sample must be entered into the software that controls the calorimeter.

15. Then we start the measurement.
16. The calorimeter performs all the steps necessary for the measurement automatically (temperature stabilization, sample ignition, mixing of the water bath and measurement).
17. After the sample burns out, the instrument signals shut down and calculates the calorific value of the fuel sample in MJ.kg^{-1} from the entered mass.

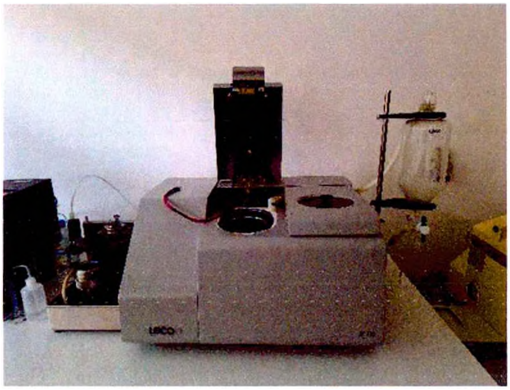

Fig. 8.9 LECO AC500 calorimetric instrument for measuring calorific value of fuels

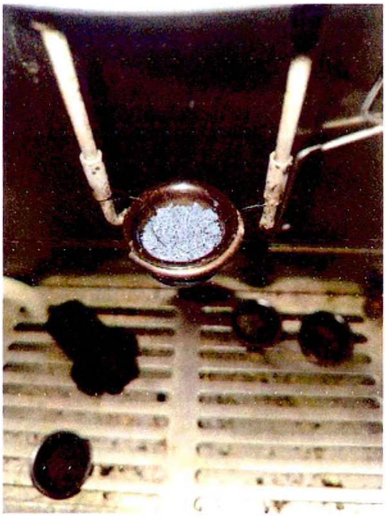

Fig. 8.10 Measuring vessel with weighed waste sludge sample with embedded ignition wire

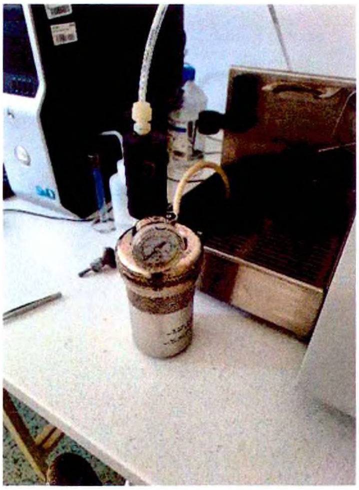

Fig. 8.11 Prepared calorimetric cylinder

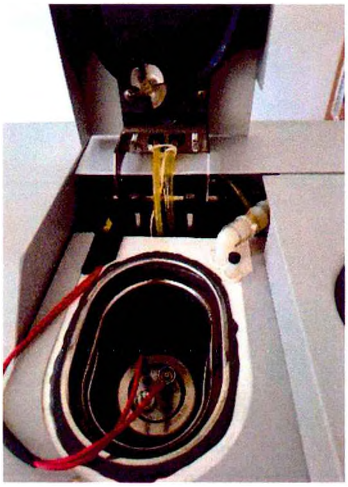

Fig. 8.12 Sample ready for calorific value measurement in the calorimeter

The results of the measured calorific values of the waste sludge samples are shown in the Tab. 8.2. For each sample, 4 measurements were taken; only 2 measurements were taken for the low calorific value samples, which were considered unsuitable for energy recovery.

As can be observed in the results, the waste sludges labelled 1+2 and 6 have very low calorific values and are not suitable for energy recovery. The calorific value of a fuel is mostly influenced by its chemical composition and, as later analyses have shown, these fuels contain almost no combustibles.

As can be seen below, some sludges also have a high energy value, comparable e.g. to wood, while others are comparable in energy value e.g. to municipal waste (sludges marked 3, 4, 5 and X). The variance in the calorific values for the different measurements for each sample are due to the fact that the first measurements were taken immediately after sampling and the others were taken some time apart. The reduction in calorific value indicates the content of volatile combustible substances which are spontaneously released into the environment. The differences also point to the inhomogeneity of the waste sludge material.

Table 8.2
Fuel calorific value

Sample marking	**Calorific value [MJ.kg^{-1}]**
Sludge 1+2, sample 1	1.724
Sludge 1+2, sample 2	1.508
Sludge 3, sample 1	16.623
Sludge 3, sample 2	12.348
Sludge 3, sample 3	13.060
Sludge 3, sample 4	13.368
Sludge 4, sample 1	16.286
Sludge 4, sample 2	9.422
Sludge 4, sample 3	9.817
Sludge 4, sample 4	10.941
Sludge 5, sample 1	8.350
Sludge 5, sample 2	7.884
Sludge 5, sample 3	7.644
Sludge 5, sample 4	7.807
Sludge 6, sample 1	0.028
Sludge 6, sample 2	0.001
Sludge X, sample 1	10.630
Sludge X, sample 2	7.884
Sludge X, sample 3	7.644
Sludge X, sample 4	7.807

Sludges that do not have a high energy value may not be of energy benefit in incineration plants, but what is important in this case is their disposal, chemical stabilization and the non-leachability of the residues after the incineration process in a landfill after such treatment which, in most cases, can be achieved by thermal processes and the subsequent landfilling of the waste in a conventional landfill.

8.4.4 Elemental analysis of waste sludge samples

CHNO analysis: it determines the mass percentage of carbon, hydrogen and nitrogen, and oxygen is added. From this analysis and practically, we can see the main elements such as carbon and hydrogen, which are the main components influencing calorific value. Nitrogen is not involved in combustion and is ballast in the fuel. The results of this analysis are presented in Table 8.3 below. The content of these substances is determined from the dry weight of the samples (absolute dry samples). The content in the original samples is shown in Table 8.4.

Analysis of other elements: other elements present in the samples include alkaline earth metals, alkali metals, metals, phosphorus and sulphur. The representation of these elements varies from sample to sample and depends on the individual technology where the sludge is produced. The waste sludge contains elements that are expected for an automotive paint shop, as these are typical elements present in paints, pigments, varnishes and automotive finish fillers. The results of the analyses are shown in Tables 8.5 to 8.10. The chemical elements found in the samples include both environmentally benign and hazardous elements.

Table 8.3

CHNO analysis – dry weight

Sample	C m/m%	H m/m%	N m/m%	O m/m%	CHNO m/m%
1+2	10.22	1.64	0.00	55.15	67.00
3	47.54	6.89	2.90	27.88	85.20
4	51.20	7.20	4.85	25.87	89.11
5	20.76	2.81	1.17	44.28	69.00
6	1.12	0.46	0.00	57.04	58.61
X	28.73	3.99	1.99	35.50	70.20

Table 8.4

CHN analysis – original state

Sample	C m/m%	H m/m%	N m/m%
1+2	10.22	1.64	0.00
3	24.95	8.92	1.39
4	27.87	9.23	2.33
5	17.74	4.49	0.79
6	0.05	0.1	0.00
X	25.41	8.29	1.62

Table 8.5

Analysis of other elements – sludge 1+2

Element	m/m%	StdErr%
Ca	24.410	0.210
Px	2.770	0.0800
Fe	2.000	0.070
Mg	0.791	0.039
Si	0.584	0.029
Sx	0.490	0.024
Al	0.468	0.023
Cl	0.403	0.020
Mn	0.298	0.015
No	0.281	0.014
Zn	0.247	0.012
Ba	0.0758	0.0038
K	0.0680	0.0034
Ti	0.0555	0.0028
Zr	0.0252	0.0013
Sr	0.0212	0.0011
Bi	0.0106	0.0005
Cr	0.0056	0.0007

Table 8.6

Analysis of other elements – sludge 3

Element	m/m%	StdErr%
Ti	7.670	0.130
Al	2.450	0.080
Si	1.990	0.070
Mg	0.978	0.049
Ca	0.902	0.045
Fe	0.244	0.012
Sx	0.163	0.008
Cl	0.135	0.007
Ba	0.069	0.0034
K	0.0625	0.0031
Sn	0.0413	0.0021
Cr	0.0316	0.0016
Zr	0.0292	0.0015
Cu	0.0151	0.0008
Sr	0.0102	0.0005
Br	0.0057	0.0003

Table 8.7

Analysis of other elements – sludge 4

Element	m/m%	StdErr%
Ti	3.860	0.100
Si	2.010	0.070
Ca	1.340	0.060
Ba	1.120	0.050
Mg	0.972	0.048
Al	0.813	0.040
Sx	0.337	0.017
Fe	0.135	0.007
Cl	0.113	0.006
Br	0.518	0.0026
K	0.0504	0.0025
Sr	0.0438	0.0022
Zr	0.013	0.0007
Cu	0.0105	0.0005
Sn	0.0104	0.0005
Bi	0.0088	0.0004

Table 8.8

Analysis of other elements – sludge 5

Element	m/m%	StdErr%
Ba	21.360	0.200
Sx	4.980	0.110
Si	1.910	0.070
Mg	0.815	0.041
Ca	0.806	0.040
Sr	0.573	0.029
Al	0.552	0.028
Cu	0.0074	0.0007

Table 8.9

Analysis of other elements – sludge 6

Element	m/m%	StdErr%
Na	27.610	0.220
Al	9.340	0.150
Px	1.710	0.060
Fe	0.967	0.048
Si	0.465	0.023

Ca	0.406	0.020
Zn	0.359	0.018
Mn	0.149	0.007
K	0.122	0.006
Ba	0.0912	0.0046
Zr	0.0814	0.0041
No	0.0693	0.0035
Cr	0.0073	0.0004
Sn	0.0059	0.0003
Sr	0.0035	0.0002

Table 8.10
Analysis of other elements – sludge X

Element	**m/m%**	**StdErr%**
Ba	17.370	0.190
Sx	3.650	0.090
Ca	3.610	0.090
Si	2.350	0.080
Mg	1.080	0.050
Al	0.643	0.032
Sr	0.506	0.025
Cl	0.343	0.017
Fe	0.189	0.009
K	0.0442	0.0023
Cu	0.0077	0.0006
Nb	0.0065	0.0003
Sn	0.0042	0.0004
Br	0.004	0.0002

Chromatographic analysis: carried out using a gas chromatograph with mass spectroscopic detector – SHIMADZU GCMS QP2010PLUS. The instrument detects ions that are formed by ionization of analytes. The first step is to convert the analytes dissolved in the mobile phase to ions in the gas phase. In the next step, the ions are analyzed, i.e. the mass-to-charge ratio (m/z) is determined. Ion sources operate at atmospheric pressure, analyzers at vacuum. This method of analysis is both versatile and highly selective, using a very sensitive detector. It allows the identification of analytes based on their mass spectra, which it compares with a database of known elements and compounds. From this it follows that the only limitation of this method is the database itself; the obtained results are influenced by the database of the measuring device.

The results of the analyses are summarized in the chromatograms in Annexes 1 to 6, expressed both graphically and numerically. The area of each chromatogram that is separated by dashed lines is the detection region of the solvent in which the sample is dissolved prior to analysis. Measurement in this area is interrupted to avoid overloading the detector. The hydrocarbon content of the sample generally reflects the predicted calorific value of the fuel. As previously anticipated, waste sludge sample 1+2 is not suitable for energy recovery; the other samples contain significant amounts of burnable and energetically significant hydrocarbon compounds.

8.5 Conclusion

The task of the research team of the University of Žilina was research in the field of energy recovery and disposal of waste sludge from the automotive industry. The aim of the task was to determine the optimal method of energy recovery or disposal of these sludges, which were taken for the initial phase of the solution from the automotive production of the Volkswagen Slovakia, a.s. plant in Bratislava. The sludge samples were subjected to chemical composition and fuel analyses, particularly moisture and calorific value.

Moisture analyses indicate a high degree of dewatering of the effluent sludge as it leaves production, and no further steps are required to reduce moisture. However, the observed moisture content reflects the actual production at that time and, according to the employees, the moisture content is much higher when the production line is under higher load and therefore the production of waste sludge increases. For this finding it is necessary to take additional samples also at this condition, i.e. at higher load on the production line. However, in this state of solution it can be stated that the moisture content of the waste sludge did not exceed 20.01 %, which corresponds to the maximum moisture content recommendations for firewood, for example.

Calorific value analyses indicate the energy content of individual waste sludge samples. Sludge samples 1+2 and 6 can be considered as unsuitable for energy recovery as their calorific value is too low, for sludge sample 6 almost zero. Sludge samples 3, 4, 5 and X are energetically interesting, similar in calorific value to municipal waste suitable for incineration in an incinerator, or low-grade coal. The variation in the observed calorific value for the individual samples is due to the measurement methodology, where the first series of calorific value measurements were taken immediately after sampling and the subsequent ones were taken some time apart. The decrease in calorific value is a reflection of the volatile matter content, which is gradually released spontaneously from the sludge.

The chemical composition analyses were focused on the assessment of the energetic elements, i.e. carbon and hydrogen, and the associated elements, i.e. nitrogen and oxygen, and later on the content of other selected chemical elements. Each of the sludge samples, except samples 1+2 and 6, has a significant carbon content (from 28.73 to 51.20 wt.%), of hydrogen (from 2.81 to 7.20 wt.%), but also a significant proportion of ballast in the form of nitrogen and oxygen. The assessment of other elements mainly points to elements found in paints or their pigments. The content of these elements is perceived as ballast from the point of view of energy recovery and as undesirable in the flue gases produced, e.g. during combustion. The hydrocarbon contents of the samples were confirmed by chromatographic analyses; these are generally considered to be indicative of the predicted achievable calorific value of the fuel. It was again confirmed that in particular waste sludge sample 1+2 is not suitable for energy recovery. The identified chemicals in the samples correspond only to the database of the chromatographic instrument and therefore cannot be considered as a total comprehensive assessment of the chemical composition.

From the analyses carried out, it can be concluded that waste sludge samples 3, 4, 5 and X are the most suitable for energy recovery; for these samples we will look for the optimal way of their energy recovery in further research. Sludge samples 1+2 and 6 are not directly suitable for energy recovery but can be disposed of and stabilized to be environmentally benign by appropriate thermal processes.

In the next step of solving the research task, it is possible to apply two different progressive approaches of energy recovery of waste sludge, either by applying pyrolysis process or co-incineration with wood sawdust to create fuel pellets. In pyrolysis, all products of the process that will take place in the experimental pyrolysis reactor (synthetic gas produced, pyrolysis oil and solid residue), its optimum working parameters (working temperature and residence time), as well as the energy consumption of the process itself, will be analyzed. In co-incineration, we will create mixtures of waste sludge with wood sawdust with varying proportions of sludge; from these mixtures we will produce fuel pellets in the pellet press, which we will then burn. We will be interested in the amount of heat released and, in particular, the chemical composition of the flue gases and ash produced after combustion. Both processes are particularly challenging from an environmental point of view because, as chemical analyses have shown, the waste sludge contains many undesirable elements.

Annex 1 Chromatogram, sludge sample 1+2

Peak	R.T.	I.T.	F.T.	Area	Area %	Height	Height %	A/H	Name
1	3.67	3.64	3.70	69391	58.02	46778	53.27	1.48	Propanoyl chloride, 2-methyl-
2	6.20	6.18	6.23	50214	41.98	41043	46.73	1.22	Ethanol, 2-butoxy-

R.T.- R. Time; I.T. – I. Time; F.T. – F. Time

Annex 2 Chromatogram, sludge sample 3

Peak	R.T.	I.T.	F.T.	Area	Area %	Height	Height %	A/H	Name
1	3.67	3.64	3.69	343992	4.35	21956	4.49	1.62	Pentane, 2-nitro-
2	3.71	3.69	3.75	214057	2.71	116517	2.47	1.84	Formic acid, butyl ester
3	3.87	3.84	3.94	154565	1.96	57452	1.22	2.69	Methane, trimethoxy-
4	5.11	5.08	5.14	73756	0.93	54242	1.15	1.36	2-Hexanol, (R)-
5	5.23	5.14	5.26	175865	2.22	127197	2.69	1.38	3,3-Dimethoxy-2-butanone
6	5.60	5.57	5.63	56385	0.71	47062	1.00	1.20	1-Hexyn-3-ol, 3,5-dimethyl-
7	7.85	7.82	7.89	115301	1.46	56371	1.19	2.05	Dodecane, 2,6,10-trimethyl-
8	8.08	8.05	8.13	197570	2.50	95543	2.02	2.07	Heptane, 5-ethyl-2,2,3-trimethyl-
9	8.17	8.13	8.20	213652	2.70	103633	2.19	2.06	Hexane, 2,2,5-trimethyl-
10	8.33	8.29	8.38	192298	2.43	81300	1.72	2.37	Decane, 3,7-dimethyl-

11	11.61	11.57	11.64	4188513	52.98	2822154	59.76	1.48	2,4,7,9-Tetramethyl-5-decyn-4,7-diol
12	11.69	11.64	11.72	1158348	14.65	543636	11.51	2.13	2,4,7,9-Tetramethyl-5-decyn-4,7-diol
13	11.73	11.72	11.75	53238	0.67	39721	0.84	1.34	Heptadecane
14	12.11	12.02	12.15	432768	5.47	96847	2.05	4.47	Pentadecane
15	12.39	12.37	12.42	49154	0.62	40035	0.85	1.23	7-Oxabicyclo[4.1.0]heptane, 1-methyl-4-(1
16	13.19	13.17	13.21	46166	0.58	40135	0.85	1.15	Isophorone diisocyanate
17	13.41	13.38	13.45	240309	3.04	188638	3.99	1.27	Isophorone diisocyanate

R.T.- R. Time; I.T. – I. Time; F.T. – F. Time

Annex 3 Chromatogram, sludge sample 4

Peak	R.T.	I.T.	F.T.	Area	Area %	Height	Height %	A/H	Name
1	3.70	3.62	3.77	103838655	51.02	29266575	38.06	3.55	Trichloromethane
2	3.97	3.88	4.01	6313702	3.10	3615847	4.70	1.75	1-Butanol
3	6.17	6.09	6.24	806902	0.40	262451	0.34	3.07	Ethanol, 2-butoxy-
4	9.05	9.02	9.12	893670	0.44	355665	0.46	2.51	1,6-Hexanediol
5	10.64	10.59	10.77	6080328	2.99	3789621	4.93	1.60	Piperidin-4-ol, 2,5-dimethyl-1-(1-methylethyl
6	11.43	11.35	11.54	3021344	1.48	1184584	1.54	2.55	2,4,7,9-Tetramethyl-5-decyn-4,7-diol
7	11.72	11.60	11.78	26366939	12.95	13150871	17.10	2.00	2,4,7,9-Tetramethyl-5-decyn-4,7-diol
8	12.40	12.31	12.48	2339199	1.15	793814	1.03	2.95	3,7-Dimethyl-6-nonen-1-ol acetate
9	12.58	12.48	12.66	5304708	2.61	3555359	4.62	1.49	Tributyl phosphate
10	13.42	13.39	13.56	1944912	0.96	968836	1.26	2.01	Isophorone diisocyanate
11	16.49	16.43	16.56	716742	0.35	314420	0.41	2.28	3-Aminomethyl-3,5,5-trimethylcyclohexan
12	16.66	16.57	16.75	838163	0.41	300723	0.39	2.79	2-N-n-Butylmelamine
13	17.34	17.26	17.48	6567024	3.23	2372436	3.09	2.77	Carbonic acid, decyl 2-ethylhexyl ester
14	20.19	20.12	20.27	799318	0.39	351151	0.46	2.28	2-N-n-Butylmelamine
15	21.44	21.38	21.52	1409193	0.69	680767	0.89	2.07	
16	22.99	22.94	23.07	1095863	0.54	499584	0.65	2.19	Butylphosphonic acid, neopentyl nonyl ester
17	23.73	23.67	23.83	11652989	5.73	5708900	7.42	2.04	Ethanol, 2-butoxy-, phosphate (3:1)
18	24.15	24.09	24.21	746237	0.37	251846	0.33	2.96	
19	24.35	24.21	24.41	1628413	0.80	926211	1.20	1.76	Hexa(methoxymethyl) melamine
20	24.60	24.41	24.68	8176708	4.02	4000031	5.20	2.04	Hexanoic acid, 3,5,5-trimethyl-, oct-3-en-2-
21	24.81	24.76	24.92	3335504	1.64	1509105	1.96	2.21	Hexanoic acid, 3,5,5-trimethyl-, tetradec-5-
22	26.18	26.13	26.26	1496858	0.74	803583	1.05	1.86	Hexanoic acid, 3,5,5-trimethyl-, tetradec-5-
23	27.64	27.56	27.73	1253706	0.62	382616	0.50	3.28	

24	29.94	29.86	30.04	1571585	0.77	536817	0.70	2.93	Hexanoic acid, 3,5,5-trimethyl-, 3-chlorophenyl
25	32.30	32.20	32.45	5328539	2.62	1310567	1.70	4.07	Hexanoic acid, 3,5,5-trimethyl-, 2-chloro-6-

R.T.- R. Time; I.T. – I. Time; F.T. – F. Time

Annex 4 Chromatogram, sludge sample 5

Peak	R.T.	I.T.	F.T.	Area	Area %	Height	Height %	A/H	Name
1	3.67	3.61	3.72	83101221	39.04	27409009	39.75	3.03	Trichloromethane
2	4.86	4.78	4.92	1194152	0.56	433684	0.63	2.75	2-Butanone, oxime
3	6.57	6.53	6.69	4650098	2.18	1602708	2.32	2.90	Neopentyl glycol
4	6.92	6.88	7.03	1879897	0.88	501292	0.73	3.75	Ethanol, 2,2'-oxybis-
5	7.48	7.41	7.52	2592954	1.22	869865	1.26	2.98	3,5-Dimethylpyrazole
6	7.85	7.80	7.93	851746	0.40	324830	0.47	2.62	Dodecane, 2,6,10-trimethyl-
7	8.06	7.96	8.14	3635938	1.71	469208	0.68	7.75	Hexane, 2,2,5-trimethyl-
8	8.17	8.14	8.25	2205854	1.04	784244	1.14	2.81	Hexane, 2,2,5-trimethyl-
9	8.33	8.25	8.39	2082633	0.98	585438	0.85	3.56	Nonane, 3-methyl-5-propyl-
10	9.18	9.01	9.41	8748804	4.11	1109626	1.61	7.88	2-Oxepanone
11	10.51	10.44	10.63	4067145	1.91	1255551	1.82	3.24	1,3-Propanediol, 2-ethyl-2-(hydroxymethyl
12	10.82	10.63	10.91	3439707	1.62	607118	0.88	5.67	1-Propanol, 2-(2-hydroxypropoxy)-
13	11.01	10.91	11.09	3843667	1.81	694337	1.01	5.54	2-Propanol, 1-(2-methoxy-1-methylethoxy
14	11.32	11.26	11.43	3820540	1.79	1539177	2.23	2.48	Hexane, 1,6-diisocyanato-
15	11.71	11.64	11.79	7548528	3.55	4709481	6.83	1.60	2,4,7,9-Tetramethyl-5-decyn-4,7-diol
16	12.13	12.02	12.18	3684154	1.73	778310	1.13	4.73	Heneicosane
17	12.21	12.18	12.25	2246066	1.06	1441468	2.09	1.56	
18	12.36	12.25	12.49	2901986	1.36	396952	0.58	7.31	Heptadecane, 7-methyl-
19	12.52	12.49	12.58	660565	0.31	274490	0.40	2.41	Dodecane, 2-methyl-
20	13.88	13.78	13.98	3097211	1.46	773936	1.12	4.00	1-Pentanol, 4-methyl-2-propyl-
21	14.08	13.98	14.12	2584500	1.21	639532	0.93	4.04	1-Decanol, 2-methyl-
22	14.34	14.25	14.39	2668224	1.25	868583	1.26	3.07	Cyclopentanecarboxylic acid, octyl ester
23	14.51	14.39	14.57	3913864	1.84	643271	0.93	6.08	1-Undecene, 9-methyl-
24	14.61	14.57	14.74	5291170	2.49	741512	1.08	7.14	Eicosane
25	14.79	14.74	14.85	2589449	1.22	640958	0.93	4.04	Dodecyl nonyl ether
26	14.90	14.85	14.98	1985072	0.93	434994	0.63	4.56	1-Dodecanol, 2-hexyl-
27	15.01	14.98	15.08	2710939	1.27	661822	0.96	4.10	Oxirane, [(dodecyloxy)methyl]-
28	15.11	15.08	15.18	1500857	0.71	443677	0.64	3.38	Dodecyl octyl ether
29	15.21	15.18	15.26	1214568	0.57	505347	0.73	2.40	Octane, 1,1'-oxybis-
30	15.57	15.50	15.61	3990588	1.87	1753256	2.54	2.28	2-((2-Ethylbutoxy)carbonyl) benzoic acid

31	15.65	15.61	15.72	4886484	2.30	2088199	3.03	2.34	1,2-Benzenedicarboxylic acid, monobutyl e
32	16.71	16.63	16.75	6071647	2.85	2070082	3.00	2.93	2-N-n-Butylmelamine
33	16.99	16.95	17.16	3879755	1.82	1414040	2.05	2.74	2-((2-Methoxyethoxy)carbonyl)benzoic acid
34	19.06	19.01	19.15	2008391	0.94	886556	1.29	2.27	(E)-2-((Hex-3-enyloxy)carbonyl)benzoic a
35	21.15	21.06	21.27	3813250	1.79	1346905	1.95	2.83	2-((Pent-4-enyloxy)carbonyl)benzoic acid
36	21.45	21.27	21.52	3996991	1.88	1653207	2.40	2.42	
37	22.10	22.05	22.23	4734835	2.22	1850516	2.68	2.56	Adipic acid, octyl pent-4-en-2-yl ester
38	24.12	24.07	24.23	2601286	1.22	1022584	1.48	2.54	Phthalic acid, 3-methylbenzyl tetradecyl es
39	25.51	25.47	25.56	3463812	1.63	1522063	2.21	2.28	
40	25.58	25.56	25.65	800575	0.38	404757	0.59	1.98	
41	26.09	26.04	26.17	1885391	0.89	799674	1.16	2.36	

R.T.- R. Time; I.T. – I. Time; F.T. – F. Time

Annex 5 Chromatogram, sludge sample 6

Peak	R.T.	I.T.	F.T.	Area	Area %	Height	Height %	A/H	Name
1	2.52	2.51	2.53	300084	2.16	265607	3.47	1.13	Carbamic acid, monoammonium salt
2	3.83	3.81	3.87	333874	2.40	150850	1.97	2.21	Acetic acid ethenyl ester
3	3.90	3.87	3.97	252368	1.82	211938	2.77	1.19	Hexane, 2,2-dimethyl-
4	5.20	5.17	5.24	172368	1.24	122285	1.60	1.41	2-Hexanol, (R)-
5	6.55	6.51	6.61	284381	2.05	150623	1.97	1.89	Neopentyl glycol
6	7.95	7.92	8.00	186928	1.35	121988	1.59	1.53	Cyclopentanol
7	8.92	8.87	9.04	305794	2.20	82015	1.07	3.73	1,6-Hexanediol
8	9.06	9.04	9.12	435986	3.14	309043	4.03	1.41	2-Oxepanone
9	10.83	10.79	10.90	369737	2.66	235430	3.07	1.57	1,2-Benzenedicarboxylic acid
10	10.98	10.90	11.07	2161948	15.56	1553968	20.29	1.39	Phthalic anhydride
11	11.30	11.27	11.34	133575	0.96	64375	0.84	2.07	Hexane, 1,6-diisocyanato-
12	11.36	11.34	11.41	198655	1.43	124716	1.63	1.59	1,3-Isobenzofurandione, hexahydro-, trans-
13	12.02	12.00	12.06	122244	0.88	93981	1.23	1.30	1H-Isoindole-1,3(2H)-dione, 2-methyl-
14	12.23	12.20	12.28	266984	1.92	157716	2.06	1.69	Phthalimide
15	12.38	12.34	12.45	1402179	10.09	975950	12.74	1.44	Phthalimide
16	15.56	15.51	15.60	259533	1.87	122787	1.60	2.11	Phthalic acid, butyl oct-3-yl ester
17	15.63	15.60	15.69	331636	2.39	186149	2.43	1.78	1,2-Benzenedicarboxylic acid, butyl 2-ethylhexyl
18	19.04	19.00	19.11	398368	2.87	185641	2.42	2.15	(E)-2-((Hex-3-enyloxy)carbonyl)benzoic acid
19	19.86	19.83	19.92	242514	1.75	115222	1.50	2.10	Heneicosane
20	21.09	21.04	21.19	647972	4.66	187605	2.45	3.45	Hexadecanoic acid, butyl ester
21	21.30	21.25	21.35	315522	2.27	151631	1.98	2.08	Heneicosane

22	22.58	22.54	22.63	220725	1.59	107949	1.41	2.04	Heneicosane
23	23.58	23.53	23.63	451230	3.25	233706	3.05	1.93	Octadecanoic acid, butyl ester
24	23.73	23.69	23.78	155241	1.12	78897	1.03	1.97	Heneicosane
25	24.70	24.66	24.74	169812	1.22	68090	0.89	2.49	Benzene, 1,1'-(1-methylethylidene)bis[4-(2-propenyloxy
26	24.77	24.74	24.84	1360942	9.80	708903	9.26	1.92	Carbonic acid, 2-ethylhexyl undecyl ester
27	25.73	25.68	25.79	253187	1.82	118458	1.55	2.14	Eicosane
28	26.67	26.63	26.71	206909	1.49	110792	1.45	1.87	Heneicosane
29	27.67	27.63	27.72	209649	1.51	101776	1.33	2.06	Heneicosane
30	28.77	28.73	28.82	254185	1.83	107411	1.40	2.37	Tetratetracontane
31	28.98	28.93	29.04	440269	3.17	197542	2.58	2.23	Oxirane, 2,2'-[(1-methylethylidene)bis(4,1-p
32	29.57	29.49	29.67	850912	6.13	176200	2.30	4.83	Oxirane, 2,2'-[(1-methylethylidene)bis(4,1-p
33	30.03	29.99	30.09	196673	1.42	80242	1.05	2.45	Hexatriacontane

R.T.- R. Time; I.T. – I. Time; F.T. – F. Time

Annex 6 Chromatogram, sludge sample X

Peak	R.T.	I.T.	F.T.	Area	Area %	Height	Height %	A/H	Name
1	3.85	3.83	3.92	1883175	0.91	910471	1.31	2.07	Butane, 2-chloro-2-methyl-
2	3.96	3.92	4.07	8995549	4.36	4270949	6.13	2.11	1-Butanol
3	6.22	6.18	6.30	2564959	1.24	1020434	1.46	2.51	Ethanol, 2-butoxy-
4	6.57	6.50	6.75	4594007	2.22	1083725	1.55	4.24	Neopentyl glycol
5	8.92	8.83	8.98	1816758	0.88	1181598	1.69	1.54	Benzyl isocyanate
6	9.08	9.02	9.16	14633141	7.09	3763548	5.40	3.89	1,6-Hexanediol
7	9.19	9.16	9.44	8304639	4.02	1721981	2.47	4.82	2-Oxepanone
8	10.52	10.45	10.62	2470512	1.20	965130	1.38	2.56	1,3-Propanediol, 2-ethyl-2-(hydroxymethyl
9	11.72	11.60	11.82	25759455	12.48	12569053	18.03	2.05	2,4,7,9-Tetramethyl-5-decyn-4,7-diol
10	11.86	11.82	11.96	3205366	1.55	655937	0.94	4.89	1-Decanol, 2-hexyl-
11	12.03	11.96	12.09	3592438	1.74	562077	0.81	6.39	Cyclopentane, 1-pentyl-2-propyl-
12	12.21	12.09	12.30	6750775	3.27	1168193	1.68	5.78	
13	12.33	12.30	12.35	662853	0.32	346849	0.50	1.91	1-Octanol, 2-butyl-
14	12.40	12.35	12.51	1781707	0.86	579367	0.83	3.08	3-Phenyl-2-ethoxypropylphthalimide
15	13.20	13.04	13.27	5897520	2.86	2376507	3.41	2.48	Isophorone diisocyanate
16	13.43	13.27	13.56	13337903	6.46	7783243	11.16	1.71	Isophorone diisocyanate
17	13.66	13.56	13.78	2943339	1.43	1011699	1.45	2.91	Benzene, 1,3-bis(1-isocyanato-1-methylethyl
18	13.87	13.78	13.97	2063941	1.00	410844	0.59	5.02	1-Octanol, 2-butyl-
19	14.08	13.97	14.13	2894368	1.40	677825	0.97	4.27	1-Dodecanol, 3,7,11-trimethyl-
20	14.32	14.13	14.39	5135497	2.49	639165	0.92	8.03	Dodecyl nonyl ether
21	14.52	14.39	14.58	6024262	2.92	874229	1.25	6.89	5-Eicosene, (E)-
22	14.68	14.58	14.74	5438786	2.63	635610	0.91	8.56	Octadecane, 1-chloro-
23	14.79	14.74	14.86	3570498	1.73	716944	1.03	4.98	Hexadecane, 2,6,11,15-tetramethyl-

24	15.01	14.86	15.09	5418662	2.62	625751	0.90	8.66	Oxalic acid, 2-ethylhexyl tetradecyl ester
25	15.11	15.09	15.18	1581606	0.77	511986	0.73	3.09	Dodecyl octyl ether
26	15.21	15.18	15.30	2428338	1.18	1125978	1.61	2.16	Cyclohexane, 1,1'-[methylenebis(oxy)]bis
27	15.56	15.51	15.61	2951062	1.43	1085157	1.56	2.72	Bis-(3,5,5-trimethylhexyl) phthalate
28	15.65	15.61	15.72	2705063	1.31	716143	1.03	3.78	Phthalic acid, butyl undecyl ester
29	16.29	16.26	16.44	1517445	0.73	264500	0.38	5.74	Decane, 1,1'-oxybis-
30	16.55	16.44	16.64	6687749	3.24	1560463	2.24	4.29	3-Aminomethyl-3,5,5-trimethylcyclohexan
31	16.70	16.64	16.76	6210991	3.01	2037843	2.92	3.05	Methyl 4,6-decadienyl ether
32	16.79	16.76	16.84	1042848	0.51	338146	0.48	3.08	Carbonic acid, decyl nonyl ester
33	16.99	16.84	17.03	3407523	1.65	614037	0.88	5.55	Bis(tridecyl) phthalate
34	17.06	17.03	17.15	1370584	0.66	377009	0.54	3.64	Decane, 1,1'-oxybis-
35	17.34	17.27	17.47	4390592	2.13	1431705	2.05	3.07	2-Isopropyl-5-methyl-1-heptanol
36	17.61	17.55	17.68	1301074	0.63	392712	0.56	3.31	Cyclopentanecarboxylic acid, 2-pentadecyl
37	17.78	17.68	17.86	1208305	0.59	216302	0.31	5.59	Nonyl tetradecyl ether
38	19.06	19.02	19.11	831205	0.40	372980	0.53	2.23	(E)-2-((Hex-3-enyloxy)carbonyl)benzoic a
39	20.21	20.17	20.31	2250793	1.09	886933	1.27	2.54	2-N-n-Butylmelamine
40	20.35	20.31	20.45	1048100	0.51	332138	0.48	3.16	Cyclohexanepropanol-
41	21.45	21.40	21.54	4599049	2.23	2066711	2.96	2.23	
42	22.09	22.05	22.20	886436	0.43	338986	0.49	2.61	Adipic acid, octyl pent-4-en-2-yl ester
43	22.99	22.95	23.09	2236545	1.08	1027902	1.47	2.18	Butylphosphonic acid, neopentyl nonyl ester
44	24.35	24.30	24.41	1918404	0.93	1056566	1.52	1.82	Hexa(methoxymethyl) melamine
45	24.59	24.52	24.67	3965436	1.92	1999746	2.87	1.98	Hexanoic acid, 3,5,5-trimethyl-, oct-3-en-2
46	24.81	24.67	24.89	2055277	1.00	712231	1.02	2.89	Hexanoic acid, 3,5,5-trimethyl-, tetradec-5-
47	25.73	25.67	25.81	992259	0.48	394767	0.57	2.51	
48	26.99	26.95	27.02	1311680	0.64	640064	0.92	2.05	Citronellyl tiglate
49	27.06	27.02	27.16	1884405	0.91	747749	1.07	2.52	Hexanedioic acid, mono(2-ethylhexyl)ester
50	27.43	27.36	27.47	1374358	0.67	636687	0.91	2.16	
51	29.26	29.21	29.37	1101397	0.53	347462	0.50	3.17	
52	29.94	29.86	30.03	1015554	0.49	312843	0.45	3.25	
53	32.29	32.20	32.40	2473437	1.20	627055	0.90	3.94	

R.T.- R. Time; I.T. – I. Time; F.T. – F. Time

References

[1] Đurđević, D., Blecich, P., Jurić, Ž. 2019. Energy Recovery from Sewage Sludge: The Case Study of Croatia. Energies, 2019, 12, 1927.

[2] Geffertová, J., Geffert, A. 2011. Energy potential of selected wastes containing biomass (in Slovak). Acta facultatis xylologiae Zvolen, 53 (1), 93-99.

[3] Hušek, M., Moško, J., Pohořelý, M. 2022. Sewage sludge treatment methods and P-recovery possibilities: Current state-of-the-art. Journal of Environmental Management. 2022. DOI:10.1016/j.jenvman.2022.115090

[4] Lu, T., et al. 2016. Characteristic of heavy metals in biochar derived from sewage sludge. J. Mater. Cycles Waste Manag., 18, 2016, 725–733.

[5] Karagiannidis, A. 2012. Waste to Energy, Opportunities and Challenges for Developing and Transition Economies. Springer, 2012.

[6] Wang, Z., et al. 2021. Effect of temperature on pyrolysis of sewage sludge: biochar properties and environmental risks from heavy metals. E3S Web of Conferences 237, 2021.

[7] Wang, Z., et al. 2021. Effects of biochar derived from sewage sludge and sewage sludge/cotton stalks on the immobilization and phytoavailability of Pb, Cu, and Zn in sandy loam soil. Journal of Hazardous Materials, 419.

[8] Wang, Z., et al. 2020. Syngas evolution and energy efficiency in CO_2-assisted gasification of pine bark. Applied Energy, 269, 114996, DOI: 10.1016/j.apenergy.2020.11499

[9] Ni, B., et al. 2020. Microplastics Mitigation in Sewage Sludge through Pyrolysis: The Role of Pyrolysis Temperature. Environmental Science & Technology Letters, 7(12), 961-967.

[10] Wang, C., et al. 2022. Biochar-based slow-release of fertilizers for sustainable agriculture: A mini review. Environmental Science and Ecotechnology, 10, 2022.

[11] Wang, J., Fu, R., Xu, Z. 2017. Stabilization of heavy metals in municipal sewage sludge by freeze-thaw treatment with a blend of diatomite, $FeSO_4$, and $Ca(OH)_2$. Journal of the Air & Waste Management Association, 67 (8), 847-853.

[12] Jandačka, J. 2014. Energy use of municipal waste (in Slovak). Uniza-EDIS. 2014.

[13] Envites 2024.

[14] IEA Press 2024.

[15] www.slovakia.andritz.sk 2024.

[16] www.filterpressmachine.com 2024.

UNIVNET 2024

UNIVNET – University and Industrial Research and Education Platform of the Recycling Society

Title: Progressive Automotive Waste Utilization Technologies as Driving Forces of Sustainable Development

Editors and technical editing: Iveta Čabalová
Jozef Krilek
Technical University in Zvolen

Published by: RAM-Verlag, Germany

Year: 2024

© Copyright 2024 by RAM-Verlag
Publisher:
RAM-Verlag
Stüttinghauser Ringstr. 44
D-58515 Lüdenscheid
Germany
RAM-Verlag@t-online.de
http://ram-verlag.eu
The publisher cannot be held responsible for any linguistic errors in book:
Such responsibility is only up to the authors.

ISBN 978-3-96595-042-9

ISBN 978-3-96595-042-9

https://en.univnet.sk/

Zvolen, 2024